REGULATION OF THE WNT/β-CATENIN PATHWAY IN THE DISEASE PROGRESSION OF OSTEOSARCOMA

LEOW PAY CHIN

(B. Sc Pharm (Hons.), NUS)

A THESIS SUBMITTED

FOR THE DEGREE OF DOCTOR OF PHILOSOPHY

DEPARTMENT OF PHARMACY

NATIONAL UNIVERSITY OF SINGAPORE

2010

ACKNOWLEDGEMENTS

LIST OF PUBLICATIONS AND PRESENTATIONS

Publications:

1. **Leow PC**, Yang Z, Ee PL. Potential role of Secreted Frizzled-related proteins as tumor suppressors in osteosarcoma. Manuscript in preparation.

2. **Leow PC**, Boon CP, Lee CY, Go ML, Ee PL. Functionlization of curcumin analogues as Wnt antagonists in osteosarcoma. Manuscript in preparation.

3. **Leow PC**, Ong ZY, Ee PL (2010). Natural compounds as antagonist of canonical Wnt/β-catenin signaling. *Current Chemical Biology* (4): 49-63.

4. **Leow PC**, Tian Q, Ong ZY, Yang Z, Ee PL (2009). Antitumor activity of natural compounds, curcumin and PKF118-310, as Wnt/β-catenin antagonists against human osteosarcoma cells. *Invest New Drugs* DOI: 10.1007/s10637-009-9311-z

5. Nayak TR, **Leow PC**, Ee PL, Arockiadoss T, Ramaprabhu S, Pastorin G. (2010) Crucial Parameters responsible for Carbon Nanotubes toxicity. *Current Nanoscience*. 6(2): 141-154.

6. Kwa AL, Low JG, Lim TP, **Leow PC**, Kurup A, Tam VH. (2008) Independent predictors for mortality in patients with positive Stenotrophomanas maltophilia cultures. *Ann Acad Med Singapore*. 37(10):826-30.

7. Chan EC, Yap SL, Lau AJ, **Leow PC**, Toh DF, Koh HL. (2007) Ultra-performance liquid chromatography/time-of-flight mass spectrometry based metabolomics of raw and steamed Panax notoginseng. *Rapid Commun Mass Spectrom*. 21(4):519-28.

Conference Abstracts

1. Leow PC, Yang Z, Ee PL. Role of Secreted Frizzled-related proteins in inhibiting growth and invasion in human osteosarcoma. American Association for Cancer Research Annual Meeting, 17-21 April 2010, Washington D.C, USA.

2. Leow PC, Boon CP, Lee CY, Go ML, Ee PL. Design and synthesis of curcumin analogues as Wnt/ß-catenin antagonists. American Association for Cancer Research Annual Meeting, April 2010, Washington D.C, USA. 17-21

3. Leow PC, Yang Z, Ee PL. Inhibition of osteosarcoma cell proliferation, invasion and migration by PKF118-310, a specific antagonist of the Wnt/β-catenin pathway. Singapore Nanomedicine Workshop 2008, 22-25 Oct 2008, Singapore.

4. Leow PC, Yang Z, Ee PL. Curcumin inhibits human osteosarcoma cell invasion by disrupting the Wnt/β-catenin pathway. Oral presentation: 9th Frontier Science Symposium, 15-17 Oct 2008, Singapore.

5. Leow PC, Yang Z, Ee PL. Curcumin inhibits cell proliferation, invasion and migration in U2OS human osteosarcoma cells. PharmSci@Asia 2008, 26-27 Jun 2008 ,Nanjing, China.

6. Leow PC, Yang Z, Ee PL. Curcumin inhibits cell proliferation, invasion and migration in human osteosarcoma cells. American Association for Cancer Research Annual Meeting, 12-16 April 2008, San Diego, USA.

TABLE OF CONTENTS

CHAPTER 4: FUNCTIONALIZATION OF CURCUMIN ANALOGUES AS WNT ANTAGONISTS IN OSTEOSARCOMA

SUMMARY

Osteosarcoma is the most common primary malignancy of the bone with an extremely high propensity for aggressive growth and metastasis. While the precise molecular mechanism underlying the disease is poorly understood, emerging evidence has implicated the canonical Wnt/β-catenin signaling pathway. The overall goal of this study is to develop novel Wnt-targeted therapies for the treatment of osteosarcoma. We hypothesized that osteosarcoma progression may be delayed by disrupting the Wnt/β-catenin pathway either by using small molecule inhibitors or by manipulating the levels of the endogenous antagonists, the family of secreted frizzled-related proteins (SFRPs).

To test our hypothesis, we explored three specific aims:

(1) Assess the role and mechanism of action of small molecule Wnt/β-catenin inhibitors in regulating osteosarcoma cell proliferation, motility and invasion.

(2) Synthesize and evaluate a set of lead compounds with improved potency and selectivity as Wnt/β-catenin antagonists; identify the critical structural motifs for Wnt inhibitory activity and examine the underlying mechanism of Wnt inhibition of selected curcumin analogues

(3) Examine the functional roles and mechanism of SFRPs as tumor suppressors in regulating osteosarcoma cell proliferation, motility and invasion.

In **Aim (1)**, we successfully showed that curcumin, PKF118-310 and artemisinin decreased the transcriptional activity of the β-catenin/TCF complex and significantly

inhibited U2OS cell invasion and migration. The observed anti-invasion effects were associated with a decrease in the expression and activities of Matrix Metalloproteinase-9, a Wnt target gene. We further demonstrated that the anti-proliferative effect of PKF118-310 is attributed to PKF118-310-induced apoptosis and G2/M phase arrest, with a corresponding decrease in proliferation-associated Wnt target oncogenes such as cyclin-D1, c-Myc, and survivin. In **Aim (2)**, using curcumin as a lead, we next synthesized and identified several analogues that were not only up to 60 times more potent than curcumin as Wnt antagonists, but were also highly selective with limited cytotoxicity. Further structure-activity-relationship analysis of these analogues suggested that conformation restriction around the dienone moiety, as well as the introduction of suitable alkoxyl and hydroxyl group substitutions on the aromatic rings of curcumin structure, dramatically enhanced Wnt-inhibitory activity. Using the Human Wnt Signaling Pathway RT^2 Profiler^{TM} PCR array, we observed down-regulation of several Wnt target oncogenes such as FOSL1, PITX2 and WISP1 in U2OS cells following treatment with the most potent analogue (**3-3**), in correspondence to its anti-invasive effects. In **Aim (3),** we found that restoration of SFRPs expressions in U2OS cells suppressed the transcriptional activity of the β-catenin/TCF complex and significantly inhibited anchorage-dependent growth, colony formation efficiency and osteosarcoma cell invasion. On the other hand, differential effects on cell migration in U2OS stable transfectants were observed. These anti-proliferative effects may be attributed to GO/G1 and/or G2/M phase arrests and perturbations of major Wnt target proliferation-associated oncogenes including cyclin-D1, c-Myc and survivin in the U2OS transfectants. Lastly, using the Human Wnt Signaling Pathway RT^2 Profiler^{TM} PCR array, we identified additional Wnt target genes

such as WISP1, Brachyury, SLC9A3R1 and JUN that might play a significant role in regulating osteosarcoma tumorigenesis and metastasis with over-expressions of SFRP2 or SFRP5. This analysis of gene perturbations provided valuable insights on the interactions of SFRPs with the Wnt pathway and may aid us in designing more effective SFRPs-based therapeutics. In conclusion, our findings not only provided deeper insights into the contributory role of aberrant canonical Wnt/β-catenin signaling in osteosarcoma disease progression, but also a greater understanding of the potential of small molecules and SFRPs as Wnt antagonists in osteosarcoma. These knowledge may be useful for the subsequent discovery and development of novel targeted therapy for osteosarcoma.

LIST OF TABLES

LIST OF FIGURES

Figure 5-6. SFRPs over-expression inhibited OS cell metastasis through suppressing MMP-2 and MMP-9 proteins.

Figure 6-1. Proposed modifications of curcumin template for improved Wnt inhibitory activity.

LIST OF SYNTHETIC SCHEMES

Scheme 4-1. General method for the synthesis of Series 1 curcumin analogues.

Scheme 4-2. Curcumin analogues from Series 2, 3, 4 and 5.

Scheme 4-3. General method for the synthesis of Series 2, 3 and 4 curcumin analogues.

Scheme 4-4. Protection and deprotection of phenolic hydroxyl groups for the synthesis of compound 2-6.

LIST OF ABBREVIATIONS

APC	Adenomatous Polyposis Coli
BCL9-2	B-Cell Lymphoma 9-2
β-TrCP	β-Transducin Repeat-Containing Protein
CBP	cAMP Response Element Binding Protein
CRD	Cysteine Rich Domain
CK-1α	Casein Kinase-1α
CM	Conditioned Medium
COX-2	Cyclooxygenase-2
CRT	Wnt-3A CM-induced β-catenin response transcription
DKK	Dickkopf
DMEM	Dulbecco's modified eagle's medium
DMSO	Dimethyl Sulfoxide
DN-LRP5	Dominant-Negative LRP5
DVL	Dishevelled
EGF	Endothelial Growth Factor
FADD	Fas-Associated via Death Domain
FBS	Fetal Bovine Serum
FOSL1	Fos-Like Antigen 1
FZD	Frizzled receptors
GSK-3β	Glycogen Synthase Kinase-3β
HBP1	HMG-Box Transcription Factor 1
HDAC	Histone Deacetylases

HFOB	Human Fetal Osteoblast
HMG	High Mobility Group
HPLC	High Pressure Liquid Chromatography
HTS	High Throughput Study
IGF	Insulin-like Growth Factor
LEF	Lymphoid Enhancer binding Factor
LRP	Low-density Lipoprotein Receptor-related Protein
MAPK	Mitogen-Activated Protein Kinase
MIRK	Minibrain-Related Kinase
MMP	Matrix Metalloproteinase
MT1-MMP	Membrane-Type Matrix Metalloproteinase 1
mTOR	Mammalian Target of Rapamycin
MTT	3-(4, 5 dimethyl-thiazol-2-yl)-2, 5-diphenyltetrazolium bromide
NF-κB	Nuclear Factor kappa-light-chain-enhancer of activated B cells
NKD1	Naked Cutile Homolog 1
NSAIDs	Non-Steriodal Anti-Inflammatory Drugs
PBS	Phosphate Buffer Saline
PCP	Planar Cell Polarity
PI	Propidium Iodide
PITX2	Paired-Like Homeodomain 2
Pygo	Pygopus
RNAi	RNA Interefence
SAR	Structure-Activity-Relationship

SEM	Standard Error Mean
SFRP	Secreted Frizzled-Related Protein
SiRNA	Small-interefering RNA
STAT3	Signal Transducer and Activator of Transcription 3
TCF	T-Cell-specific Transcriptional Factor
TCF7L1	T-Cell-specific Transcriptional Factor Like 1
TIMP-2	Tissue Inhibitor of Metalloproteinases
TMS	Tetramethylsilane
TNF-α	Tumor Necrosis Factor-α
TLC	Thin Layer Chromatography
TLE2	Transducin-like Enhancer of Split 2
RT	Room Temperature
RT-PCR	Reverse Transcriptase–Polymerase Chain Reaction
PI	Propidium Iodide
uPAR	Urokinase Plasminogen Activator Receptor
VEGF	Vascular Endothelial Growth Factor
WIF-1	Wnt Inhibitory Factor-1
WISP1	WNT1-Inducible Secreted Protein 1

CHAPTER 1.   Introduction

1.1 Osteosarcoma

Osteosarcoma is the most frequent malignancy of the bone which predominantly affects rapidly growing bones such as the metaphyses of long tubular bones, especially the distal femur or proximal tibia in adolescents and children, and there is no sex- or race-based predilection [1]. High grade central osteosarcoma is by far the most frequent sub-type, comprising up to 80 % of all osteosarcomas. The other osteosarcoma variants, which differ in site, histology or biological behavior, include small cell osteosarcoma, osteosarcoma occurring as secondary malignancy, extra skeletal osteosarcoma, surface osteosarcoma and craniofacial osteosarcoma. Risk factors for osteosarcoma include states associated with increased osteoblast proliferation such as chronic osteomyelitis, Paget's disease of bone, ionizing radiation and various rare inherited syndromes such as retinoblastoma and multiple exostoses [2].

Osteosarcoma is a mesenchymal neoplasm characterized by locally aggressive growth and early metastatic potential as a result of morphologically abnormal osteoblastic cells producing defective immature bone (osteoid). An alarming high proportion of 20-25 % of patients presents with clinically detectable distant metastases at the time of diagnosis. The rest has a 50-60 % risk of developing metastases and often microscopic subclinical metastases are detected at first presentation. Effective treatment options are very limited for osteosarcomas that have metastasized [3, 4]. The presence of metastatic disease is the worst prognostic factor in both univariate and multivariate analyses; fewer than 20 % of

these patients have a disease-free survival at five years [5, 6]. Furthermore, loss of differentiation occurs in more than 80 % of osteosarcoma, correlates with higher grade and confers a 10 % to 15 % decrease in survival.

The current standard treatment for osteosarcoma uses a multi-modal treatment approach consisting of preoperative neo-adjuvant systemic polychemotherapy, local surgical resection to safely remove the tumor yet preserve as much extremity as possible, followed by post-operative adjuvant chemotherapy. Chemotherapeutic agents aimed at eradicating clinically detectable metastases in osteosarcoma include doxorubicin, cisplatin, high-dose methotraxate and ifosfamide, which are generally given in combination over six to 12 months. With this standard multi-modal regimen, the five-year relapse-free survival rates of patients with non-metastatic osteosarcoma remains low at approximately 60-70 % while the survival rate for patients with distance metastasis is less than 20 % [1]. Further, exploitation of the most commonly used chemotherapeutic agents against osteosarcoma has been hampered by severe and life-threatening side effects including antracyclin-induced cardiomyopathy, glomerular dysfunction and secondary cancers such as treatment-related leukemia particularly after high-dose cisplatin, hemorrhagic cystitis caused by ifosamide as well as renal dysfunction with methotrexate. At present, there is no standard chemotherapy treatment regimen for osteosarcoma which relapses following multi-modal first-line treatment [7, 8]. Despite significant clinical improvements through the use of combination intensive chemotherapy and surgical resection over the past few decades, prognosis for osteosarcoma patients with pulmonary metastasis is still unsatisfactory. Respiratory failures due to lung

metastases are very common events and the major cause of death in these patients [5, 9]. Moreover, effective therapeutic options available for patients who either relapse following administration of currently approved chemotherapeutic agents or suffer intolerable acute and long term toxicities from chemotherapy treatments are seriously lacking. Therefore, more effective treatment strategies are urgently needed to prevent or reduce osteosarcoma disease progression and improve patient survival rates.

1.2 Molecular mechanisms involved in osteosarcoma tumor progression and metastasis

Identifying molecular signaling mechanisms involved in osteosarcoma tumorigenesis and metastasis may be the key to designing novel, safe and effective treatment therapies against this malignant phenotype. While the precise molecular mechanisms that regulate osteosarcoma disease progression and metastasis are poorly understood, numerous reports on the involvement of multiple interacting and cross talked molecular signaling pathways associated with Cyclooxygenase-2 (COX-2), Nuclear Factor Kappa-light-chain-enhancer of activated B cells (NF-κB) and several receptor tyrosine kinase signaling have expanded our understanding of the pathogenesis of osteosarcoma. For instance, both *in vivo* and *in vitro* studies showed that treatments with COX-2 inhibitors abrogated enhanced cell invasiveness and motility in osteosarcoma over-expressing COX-2 [10, 11]. NF-κB signaling is implicated in osteosarcoma metastasis as demonstrated by Harimaya et al. who found that forced expression of NF-κB decoy attenuated Tumor Necrosis Factor-α (TNF-α)-induced motility and invasiveness of osteosarcoma cell lines [12]. Flex et al. later reported that ET-1 and its receptors were

over-expressed in osteosarcoma cells, and the inhibition of ET receptors effectively suppressed both basal and ET-1-induced osteosarcoma cell invasion through a NF-κB-dependent mechanism [13]. Moreover, using microarray analysis studies, osteosarcoma cultured cell lines and tissues samples were found to over-express multiple cell-signaling related genes, ligands, receptors and downstream signaling molecules of the receptor tyrosine kinase family, and their over-expressions were closely associated with high potential for metastasis and bad prognosis. Examples include the Vascular Endothelial Growth Factor (VEGF) [14], Insulin-like Growth Factor (IGF) [15], Endothelial Growth Factor (EGF) [16], Signal Transducer and Activator of Transcription 3 (STAT3) [17, 18], Mitogen-Activated Protein Kinase (MAPK) [19], Mammalian Target of Rapamycin (mTOR) [20], Orphan receptor tyrosine kinase (ROR2) [21, 22] and Minibrain-Related Kinase (MIRK) [23].

Many other genes in a myriad of tumorigenic pathways are continuously being identified in microarray profiling studies in the examination of causal biomolecular processes and novel pathways associated with osteosarcoma pathogenesis. Examples include genes that regulate growth and cell cycle progression (cyclins and cyclin dependent kinases), apoptosis (Fas, MAPKKK5), invasion and motility (AXL, chemokine receptor CXCR4, collagen VII, ezrin, galectin-3, Her-2/neu, MKK6, thrombospondin, fibronectin), angiogenesis (VEGF), DNA replication and transcription (E2F4, E2F5, Runx2) as well as chemotherapy resistance (P-gycoprotein, cytochrome P450) [24-28].

Recently, accumulating evidence has implicated the canonical Wnt/β-catenin signaling pathway in osteosarcoma tumorigenesis and metastasis. Although its role has been well studied in many other types of malignancies, there are limited reports on the contributory role of aberrant Wnt/β-catenin signaling in osteosarcoma disease progression, and even fewer reports, if any, on the application of Wnt therapeutics in osteosarcoma treatment, thus there lies the potential and scope for novel research.

1.3 Overview of Wnt/β-catenin signaling pathway and its implication in oncology

The term 'Wnt' was coined from a combination of the Drosophila segment polarity gene *Wingless*, which is involved in segment polarity during development [29] and the murine proto-oncogene *Int-1*, that is required for the development of the forebrain, midbrain, cerebellum and neural crest [30, 31]. The Wnt-dependent signaling pathway is highly conserved among *Drosophila, Dictyostelium, C. elegans, Xenopus* and mammals [32, 33]. Wnt signaling plays pivotal roles in the regulation of body axis formation, cell proliferation and organogenesis in many organisms, and are important for homeostatic self-renewal in various tissues. Given the critical and pleiotropic roles of Wnt, it is not surprising that perturbations in Wnt signaling have been implicated in a range of human diseases and cancers [34-36]. Wnt proteins are secreted glycoproteins that act on target cells by binding to Frizzled receptors (FZD) and low-density lipoprotein receptor-related protein 5/6 (LRP5/6) co-receptors. To date, a total of 19 Wnt genes and 10 different FZD family members have been identified in mammals [37, 38].

The complexity of molecular players on the cell surface is further illustrated inside the cell by the existence of at least four Wnt-dependent downstream pathways whose activation is dependent on the specificity of the Wnt ligands and FZD receptors, as well as other cellular components. These four signaling pathways include: (1) the canonical Wnt/β-catenin pathway that regulates the expression of Wnt target genes through TCF/β-catenin; (2) the planar cell polarity (PCP) pathway that establishes asymmetric cell polarities and coordinates cell shape changes and cellular movements; (3) Wnt/Ca^{2+} pathway which controls cell adhesion and motility [39]; and (4) the most recently discovered Protein kinase A pathway that plays a role in myogenesis [40]. More than 50 signaling component proteins have since been identified to transduce these Wnt signals to mediate diverse cellular responses. Among these four known Wnt pathways, the canonical Wnt/β-catenin signaling pathway is the best understood and has been identified as the main culprit in the cellular events that leads to cancer, whereas the role of the non-canonical Wnt pathway is poorly understood and difficult to address. At least six of the 19 Wnt ligands, including Wnt 1, Wnt 2, Wnt 3, Wnt 3a, Wnt 8 and Wnt 8b, have been reported to activate the canonical Wnt/β-catenin pathway while Wnt 4, Wnt 5a and Wnt 11 can activate the non-canonical Wnt signaling. As presented in Table 1-1, various Wnt/β-catenin pathway components contributing to a wide spectrum of cancer types have been identified. This list continues to be added onto, giving it many layers of complexity to the role of Wnt/β-catenin pathway in human cancer.

Table 1-1. Canonical Wnt/β-catenin signaling pathway components involved in cancer.

Pathway components	Observed alterations	Oncologic disease	Reference
Cell surface			
Wnt ligands	Increased expression	colon cancer, breast cancer, melanoma, head and neck cancer, non-small-cell lung cancer, gastric cancer, mesothelioma, osteosarcoma	[41-48]
FZD	Increased expression	colon cancer, breast cancer, head and neck cancer, gastric cancer	[43, 44, 47, 49, 50]
LRP5	Gain-of-function mutation, Increased expression	osteosarcoma, hyper-parathyroid tumors	[47, 51-53].
SFRPs	Reduced expression	osteosarcoma, non-small-cell lung cancer, mesothelioma, chronic lymphatic leukemia, gastric, breast, esophageal adenocarcinoma	[49, 54-62]
DKK3	Reduced expression	osteosarcoma	[63]
WIF-1	Reduced expression	colon cancer, breast cancer, prostate cancer, lung cancer, bladder cancer, mesothelioma, osteosarcoma	[64-69]
Within the cytoplasm			
DVL	Increased expression	mesothelioma, non-small-cell lung cancer, cervical cancer	[70-72]
β-catenin	Gain-of-function mutations Increased expression	colon cancer, osteosarcoma, Lung cancer, liver, endometrial ovarian cancer, pilomatricoma skin cancer, prostate cancer, melanoma, osteosarcoma,	[73-78].

		wilms tumor	
APC	Loss-of-function mutations/ Reduced expression	colon cancer	[79-81]
Axin 1	Loss-of-function mutations	liver cancer medulloblastomas , esophageal squamous cell carcinoma	[82-84]
Axin 2	Loss-of-function mutations	colon cancer, hepatocellular cancer	[85-87]
Tyrosine kinases, Met	Over-expressions	colorectal cancer	[88]
Tyrosine phosphatase genes	Mutations	colorectal cancer	[89]
BCL9-2	Increased expression Rearrangement of the BCL9-2 loci	colon cancer, acute myeloid leukemia, acute lymphoid leukemia, advanced colon carcinoma	[90-92]
In the nucleus			
TCF-4	Frame shift Mutation	colorectal cancer	[93]
Transcriptional co-repressors: Groucho, HDAC, HBP1	Decreased function/ expression	breast cancer, colon cancer	[94, 95]
Transcriptional co-activator proteins: CBP/p300	Increased function/ expression	colorectal cancer	[96]
Wnt target oncogenes	Increased function/ expression	breast cancer, colorectal cancer. intestinal cancer, liver cancer,	[60, 97-103]

Abbreviations: APC: Adenomatous polypopsis coli; **BCL9-2**: B-cell lymphoma 9-2**; CBP**: Camp response element binding protein **DKK**:

Dickkopf; **DVL**: Dishevelled; **FZD**: Frizzled receptor; **HBP1**: High-mobility-group-box transcription factor 1; **HDAC**: Histone deacetylase**;**

SFRP: Secreted frizzled-related protein; **LRP**: Low density lipoprotein receptor-related protein; **WIFs**: Wnt inhibitory factor-1

On the cell surface: Initiation of Wnt/β-catenin signaling cascade

Canonical Wnt/β-catenin signaling pathway is initiated when both the FZD and LRP5/6 co-receptors complex with Wnt ligands [37, 38] (Figure 1-1). However, the binding affinities of native FZD-Wnt complexes remained undetermined due to the lack of purified Wnt ligands. During development, Wnt/β-catenin signaling plays an important role in cell fate specification, tissue patterning and control of asymmetrical cell division where the expression of the Wnt genes is developmentally regulated in a coordinated temporal and spatial manner. Activation of Wnt/β-catenin signaling is also tightly regulated by four families of Wnt antagonists that can be classified into two sub-groups according to their mode of action: the Secreted Frizzled-Related Protein (SFRP) family, Wnt Inhibitory Factor-1 (WIF-1) and Cerberus act as Wnt antagonists by directly squelching Wnt ligands, thus preventing FZD-Wnt binding, while the Dickkopf (DKK) family inhibits Wnt signaling by binding to LRP and Kremen receptors, and sterically hindering Wnt interaction with LRPs [54, 104]. The formation of the LRP-DKK-Kremen ternary complexes disengages the LRP receptor from the Wnt-FZD complex, precluding signal transduction by Wnt [104, 105]. The loss of this coordinated control in Wnt/β-catenin signaling, however, subsequently drives the formation of numerous diseases including human cancers (Table 1-1).

Indeed, epigenetic silencing of genes encoding endogenous Wnt antagonists such as SFRPs [49, 54, 55, 57-62] and WIF-1 [64-69], or increased expression of pathway components including Wnt ligands [41-48], FZD [43, 44, 47, 49, 50], Dishevelled (DVL) family members [70-72] and LRP5 co-receptors [47, 53] account for the aberrant

activation of Wnt signaling observed in many human malignancies (Table 1-1). Dysregulation of modulators of the Wnt pathway such as proteases activator receptor-1 and Frat proteins which function as activators as well as Idax and Naked which inhibits Wnt signaling may also be implicated with cancer progression [106-108].

Within the cytoplasm: Stabilization of β-catenin

Stabilization of the β-catenin protein within the cytoplasm is the key to the activation of canonical Wnt/ β-catenin signaling (Figure 1-1). Upon binding of the Wnt ligand to the LRP/FZD complex, DVL is phosphorylated and through its association with Axin and Adenomatous Polyposis Coli (APC) tumor suppressor, prevents Glycogen Synthase Kinase-3β (GSK-3β) and Casein Kinase-1α (CK-1α) from phosphorylating β-catenin [109, 110]. Unphosphorylated β-catenin is stabilized by escaping recognition by the β-Transducin Repeat-Containing Protein (β-TrCP), a component of an E3 ubiquitin ligase complex, and subsequently translocates to the nucleus where it interacts with the T-Cell-specific Transcriptional Factor/Lymphoid Enhancer Binding Factor (TCF/LEF) to activate the expression of Wnt target genes [77, 111, 112]. Mutations of oncogenes and tumor suppressor genes including APC, Axin and β-catenin in Wnt signaling not only initiate events in cancer formation, but also facilitate their progression into malignant, invasive and metastatic cancers (Table 1-1). Approximately 90% of colon cancers showed aberrant Wnt signaling, usually as a result of mutation in APC (80 %) [79-81], and less frequently due to mutations in β-catenin [76, 77] or Axin [85, 86]. Mutations of the conserved serine/threonine phosphorylation sites of β-catenin block its targeted degradation by the ubiquitin proteasome pathway while the oncogenic mutations of APC
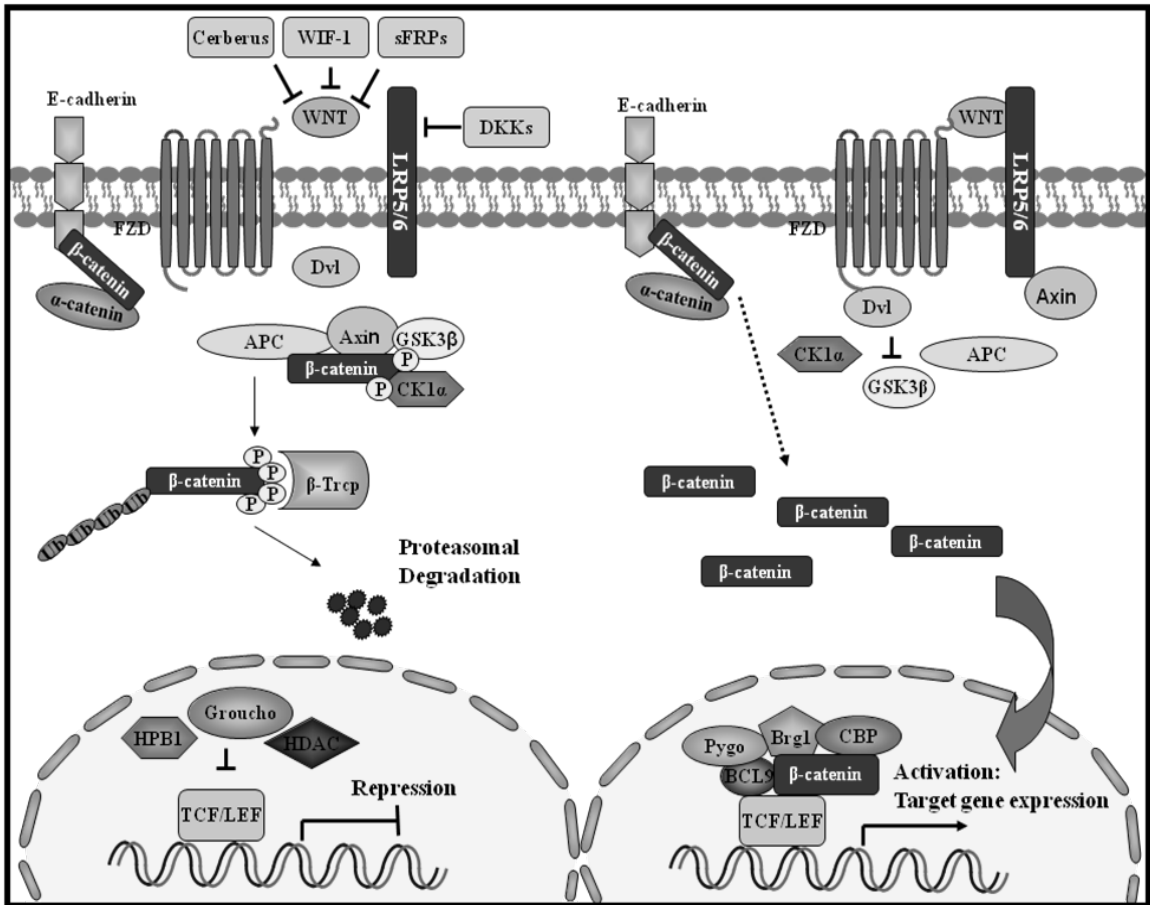
Figure 1-1. The Wnt/β-catenin signaling cascade. Left: In the absence of Wnt ligands and/or when secreted endogenous antagonists such as Cerberus, Wnt Inhibitory Factor-1 (WIF-1), Secreted Frizzled-Related Proteins (sFRPs) or Dickkopf (DKKs) are present, β-catenin levels are tightly regulated by a degradation complex comprising of Axin, Adenomatous Polyposis Coli (APC) and Glycogen Synthase Kinase-3β (GSK-3β). Transcription of TCF/LEF target genes is effectively repressed by Groucho, histone deacetylases (HDAC) and HMG-box transcription factor 1 (HBP1) transcriptional co-repressors. Right: The binding of Wnt ligands to Frizzled receptor (FZD) and low-density lipoprotein receptor-related protein 5/6 (LRP5/6) co-receptor hyperphosphorylates Dishevelled (DVL), leading to inhibition of the β-catenin degradation complex. The resultant effect is β-catenin translocation to the nucleus where it activates the transcription of target genes by directly displacing the transcriptional repressors and recruiting an array of co-activator proteins including Pygopus (Pygo), SWI/SNF chromatin-remodeling complex member (Brg1), histone acetylase CREB-binding protein (CBP) and B-Cell Lymphoma 9-2 (BCL9-2).

or Axin 1 compromises their functions as the APC-Axin-GSK3β β-catenin destruction complex. Axin 2 is an axin homologue that shows 45 % homology to Axin 1, with similar biochemical properties. Whereas Axin 1 is a constitutively expressed component of the β-catenin degradation complex, Axin 2 is up-regulated in response to increased β-catenin concentrations and functions to limit the duration and intensity of Wnt signaling. In contrast to colorectal cancers, frequent mutation of β-catenin that results in Wnt signaling dysfunction have been detected in many non-colorectal cancers such as liver cancer (hepatocellular and hepatoblastoma), endometrial ovarian cancer, pilomatricoma skin cancer, prostate cancer, melanoma and Wilms tumor [73-78]. Mutations of Axin 1 and Axin 2 were observed in some liver cancers, esophageal squamous cell carcinoma and medulloblastomas [82-84, 87] while non-colon cancers are very rarely due to loss of APC function.

Cellular re-distribution of β-catenin within the cytoplasm

In addition to its role in gene regulation, β-catenin is involved in regulating cell-cell adhesion by acting as a structural adaptor protein linking E-cadherin to the actin cytoskeleton in the plasma membrane [97, 113-117] (Figure 1-1). Both functions of β-catenin are deregulated in several cancers, thus leading to the loss of β-catenin/E-cadherin-mediated cell adhesion and a corresponding increase in β-catenin-dependent transcription. The switch between these two functions, which directly controls the shuttling of β-catenin between the plasma membrane and nucleus, is tightly regulated by several factors including the presence of E-cadherin-mediated cell adhesion, interaction of β-catenin with other proteins such as APC, as well as conformation and tyrosine

phosphorylation of β-catenin [118, 119]. Phosphorylation of tyrosine residue 654 of β-catenin by either c-scr or the epidermal growth factor receptor leads to the loss of E-cadherin binding while the tyrosine kinases Fer, Fyn or Met are capable of inducing phosphorylation of tyrosine residue 142 of β-catenin to disrupt interaction with α-catenin but promotes binding of β-catenin to the nuclear co-factor B-Cell Lymphoma 9-2 (BCL9-2) [118-123]. The β-catenin-BCL9-2 complex subsequently localizes to the nucleus and regulates the transcription of crucial target oncogenes upon interaction with the TCF/LEF DNA binding proteins [120]. Accordingly, over-expressions of tyrosine kinases and mutations in tyrosine phosphatase genes that might catalyze these phosphorylation processes have been reported in colorectal cancers [88, 89] (Table 1-1). BCL9-2 expression was found to be elevated in a series of human colon cancer samples [124]. Moreover, BCL9-2 gene is located in a region where frequent amplifications, deletions, loss of heterozygosity or gene rearrangement have been reported in several cancers including acute myeloid leukemia, acute lymphoid leukemia and advanced colon carcinoma, indicating that rearrangement of the BCL9-2 loci is involved in tumor formation and progression [90-92]. APC also plays an important role in switching the function of β-catenin between cell adhesion and Wnt signaling. APC binds directly with β-catenin, α-catenin and actin filament in the cell-cell adhesion complex linked with E-cadherin [125, 126]. As such, APC loss-of-function potentially couples loss of cell adhesion to activated Wnt signaling, in a similar manner as Y142 phosphorylation of β-catenin which shifts β-catenin from adherens junctions to the nucleus. In addition, this preferential movement of β-catenin can be influenced by distinctive conformational changes in the β-catenin. As demonstrated by Gottardi and Gumbiner, Wnt signaling

13

promotes the formation of a monomeric form of β-catenin that preferentially interacts with TCF/LEF proteins in the nucleus while another distinctive form that exists as a β-catenin-α-catenin dimer preferentially binds to E-cadherin at the plasma membrane [127].

In the nucleus: Wnt/β-catenin-mediated gene transcriptional activity

The human TCF/LEF proteins, consisting of TCF-1, LEF-1, TCF-3 and TCF-4, belong to a family of transcriptional factors that bind DNA in a sequence-specific manner through their High Mobility Group (HMG) domains, but lack the capability to activate gene transcription independently [128]. In the absence of Wnt ligands, levels of nuclear β-catenin remain low, which in turn allow the DNA binding TCF/LEF protein to interact with transcriptional co-repressors such as Groucho, Histone Deacetylases (HDAC) and HMG-Box Transcription Factor 1 (HBP1), thus blocking target gene transcription [95, 129, 130] (Figure 1-1). Although activating mutations in TCF/LEF genes are rare in human cancers, Duvel et al. has recently reported a frequent frame shift mutation in TCF-4 in human colorectal cell lines [93].

Besides regulation through the transcriptional co-repressors, nuclear APC plays a critical role in the control of nuclear β-catenin levels and activity by binding to β-catenin and inducing its nuclear export [131, 132]. Nuclear translocation of β-catenin converts the TCF/LEF protein into a potent transcriptional activator by directly displacing the transcriptional repressors and recruiting an array of co-activator proteins including histone acetylase cAMP Response Element Binding Protein (CBP/p300), SWI/SNF chromatin-remodeling complex member BRG-1, Legless/BCL9-2, Paired-Like

Homeodomain 2 (PITX2), Pygopus (Pygo), mediator and Hyrax/parafibromin (a member of the polymerase-associated factor complex) to activate transcription of at least 300-400 Wnt target genes with diverse functions [133-141]. Notorious examples of Wnt target genes include oncogenes that are involved in cancer cell proliferation (cyclin-D1, c-Myc, survivin) [97, 98, 142], adhesion (E-cadherin, neuronal cell adhesion molecule) [143], tumor metastasis (Matrix Metalloproteinases (MMPs) [99-101], keratin 1 [102], Urokinase Plasminogen Activated Receptor (uPAR) [103], CD44 [144], VEGF [145] WNT1-Induced Secreted Protein 1 (WISP-1) [146]) and cell differentiation (siamois, brachyury T gene) [147, 148]. Other Wnt responsive genes comprise of components of the Wnt pathway itself such as LRPs, Axin2, β-TrCP and TCF/LEF, suggesting an auto-regulation of Wnt signaling. The list of downstream target oncogenes will undoubtedly be expanded and it would be very useful to elucidate the relevance of these genes in human cancer.

Wnt/β-catenin signaling pathway in the disease progression of osteosarcoma

Although its role has been well studied in many other types of malignancies, the knowledge of the Wnt/β-catenin signaling in osteosarcoma is limited. Specifically, over-expression of numerous Wnt components including Wnt ligands and Frizzled receptors, as well as the epigenetic silencing of genes encoding endogenous Wnt pathway inhibitors such as SFRP3 and WIF-1, highlighted the implications of aberrant Wnt/β-catenin signaling in the development and progression of this malignant phenotype [47, 56, 65]. Elevated levels of cytoplasmic and nuclear β-catenin have also been reported in osteosarcoma tissue samples [73, 74]. In addition, the expression of the Wnt co-receptor,

LRP5, in osteosarcoma specimens correlated significantly with metastatic events [47] while Wnt10b ligand induced osteosarcoma chemotaxis and its expression correlated with reduced survival [48]. Dominant-negative LRP5 (DN-LRP5) has also been shown to inhibit both *in vitro* and *in vivo* osteosarcoma growth and metastasis by down-regulating MMPs, Twist, Slug, Snail and N-cadherin [51, 52]. Furthermore, DKK-3, an endogenous inhibitor of the pathway, inhibited the motility and invasiveness of osteosarcoma cells by affecting intracellular β-catenin [63]. Kansara et al. has also found that WIF-1 is silenced in human osteosarcoma and when deleted in mice, accelerates radiation-induced osteosarcoma formation [65]. Most recently, Rubin et al. reported that restoration of WIF-1 markedly reduced the number of lung metastasis *in vivo* in an orthopedic mouse model of osteosarcoma [149]. Given these observations, disruption of the Wnt/β-catenin signaling pathway is an attractive approach for developing effective therapies for osteosarcoma. It is thus our goal to perturb critical nodal points in the Wnt/β-catenin pathway with the aim of developing novel Wnt-targeted therapies to prevent or reduce osteosarcoma disease progression.

1.4 Strategies in inhibiting the Wnt/β-catenin signaling pathway

Overwhelming evidence implicates aberrant activation of Wnt signaling in oncogenesis and cancer progression. Given the complexity of the canonical Wnt/β-catenin signaling pathway and its tight regulation at multiple cellular levels, the pathway offers ample targeting nodal points for rationale drug development to treat cancer. Wnt therapeutic interventions can be targeted at many junctures to: (1) disrupt receptor-ligand interactions at the cell membrane; (2) stabilize APC-Axin-GSK-3β β-catenin destructive complex; (3)

enhance proteosomal degradation of cytoplasmic β-catenin; (4) interrupt β-catenin/TCF complexation and/or (5) inactivate Wnt target oncogenes transcription within the nucleus. Despite intense efforts and interest by pharmaceutical and biotechnology sectors in developing effective Wnt signaling pathway antagonists, drug development specifically targeting the aberrant Wnt/β-catenin pathway is still in its infancy, with no drugs currently in late-stage clinical trials. Nevertheless, numerous *in vitro* and *in vivo* reports on the effective use of Wnt therapeutics on cancer caused by aberrant Wnt activation are extremely encouraging and should motivate the accelerated discovery of yet more potent and novel Wnt therapeutics.

1.4.1   Existing drugs as Wnt therapeutics

A number of drugs that are either already on the market or are currently being evaluated for use in other diseases such as Non-Steriodal Anti-Inflammatory Drugs (NSAIDs) and vitamin derivatives have been reported to target Wnt signaling. NSAIDs, which are used worldwide for the treatment of pain, inflammation and fever, have recently been shown to dampen the Wnt signaling pathway in colorectal cancers and curb tumor growth *in vivo* [150]. Increasing evidence showed that the activities of the COX and Wnt signaling pathways might be inextricably linked in colon cancers and could be subject to concerted regulation in vivo by NSAIDS [151, 152]. A direct support for this was provided in study describing the substantial reduction of nuclear β-catenin levels in polyps of Familial Adenomatous Polyposis (FAP) patients treated for six months with the NSAID sulindac sulphide [150]. Furthermore, elevated COX activity in colon cancer was demonstrated to drive increase in prostaglandin levels, which might subsequently stimulate Wnt signaling

17

by interfering with the capacity of cells to degrade β-catenin [151, 152]. Thus the reduction of prostaglandin levels by inhibition of COX activity in the tumors could account for the observed ability of NSAIDS to dampen the Wnt signaling pathway and curb tumor growth. Most recently, celecoxib (a COX-2 inhibitor) was also shown to inhibit β-catenin-dependent survival of MG-63 osteosarcoma cell line [153].

Unfortunately, the clinical use of NSAIDs is limited by severe intestinal bleeding and/or kidney failure caused by COX-1 inhibitors and potential cardiovascular side effects of COX-2 inhibitors. Vitamin derivatives such as retinoids are reported to inhibit colon cancer growth *in vitro* and in animal models by reducing TCF-β-catenin complex formation [154, 155]. However, a more recent study recorded increased intestinal tumor growth in mice treated with retinoic acid and raised some doubts regarding their therapeutic potential [156].

1.4.2   Novel approaches in Wnt therapeutics

Although existing drugs in the market such as NSAIDs and vitamin derivatives seemed promising in *in vitro* and limited *in vivo* assays, their clinical potential is limited by their inability to reduce adenoma formation in approximately 50 % of treated patients and unwanted side effects. Therefore there is an urgent need to continuously develop more effective and selective Wnt inhibitors, and several of the promising approaches that are currently being explored in persuit of these inhibitors targeting Wnt-activated cancers are outlined below (Table 1-2).

Antibody-based therapeutics

Antibodies against over-expressed membrane Wnt components such as Wnt ligands and FZD proteins are particularly useful for a range of human cancers without mutations in APC, Axin or β-catenin, but instead have increased expression of more upstream pathway components. For instance, WNT1 and WNT2 monoclonal antibodies effectively suppressed Wnt signaling in several cancers over-expressing these Wnt ligands including breast [157], head and neck [44], non-small cell lung carcinoma [157], gastric [41], colon, melanoma [158], mesothelioma [157] and sarcoma [157] (Table 1-2). FZD1 and FZD2 receptors, highly expressed in breast [43] and colon cancers [159] compared to normal tissues, represent alternative targets for antibody-based therapies. Most recently, the development of antibody-based therapeutics were made even more attractive by the discovery that treatment with WNT1 antibody strongly induced apoptosis in colon cancers cell lines that over-expressed this ligand even in the presence of additional downstream mutations [61, 160]. Membrane proteins encoded by Wnt target genes are also excellent potential therapeutic targets for antibody-based therapies.

Viral-based therapeutics

The biggest advantage of viral-based therapies is their high therapeutic efficacy and selectivity. This is typically achieved by oncolytic virus which target the cancer cells by either restricting infection and replication of cell-destroying virus to the cancer cells or by selective expression of virally encoded genes that produce toxins or prodrug-converting enzymes in these cells [161] (Table 1-2). The oncolytic viral approach has been used successfully to develop adenovirus that selectively expressed the apoptotic-inducing

FADD (Fas-associated via death domain) gene or cytotoxic genes encoding diphtherin toxin A in colon cancer cell lines with hyperactive TCF/β-catenin signaling [162, 163]. Similarly, other examples that selectively target tumor cells which exhibit aberrantly high TCF/β-catenin activity include the development of replicating adenovirus that expressed tumor-selective viral E1B, E1A, E2 and E4 genes from promoters controlled by the TCF-4 transcriptional factor [164, 165]. Furthermore, several recombinant adenoviruses in combination with prodrug treatment have been shown to effectively and selectively kill cancer cells with active TCF/β-catenin activity, but spare the control normal cells. One example is the effective use of an adenovirus expressing the thymidine kinase gene under the control of a TCF-responsive promoter which selectively killed colon cancer cells with hyperactive TCF/β-catenin signaling following treatment with the prodrug ganciclovir [166]. Recent examples include selectively replicating adenovirus expressing genes encoding cytosine deaminase, which converts prodrug 5-fluorocytosine into highly

Table 1-2. Summary of current approaches to targeting Wnt/β-catenin signaling pathway for cancer therapy.

Targets	Approaches	Tumor targeted	References
Extracellular and membrane			
Wnt ligands	Antisense Monoclonal antibodies	Breast, Colon, Head and neck, NSCLS, gastric, Melanoma, Mesothelioma, soft tissue sarcoma	[41, 44, 157, 158]
FZD	Antisense Monoclonal antibodies	Breast, Colon	[43, 159]
SFRPs	sFRPs over-expression Therapeutic proteins	Breast, Cervical, Colorectal, Gastric, Mesothelioma, Liver, Lung, osteosarcoma Tetratocarcinoma,	[55, 61, 167]
WIF	sFRPs over-expression Therapeutic proteins	Breast, Bladder, Lung, Mesothelioma, Prostate, osteosarcoma	[64-69].
DKKs	wt-DKK over-expression Therapeutic proteins	Colon, Mesothelioma, NSCLC, osteosarcoma	[63, 168, 169].
Within the Cytoplasm			
APC	wt-APC over-expressions	Colon	[170]
Axin	wt-Axin over-expressions	Colon, hepatocellular carcinoma	[83]
β-catenin	Antisense oligos RNA interference Protein knockdown	Breast, Colon, NSCLS, Esophageal, squamous cell carcinoma	[171-175].
COX-2	COX-2 Inhibitors	Breast, Colon, NSCLS	[150, 176, 177]
In the Nucleus			
TCF/LEF	Retinoids Apoptotic/Suicide HSV-	Colon, NSCLS	[154, 155, 162-166, 178-181]

	TK/ganclovior Small molecule inhibitor Oncolytic virus		
CBP	Inhibition of CBP	Colon	[179]
c-MyC	Antisense oligos	Breast, Colon Liver, Prostate, Melanoma,	[182, 183]
CyclinD1	Cdk inhibitor	Breast, Colon, Glioblastoma, Leukemia, Lymphoma, Melanoma, NSCLS, Prostate, renal cell carcinoma, squamous cell carcinoma, soft tissue sarcoma, Uterine,	[184, 185]

Abbreviations: APC: Adenomatous polyposis coli; **CBP**: Camp response element binding protein; **COX-2**: Cyclooxygenase-2; **DKK**: Dickkopf; **FZD**: Frizzled receptor**; SFRP**: Secreted frizzled-related protein; **WIF**: Wnt inhibitory factor; **NSCLC**: non-small cell lung cancer; TCF/LEF: T-cell factor transcriptional factor/Lymphoid enhancer binding factor

toxic drug 5-fluorouracil [180], and *Escherichia coli* nitroreductase which activates the prodrug CB1954 [181].

Recombinant adenoviruses are also used to constitutively express Wnt components that are suppressed due to genetic mutations. For example, adenoviruses (Ad-CBR) that constitutively expressed APC induced apoptosis and growth arrest by blocking TCF-β-catenin transcriptional activity in colorectal cancer cell lines with mutant APC [170]. Similarly, adenovirus-mediated gene transfer of wild-type Axin-1 promoted apoptosis in colorectal and hepatocellular cancer cells that have aberrant Wnt activation due to Axin-1 mutation [83].

Nucleic-acid-based therapeutics (vaccines, antisense and small interfering RNA)

Antisense oligonucleotides are single stranded DNA, RNA or chimeric RNA/DNA that are designed to specifically hybridize to a target mRNA and subsequently prevent protein synthesis. As many human cancers with aberrant Wnt signaling ultimately results in increased β-catenin levels, direct targeting of this key protein using anti-sense and RNA interference (RNAi) strategies have attracted a lot of attention. Several studies using antisense oligonucleotides have demonstrated decreased β-catenin levels and inhibition of cell proliferation, adhesion, invasiveness and anchorage-dependent growth in various cancer cells and *in vivo* xenograft models [171-173] (Table 1-2). Other studies have developed and evaluated the therapeutic potential of RNAi targeting β-catenin: Van et al. created an inducible vector system expressing β-catenin small interfering RNA (siRNA) that is effective in promoting cell differentiation and G1 cell cycle arrest in colon cancer

cell lines [174]. In another study, siRNA against β-catenin suppressed *in vitro* and *in vivo* tumor growth of colon cancer [175].

Microarray analyses of TCF-dependent gene expressions in human cancer cells suggest that there are currently at least 300-400 oncogenes that regulate cancer cell proliferation, differentiation, migration, apoptosis and other processes that leads to cancer initiation and progression [186]. Given that some of these targets such as c-Myc and cyclin D1 are directly implicated in driving cancer formation, current therapeutic approaches use RNAi or small membrane-permeable antisense molecules to reduce c-Myc and cyclin D1 RNA levels [183]. AVI-4126 is an example of a c-Myc specific antisense molecule that effectively suppressed growth in various cancer xenograft murine models including breast, prostate, melanoma and liver [182].

Small molecule inhibitors

Drugs developed to disrupt TCF-β-catenin signaling activity undoubtedly have great potential as effective cancer therapeutics, given that a common feature of almost all cancers with aberrant activation of Wnt/β-catenin pathway is the constant presence of TCF-β-catenin complexes in the nuclei. Although no small-molecule inhibitors of the TCF-β-catenin has yet been identified by High Throughput Screening (HTS) of large synthetic compound libraries, three natural occurring compounds (PKF115-584, PKF222-815 and CPG049090) from a HTS of natural compounds consistently scored as effective antagonists of TCF-β-catenin complexation by binding to either TCF or β-catenin [178] (Table 1-2). Other opportunities for blocking TCF-β-catenin function in cancer cells

include development of small molecule inhibitors that prevent interaction of β-catenin with crucial transcriptional co-activator proteins such as CBP and BCL-9/pygopus. For instance, ICG-001 was found to inhibit growth of colon cancer cell lines and xenografts mouse models by selectively binding CBP, thus preventing interaction with β-catenin [179]. Small molecule inhibitor of the interaction between BCL-9 and β-catenin has also been developed. Low-molecular weight compounds that target other transcriptional co-activators such as BRG-1, Pygopus, Hyrax and components of the Mediator complex are also under scrutiny for potential therapeutic applications [187].

In addition, the increasing availability of detailed crystal structures of various components of the Wnt pathways down the whole signaling cascade, ranging from β-catenin, Axin, APC, DVL and their complexes should allow future design and testing of small molecule compounds that interfere with their activity [125, 188-191]. To this end, Shan et al. has recently developed a small molecule, NSC668036, which binds to DVL and blocks its interaction with FZD; NSC668036 is of great therapeutic value to prevent or minimize signaling relay and amplifications [192].

Natural products are traditionally excellent sources of lead compounds in the drug discovery and development process, and are gaining prominence as effective antagonists of the Wnt/β-catenin signaling pathway. Indeed, a wide variety of natural compounds ranging from phytochemicals, microorganisms, fungi, slime molds to bacteria have been identified as potent Wnt inhibitors and makes promising candidate drugs for development.

In fact, we have recently written a review entitled 'Natural compounds as antagonists of canonical Wnt/β-Catenin Signaling' published in *Current Chemical Biology* (2010). In this review, we provided a comprehensive summary on the current use of natural compounds as Wnt therapeutics and the development of more efficacious analogues using these compounds as lead structures. Increasing evidence of natural products as rich and diverse sources for lead compounds would inspire more concerted efforts to harness this largely untapped 'reservoir' for 'drug-like' molecules and accelerated their development as effective Wnt therapeutics. To this end, , we have examined the role and mechanism of actions of small molecule drugs derived from natural sources as Wnt/β-catenin inhibitors in regulating osteosarcoma cell proliferation, motility and invasion in this thesis.

Therapeutic proteins

Therapeutic proteins of endogenous Wnt antagonists such as SFRPs, WIF-1 and DKK have great therapeutic potential for the treatment of human oncology as a result of epigenetic inactivation of these secreted negative regulators. Significant transcriptional down-regulation of SFRPs gene family via hypermethylation has been observed in many human malignancies including breast, lung, cervical, liver, gastric, colorectal and osteosarcoma, just to name a few [55] (Table 1-2). Restoration of SFRP functions in these tumor types have shown to effectively attenuate Wnt signaling even in the presence of downstream mutation [61], highlighting the great potential of using SFRPs as a therapeutic strategy against cancers with elevated Wnt signaling.

Indeed, sFRPS therapeutic proteins, which functions as Wnt antagonist are currently been developed and evaluated in preclinical tumor models [167]. It is also one of our research objectives to examine the functional roles and mechanisms of SFRPs as tumor suppressors in regulating osteosarcoma cell proliferation, motility and invasion. Several recent studies have explored the anti-cancer potential of WIF-1 proteins, another group of antagonist which blocks Wnt signaling in a similar manner as SFRPs by directly squelching Wnt ligands, thus preventing FZD-Wnt binding. WIF-1 is down-regulated in prostate, mesothelioma, breast, lung, and bladder cancer, as well as osteosarcoma, and restoration of WIF-1 expression would in a similar manner prevent or reduce tumorigenesis and metastasis in these cancers [64-69]. DKK-3 is the third class of natural Wnt antagonist which has been reported to be down-regulated in many immortalized and tumor derived cell lines. However, forced expression of DKK-3 significantly inhibited cell growth and invasion in non-small cell lung cancer and osteosarcoma cells respectively [63, 168, 169]. Accordingly, exogenous proteins of these Wnt antagonists that are down-regulated in numerous cancers hold great promise as therapeutic agents for the treatment of the respective cancers.

CHAPTER 2.   Hypothesis and Aims

Evidence that implicates aberrant activation of the canonical Wnt/β-catenin signaling pathway in osteosarcoma has only recently emerged. There are very limited, if any, reports on the use of Wnt therapeutics in the treatment of osteosarcoma and there lies the potential and scope for novel research. The overall goal of this study is thus to perturb critical nodal points in the Wnt/β-catenin signaling pathway both pharmacologically and genetically with the aim of developing novel Wnt-targeted therapies to prevent or reduce osteosarcoma progression and metastasis, thereby improving the clinical outcomes of this disease.

We hypothesized that osteosarcoma progression may be delayed by disrupting the Wnt/β-catenin signaling pathway either by using small molecule inhibitors or by manipulating the levels of the endogenous antagonists, SFRPs. Our hypothesis was based on several observations: Firstly, numerous Wnt signaling components including Wnt ligands and Frizzled receptors were found to be over-expressed in osteosarcoma [47, 56, 65], while many genes encoding endogenous Wnt antagonists such as SFRP3 and WIF-1 were epigenetically silenced [47, 56, 65]. Secondly, accumulation of cytoplasmic and nuclear β-catenin was commonly observed in osteosarcoma and nuclear translocation of β-catenin protein correlated with osteosarcoma metastasis [73, 74]. Others have also reported that high expression of the Wnt co-receptor, LRP5, in osteosarcoma specimens associated with decreased patient survival [47] while increased expression of Wnt10b ligand correlated with reduced survival and induced osteosarcoma chemotaxis [48]. On

the other hand, blocking Wnt signaling using DN-LRP5 and DKK3 resulted in inhibitions of both osteosarcoma growth and metastasis through down-regulating Wnt-responsive oncogenes including MMPs, Twist, Slug, Snail and N-cadherin [51, 52], Lastly, Kansara et al reported that WIF-1 was silenced in human osteosarcoma and when deleted in mice, accelerated radiation-induced osteosarcoma formation [65]. These studies were later supported by Rubin et al. who showed that restoration of WIF-1 markedly reduced the number of lung metastasis in an orthopedic mouse model of osteosarcoma [149]. Given these observations, disruption of the Wnt/β-catenin signaling pathway is an attractive approach for developing effective therapies for osteosarcoma.

To test our hypothesis, we explored three specific aims:

(1) Assess the role and mechanism of actions of small molecules Wnt/β-catenin inhibitors in regulating osteosarcoma cell proliferation, motility and invasion.

(2) Synthesize and evaluate a set of lead compounds with improved potency and selectivity as Wnt/β-catenin antagonists; identify critical structural motifs for Wnt inhibitory activity; and examine the underlying mechanism of Wnt inhibition of selected curcumin analogue.

(3) Examine the functional roles and mechanisms of SFRPs as tumor suppressors in regulating osteosarcoma cell proliferation, motility and invasion.

Work done to address these specific aims was included in the following chapters: In Chapter 3, we provided important *in vitro* proof-of-concept for the potential use of small molecule Wnt/β-catenin inhibitors to delay osteosarcoma progression and metastasis

(Aim 1). In Chapter 4, we evaluated and identified curcumin analogues with enhanced Wnt inhibitory potency and reported critical structural motifs for Wnt inhibitory activity using structure-activity–relationship analysis (Aim 2). In Chapter 5, we reported the role of SFRPs as tumor suppressors in delaying osteosarcoma disease progression (Aim 3). Lastly, the thesis is concluded with a summary and perspectives on the subject matter (Chapter 6).

Achieving the above aims not only provided deeper insights into the contributory role of aberrant canonical Wnt/β-catenin signaling in osteosarcoma disease progression and metastasis, but a greater understanding of the role and functions of small molecule Wnt antagonists and SFRPs in osteosarcoma. These knowledge maybe useful for the subsequent discovery and development of novel molecular Wnt-targeted therapy for the treatment of osteosarcoma.

CHAPTER 3.   Antitumor activity of natural small molecule compounds as Wnt/β-catenin antagonists against human osteosarcoma cells

3.1 Introduction

Aberrant activation of the canonical Wnt/β-catenin signaling pathway has been implicated in tumorigenesis and cancer progression in many human malignancies [47, 48, 51, 52, 63, 193]. Small molecule inhibitors of Wnt/β-catenin signaling pathway clearly hold great promise as an effective therapeutic strategy for the delay of disease progression in these malignancies. While intense efforts from screening diverse natural compound libraries made in this quest for effective Wnt antagonists has led to the discovery of numerous effective candidates, drug development in this area is still in its infancy, with no drugs currently in late-stage clinical trials. Particularly, evidence of deregulated Wnt/β-catenin signaling in osteosarcoma has only recently emerged; there are thus limited, if any, reports on the use of such small molecule inhibitors derived from natural sources in delaying osteosarcoma disease progression and there lies the potential and a great scope for novel research.

Our first aim of this thesis is to assess the role and mechanism of actions of small molecule Wnt/β-catenin inhibitors in regulating osteosarcoma cell proliferation, motility and invasion. The goal of this part of the dissertation is to provide important *in vitro* proof-of-concept for the potential use of small molecule Wnt/β-catenin inhibitors to delay osteosarcoma progression and metastasis. Lead compounds identified with potent Wnt

inhibitory activities may then be modified by medicinal chemistry to increase the potency and selectivity.

Our data demonstrated that curcumin significantly inhibited Wnt/β-catenin signaling and reversed Wnt/β-catenin-induced cell invasiveness and MMP-9 expression in U2OS cells. Furthermore, another natural compound, PKF118-310, inhibited osteosarcoma cell invasion, migration and proliferation, as well as induced apoptosis and G2/M phase cell cycle arrest, through down-regulating Wnt target genes including MMP-9, cyclin D1, c-Myc and survivin. Our results strongly suggest that curcumin and PKF118-310 may be promising candidate drugs for development, given the limited chemotherapeutic options available for the treatment and prevention of osteosarcoma. Building on these promising results, we then developed analogues with increased potency and selectivity using curcumin as our lead compound in our second aim detailed in the next chapter.

3.2 Experimental Methods

3.2.1   Cell culture, transfections and plasmids

The human osteosarcoma cell lines U2OS, SaOS-2 and HOS were purchased from American Tissue Culture Collection (Rockville, MD) while CRL11226, CRL1423, OS1, OS2 and OS3 have been described previously [194] and were kindly provided by Dr Saminathan S. Nathan (Department of Orthopaedic Surgery, Yong Loo Lin School of Medicine, National University of Singapore). All cell culture reagents were purchased form Sigma Chemical Co. (St Louis, MO) unless otherwise stated. U2OS, SaOS-2 and CRL1423 cells were cultured in McCoy's 5A medium, while HOS, CRL11226, OS1-3

cells were maintained in DMEM, RPMI and RPMI: DMEM 9:1 medium respectively. All media were supplemented with 10-15 % fetal bovine serum (FBS) (Invitrogen, Carlsbad, CA), 10U/ml penicillin G and 100μg/ml streptomycin. The cells were cultured in a humidified atmosphere at 37 ºC containing 5 % CO_2. TOPglow and FOPglow reporters used in the luciferase reporter gene assays were purchased from Upstate Biotechnology (Lake Placid, NY). The pSV-β-galactosidase control vector and pcDNA3.1 empty plasmids were purchased from Promega (Madison, WI) and Invitrogen (Carlsbad, CA) respectively. The plasmids for wild-type (pcDNA β-catenin) and mutant S33Y β-catenin (pcDNA S33Y) were kindly provided by Dr Georges Rawadi (Galapagos SASU, Romainville, France) and have been described previously [76]. PKF118-310 (Asinex, Winston-Salem, NC), curcumin (Sigma Chemical Co., St Louis, MO), quercetin (Sigma Chemical Co., St Louis, MO), artemisinin (Sigma Chemical Co., St Louis, MO), artesunate (Sigma Chemical Co., St Louis, MO), LiCl (Sigma Chemical Co., St Louis, MO), BIO (Merck, Darmstadt, Germany) and SB216763 (Sigma Chemical Co., St Louis, MO) were dissolved in Dimethyl Sulfoxide (DMSO) before use. The final concentration of DMSO did not exceed 0.1 % in all instances.

3.2.2 Cell proliferation assay

The effects of test compounds on the proliferation of U2OS, SaOS-2 and HOS cells were examined using 3-(4, 5 dimethyl-thiazol-2-yl)-2, 5-diphenyltetrazolium bromide (MTT) assays. U2OS, SaOS-2 and HOS cells were seeded into 96-well plates at a density of 9 x 10^3 cells/well, 10 x 10^3 cells/well and 5.5 x 10^3 cells/well respectively and cultured for 24 h. Cells were then treated with the respective compounds at various concentrations or

DMSO (vehicle control) for 72 h. For time-response assays, U2OS cells were treated in the same manner for 24 h and 48 h. After treatment, cell growth was analyzed by adding 100 µl of 1 mg/ml MTT (Sigma Chemical Co., St Louis, MO). Following an incubation period of 4 h, DMSO was added to lyse the cells and dissolve the purple formazan crystals. The absorbance of the formazan product was determined at λmax of 595 nm using a Tecan Spectra Fluor spectrophotometer (MTX Lab Systems Inc., Vienna, VA). The IC_{50} values were obtained from the sigmoidal curve by plotting the percentage survival of cells against the concentration of curcumin or PKF118-310 using GraphPad Prism version 4.0 for Windows, GraphPad Software (San Diego, CA).

3.2.3   Luciferase reporter gene assay

U2OS cells (1.0 x 10^5/well) grown to 90–95% confluency in 24-well plates were transiently co-transfected with either 0.3µg TOPglow, a luciferase reporter construct containing four TCF consensus binding sites upstream of the firefly luciferase cDNA, or 0.3 µg FOPglow, a negative control plasmid with mutated TCF binding sites, and 0.1 µg pSV-β-galactosidase plasmids using Lipofectamine 2000 (Invitrogen, Carlsbad, CA), according to the manufacturer's instructions. For the extrinsic activation of the canonical Wnt/β-catenin signaling pathway, U2OS cells were co-transfected with one other gene, the wild-type (pcDNA β-catenin) or mutant S33Y β-catenin gene (pcDNA S33Y). The amount of DNA in each transfection was kept constant by the addition of an appropriate amount of the empty expression vector (pcDNA3.1). Five to twenty hours post-transfection, cells were treated with compounds at various concentrations for 24 h before cell lysis and harvesting. Similarly, to activate Wnt/β-catenin signaling using small

molecule GSK-3β inhibitors, U2OS cells were incubated with 5 μM BIO or 50 μM SB216763 with various concentrations of curcumin or PKF118-310 for 24 h before cells were lysed using the Reporter Lysis Buffer (Promega, Madison, WI). Luciferase assays were performed with the Luciferase assay systems kit (Promega, Madison, WI) according to the manufacturer's instructions. Cell lysates (20 µl) were incubated with 50 µl of β-galactosidase assay buffer (Promega, Madison, WI) at 37 ºC for 40 mins and absorbance at λmax of 420 nm was measured in a Tecan Spectra Fluor spectrophotometer (MTX Lab Systems Inc., Vienna, VA) to determine β-galactosidase activity. For luciferase activity, 20 µl cell lysate was mixed with luciferin (100 µl) and the light output was determined in a luminometer (Tecan, MTX Lab Systems Inc., Vienna, VA). Results were expressed as mean ± Standard Error Mean (SEM) of normalized ratios of luciferase and β-galactosidase activities for each triplicate sets. Reporter activities in compound-treated cells were expressed as the percentage of DMSO-treated samples.

3.2.4 Cell migration and invasion assays

U2OS cell migration and invasion were determined using the wound healing and Matrigel invasion assays as previously described [195]. Briefly, for wound healing assays, equal number of U2OS cells (5.0 x 10^5/well) were seeded and grown overnight to 90–95 % confluence in 6-well plates before wounds of similar size were introduced into the monolayer by a sterile pipette tip. The monolayers were rinsed with Phosphate Buffer Saline (PBS) to remove detached cells and then cultured in medium containing various concentrations of compounds. The speed of wound closure was documented 12 h and 24 h post-wounding using the Nikon Eclipse TE2000U microscope (Melville, NY). Cell

invasion assays, on the other hand, were performed using 8 µm pore size polyethylene terephthalate membrane inserts (BD Bioscience, San Jose, CA) precoated with 30 µg Matrigel (an extracellular matrix gel from Engelbreth Holm-Swarm mouse sarcoma) (BD Bioscience, San Jose, CA). Briefly, cells that were untransfected or transfected with the respective control vector or β-catenin plasmids were treated with compounds at various concentrations for 24 h. Next, viable cells (1.5×10^5/ 200 µl, confirmed by trypan blue exclusion) were seeded in serum-free medium onto the upper wells of the precoated membrane inserts, while McCoy's 5A medium supplemented with 15 % FBS was added in the lower compartment as a chemoattractant. Control wells contained serum-free medium in the lower chamber instead. Cells were allowed to invade through the precoated inserts for a period of 48 h, after which non-invasive cells were removed from the upper membrane using a cotton swab. Cells that have invaded to the lower surface of the membrane were then fixed with 70 % ethanol and stained with 0.2 % w/v crystal violet before they were counted using the Nikon Eclipse TE2000U microscope (Melville, NY). Invaded cells from ten random microscopic fields (200 x magnifications) were enumerated and all experiments were performed in triplicates at least.

3.2.5   Western blot analysis

Western blotting was used to examine the protein expression levels of β-catenin, active β-catenin, MMP-9, cyclin D1, c-Myc and survivin before and after 24 h treatment of curcumin or PKF118-310. The primary antibodies for β-catenin, MMP-9, cyclin D1, c-Myc and survivin were purchased from Santa Cruz Biotechnology, Inc. (Santa Cruz, CA), while those for active β-catenin, α-Tubulin and lamin A/C were obtained from Upstate

Biotechnology (Lake Placid, NY), Sigma Chemical Co. (St Louis, MO) and BD Bioscience (San Jose, CA) respectively. Anti-mouse (BioRad, Hercules, CA) and anti-rabbit (Santa Cruz, CA) IgG horseradish peroxidase were used as the secondary antibodies. Cells were harvested and lysed in lysis buffer containing 1 % Triton with protease inhibitor (Roche, Mannheim, Germany). The protein concentration of the soluble extracts was determined by Bradford protein assay (Sigma Chemical Co., St Louis, MO). For the collection of proteins from the cytosolic and nuclear fractions, the NE-PER cytoplasmic and nuclear protein extraction kit (Pierce, Rockford, IL) was used according to the manufacturers' protocol. Proteins (10-50 µg) were separated by electrophoresis on 8-10 % SDS-polyacrylamide gels and blotted onto nitrocellulose membranes (BioRad, Hercules, CA). Membranes were then blocked overnight at room temperature in Tris-buffered saline containing 0.1 % (v/v) Tween 20 and 5 % (w/v) fat-free dry milk and then incubated with the respective primary antibodies, followed by the secondary antibody according to the manufacturer's directions. After incubation with the antibodies, membranes were washed and incubated with the West Femto or West Pico luminal/enhancer solution (Pierce, Rockford, IL) and stable peroxide solution (Pierce, Rockford, IL) before being exposed to an X-ray film (ThermoFisher Scientific, Waltham, MA). Bands were quantified using Quantity One software (BioRad, Hercules, CA), normalized to either α-tubulin or lamin A/C loading controls, before bands in treatment group are expressed relative to DMSO control (set as 100%).

3.2.6 Gelatin zymography

The effects of curcumin and PKF118-310 on the gelatinolytic activity of MMP-9 were examined by gelatin zymography as detailed previously [195, 196]. U2OS cells that were untransfected or transfected with the respective control vector or β-catenin plasmids were treated with the indicated concentrations of curcumin or DMSO for 72 h in serum-free medium. U2OS cells were treated with PKF118-310 in a similar manner for 24 h. After treatment, serum-free conditioned media were harvested and centrifuged at 170 g to remove cellular debris. The supernatant was then concentrated using Amicon Ultra-4 centrifuge filter devices (Millipore, Billerica, MA) and stored at -80 °C until use. Protein content in the supernatant was quantified using the Bradford protein assay (Sigma Chemical Co., St Louis, MO). An equal amount of protein (25 µg) from each treatment was diluted with the loading buffer (4x) and applied to a 7.5 % sodium dodecyl sulfate (SDS)-polyacrylamide gel co-polymerized with 0.2% gelatin A (Sigma Chemical Co., St Louis, MO). After electrophoresis, the gels were stained with 0.1 % Coomassie brilliant blue (BioRad, Hercules, CA) and destained with 45 % methanol, 10 % (v/v) acetic acid until clear bands suggestive of gelatin digestion were present. Bands were quantified using Quantity One software (BioRad, Hercules, CA).

3.2.7   Apoptosis assay

The effect of PKF118-310 on U2OS cell apoptosis was assessed using an annexin-V-fluorescein/ Propidium Iodide (PI) apoptosis assay kit (Invitrogen, Carlsbad, CA) accordingly to the manufacturers' protocol. Briefly, U2OS cells (0.2×10^6 cells/well) were seeded into 6-well plates and allowed to adhere overnight. On the following day, cells were treated with PKF118-310 at various concentrations or DMSO for 24 h, after

which the cells were washed with 1x PBS and trypsinized. U2OS cells were then incubated for 15 mins at room temperature in 1x annexin-binding buffer (100 μl) containing annexin-V and PI. After incubation, 400μl 1x annexin-binding buffer was added and the stained cells were analyzed using a CyAn ADP flow cytometer (Beckman Coulter, Inc. Fullerton, CA).

3.2.8 Cell cycle analysis

The effect of PKF118-310 on the cell cycle distribution was assessed by flow cytometry after staining the cells with PI as described earlier [195]. U2OS cells (1.5×10^5 cells/well) were seeded and cultured for 24 h. Cells were then treated with PKF118-310 at various concentrations or DMSO (vehicle control). Following treatment for 24 and 48 h, both floating and adherent cells were collected and washed with 1x PBS. After which, the cells were resuspended in cold 1x PBS to obtain a single-cell suspension and added drop wise into ice cold ethanol while vortexing. Cells were then incubated overnight at -20˚ C. The following day, cells were washed with cold 1x PBS, resuspended in fluorescence-activated cell sorting solution (PI/Triton X-100, with RNase A, 1 ml) and incubated in the dark for 30 mins at room temperature. Samples were then analyzed using a CyAn ADP flow cytometer (Beckman Coulter, Inc. Fullerton, CA).

3.2.9 Statistical analysis

Statistical significance for treatment groups were analyzed using the two-tailed Student's t-test (SPSS, Chicago, IL). The difference between values for each treatment

concentration and the respective controls was considered to be statistically significant when $P < 0.05$.

3.3 Results

3.3.1 Evaluation of canonical Wnt/β-catenin signaling activity in osteosarcoma cells

To investigate Wnt/β-catenin signaling status in osteosarcoma, we first evaluated the endogenous expression of β-catenin protein in a panel of osteosarcoma cell lines from various origins, given that the stabilization and nuclear accumulation of β-catenin protein is a hallmark of canonical Wnt/β-catenin signaling. Several of the cells lines including SaOS-2, U2OS, HOS, CRL11226 and CRL1423 were derived from Caucasian patients while OS1, OS2 and OS3 originated from the pre-chemotherapeutic tumor in either the femur or proximal humerus of three different Chinese patients [194]. Western blot analysis using an anti-β-catenin antibody revealed high expression of endogenous β-catenin in all of the osteosarcoma cell lines tested, except CRL1423 cell line (Figure 3-1). Since β-catenin activation is the hallmark of Wnt signaling, we also investigated the protein expression of the active form of β-catenin, which is dephosphorylated on Ser37 and Thr41. Active β-catenin expression was detected in five of the eight osteosarcoma cell lines, although the levels of protein expression varied considerably among these cell lines (Figure 3-1). Our findings are consistent with previous studies, which demonstrated significant accumulation of β-catenin protein in osteosarcoma patients' specimens [73, 74]. Together with previous studies, our results confirmed the frequent activation of

Wnt/β-catenin signaling in most of the osteosarcoma cell lines tested, although the apparent degree of activation varied.
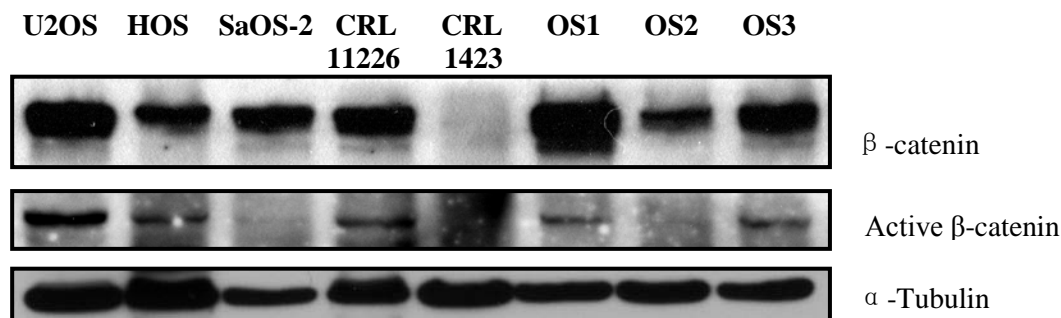
Figure 3-1. Evaluation of canonical Wnt signaling in osteosarcoma cell lines. Western blot analysis of β-catenin in eight OS cell lines using anti-β-catenin and anti-active- β-catenin antibodies. α-Tubulin was used as a loading control. The blots shown were representatives of three independent experiments.

3.3.2   Wnt/β-catenin inhibitors selected for our study

Numerous studies on small molecule inhibitors of the Wnt/β-catenin pathway and their inhibitory mechanisms have been reported [197]. To date, no small molecule antagonists have been identified from large synthetic compound libraries, although several natural compounds ranging from plant-derived polyphenols, anti-malaria artemisinins, marine organisms to microorganisms as well as a number of exciting drugs such as NSAIDS and vitamin derivatives have scored as potent Wnt antagonists in both *in vitro* and *in vivo* studies (316). We have conducted a detailed literature review and selected five natural-occurring small molecule compounds to perform initial screening for Wnt inhibitory activity, based on their commercial availability. These inhibitors are curcumin, quercetin, PKF118-310, arteminsinin and artesunate. The chemical structures of these compounds are shown in Figure 3-2. It is important to note that all these compounds except

41

artemisinin have been shown to disrupt the Wnt/β-catenin pathway in various cancer cell lines [198-201], but none has been tested in the context of osteosarcoma.

Curcumin, a dietary pigment found in the spice turmeric, has been shown to be anti-proliferative, anti-invasive and anti-angiogenic in multiple myeloma, prostate, colorectal, pancreatic, lung and breast cancer cell lines [202, 203] while quercetin, a major member of the flavonol subclass of dietary flavonoids, has been found to display both anti-oxidant and anti-tumor activities in colon carcinoma [204-206]. PKF118-310, on the other hand, is a natural compound of microbial origin and has been selected through the screening of libraries of natural compounds for small molecule inhibitors of the TCF/β-catenin protein complex [178]. Initial studies with these three compounds showed that they disrupted the Wnt/ß-catenin pathway by decreasing nuclear β-catenin levels, resulting in a reduced association of β-catenin with TCF-4, which in turn gave rise to reduced binding of the complexes to DNA response elements in target genes [178, 200, 201]. Curcumin was also reported to disrupt Wnt/ß-catenin signaling at various intersections of the pathway such as inducing caspase-3-mediated cleavage and degradation of ß-catenin, inhibiting the phosphorylation of GSK-3β and suppressing the transcriptional co-activator, p300 [96, 193, 207, 208]. Artemisinin and its derivative, artesunate (a prodrug of artemisinin) are anti-malarial drugs with *in vitro* and *in vivo* anticancer activities [209, 210]. Li et al. has recently shown that artesunate disrupted the Wnt/β-catenin pathway via membranous translocation of β-catenin and down-regulation of Wnt targeted genes such as c-myc and survivin in human colorectal carcinoma [211]. Based on this observation, we have also

included artemisinin (the active metabolite of artesunate) in our preliminary screening for Wnt antagonists.
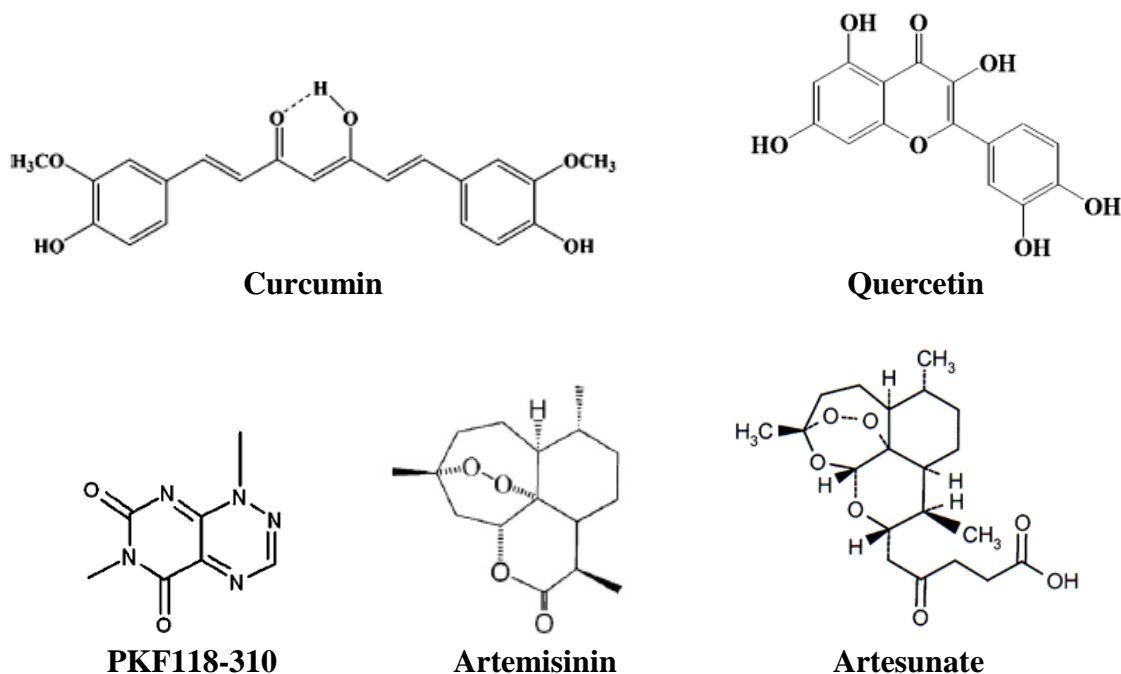
Figure 3-2 Chemical structures of Wnt/β-catenin modulators used in our study

3.3.3 Cytotoxicity of Wnt/β-catenin modulators on osteosarcoma cells

It is necessary to profile the cytotoxic effect of our compounds in osteosarcoma cells to eliminate compounds that either promote survival or are too toxic. Since high levels of endogenous Wnt antagonist, DKK-1, have been reported to allow tumor cells to re-enter the cell cycle by inhibiting the canonical Wnt/β-catenin pathway and promote osteosarcoma cell survival [212], our selected compounds may act similarly. On the other hand, disruption of the pathway could instead have a cytostatic effect on osteosarcoma cell growth, given that Wnt/β-catenin affects the transcriptional regulation of genes associated with proliferation of tumor cells. Lastly, it may also be possible that these

compounds are toxic to osteosarcoma cells by some other non-selective and non-specific mechanism. The expression levels of Wnt signaling components including Wnt ligands, FZD and LRP5 in various human osteosarcoma cell lines have previously been reported [47] and using this information, we have chosen three heterogeneous representative osteosarcoma cell lines namely U2OS, HOS and SaOS-2 for our experiments.

Accordingly, MTT cell proliferation assays were first performed on these three representative human osteosarcoma cell lines to profile the cytotoxicity effects of the compounds. All compounds inhibited growth of the osteosarcoma cells *in vitro* in a concentration-dependent manner (Figure 3-3), with the IC_{50} values at 72 h presented in Table 3-1. Comparison of the IC_{50} values showed that these osteosarcoma cell lines have relatively similar sensitivity to curcumin and artemisinin while PKF118-310 and quercetin had the most potent anti-proliferation effects against U2OS cells. Among the three cell lines, U2OS has been previously reported to be highly invasive [213] and was found to express the highest levels of β-catenin protein (Figure 3-1). It was thus used in subsequent studies to investigate various anti-cancer effects of the Wnt/β-catenin modulators. To determine an optimum (i.e. effective yet non-toxic) dose range for anti-invasion and anti-migration studies, time-response cytotoxic assays were next performed. Figure 3-4 shows that treatment of U2OS cells with curcumin beyond 20 μM at 24 h, 48 h and 72 h resulted in statistically significant toxicities and hence the maximum concentration employed in these studies was limited at 20 μM. The maximum concentration used for artemisinin and PKF118-310 was limited at 400 μM and 0.15 μM

respectively for similar reasons (Figure 3-4), although higher toxic concentrations were used to further investigate the anti-proliferation and apoptotic effects of PKF118-310.
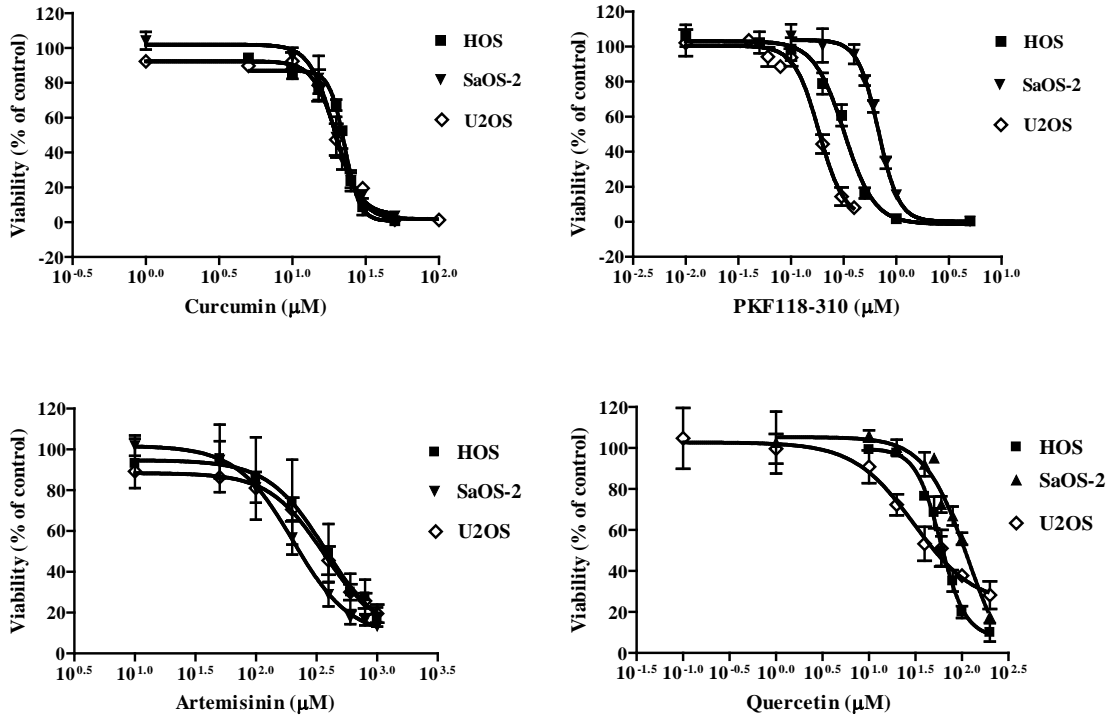
Figure 3-3. Effect of Wnt/β-catenin modulators on osteosarcoma cell viability. MTT assays were used to profile the cytotoxicity effects of Wnt/β-catenin modulators in three osteosarcoma cell lines (U2OS (◊), SaOS-2 (▼) and HOS (■)) for 72 h at the concentrations indicated. Data is presented as mean IC_{50} ± SEM (Standard Error Mean) relative to DMSO (vehicle control) from three independent experiments repeated in triplicate.

	IC_{50} ± SEM			
	Artemisinin (μM)	**QUERCETIN** (μM)	**PKF118-310** (μM)	**CURCUMIN** (μM)
HOS	351.85 ± 41.03	55.31 ± 1.06	0.32 ± 0.02	22.72 ± 0.38
SaOS-2	206.90 ± 26.50	105.17 ± 6.42	0.64 ± 0.03	18.51 ± 1.67
U2OS	353.80 ± 31.71	33.84 ± 3.76	0.19 ± 0.01	19.94 ± 1.48

Table 3-1. MTT proliferation assays were performed on HOS, SaOS-2 and U2OS cells 72 hours after the addition of test compounds. Results were obtained with six repeats in each of the three independent experiments. IC_{50} values shown are mean ± SEM of three independent experiments.
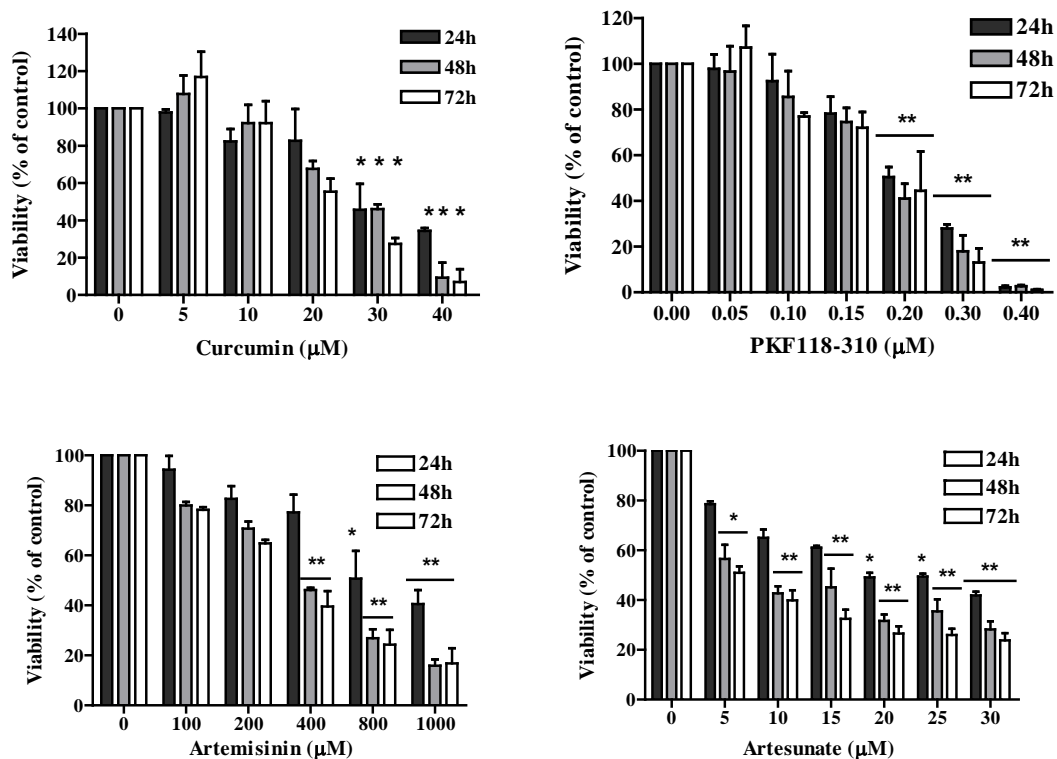
Figure 3-4. Dose- and time-dependent inhibition of U2OS cell viability by curcumin, PKF118-310, artemisinin and artesunate. MTT assays were used to establish an optimum concentration range of these compounds for subsequent experiments. U2OS cells were treated with curcumin, PKF118-310, artemisinin or artesunate for 24, 48 and 72 h at the concentrations indicated. The results shown were means ± SEM from three independent experiments repeated in triplicate. Cell viability in compound-treated cells was expressed as the percentage of DMSO-treated samples. *, $P<0.05$, **, $P<0.01$

3.3.4 Effects of selected Wnt/β-catenin inhibitors on β-catenin/TCF transcriptional activity in HCT116 colon cancer and U2OS cell lines

The effects of selected Wnt/β-catenin inhibitors on intrinsic downstream β-catenin/TCF transcriptional activities were first evaluated using a reporter gene containing four copies of the TCF-binding site (TOPglow). This was done to examine the magnitude of their Wnt inhibitory activities in the context of osteosarcoma cells. Cells were transiently transfected with TOPglow or the inactive mutant FOPglow luciferase reporter plasmids

46

and pSV-β-galatosidase control vector for normalization of transfection efficiency. The transfectants were then treated with increasing concentrations of the compounds for 24 h before cell lysates were collected for luciferase assays. Human colon carcinoma HCT116 cells were used as positive control cells as they express high levels of β-catenin due to a mutation that eliminates the phosphorylation site (serine 45) in β-catenin required for its ubiquitination and subsequent degradation [214] while U2OS cells were used as our model cell line.

As shown in Figures 3-5 and 3-6, both curcumin and artemisinin significantly suppressed β-catenin/TCF transcriptional activity in a dose-dependent manner in both HCT116 and U2OS cells. Statistical significance was observed beyond 10 μM and 20 μM for curcumin in U2OS and HCT116 cell lines respectively. Compared with the control, curcumin at 20 μM and artemisinin at 400 μM inhibited β-catenin/TCF signaling in the two cell lines by 56–59 % and 46-48 %, respectively. PKF118-310, on the other hand, inhibited the transcriptional activity of β-catenin/TCF in U2OS cells in a concentration-dependent manner but had no effect in HCT116 cells. As shown in Figure 3-6 , β-catenin/TCF signaling was inhibited by PKF118-310 by approximately 59 % and 48 % at doses of 0.10 μM and 0.15 μM in U2OS cells respectively. Much to our surprise and contrary to published reports, quercetin increased β-catenin/TCF transcriptional activity in U2OS cells and had no dose-response relationship in HCT116 cells [200]. Artesunate did not show any significant effect in both HCT116 and U2OS cells. LiCl, a well known Wnt/β-catenin agonist, was used as a positive control here. As expected, LiCl increased β-catenin/TCF transcriptional activity drastically in HCT116 cells (Figure 3-5).

Transcriptional activities of the FOPglow plasmid were not affected by treatment of all compounds. The inhibitory effects of curcumin, PKF118-310 and artemisinin on β-catenin/TCF signaling in osteosarcoma is the first of such report although similar effect has been observed in colon and prostate cancer cell lines recently [178, 193, 201, 215]. Two of these compounds, namely curcumin and PKF118-310, showed the best profile in terms of suppression the β-catenin/TCF transcriptional activity in U2OS cells and were thus selected to further investigate their specific mechanisms of Wnt inhibitions.
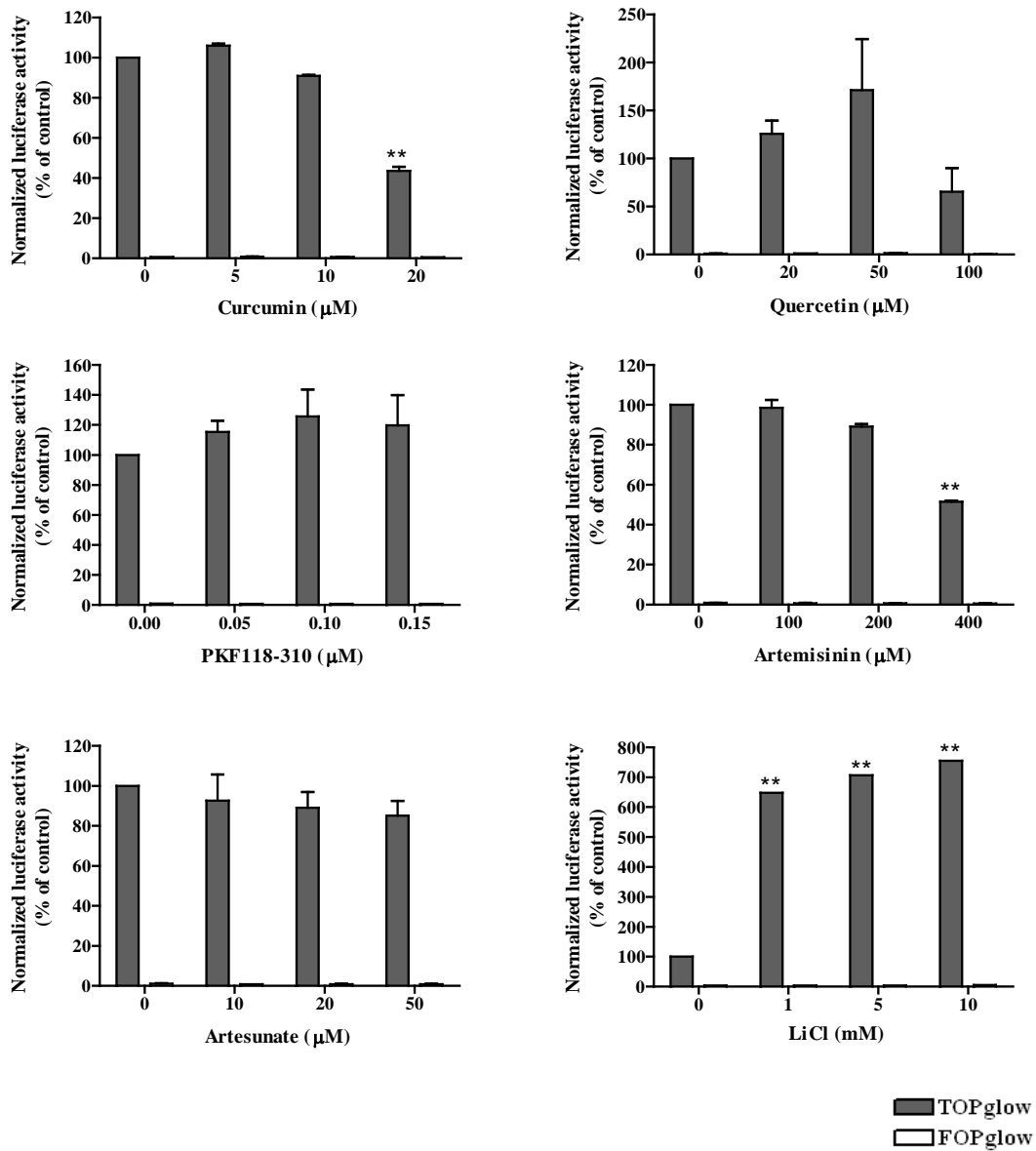
Figure 3-5. Effects of Wnt/β-catenin modulators on the transcriptional activity of β-catenin/TCF in HCT116 cell line. HCT116 cells were co-transfected with reporter genes harboring TCF-4 binding sites (TOPglow) or a mutant TCF-4 binding site (FOPglow) and β-galactosidase gene. 20 hours post-transfection, increasing amount of test compounds were added to the cells. Luciferase activity was determined 24 h post-treatment, normalized against values for the corresponding β-galactosidase activity. Results were expressed as the means ± SEM of normalized ratios of luciferase and β-galactosidase measurements of three independent experiments. Reporter activity in compound-treated cells is expressed as the percentage of DMSO-treated samples. * $P<0.05$, ** $P<0.01$.
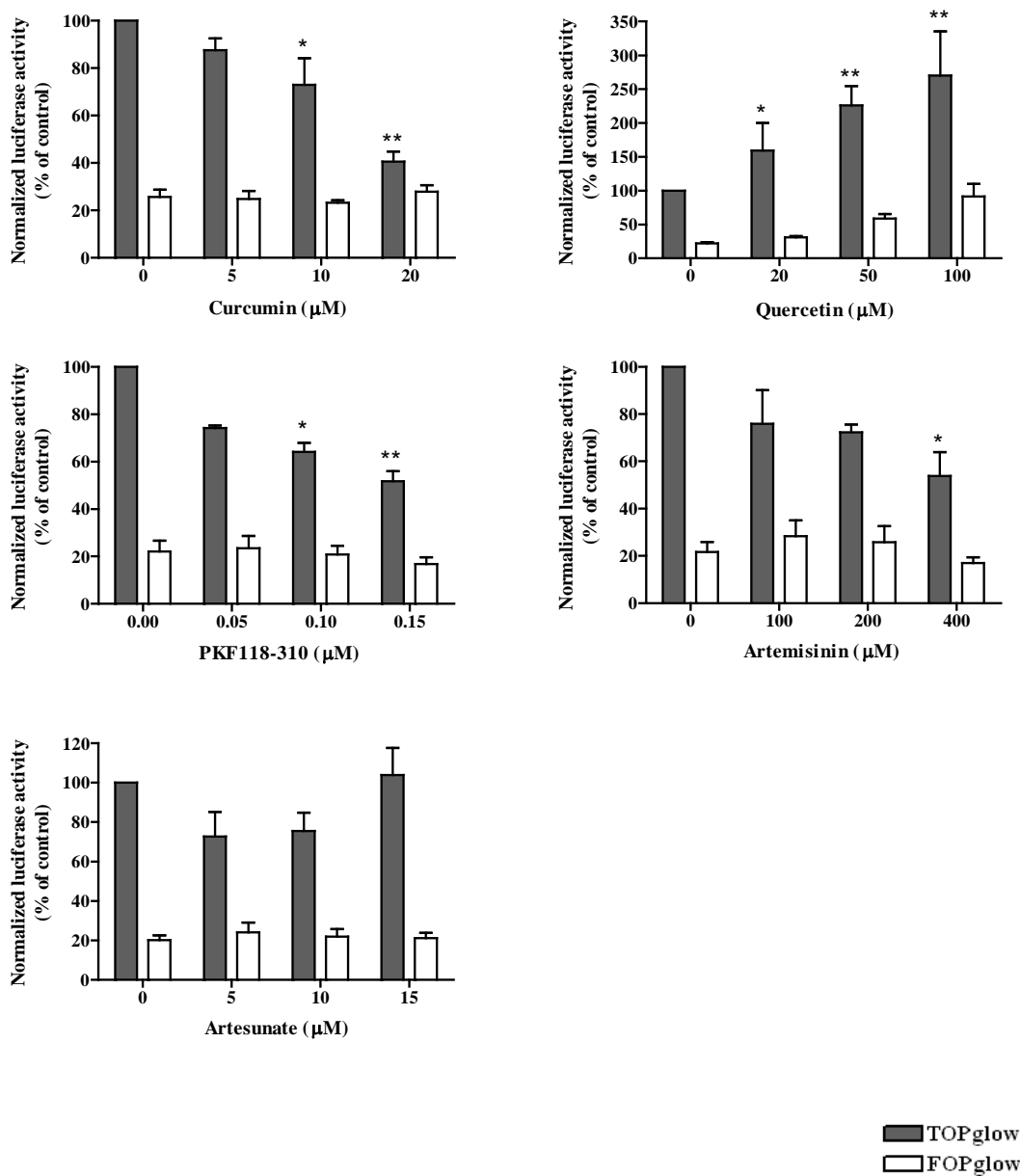
Figure 3-6. Effects of Wnt/β-catenin modulators on the transcriptional activity of β-catenin/TCF in U2OS cell line. U2OS cells were co-transfected with reporter genes harboring Tcf-4 binding sites (TOPglow) or a mutant TCF-4 binding site (FOPglow) and β-galactosidase gene. 20 hours post-transfection, increasing amount of test compounds were added to the cells. Luciferase activity was determined 24 h post-treatment, normalized against values for the corresponding β-galactosidase activity. Results were expressed as the means ± SEM of normalized ratios of luciferase and β-galactosidase measurements of three independent experiments. Reporter activity in compound-treated cells is expressed as the percentage of DMSO-treated samples. * P<0.05, ** P<0.01.

Next, to demonstrate that extrinsic activation of the canonical Wnt/β-catenin pathway can be inhibited by curcumin and PKF118-310, similar reporter assays were repeated in U2OS cells, but with the inclusion of two specific GSK-3β inhibitors (BIO and SB216763), as well as plasmids for both wild-type pcDNA β-catenin and mutant S33Y β-catenin, in separate treatments. BIO (a synthetic derivative of 6-bromoindirubin) is a natural product isolated from the Mediterranean mollusc Hexaplex trunculus [199], while SB216763 is a maleimide derivative identified from a high throughput screen against human GSK-3α and GSK-3β [198]. Both compounds have been shown to be potent and selective GSK-3β inhibitors [198, 199]. As expected, β-catenin/TCF transcriptional activities were increased approximately 730- and 220-fold with 5 μM BIO and 50 μM SB216763 treatment in our experiments respectively, most possibly due to a decrease in β-catenin degradation mediated by GSK-3β. Such extrinsic Wnt/β-catenin activation, however, could be effectively blocked by concomitant treatments with either curcumin (Figure 3-7a) or PKF118-310 (Figure 3-7b), in a dose-dependent manner.

Similarly, β-catenin/TCF transcriptional activities were increased dramatically by 30- and 580-fold with the forced expression of both wild-type and mutant S33Y β-catenin, respectively. The product of the mutant S33Y β-catenin gene is resistant to degradation by the Axin–APC–GSK3β complex [76] and hence gave rise to a much greater increase in reporter activity compared to that of the wild-type β-catenin gene. Again, treatment with either curcumin (Figure 3-7c) or PKF118-310 (Figure 3-7d) effectively suppressed β-catenin activation dose-dependently. At 20 μM, curcumin significantly reduced β-catenin/TCF transcriptional activation by the wild-type and mutant S33Y β-catenin gene

by 32.1 % and 56.3 % respectively. Such suppression was statistically significant at all doses used for PKF118-310.

Taken together, we have identified curcumin and PKF118-310 as the two most potent antagonists of Wnt signaling in the context of osteosarcoma. Our findings suggest that both curcumin and PKF118-310 act specifically at the level or downstream of β-catenin along the axis of the Wnt/β-catenin signaling pathway, independent of GSK3β, rather than upstream of or at the level of the β-catenin degradation machinery. Transcriptional activities of the negative control FOPglow plasmids were unaffected in all instances, indicating the specificity of Wnt inhibition.
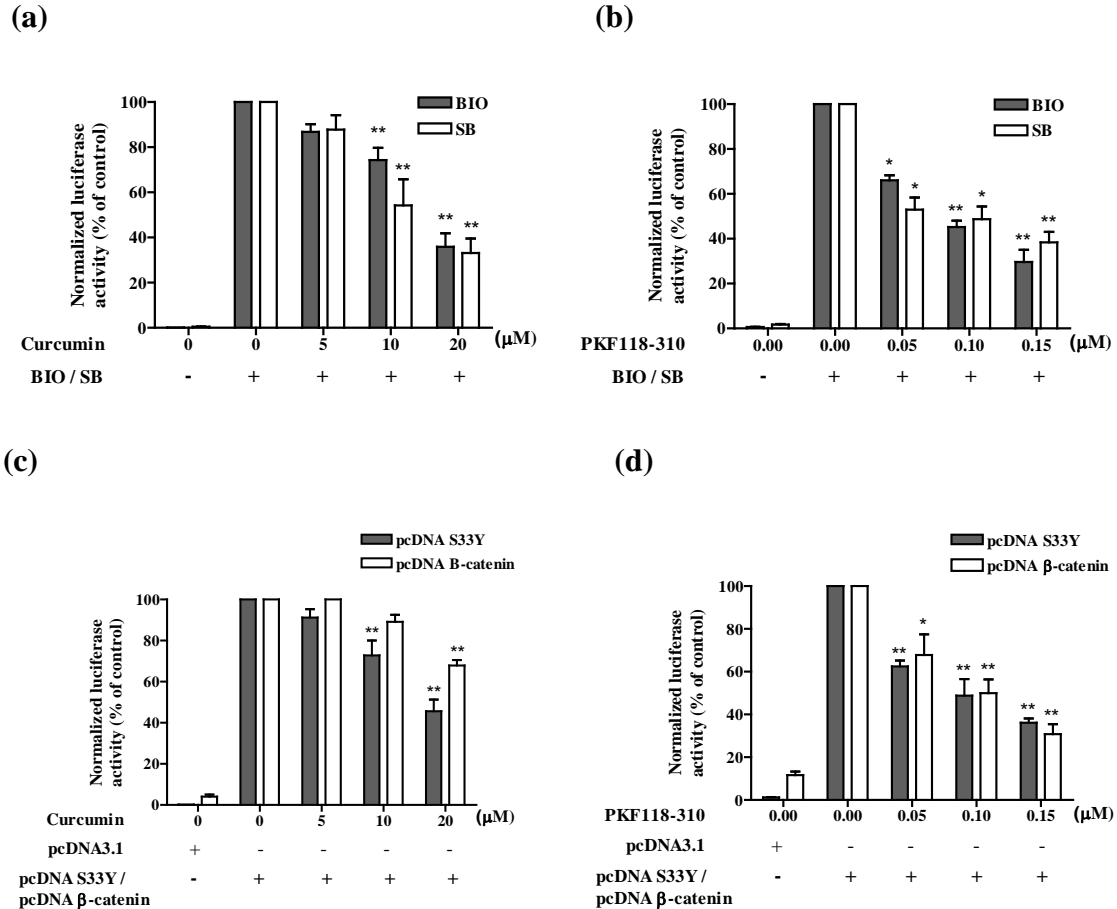
Figure 3-7. Effects of Wnt/β-catenin modulators on the extrinsic transcriptional activity of β-catenin/TCF in U2OS cell line. (a-b) U2OS cells were co-transfected with TOPglow or a mutant Tcf-4 binding site (FOPglow) and pSV-β-galactosidase control vector. Five hours post-transfection, various amounts of curcumin and PKF118-310 together with GSK-3β inhibitors BIO (5 μM) or SB216763 (50 μM) were added to the cells. **(c-d)** U2OS cells were co-transfected with TOPglow or a mutant Tcf-4 binding site (FOPglow), pSV-β-galactosidase control vector and pcDNA β-catenin (wild type β-catenin gene) or pcDNA S33Y (S33Y mutant β-catenin gene). The amount of DNA in each transfection was kept constant by the addition of an appropriate amount of empty expression vector, pcDNA3.1. Five hours post transfection increasing amounts of curcumin or PKF118-310 were added to the cells. Luciferase activities were determined 24 h after treatment with curcumin and PKF118-310, normalized against values for the corresponding β-galactosidase activities. Data were represented as means ± SEM. of normalized ratios of luciferase and β-galactosidase measurements of three independent experiments. Reporter activities in compound-treated cells were expressed as the percentage of DMSO-treated samples. *, $P<0.05$, **, $P<0.01$, compared with the GSK-3β inhibitor-only, pcDNA β-catenin or pcDNA S33Y-only group.

3.3.5 Effects of curcumin and PKF118-310 on the cellular accumulation of β-catenin

As the activation of β-catenin/TCF transcriptional activity results from the accumulation of nuclear β-catenin [77], we subsequently examined whether curcumin or PKF118-310 treatments was associated with changes in the cellular contents and localization of β-catenin protein, after having shown that these compounds significantly suppressed both the intrinsic and extrinsic transcriptional activities of β-catenin/TCF in U2OS cells. Following 24 h treatment with either curcumin or PKF118-310, both nuclear and cytosolic cell lysates were collected and used for western blot analysis to determine the amount of β-catenin in each cellular fraction. As shown in Figure 3-8a-b, we found that the amount of β-catenin in the cytoplasmic fraction was not altered by curcumin treatment, whereas that in the nuclear fraction which represent the active unphosphorylated form was markedly decreased by curcumin at 20 μM. Similarly, β-catenin protein in the nuclear fraction was decreased in a dose-dependent manner by PKF118-310 while that in the cytoplasmic fraction remained unchanged (Figure 3-8c-d).

(a)

Cytoplasmic

| Curcumin | 0 | 5 | 10 | 20 | (µM) |

β-catenin

α-Tubulin

Nuclear

| Curcumin | 0 | 5 | 10 | 20 | (µM) |

β-catenin

Lamin A/C
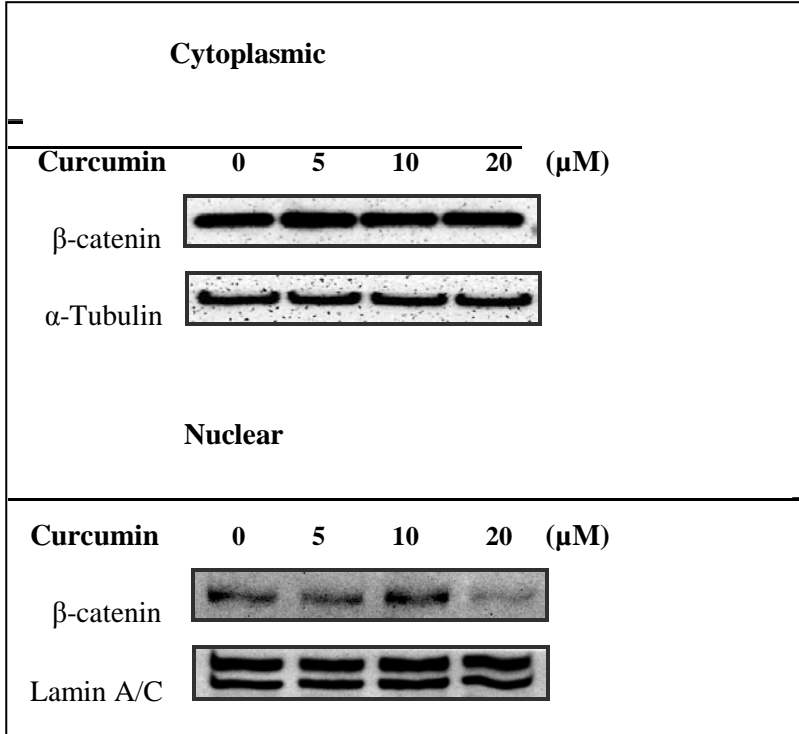
(b)
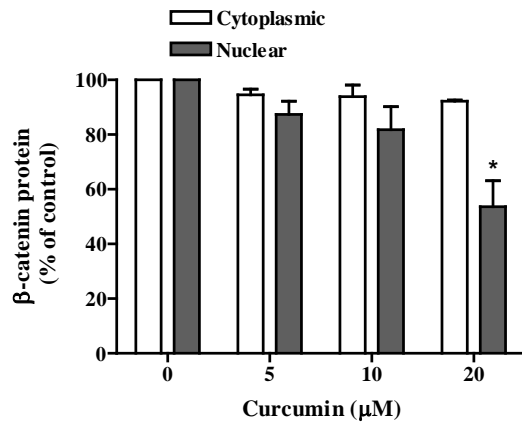
(c)
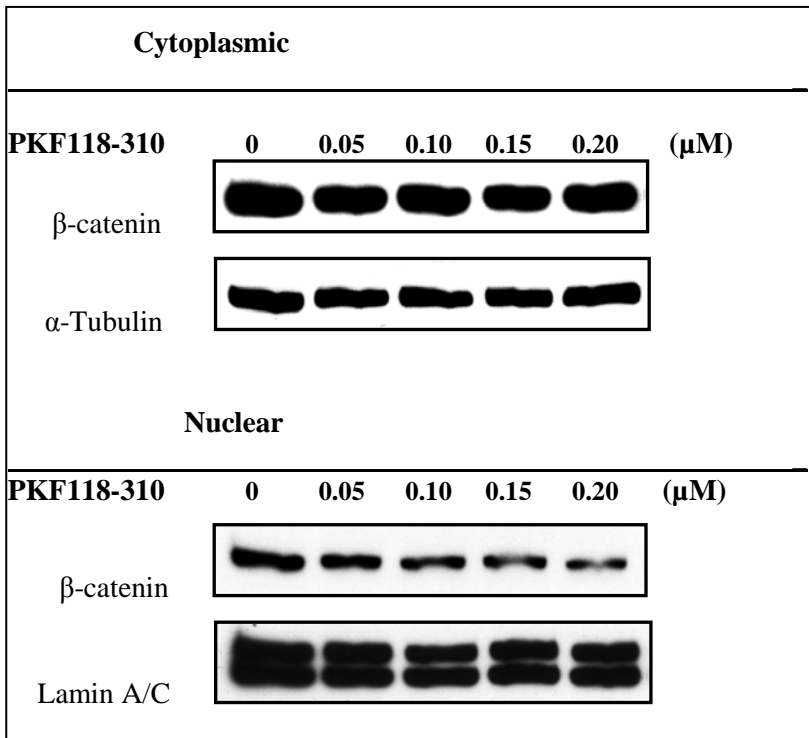
(d)
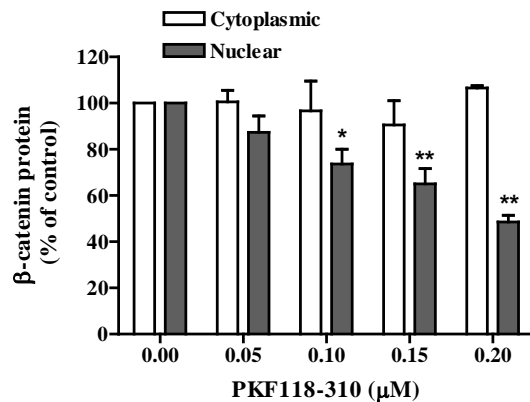
Figure 3-8. Effects of curcumin and PKF118-310 treatment on the cellular and nuclear accumulation of β-catenin. U2OS cells were pre-treated with curcumin **(a)** or PKF118-310 **(c)** at the stated concentrations for 24 h, followed by collection of protein from the cytoplasmic and nuclear fraction. α-tubulin and lamin A/C were used for cytoplasmic and nuclear protein loading controls respectively. β-catenin protein expression in curcumin- **(b)** or PKF118-310-treated **(d)** cells were expressed as the percentage of DMSO-treated samples. *,$P<0.05$, ** $P<0.01$.

3.3.6 Effects of curcumin and PKF118-310 on osteosarcoma cell migration and invasion

Recent reports showed that the inhibition of the Wnt/β-catenin pathway by the dominant-negative form of the co-receptor, DN-LRP5, and the endogenous inhibitor, DKK-3, could result in a reduction of motility and invasiveness of osteosarcoma cells [51, 63]. To investigate if curcumin, PKF118-310 and artemisinin could exert similar effects after having established that these compounds could effectively block Wnt/β-catenin signaling in preceding studies, we performed wound healing and Matrigel invasion assays using U2OS cells. U2OS has been reported to be highly metastatic [213], but as shown in Figure 3-9, curcumin, PKF118-310 and artemisinin were able to markedly inhibit U2OS cell migration in a dose- and time-dependent manner in wound healing assays performed over a period of 24 h. Of these compounds, curcumin had the greatest anti-migratory effects on U2OS cells. These results were also supported by Matrigel invasion assays whereby curcumin and artemisinin significantly reduced the ability of U2OS cells, again in a dose-dependent manner, to invade through the Matrigel-coated inserts over a period of 48 h (Figure 3-10a, c). Similar to the cell migratory studies, curcumin had the most anti-invasive effects on U2OS cells. Specifically, curcumin treatment significantly reduced the invasive capacity of U2OS cells by 29.0 ± 5.1 %, 77.3 ± 3.3 % and 85.8 ± 1.2 % at 5 μM, 10 μM and 20 μM respectively (Figure 3-10a). Artemisinin, on the other hand, significantly suppressed U2OS cell invasion by 41.4 ± 13.7 %, 38.9 ± 15.5 % and 51.7 ± 5.8 % at 100 μM, 200 μM and 400 μM respectively (Figure 3-10c).

(a)

Curcumin (µM)   0   5   10

0 h

12 h

24 h

(b)
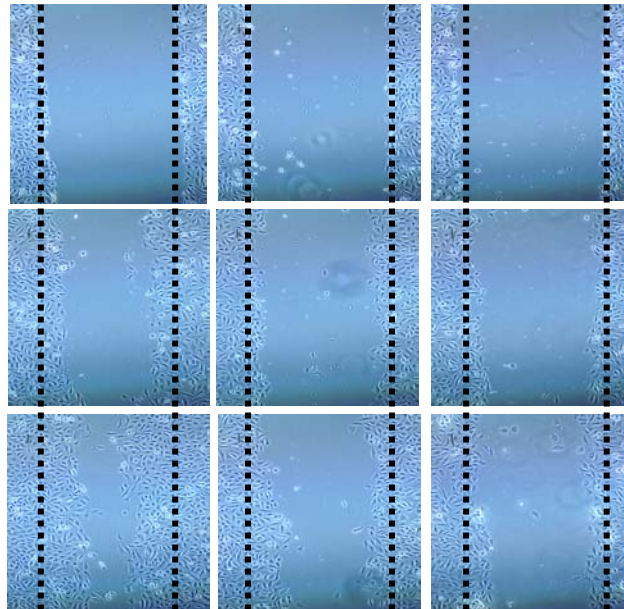
Artemisinin (µM)   0   100   200   400

0 h

12 h

24 h

(c)
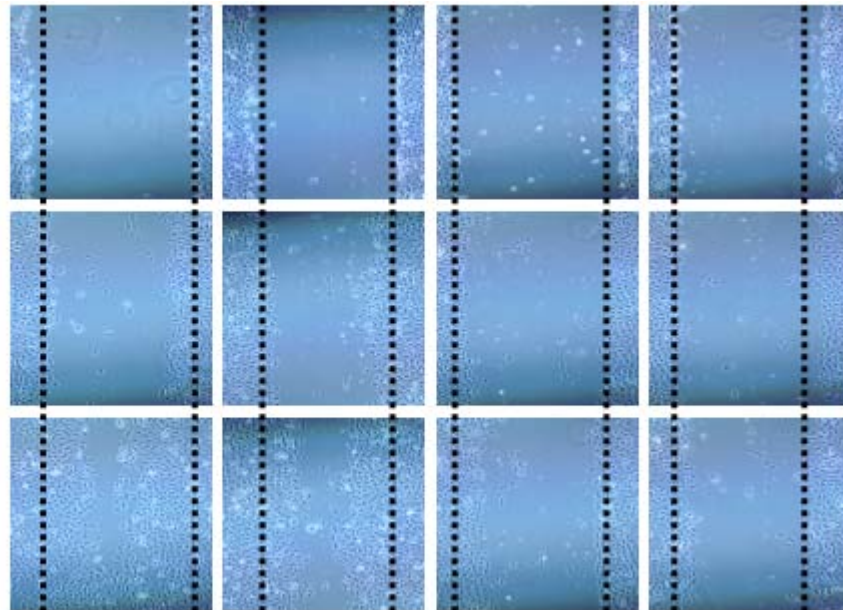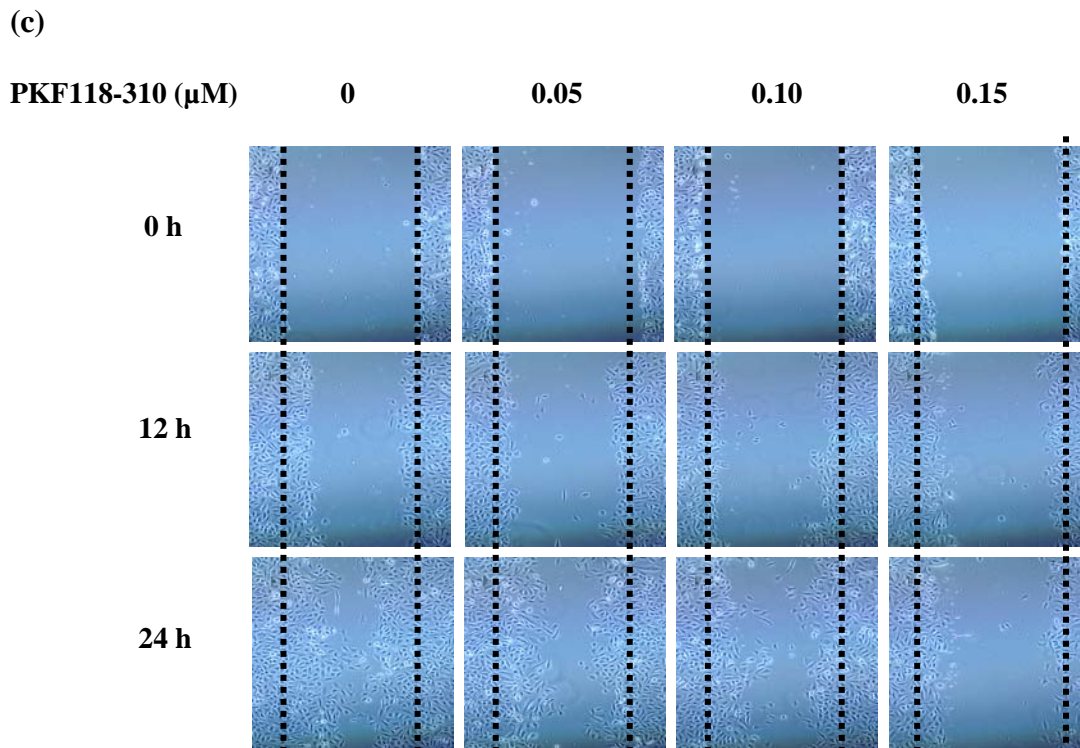
Figure 3-9. Suppression of U2OS cell migration by Wnt/β-catenin inhibitors is concentration- and time-dependent. Representative images from three independent experiments showing a dose- and time-dependent inhibition of U2OS migration by curcumin **(a)** artemisinin **(b)** and PKF118-310 **(c)** using the wound healing assays. Uniform scratches were created in confluent cultures which were treated with compounds over a period of 24 h. Images of differential wound closure rates were captured using a microscope at 10x objective.

(a)

Curcumin (μM)   0   5   10   20

(b)

Curcumin (μM)   0   0   5   10   20

pcDNA 3.1   pcDNA β-catenin

Curcumin	0	0	5	10	20	(μM)
pcDNA β-catenin	-	+	+	+	+	
pcDNA3.1	+	-	-	-	-	

60

(c)
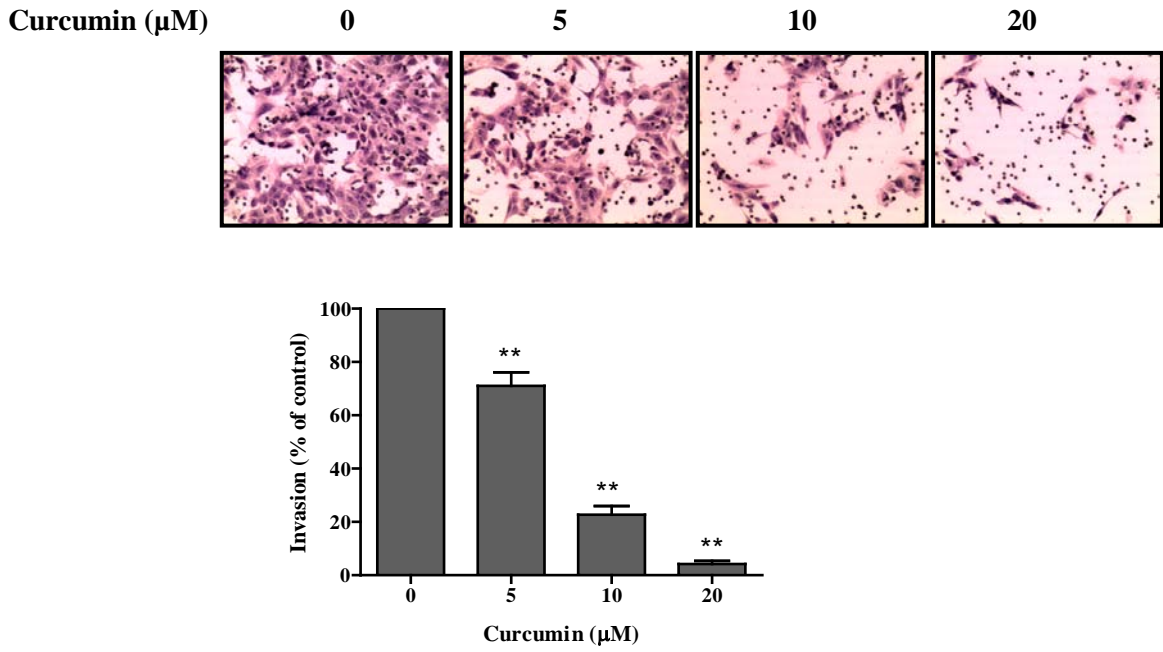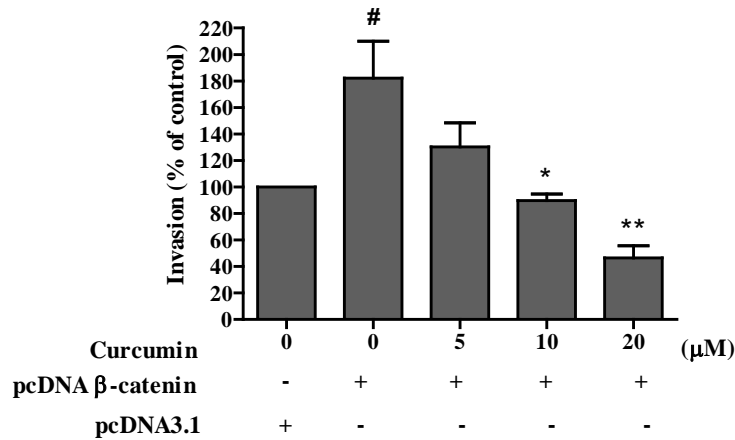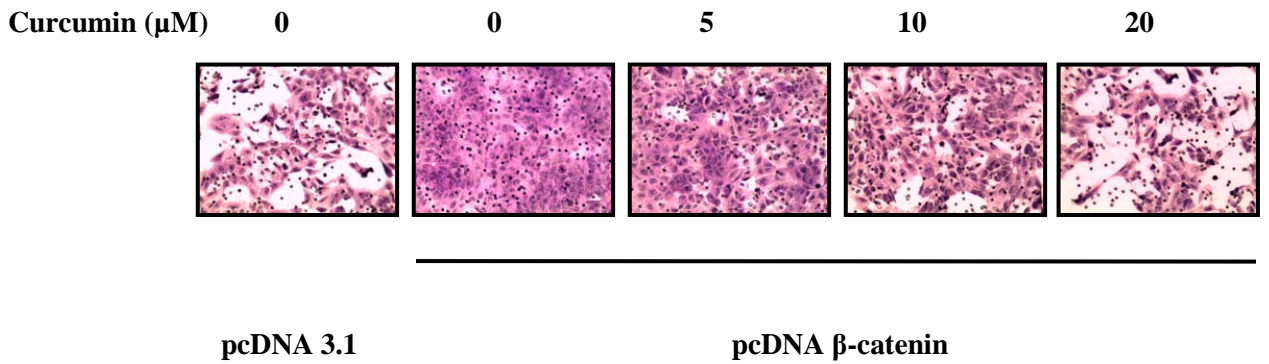
Artemisinin (µM)   0   100   200   400

(d)
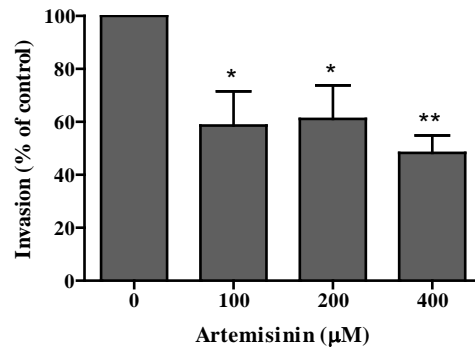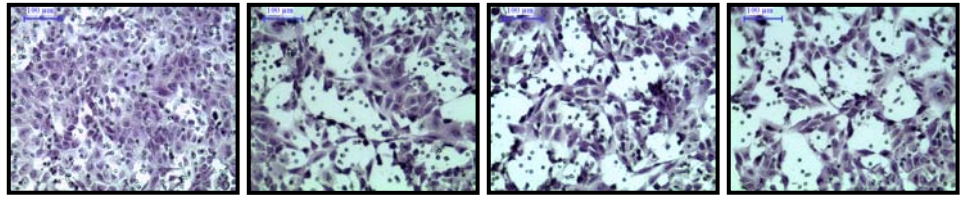
PKF118-310 (µM)   0   0.05   0.10   0.15
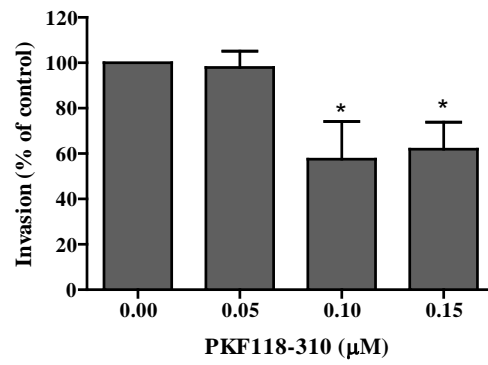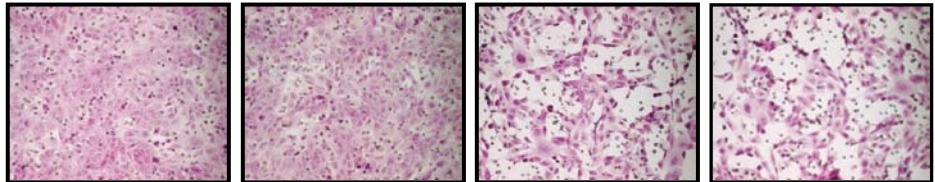
Figure 3-10. Dose-dependent inhibition of U2OS cell invasion by curcumin, artemisinin and PKF118-310. U2OS cells pre-treated with curcumin (**a**), artemisinin (**c**), PKF118-310 (**d**) or DMSO (vehicle control) for 24 h were seeded into Matrigel-coated inserts. In (**b**), to examine β-catenin-enhanced U2OS cell invasion by curcumin, U2OS cells were first transfected with pcDNA β-catenin plasmids or pcDNA3.1 control vector, followed by treatment with various concentrations of curcumin or DMSO (vehicle control) for 24 h before seeding into Matrigel-coated inserts. Cells that invaded to the lower surface of the insert over a period of 48 h were captured with a light microscope at 200x magnification after staining with crystal violet dye. Ten random fields were counted for the number of invaded U2OS cells. Data were presented as means ± SEM of three independent experiments. Cell invasion in compound-treated cells and β-catenin transfected cells was expressed as the percentage of DMSO-treated samples (*, $P<0.05$, **, $P<0.01$) and that transfected with the control vector, pcDNA3.1 (* $P<0.05$, ** $P<0.01$, compared with the β-catenin-only group; #, $P<0.01$, compared with the pcDNA 3.1-only group) respectively.

Since both curcumin and artemisinin may be non-specific inhibitors of Wnt/β-catenin signaling and may have exerted anti-invasive effects through other signaling pathways, we further used PKF118-310, which is a more selective compound, in similar studies to ascertain the involvement of Wnt/β-catenin signaling in osteosarcoma cell migration and invasion. As shown in Figure 3-9c, PKF118-310 was able to significantly inhibit U2OS cell migration in a dose- and time-dependent manner. In parallel to its anti-migration effects, PKF118-310 treatment significantly reduced the invasive capacity of U2OS cells by 42.4 ± 16.6 % and 38.1 ± 12.0 % at 0.10 μM and 0.15 μM respectively (Figure 3-10d). The anti-metastatic effects of curcumin, artemisinin and PKF118-310 were observed at concentration ranges that are shown to inhibit downstream β-catenin/TCF transcriptional activities (Figure 3-6) as well as nuclear translocations of the β-catenin protein (Figure 3-8) and were not a result of cell toxicity as U2OS cells did not exhibit significant growth inhibition at these concentrations as shown previously in Figure 3-4 .

To confirm the contribution of Wnt/β-catenin activation in affecting osteosarcoma cell invasion, we next transfected U2OS cells with the wild-type β-catenin plasmid followed by curcumin treatment and performed similar Matrigel invasion assays. The pre-treated U2OS cells were allowed to invade through the Matrigel-coated inserts for a period of 48 h. As shown in Figure 3-10b, Wnt/β-catenin activation via the forced expression of wild-type β-catenin dramatically enhanced the invasion capacity of U2OS cells, but this effect could be effectively reversed by curcumin treatment in a dose-dependent manner. Specifically, curcumin treatment significantly inhibited β-catenin-induced U2OS invasiveness by 50.7 ± 4.9 % at 10 μM and 74.5 ± 9.2 % at 20 μM respectively.

Altogether, our results strongly suggest that the Wnt/β-catenin pathway is involved, possibly in part, in the regulation of the invasive behavior of U2OS cells and that osteosarcoma cell invasion may be delayed by disrupting the Wnt/β-catenin pathway using small molecule inhibitors such as curcumin, artemisinin and PKF118-310.

3.3.7 Effects of curcumin and PKF118-310 on MMP-9 activity and protein expression in U2OS cells

MMPs play important roles in the degradation of extracellular matrix to facilitate cancer cell invasion and metastasis [216]. In particular, MMP-9 is a well known Wnt target gene that is constitutively over-expressed in U2OS cells and its increased expression is closely associated with enhanced osteosarcoma tumor invasion and metastasis [217-219]. Using Western blotting, we selected the two most potent antagonists, namely curcumin and PKF118-310 and examined whether reduced invasion with treatment of these compounds

correlated with MMP-9 protein levels in U2OS cells. As shown in Figure 3-11a, we observed a dose-dependent reduction in MMP-9 protein expression with curcumin treatment. Specifically, MMP-9 protein expression was significantly down-regulated by 27.5 ± 2.4 % at 10 μM and 48.8 ± 6.1 % at 20 μM. Parallel to the western blot results, gelatin zymography assays demonstrated that curcumin significantly reduced MMP-9 activity dose-dependently over a period of 72 h. As shown in Figure 3-11b, MMP-9 activity was significantly reduced by 32.1 ± 5.1 % at 10 μM and 59.2 ± 8.8 % at 20 μM, respectively.

In addition, the effects of Wnt/β-catenin activation via the exogenous expression of wild-type β-catenin on MMP-9 protein levels and activities were further investigated. As shown in Figure 3-11c, β-catenin protein levels were elevated, indicating successful transfection of the wild-type β-catenin plasmid in U2OS cells. Over-expression of β-catenin significantly up-regulated MMP-9 protein levels but this increase could be suppressed with curcumin treatment in a dose-dependent manner. Beyond 10 μM, MMP-9 protein levels returned to basal levels with curcumin treatment. In parallel, gelatin zymography assays showed that MMP-9 activity was also increased with β-catenin over-expression (Figure 3-11d). As a result of curcumin treatment, MMP-9 activity eventually decreased and returned to basal levels at a concentration of 20 μM. Similarly, we observed dose-dependent reductions in both MMP-9 protein expression and activity with PKF118-310 treatment (Figure 3-11e and Figure 3-11f). With PKF118-310 treatment, MMP-9 expression was significantly reduced by 29.6 ± 9.9 % at 10 μM and 63.9 ±

19.3 % at 20 μM while MMP-9 activity was significantly suppressed by 37.8 ± 2.5 % at 10 μM and 54.3 ± 1.4 % at 20 μM respectively.

Taken together, our findings suggest that curcumin and PKF118-310 elicited a reduction in the secretion of MMP-9 under conditions of either endogenous and/or exogenous Wnt/β-catenin activation, possibly giving rise to reduced invasiveness and migration of U2OS cells as seen in Figures 3-9 and 3-10.

(a)

(b)

(c)

(d)

MMP-9

Curcumin (µM)	0	0	5	10	20
pcDNA β-catenin	-	+	+	+	+
pcDNA3.1	+	-	-	-	-

Curcumin	0	0	5	10	20	(µM)
pcDNA β-catenin	-	+	+	+	+	
pcDNA3.1	+	-	-	-	-	

(e)

PKF118-310	0	0.05	0.10	0.15	(µM)

MMP-9

α-Tubulin

PKF118-310	0.00	0.05	0.10	0.15	(µM)

(f)

PKF118-310   0   0.05   0.10   0.15   (μM)
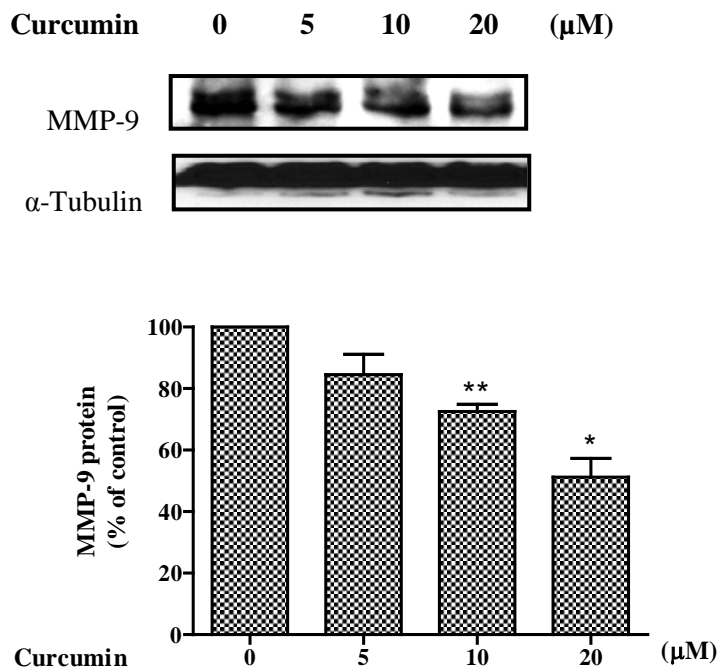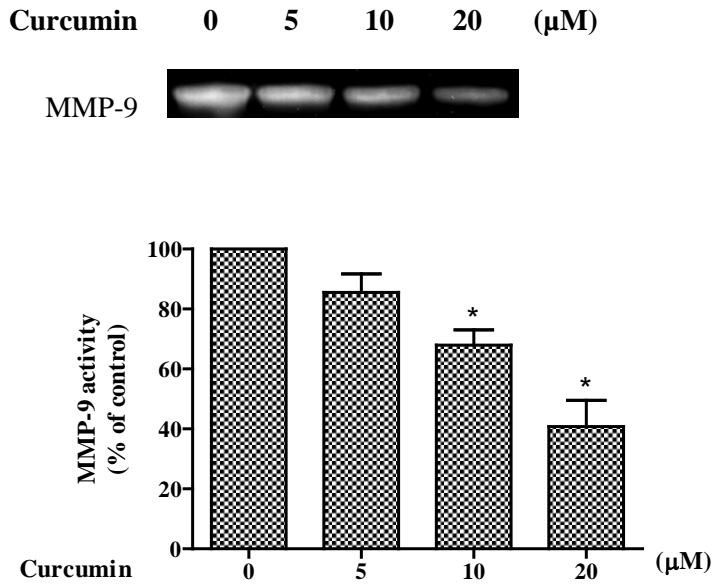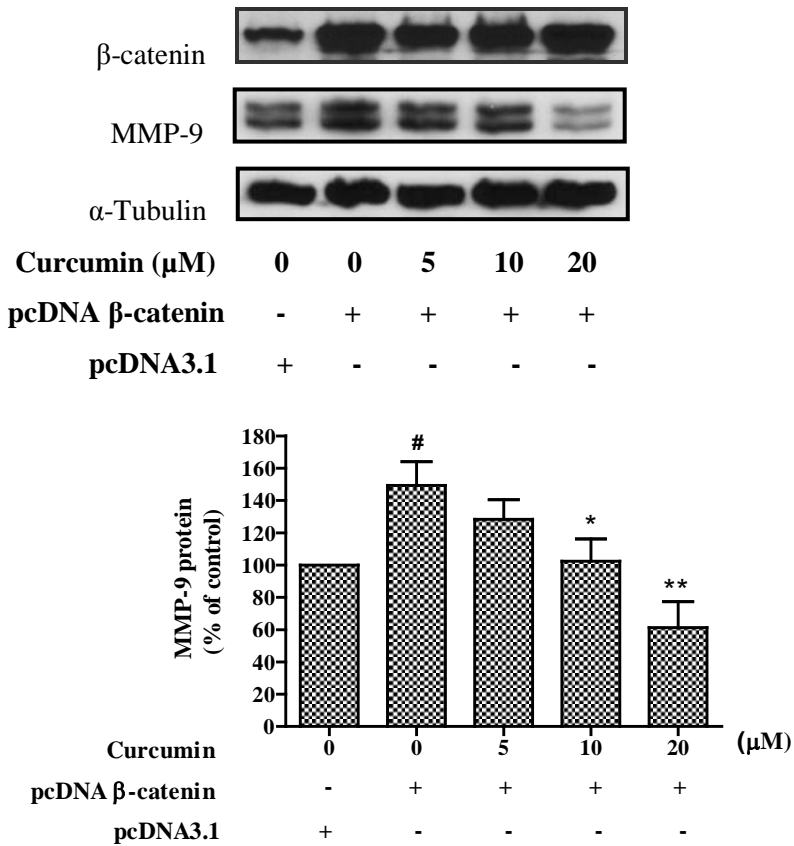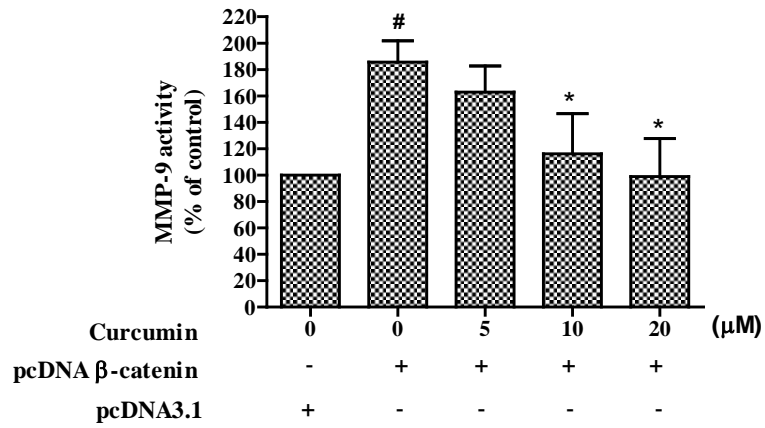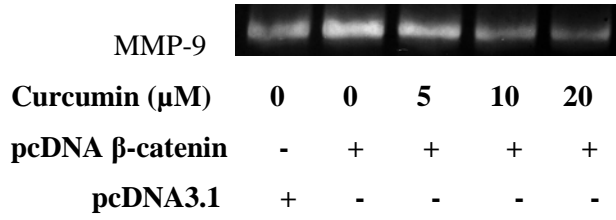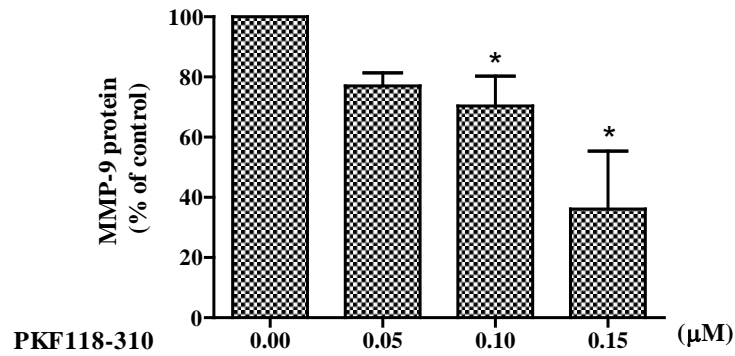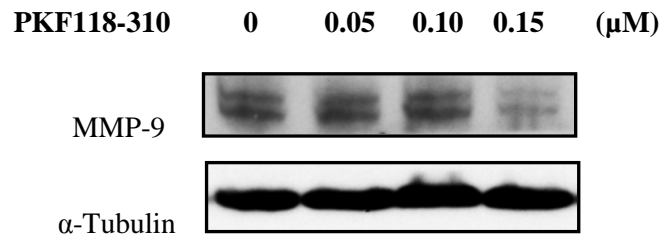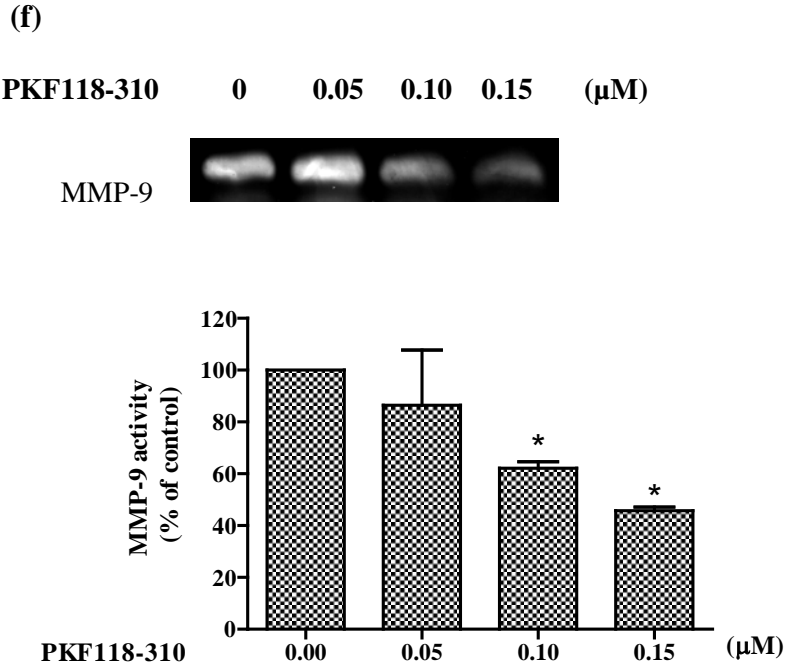
Figure 3-11. Curcumin and PKF118-310 inhibit MMP-9 activities and protein expressions in osteosarcoma. (a, e) Inhibition of MMP-9 protein expressions by curcumin or PKF118-310. U2OS cells were treated with indicated concentrations of curcumin, PKF118-310 or DMSO (vehicle control) for 24 h before proteins were collected for western blot. **(b, f)** Curcumin and PKF118-310 inhibited MMP-9 activities. U2OS cells were treated with indicated concentrations of curcumin, PKF118-310 or DMSO for 72 h in serum free medium. The conditioned media were then harvested and concentrated. MMP-9 activity was assessed by gelatin zymography and identified by clear zones of digested gelatin. **(c)** Effect of curcumin on MMP-9 protein expression in β-catenin-transfected U2OS cells. U2OS cells transfected with pcDNA β-catenin plasmid were treated with indicated concentrations of curcumin or DMSO for 24 h. Proteins were collected for western blot. **(d)** Effect of curcumin on MMP-9 activity in β-catenin-transfected U2OS cells. U2OS cells transfected with pcDNA β-catenin plasmid were treated with indicated concentrations of curcumin or DMSO for 72 h in serum free medium. The conditioned media were then harvested and concentrated. The MMP-9 activity was assessed by Gelatin zymography. All blots and zymograms shown in Figure 3-11 were representative of three independent experiments. α-Tubulin was used as a loading control in all the western blot analysis. MMP-9 protein expressions or activities in compound-treated cells were expressed as the percentage of DMSO-treated samples. * ,$P<0.05$, ** $P<0.01$. MMP-9 protein expressions or activities in compound-treated cells that over-expressed β-catenin were expressed as the percentage of control vector, pcDNA3.1. * ,$P<0.05$, ** $P<0.01$, compared with the β-catenin-only group. #, $P<0.05$, compared with the pcDNA 3.1-only group.

3.3.8 Effects of PKF118-310 on osteosarcoma cell proliferation, apoptosis and cell cycle progression in U2OS cells

It has recently been reported that disruption of the Wnt/β-catenin signaling suppressed both *in vitro* and *in vivo* cell proliferation in osteosarcoma cells [51, 220]. Given that β-catenin/TCF-dependent signaling and its gene products are known to regulate cell proliferation, cell cycle distribution and apoptosis, we investigated the effect of PKF118-310 on these processes, after having demonstrated that PKF18-310 had the most potent anti-proliferative effect among other Wnt/β-catenin modulators against U2OS cells. Figure 3-3 shows that treatment with PKF118-310 inhibited U2OS cell proliferation dose- and time-dependently, with an IC_{50} of 0.19 ± 0.01 µM (Table 3-1) and PKF118-310 beyond 0.20µM at 24 h, 48 h and 72 h resulted in statistically significant toxicities (Figure 3-4). Resistance against apoptosis is critical for survival and contributes to drug resistance in many cancers, including osteosarcoma [221]. Given the potent anti-proliferation effects of PKF118-310, we were interested in determining whether PKF118-310 also induces apoptosis in U2OS cells at higher toxic concentrations. PKF118-31-induced apoptosis was evaluated by accessing the cell population using flow cytometry analysis after incubating PKF118-310-treated cells with annexin-V and PI. As shown in Figure 3-12a, treatment with PKF118-310 resulted in a dose-dependent increase in the number of early (stained with annexin-V only) and late (stained with both annexin-V and PI) apoptotic cells. Specifically, PKF118-310 treatment significantly induced the rate of early apoptosis by 328% and 290% at 0.20 µM and 0.30 µM respectively. The late apoptotic rate was significantly increased about 2-fold with 0.30 µM PKF118-310.

In addition, cell cycle distribution of U2OS cells was examined following 24 h and 48 h treatment of increasing concentration of PKF11-310 using flow cytometry. As shown in Figure 3-12b, treatment with PKF118-310 resulted in an increase in the number of cells in the G2/M phase and a corresponding decrease in number of cells in the G0/G1 phase, indicating a PKF118-310-induced G2/M phase arrest. This trend is seen after treatment with PKF118-310 for 24h and 48h, although G2/M phase arrest is only statistically significant at 0.30 μM PKF118-310 treatment over 48 h. In parallel with the apoptotic assays, we also observed an increase in the number of cells in the sub-G1 phase of the cell cycle with PKF118-310 treatment (data not shown), confirming that PKF118-310 promoted apoptosis in U2OS cells.

(a)
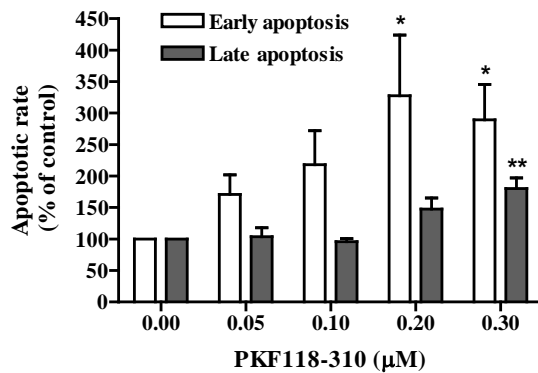
(b)
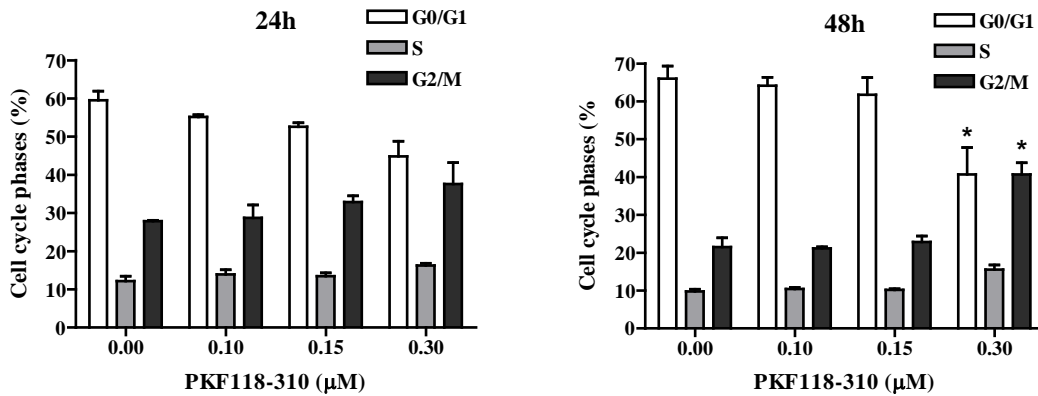
Figure 3-12. PKF118-310 induces apoptosis and disrupts cell cycle distribution in U2OS cells. (a) PKF118-310 induced apoptosis in U2OS cells. U2OS cells pre-treated with PKF118-310 or DMSO for 24 h were stained with annexin-V and PI and analyzed by flow cytometry. Data were presented as means ± SEM of three independent experiments. PKF118-310-treated cell which undergone early (stained with annexin-V only) and late (stained with both annexin-V and PI) apoptosis were expressed as the percentage of DMSO-treated samples. *, $P<0.05$. **, $P<0.01$. **(b)** PKF118-310 induced G2/M phase cell cycle arrest in U2OS cells. U2OS cells were treated with increasing concentration of PKF118-310 for 24 and 48 h before they were stained with PI. Cell cycle distribution of the cells was measured by flow cytometry and the results were plotted as the percentage of cells in each cell cycle phase. Data were presented as means ± SEM of three independent experiments. *, $P<0.05$ indicated the difference in the various cell cycle phases compared to the control cells.

3.3.9   Effects of PKF118-310 on the protein expressions of proliferation-associated

Wnt-responsive genes

Given that PKF118-310 inhibited anti-proliferative effect as well as induced apoptosis

and G2/M phase arrest in U2OS cells, we asked whether these anti-cancer effects with

PKF118-310 treatment correlated with protein expressions of proliferation-associated β-

catenin/TCF target genes such as cyclin D1, c-Myc and survivin. Both cyclin-D1 and c-

Myc are critical for tumor growth and survival [97, 98] while survivin is both an inhibitor

of apoptosis as well as an important regulator of the G2/M phase of the cell cycle [222-

225]. U2OS cells expressed high levels of cyclin D1, c-Myc and survivin demonstrating

an active Wnt/β-catenin signaling, however, treatment with PKF118-310 significantly

suppressed the expression of these Wnt target proteins dose-dependently (Figure 3-13).

Taken together, our findings strongly suggest that PKF118-310 suppressed the expression

of several proliferation-associated Wnt-target genes such as cyclin-D1, c-Myc and

survivin, possibly giving rise to reduced proliferation, enhanced apoptosis and G2/M

phase arrest of U2OS cells.
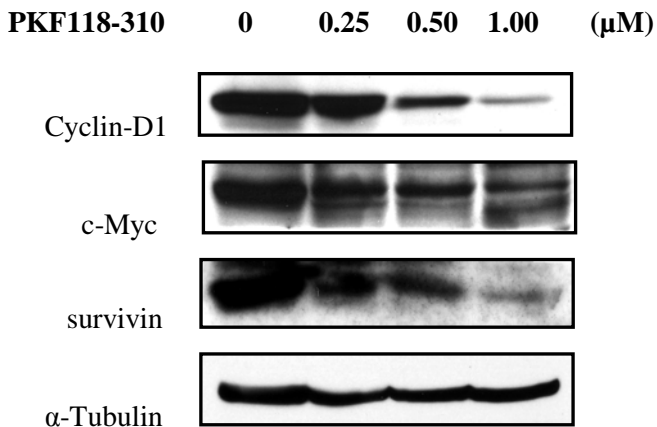
Figure 3-13. Concentration-dependent decrease of cyclin D1, c-Myc and survivin protein expressions with PKF118-310 treatment. U2OS cells were treated with indicated concentrations of PKF118-310 or DMSO for 24 h and total cellular proteins were collected for western blot. α-Tubulin was used as a loading control. The blots shown were representative of three independent experiments

3.4 Discussion

Despite mounting evidence implicating the importance of Wnt/β-catenin in the

development and progression of osteosarcoma, the therapeutic potential of small

molecule inhibitors targeting this pathway in osteosarcoma remained largely unreported.

Therefore, in this chapter, we aimed to perturb the Wnt/β-catenin signaling pathway

using small molecule antagonists to prevent or reduce osteosarcoma tumorigenesis and metastasis, with the hope of improving the clinical outcome of the disease.

In this study, we first sought to assess Wnt/β-catenin signaling in a panel of eight metastatic osteosarcoma cell lines from various origins and detected abundant levels of β-catenin protein in most of these osteosarcoma cells (Figure 3-1) This suggests that frequent activation of canonical Wnt/β-catenin signaling is observed in osteosarcoma, although the apparent degree of activation varied among the cell lines. Our findings are consistent with previous studies, which demonstrated significant accumulation of β-catenin protein in osteosarcoma patients' samples [73, 74]. Together with previous reports on the expressions of Wnt signaling components including Wnt ligands, FZD, LRP5 and β-catenin protein observed in various human osteosarcoma cell lines and patient samples [47, 51, 63, 73, 74], our results supported the notion that canonical Wnt/β-catenin signaling is active in osteosarcoma.

The choice of the main osteosarcoma cell lines for subsequent experiments is challenging given the heterogeneous nature of the cancer type. While there are numerous commercially available human osteosarcoma cell lines, limited information is available on their disease status and pathophysiological relationship with Wnt signaling. Our selection of the osteosarcoma cell lines was guided primarily by previous publication supporting a role for canonical Wnt signaling in the pathobiology and progression of osteosarcoma [51, 52, 63]. The highly invasive U2OS cells [213] was found to express the highest levels of β-catenin protein (Figure 3-1) while SFRPs proteins were shown to

be absent or markedly silenced, compared to the normal osteoblast cells (Figure 5-1). U2OS was thus chosen as the main cell line in subsequent studies to investigate various anti-cancer effects of the Wnt/β-catenin modulators. It is noteworthy that the expression of the Wnt co-receptor, LRP5, in osteosarcoma specimens has been previously reported to correlate significantly with metastatic events [47]. Given that U2OS cells highly express LRP5, this cell lines closely represent the clinical state of osteosarcoma characterized by rapid growth and aggressive metastasis. In contrast to previous reports supporting a significant role for canonical Wnt signaling in the pathobiology and progression of HOS and SaOS-2 osteosarcoma cell, very low expression of active β-catenin was detected in these cells (Figure 3-1) [51, 52, 63]. Nevertheless, MTT assay was performed using HOS and SaOS-2 cell lines to compare the cytotoxicity profile of the test compounds in various osteosarcoma cell lines (Figure 3-3).

Effective inhibitions of Wnt/β-catenin pathway by the various compounds used in our studies were evidenced by the suppression of intrinsic β-catenin/TCF transcriptional activities using luciferase reporter assays (Figures 3-5 and 3-6). Curcumin and artemisinin were identified as good inhibitors of the Wnt/β-catenin pathway in both U2OS and HCT116 colon cancer cells. PKF118-310, on the other hand, inhibited the transcriptional activity of β-catenin/TCF in U2OS cells but had no effect in HCT116 cells at the highest non-toxic concentration used (0.15 µM). Although PKF118-310 was reported to inhibit β-catenin/TCF transcriptional activity in HCT116 cells at an EC_{50} of 0.3 ± 0.02 µM [178], Wnt inhibitory activity of PKF at concentrations beyond 0.15µM was not tested since significantly cell death at these concentrations may confound Wnt

inhibitory effects interpretation. Artesunate did not show any significant effect in both HCT116 and U2OS cells. These results did not agree with previous reports possibly because of the lower concentrations used in our study [211]. Contrary to expected, we found that quercetin increased β-catenin/TCF transcriptional activity in U2OS cells and had no dose-response relationship in HCT116 cells. A similar induction of transcriptional activity was reported in HEK293 human embryonal kidney cells [226]. This conflicting observation whereby known inhibitors enhanced the β-catenin/TCF transcriptional activity also occurred in the case of indomethacin and rofecoxib in SW480 cells [227]. Intrinsic resistance of cells against such inhibitors may have resulted in this anomaly. Other reasons to the discordant results may include the variation in levels of intrinsic Wnt signaling in different tissues, biphasic responses to increasing concentrations of compounds and difference in potency of the compounds in different cell lines. Given that compounds derived from natural sources are known to be multi-targeted, we also cannot rule out multiple inhibitory effects of these compounds on different targets. Further studies are needed to characterize their specificity on Wnt inhibition.

Given that curcumin and PKF118-310 showed the best profiles in terms of suppression the β-catenin/TCF transcriptional activity in U2OS cells, we further investigated their mechanisms of Wnt inhibitions and anti-metastatic effects. In agreement with previous findings [178, 201, 228], the inhibitory effects of both compounds were not related to the β-catenin degradation machinery, but rather to downstream components. This was supported by the following observations: Firstly, both curcumin (Figure 3-7a) and PKF118-310 (Figure 3-7b) were found to suppress β-catenin/TCF signaling in the

presence of specific GSK-3β inhibitors, BIO and SB216763; secondly, the inhibitory effect of curcumin (Figure 3-7c) and PKF118-310 (Figure 3-7d) were unaffected when the Wnt/β-catenin pathway was activated with over-expression of constitutively active mutant S33Y β-catenin gene, whose product is resistant to degradation by the Axin–APC–GSK3β complex; and lastly both compounds were capable of disrupting nuclear β-catenin translocation without changing the total cellular levels (Figure 3-8). Similar to the phenomenon previously reported by Park et al., we observed a more pronounced inhibitory effect on the extrinsic transcriptional activity by curcumin with either forced expression of mutant S33Y β-catenin gene or treatment with GSK-3β inhibitors compared to the over-expression of wild-type β-catenin, although the transcriptional activity of the latter was increased much less than other treatments [201]. These observations may be explained by the fact that both treatments with the mutant S33Y β-catenin and GSK-3β inhibitors negatively affected β-catenin degradation [76, 198, 199], which in turn may have resulted in the stabilization of β-catenin protein and consequently a much greater increase in its nuclear translocation compared to treatment with the wild-type β-catenin gene. Curcumin could have acted effectively in disrupting the nuclear translocation of β-catenin protein in these treatments giving rise to a more pronounced decrease in transcriptional activity, but further experiments are required to confirm this. On the other hand, these differences were not observed for PKF118-310 since it is capable of antagonizing Wnt/β-catenin signaling at various juncture of Wnt signaling such as preventing the translocation of nuclear β-catenin, as well as inhibiting the complexation of β-catenin/TCF [178]. Synergistic antagonism at various critical points of the cascade by PKF118-310 could have also contributed to its superior and potent Wnt

inhibitory effects. As several Wnt components including cell-surface receptor (LRP5), Wnt ligands (Wnt 10b) as well as natural antagonist (DKK-3) have recently been shown to regulate cellular invasion in osteosarcoma [47, 48, 51, 52, 63, 73, 193], we next asked if curcumin, artemisinin and PKF118-310 could act as anti-invasive agents in U2OS cells after having established their inhibitory effects on Wnt/β-catenin signaling (Figures 3-5, 3-6 and 3-7). Indeed, we showed that U2OS cell migration and invasiveness were significantly reduced using non-toxic concentrations of curcumin and artemisinin (Figures 3-9 and 3-10). The demonstration that PKF118-310, a selective antagonist of Wnt/β-catenin signaling, inhibited osteosarcoma cell migration and invasiveness further supported the involvement of the pathway in osteosarcoma cell metastasis (Figure 3-9c and 3-10d). As an alternative confirmatory approach to correlate osteosarcoma invasiveness with the Wnt/β-catenin pathway, we transfected U2OS cells with wild-type β-catenin plasmid and demonstrated that the activation of the Wnt/β-catenin pathway with the **over-expression** of the wild-type β-catenin gene resulted in enhanced invasion capacity of osteosarcoma cells, promoting their ability for transmigration through the extracellular matrix. Again, curcumin effectively reversed this phenomenon (Figure 3-10b).

Although we do not fully understand the specific mechanisms of their anti-invasive effects, curcumin and PKF118-310 may suppress osteosarcoma cell invasion through Wnt-targeted genes such as MMPs [100, 101, 229]. Given the myriad of MMPs that may be affected, we focused on MMP-9 since several groups have shown that MMP-9 is the major extracellular matrix degradation enzymes that is highly expressed in osteosarcoma

and that its increased expression is associated with osteosarcoma tumor aggressiveness, metastasis and poor prognosis [217-219]. Indeed, the suppression of U2OS cell invasion by curcumin and PKF118-310 was found to correlate with the inhibition of MMP-9 activity and protein levels (Figure 3-11e-f). This observation may be explained by the fact that the MMP-9 gene contains consensus TCF/LEF-binding elements in the promoter region and has been shown to be highly regulated by Wnt/β-catenin signaling [230]. Hence, PKF118-310, a selective Wnt/β-catenin antagonist, was able to inhibit MMP-9 protein expression and activity (Figure 3-11e-f). In addition, curcumin was shown to suppress MMP-9 protein levels and activities under both conditions of intrinsic (Figure 3-11a-b) and extrinsic (Figure 3-11c-d) Wnt/β-catenin activation. It is noteworthy that the inhibitory effect by curcumin was more pronounced under Wnt-stimulated conditions, further supporting the notion that MMP-9 is regulated by Wnt/β-catenin signaling. Taken together, our findings suggest that curcumin and PKF118-310 down-regulated MMP-9 under conditions of either endogenous and/or exogenous Wnt/β-catenin activation, possibly giving rise to reduced invasiveness and migration of U2OS cells.

Besides MMP-9, other Wnt-targeted oncogenes may possibly be involved in regulating the invasive behavior of osteosarcoma. For instance, attenuating Wnt/β-catenin signaling using DN-LRP5 inhibited both in vitro and in vivo metastasis in several osteosarcoma cells by suppressing MMP-2, MMP-14, Twist, Slug and Snail [51, 52]. Several other metastatic-associated Wnt responsive genes including MMP-2, MMP-7, membrane-type matrix metalloproteinase 1 (MT1-MMP) and uPAR were previously reported to regulate the invasiveness of several other human tumors [100, 103, 231, 232]. Therefore, further

studies are required to investigate the effects of curcumin and PKF118-310 on the levels of MMPs and metastatic-associated Wnt target genes, as well as fully elucidate their roles in regulating osteosarcoma cell metastasis.

Given that curcumin is a multi-targeted compound, we cannot exclude the possibility that curcumin reduced osteosarcoma cell invasiveness through a combination of Wnt-dependent and Wnt-independent effects. A recent report showed that curcumin was able to transcriptionally activate the tumor suppressor HLJ1 through the JNK/JunD pathway, resulting in the up-regulation of E-cadherin which in turn leads to the inhibition of cancer cell invasion and metastasis in human lung adenocarcinoma [233]. Further experiments are needed to examine the effect of curcumin on the relative expression of epithelial and mesenchymal markers in osteosarcoma. Nevertheless, our studies provide first evidence that curcumin and PKF118-310 effectively reduced the metastatic capacity of osteosarcoma by mediating, at least in part, the Wnt/β-catenin signaling pathway through inhibiting MMP-9 protein and activity.

Apart from its potent anti-invasive effects at lower non-toxic concentrations, PKF118-310 was also found to demonstrate anti-proliferative effect in U2OS cells, attributed to PKF118-310 induced apoptosis and G2/M phase arrest, at higher toxic concentrations (Figure 3-12). Previous reports on prostate and colon cancer cell lines supported the potent anti-proliferative effect of PKF118-310 [178, 215]. Given that several survival-associated Wnt target genes such as cyclin D1, c-Myc and survivin have been reported to be over-expressed in osteosarcoma cell lines and their increased expression correlated

significantly with reduced survival time and prognosis [234-241], we further examined the expression of these genes with PKF118-310 treatment. Cyclin D1 and c-Myc regulate cell proliferation and cell cycle progression [97, 98] while survivin is both an inhibitor of apoptosis and a regulator of mitosis in the G2/M checkpoints of the cell cycle [222-225]. Indeed, we found that the suppression of cell proliferation through induction of apoptosis and G2/M phase cell cycle arrest in U2OS cells by PKF118-310 correlated with the down-regulation of cyclin D1, c-Myc and survivin protein expressions (Figure 3-13).

Downregulation of genes that regulate apoptosis such as c-Myc and survivin represent an advantage in controlling metastatic behavior in osteosarcoma [240, 242]. For instance, c-myc was previously reported to induce a more aggressive phenotype and metastatic features in osteosarcoma while a synchronous over-expressions of c-Myc and c-fos were strongly correlated to the development of metastases [240]. In another study, survivin expression was found to be significantly down-regulated in a U2OS cell model with markedly reduced invasiveness and metastatic potential as a result of the forced expression of L/B/K ALP (Liver-bone-kidney alkaline phosphatase) or CD99 [242]. Altogether, our results suggested that the suppression of c-Myc, cyclin D1, survivin and MMP-9 by PKF118-310 treatment may collectively delayed tumorigenesis and metastasis in osteosarcoma.

CHAPTER 4.   Functionalization of curcumin analogues as Wnt antagonists in osteosarcoma

4.1 Introduction

In the previous chapter, we have reported the therapeutic potential of curcumin as an anti-invasion agent in osteosarcoma and found that its anti-invasive activity was associated with the suppression of intrinsic and extrinsic Wnt/β-catenin signaling, as well as the down-regulation of metastatic-related Wnt target gene, MMP-9 [195]. Our findings were supported by others which showed that curcumin exert its anti-cancer properties through disrupting Wnt signaling in other malignancies such as colon, gastric and stomach cancer [193, 201, 207, 208, 228]. However, the clinical application of curcumin as an effective Wnt antagonist is limited by its low bioavailability due to poor absorption and rapid metabolism [243-245]. As such, the effective but high concentrations used in previous studies may not be feasible for human clinical intervention studies. Therefore, a requirement obviously exists for access to compounds that combine improved Wnt inhibitory potency (lower EC_{50}) and selectivity with a suitable drug-like character that would circumvent the limitations encountered with curcumin. Furthermore, identification of critical targets for Wnt inhibition as well as elucidation of structure-activity-relationships (SAR) that critically influence Wnt inhibitory activity would provide useful direction for designing novel derivatives with desirable drug-like profiles. The objectives of this chapter are thus to (1) synthesize, evaluate and identify curcumin analogues with enhanced potency and good selectivity as Wnt antagonists to prevent or delay osteosarcoma disease progression; (2) study the SAR of Wnt inhibitory activity so as to

identify crucial structural motifs leading to improved potency and selectivity as Wnt inhibitors and (3) examine the underlying mechanism of Wnt inhibition of selected curcumin analogue by evaluating the perturbations in gene expression of various Wnt signaling components using the Human Wnt Signaling Pathway RT^2 Profiler^{TM} PCR array.

To study the effect of structural modification on Wnt inhibition, we modified the lead compound, curcumin (**1-1**) to produce five series of curcumin analogues with diverse linkers joining the terminal phenyl rings as well as different substituent at the phenyl rings. These compounds were synthesized by base-catalyzed Clasien-Schmidt condensation reactions of substituted aromatic aldehydes with the appropriate acetophenones (see Material and methods). The structures of curcumin analogues are presented in Table 4-1. Series 1 consists curcumin-type compounds that retain the 7-carbon spacer between the terminal phenyl rings known as the diarylheptanoids while Series 2 represents diarylpentanoid analogues with a 5-carbon spacer between the terminal phenyl rings. Series 3 (dibenzylidene-cyclohexanones) and 4 (dibenzylidene-cyclopentanones) consist of diarylpentanoid-type compounds in which flexibility of the 5-carbon chain is constrained by incorporating it as part of a cyclohexanone and cyclopentanone ring respectively. Lastly, Series 5 compounds, known as chalcones, were considered as structures equivalent to "half a curcuminoid" with loss of symmetry and a shortened linker.

The choice of these templates and the associated substitutions at the terminal phenyl rings were prompted by the following observations: Firstly, natural derivatives of curcumin with different substitutions on the end rings were reported to suppress β-catenin/TCF transcription. Hence, regioisomers of diarylheptanoids (Series 1) were included to determine how changes in substitution pattern would impact inhibitory activity [96]. Second, the deletion of the β-ketone moiety in curcumin to give diarylpentanoids (Series 2), dibenzylidene-cyclohexanones (Series 3) and dibenzylidene-cyclopentanones (Series 4) is known to give rise to analogues with improved pharmacological and metabolic profiles [243, 244, 246]. These compounds may also be more potent inhibitors of the Wnt/β-catenin signaling pathway. Finally, the substitution pattern on the terminal phenyl rings were kept symmetrical (i.e. both rings share the same substitution pattern) and largely restricted to groups present on curcumin. Thus the 3'OCH$_3$-4'OH substitution pattern of curcumin was modified by (i) excluding either one substituent to give 3'OCH$_3$ or 4'OH analogs; (ii) removing both substituent; (iii) switching their positions to give 3'OH-4'OCH$_3$ substituted rings; and (iv) introducing an additional OCH$_3$ in place of OH. An exception was the introduction of fluorine which was made in view of the bioisosteric relationship between F and H, as well as the anomalous properties of fluorine which have led to improved activities in many instances [247-249]. It is noteworthy that except for some fluorinated analogues, other compounds have physicochemical properties that comply with the Lipinski's Rule of Five [250] which provide guidelines for drug-like profiles related to good oral bioavailability. In fact, 38 of the 43 synthesized analogues have enhanced lipohilicity compared to parental curcumin (Appendix 1). For example, the LogP for analogue **3-7** is 5.76 compared to 2.94 for parental curcumin.

Table 4-1. Structures of curcumin analogues (Series 1-5).

Compound	R1 (3')	R2 (4')
Series 1		

Compound	R1 (3')	R2 (4')
1-1 (curcumin)	OCH_3	OH
1-2	OCH_3	OCH_3
1-3	OH	OCH_3
1-4	H	H
1-5	OCH_3	H
1-6	H	OH
1-7	F	F

Series 2

Compound	R1 (3')	R2 (4')
2-1	OCH_3	OH
2-2	OCH_3	OCH_3
2-3	OH	OCH_3
2-4	H	H
2-5	OCH_3	H
2-6	H	OH
2-7	F	F

Series 3

Compound	R1 (3')	R2 (4')
3-1	OCH_3	OH
3-2	OCH_3	OCH_3
3-3	OH	OCH_3
3-4	H	H
3-5	OCH_3	H

3-6	H	OH
3-7	F	F
3-8	2'F	
3-9	F	H
3-10	H	F

Series 4
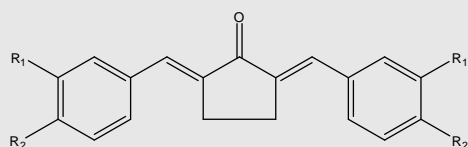
4-1	OCH$_3$	OH
4-2	OCH$_3$	OCH$_3$
4-3	OH	OCH$_3$
4-4	H	H
4-5	OCH$_3$	H
4-6	H	OH
4-7	F	F
4-8	2'F	
4-9	F	H
4-10	H	F

Series 5
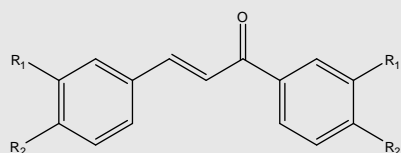
5-1	OCH$_3$	OH
5-2	OCH$_3$	OCH$_3$
5-3	OH	OCH$_3$
5-4	H	H
5-5	OCH$_3$	H
5-6	H	OH
5-7	F	F
5-1	OCH$_3$	OH
5-2	OCH$_3$	OCH$_3$
5-3	OH	OCH$_3$
5-4	H	H
5-5	OCH$_3$	H
5-6	H	OH
5-7	F	F

In total, we evaluated the effects of 43 curcumin analogues on the Wnt/β-catenin pathway and identified 6 promising analogues that were effective in suppressing β-catenin/TCF transcriptional activities in osteosarcoma with a lower EC_{50} compared to parental curcumin. Results from invasion assays further demonstrated that these analogues were more potent than curcumin in osteosarcoma, possibly through suppressing MMP-9. Perturbations of genes related to Wnt signaling components and other Wnt-targeted genes following treatment with the most potent analogue (**3-3**) indicated that **3-3** may be capable of disrupting Wnt signaling in U2OS cells at multiple intersections of the Wnt cascade including interrupting cell surface FZD receptor-Wnt ligand interactions, inducing proteasomal degradation of cytoplasmic β-catenin, preventing β-catenin/TCF complexation and transcription and down-regulating Wnt target oncogenes. In addition, Wnt inhibitory effects were observed to be markedly enhanced by shortening and restraining the flexibility of the 7-carbon linker moiety connecting the terminal aromatic rings of curcumin. Our results strongly suggest that curcumin analogues especially those with the dibenzylidene-cyclohexanone and dibenzylidene-cyclopentanone scaffolds are promising templates for lead optimization and may yield clinically useful candidate drugs for the treatment and prevention of osteosarcoma.

4.2 Experimental Methods

4.2.1 General experimental details for synthesis

Reagents (synthetic grade or better) were obtained from Sigma-Aldrich Chemical Company Inc (Singapore) and used without further purification. Melting points were determined in open capillary tubes on a Gallenkamp melting point apparatus and were

uncorrected. Mass spectra were captured on an LCQ Finnigan MAT equipped with an Atmospheric Chemical Ionization probe and m/z ratios for the molecular ions $(M+1)^+$ were reported. Chemical shifts of ^{1}H-NMR and ^{13}C-NMR spectra, obtained on a Bruker Spectrospin 300 Ultrashield spectrometer at 300 MHz and 75 MHz respectively, were analyzed using MestRec-C 4.9.9.6 (Mestrelab Research SL, Spain) and reported in δ (ppm) relative to tetramethylsilane (TMS) as an internal standard. Silica 60 F254 sheets (Merck, Darmstadt, Germany) and silica gel 60 (0.040-0.063) (Merck, Darmstadt, Germany) were used for Thin Layer Chromatography (TLC) and flash chromatography respectively. Purity of the final compounds were verified either by elemental analysis on a Perkin Elmer PRE-2400 Elemental Analyzer or by High Pressure Liquid Chromatography (HPLC) using two different solvent systems. Spectroscopic data, melting points, yields and purities of individual compounds were listed in Appendix 2.

4.2.2 Mechanism of reaction for Series 1 curcumin analogues

Various methods to prepare Series 1 curcumin analogues were previously reported [251-253]. Their basic principles remained the same, but differed in technique, reaction time and temperature. Generally, the first step is the protection of the active methylene group by reacting acetylacetone with boron anhydride to yield the acetylacetone-boric anhydride complex in order to avoid Knoevenagel condensation reaction of the active methylene group (Scheme 4-1). Subsequently, the less reactive methyl terminals of this complex will react with aromatic aldehyde to give Series 1 curcumin analogues in the form of the complex with boron, which is easily hydrolyzed by dilute hydrochloric acid.
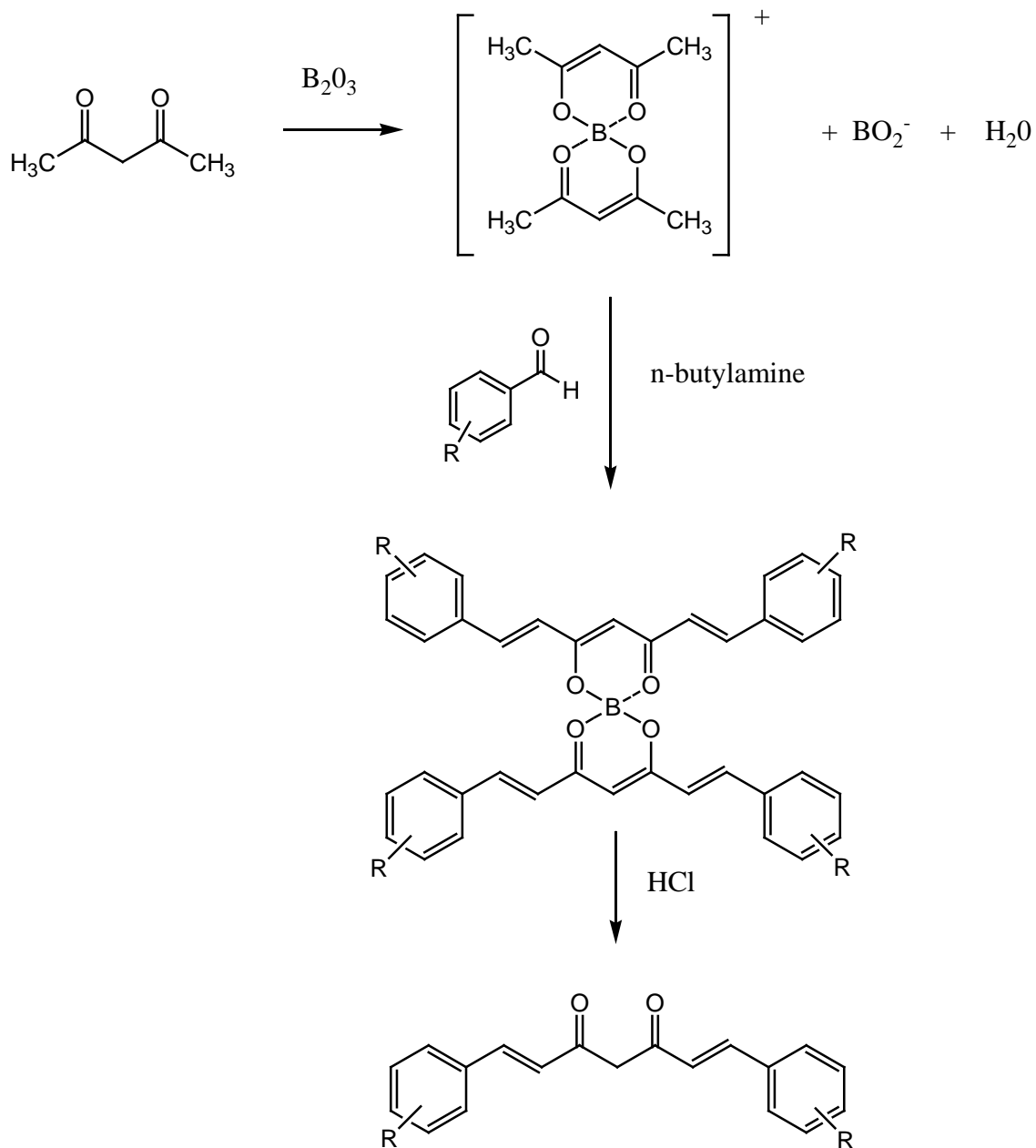
Scheme 4-1. General method for the synthesis of Series 1 curcumin analogues

4.2.2.1 General procedure for the synthesis of Series 1 curcumin analogues

Specifically, our curcumin analogues from Series 1 were prepared according to Pedersen method with slight modifications [251]. A mixture of boric anhydride (0.35 g, 5 mmol), suspended in ethyl acetate (EtOAc), and acetylacetone (1.00 g, 10 mmol) was first stirred

for 3 h at 70 ℃. After removing the solvent, the resultant white residue was washed with hexane. Following this, substituted aldehyde (20 mmol), tributyl borate (4.60 g, 20 mmol) and 20 ml EtOAc were added and stirred at room temperature for a further 30 mins. Butylamine (73 mg, 1 mmol) dissolved in EtOAc (5 ml) was then added drop wise over 15 mins and the mixture was stirred at 70 ℃ for another 24 h. Next, the reaction mixture was heated for 30 mins at 60 ℃ after adjusting to pH5 by adding 1 N HCl. EtOAc (3 x 50 ml) was then used to extract the crude product from the water layer. The organic layer was washed with brine, dried with anhydrous $NaSO_4$ and evaporated *in vacuo* to give either a solid or liquid residue and purified by column chromatography on silica gel using hexane: ethyl acetate as eluting solvents. Further purification by re-crystallization from ethyl acetate yielded yellow crystals.

4.2.3   Mechanism of reaction for Series 2, 3, 4 and 5 curcumin analogues

The alkoxylated Series 2, 3, 4 and 5 curcumin analogues were synthesized using a base-catalyzed Clasien-Schmidt condensation of a substituted aromatic aldehyde with the appropriate acetophenone in the ratio of 2:1 (Series 2-4) and 1:1 (Series 5) (Scheme 4-2) [246].
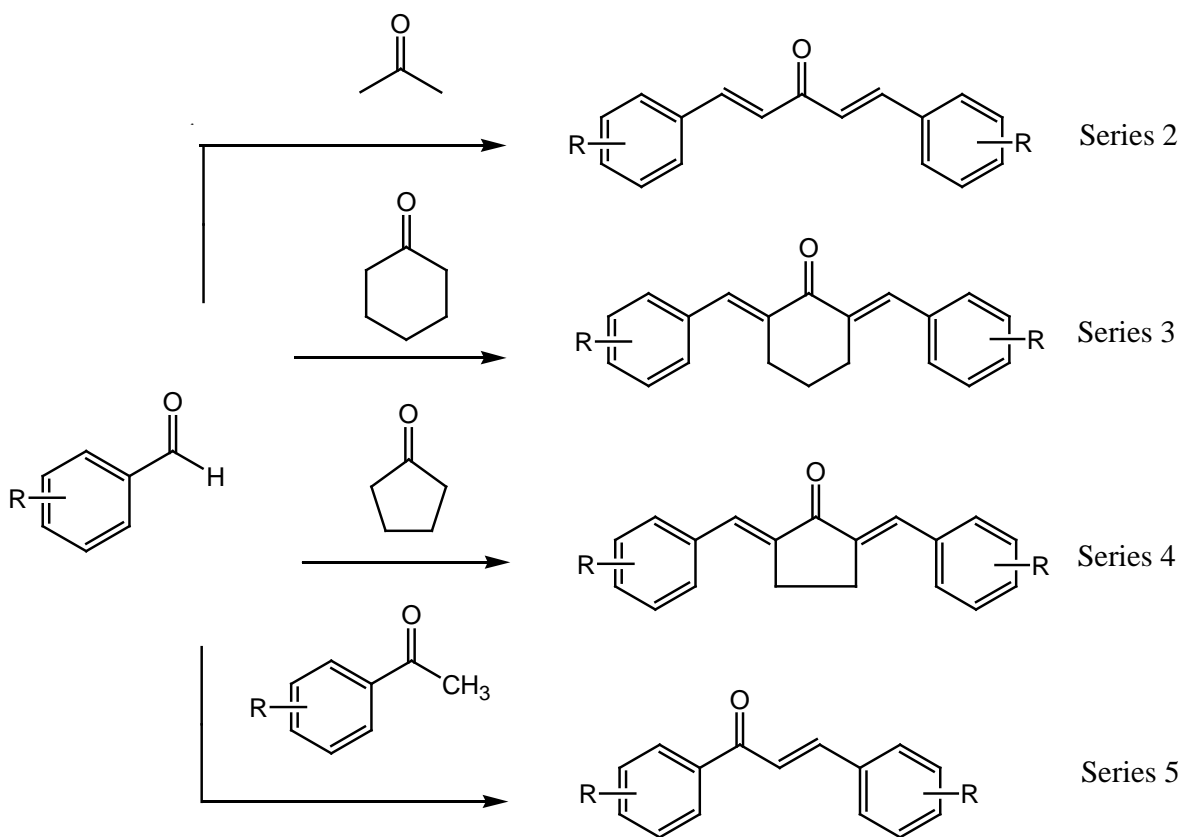
Scheme 4-2. Curcumin analogues from Series 2, 3, 4 and 5

Briefly, sodium hydroxide (20% w/v) acted as a base catalyst to protonate the methyl group of the acetophenone, forming a carbanion. The resultant carbanion attacks the carbonyl carbon of the substituted benzaldehyde via a nucleophilic addition reaction to obtain the final α, β unsaturated ketone product (Scheme 4-3).
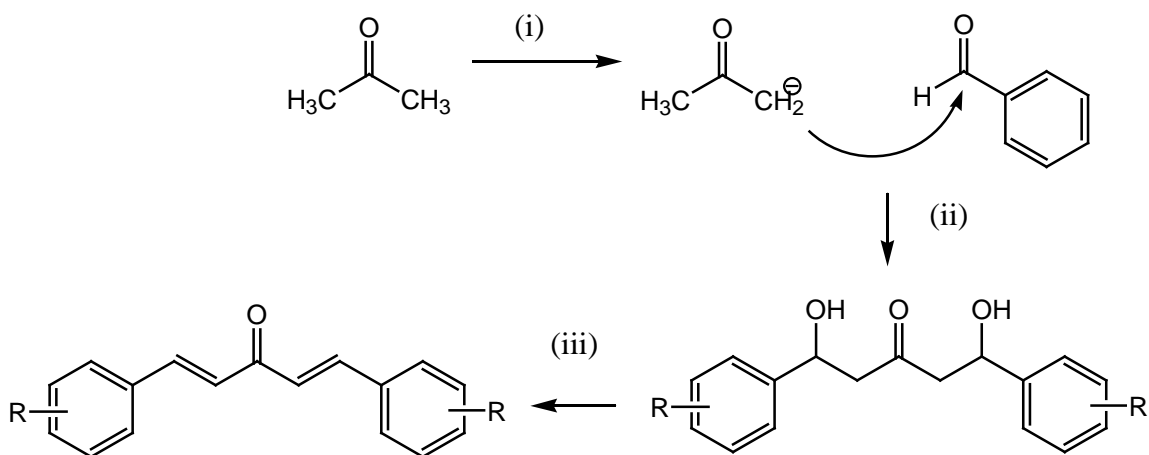
Scheme 4-3. General method for the synthesis of Series 2, 3 and 4 curcumin analogues. Reagents and conditions: (i) 20% NaOH, RT, 3h. (ii) carbanion attacks aldehyde by nucleophilic addition. (iii) Dehydration.

For the synthesis of the hydroxylated analogues from Series 2-4, protection of the phenolic groups on the aromatic aldehyde with 2H-3, 4-dihydropyran is necessary to minimize reaction between these OH groups and the carbonyl group of the benzaldehyde for improved yields (Scheme 4-4). In the case of Series 5 analogues, phenolic groups from both the aromatic aldehyde and ketone were needed. Protection converts the OH groups to tetrahydropyranyl ethers which can easily be removed by acid hydrolysis to give the desire curcumin analogues.

The dihydropyran is an enol ether which is susceptible to electrophilic attack by an acid provided by the pyridinium cation of pyridinium p-toluenesulphonate. The phenolic OH, to be protected, act as a nucleophile and attacks the α-carbon on the pyran ring, resulting in the removal of a proton form the intermediate by pyridine (which is a stronger base than p-toluenesulphonate), thus reforming pyridinium p-toluenesulphonate. The aromatic

aldehyde with its hydroxyl groups protected is then subjected to based-catalyzed Claisen-Schmidt condensation as described earlier (Scheme 4-3).
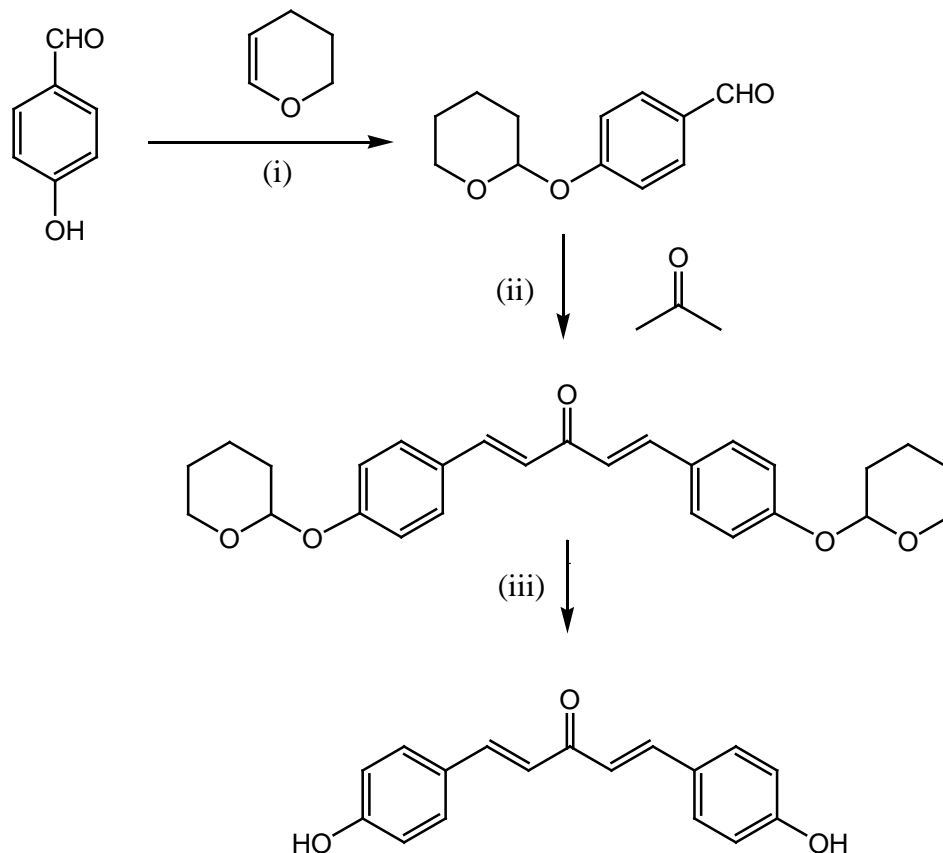
Scheme 4-4. Protection and deprotection of phenolic hydroxyl groups for the synthesis of compound 2-6. Reagents and conditions: (i) pyridinium p-toluenesulphonate, RT, 4 h. (ii) 20% NaOH, RT, 3h. (iii) 4M HCl, RT, 4 h.

4.2.3.1 General procedure for the synthesis of Series 2, 3, 4 and 5 alkoxylated curcumin analogues

The method by Liang et al. was followed [246]. To a solution of substituted benzalaldehyde (30 mmol) in methanol (20 ml) was added appropriately substituted ketone (15 mmol) such as acetone (Series 2), cyclohexanone (Series 3) and cyclopentanone (Series 4). For the synthesis of Series 5 analogues, 15 mmol of

substituted benzalaldehyde and 15 mmol of substituted ketone were used instead. The resultant mixture was stirred at room temperature for 20 mins before 20 % (w/v) NaOH (3.0 ml, 15 mmol) was added drop wise. After the reaction has completed, the residue was poured into saturated NH_4Cl solution and filtered. The precipitate was washed with brine and cold ethanol, dried with anhydrous $NaSO_4$, evaporated *in vacuo* to give either a solid or liquid residue and purified by column chromatography on silica gel using hexane: ethyl acetate as eluting solvents. Further purification by re-crystallization from ethyl acetate or ethanol yielded yellow crystals.

4.2.3.2 General procedure for the synthesis of Series 2, 3 and 4 hydroxylated curcumin analogues

For compounds with phenolic hydroxyl substituent, additional protection and de-protection of the phenolic hydroxyl groups on the benzalaldehyde were required and the method by Liang et al. was followed [246]. A solution of 3, 4-dihydro-α-pyran (44 mmol) in dichloromethane (40 ml) was added drop wise to a well stirred suspension of hydroxyl benzalaldehyde (28.8 mmol) and pyridium p-tolenesulfonate (0.32 mmol) in dichloromethane (80 ml) and stirred at room temperature for 4 h. The reaction mixture was then washed with 1 M $NaCO_3$ solution (60 ml x 3) and brine (60 ml x 3), dried with anhydrous Na_2SO_4, evaporated *in vacuo* and purified by column chromatography on silica gel using hexane: ethyl acetate as eluting solvents to yield 4-(tetrahydropyran-2-yloxy) as a pale yellow oil. This purified protected derivative was condensed with substituted ketone at a ratio of 2:1 using similar procedures as described earlier for alkoxylated curcumin analogues (Section 4.2.3.1). At the end of the reaction, the

protecting groups were removed by acidifying with 4 M HCl, followed by stirring the mixture for 4 h at room temperature. The reaction mixture was then diluted with water, followed by extracting with ethyl acetate (50 ml x 3) and the combined organic phase was washed with brine (50 ml x 3), dried over anhydrous NaSO₄, evaporated *in vacuo* and purified by column chromatography and/or re-crystallization as described earlier in Section 4.2.3.1.

4.2.3.3 General procedure for the synthesis of Series 5 hydroxylated chalcones

For chalcones with phenolic hydroxyl substituent, additional protection and de-protection of the phenolic hydroxyl groups on both the acetophenone and substituted aromatic aldehyde were required. The benzaldehyde (15 mmol) and aromatic ketone (15 mmol), were reacted separately each with pyridinium p-toluenesulphonate (1 mmol) and 3,4-dihydro-2H-pyran (40 mmol) in dichloromethane (40ml) and stirred at room temperature for 4 h. The reaction mixture was then washed with 1 M NaHCO₃ solution (60 ml x 3) and brine (60 ml x 3), dried with anhydrous Na₂SO₄, evaporated *in vacuo* to yield the crude tetrahydropyranyl ether as a pale yellow oil and used without purification. This crude protected aromatic aldehyde and ketones were then reacted at a ratio of 1:1 using similar procedures as described earlier for alkoxylated Series 5 analogues (Section 4.2.3.1). At the end of the reaction, the protecting groups were removed by acidifying with 4 M HCl, followed by stirring the mixture for 4 h at room temperature. The reaction mixture was then diluted with water, followed by extracting with ethyl acetate (50 ml x 3) and the combined organic phase was washed with brine (50 ml x 3), dried over anhydrous

NaSO$_4$, evaporated *in vacuo* and purified by column chromatography and/or re-crystallization as described earlier (Section 4.2.3.1).

4.2.4 High Pressure Liquid Chromatography (HPLC) analysis of compounds

The purity of most analogues was verified by HPLC using Waters Delta 600-2487 systems. Briefly, the compounds were dissolved in methanol and injected through a 50 µl loop at a flow rate of 1 ml/min in a Nova Pak C$_{18}$ column (2.0 x 150 mm, 10 µm particle size, (Waters Corp., Milford, USA) with UV detection at λ$_{max}$ 254 nm. Elution was done using two different mobile phases namely methanol: water (80:20) and acetonitrile: water (80:20). The retention times and peak Area Under Curve (AUC) were recorded from at least two independent determinations for each compound. Peaks were found to have >95% AUC for all compounds.

4.2.5 Cell culture, transfection and plasmids

All cell culture reagents were purchased from Sigma Chemical Co. (St Louis, MO) unless otherwise stated. The U2OS human osteosarcoma cell line was purchased from American Tissue Culture Collection (Rockville, MD) and cultured in McCoy's 5A medium. The human embryonic kidney cells HEK293T was a gift from Dr Yang Yi Yan (Institute of Biotechnology and Nanotechnology, (IBN), Singapore). These cells were grown in DMEM. Both control L cells and L cells stably transfected with a Wnt-3A expression factor (L Wnt-3A cells) were kindly provided by Professor Victor Nurcombe (Institute of Medical Biology, A*STAR, Singapore) and were maintained in DMEM supplemented with 400 µg/ml of G418. All culture media were also supplemented with 10-15 % FBS

(Invitrogen, Carlsbad, CA), 10U/ml penicillin G and 100μg/ml streptomycin. The cells were cultured in a humidified atmosphere at 37 ℃ containing 5 % CO_2. For the preparation of Wnt-3A conditioned medium (Wnt-3A CM), Wnt-3A secreting L Wnt-3A cells were cultured in DMEM supplemented with 10 % FBS for four days before this first batch of CM was harvested. Fresh medium was added and the cells were cultured for another three days. Following this, the medium was collected, combined with the previous batch and filtered using a 0.22 µM filter. TOPglow and FOPglow reporters used in the dual luciferase reporter gene assays were purchased from Upstate Biotechnology (Lake Placid, NY). The pCMV-RL renilla control vector was purchased from Promega (Madison, WI). The synthesized curcumin analogues were dissolved in DMSO before use. The final concentration of DMSO did not exceed 0.1 % in all instances.

4.2.6   Luciferase reporter gene assay

HEK cells ($1.4x\ 10^6$) grown to 40% confluency in 60 mm culture dish were transiently co-transfected with either 3ug TOPGlow, or 3ug FOPGlow, a negative control plasmid, and 0.012ug pCMV-RL Renilla control plasmids for normalization of transfection efficiency using Lipofectamine 2000 (Invitrogen, Carlsbad, CA), according to the manufacturer's instructions. On the other hand, U2OS cells (1.0×10^5/well) grown to 90–95% confluency in 24-well plates were transiently co-transfected with either 0.3μg TOPGlow or 0.3 µg FOPglow, and 1.2 ng pCMV-RL renilla plasmids. Twenty hours post transfection, both type of cells were treated with curcumin analogues at various concentrations (0.01 - 20μM) for 24 h before cell lysis and harvesting. For HEK293T cells, they were re-seeded into 96-well plates at a density of 18×10^3 cells/well before

treatment. To activate the Wnt/β-catenin signaling pathway, HEK cells were co-incubated with Wnt-3A CM and the curcumin analogues for 24 h. Luciferase assays were performed with the Dual Luciferase assay kit (Promega, Madison, WI) according to the manufacturer's instructions. For firefly luciferase activity, 20 µl cell lysate was mixed with Dual-Glo® Luciferase Reagent (100 µl) and the light output was determined in a luminometer (Tecan, MTX Lab Systems Inc., Vienna, VA). An equal volume of Dual-Glo® Stop & Glo® Reagent (100 µl) was subsequently added to the same samples and a second luminescence measurement was taken for the Renilla luciferase activity. Results were expressed as mean ± SEM of normalized ratios of Firefly luciferase and Renilla luciferase activities for each triplicate sets. Reporter activities in curcumin analogue-treated cells were expressed as the percentage of DMSO-treated samples. For HEK293T cells, the EC_{50} values were obtained from the sigmoidal curve by plotting the percentage normalized luciferase activity against the concentration of curcumin analogues using GraphPad Prism version 4.00 for Windows, GraphPad Software (San Diego, CA).

4.2.7 MTS cell cytotoxicity assay

MTS cell cytotoxicity assay was used to evaluate the cytotoxic profile of the curcumin analogues. Briefly, HEK293T and U2OS cells were seeded into 96-well plates at a density of 18 x 10^3 cells/well and 10 x 10^3 cells/well respectively and cultured for 24 h. HEK293T cells were then treated with curcumin analogues at their respective concentrations for 24 h while U2OS cells were treated with selected curcumin analogues at 1 and 5 µM. After treatment, cell viability was analyzed by adding 20 µl of CellTiter 96 AQ$_{ueous}$ One Solution Reagent (Promega, Madison, WI). Following an incubation

period of 4 h, the absorbance of the formazan product was determined at λ_{max} of 490 nm using a Tecan Spectra Fluor spectrophotometer (MTX Lab Systems Inc Vienna, VA). The percent cell viability after treatment with curcumin analogues was calculated using the following formula: % viability = ($A_{Analogues}$ − A_{Blank})/ ($A_{Control\ (DMSO)}$ − A_{Blank}) X 100%, where $A_{Analogue}$ = absorbance of wells with cells treated with curcumin analogues, A_{Blank} = absorbance of wells with media and $A_{Control\ (DMSO)}$ = absorbance of wells with cells treated with DMSO (vehicle control). Each concentration of curcumin analogue was performed in triplicate on three separate occasions.

4.2.8 Western blot analysis

Western blotting was used to examine the protein expression levels of β-catenin, MMP-9, and cyclin D1 before and after 24 h treatment of curcumin analogues using similar methods detailed in section 3.2.5. Primary and secondary antibodies used were similar to those mentioned earlier (section 3.2.5). For the collection of proteins from the cytosolic and nuclear fractions, the NE-PER cytoplasmic and nuclear protein extraction kit (Pierce, Rockford, IL) was used according to the manufacturers' protocol. Bands were quantified using Quantity One software (BioRad, Hercules, CA), normalized to either α-tubulin or lamin A/C loading controls, before bands in treatment group are expressed relative to DMSO control (set as 100%).

4.2.9 Cell invasion assay

U2OS cell invasion were determined using the Matrigel invasion assays as previously described in section 3.2.4. Briefly, cells were treated with curcumin analogues at various

concentrations for 24 h and allowed to invade through the precoated inserts for a period of 48 h. Cells that have invaded to the lower surface of the membrane were then fixed with 70% ethanol and stained with 0.2% w/v crystal violet before they were counted using the Nikon Eclipse TE2000U microscope (Melville, NY). Invaded cells from ten random microscopic fields (200 x magnifications) were enumerated and all experiments were performed in triplicates at least.

4.2.10 Gene expression profiling using real-time PCR array

The Human Wnt Signaling Pathway RT^2 Profiller^{TM} PCR Array (SA Bioscience, MD) was used to identify changes in expression of 84 key genes related to Wnt-mediated signaling transduction with curcumin analogue treatment. The 84 genes comprises representative upstream and downstream components of the Wnt pathway including glycosylated extracellular signaling molecule and ligands belonging to Frizzled family, cell surface receptors serving as ligands of the Wnt genes, competitive Wnt binding antagonists, intracellular signaling molecules, targets genes implicated in cancer tumorigenesis and metastasis, as well as those involved in protein modifications downstream of Wnt signaling. These genes are shown in Appendix 3. Total RNA from the osteosarcoma cell lines, treated with compounds or DMSO for 24 h, were extracted using Qiagen's RNeasy mini kit (Qiagen, Valencia, CA), followed by on-column DNase treatment to remove genomic contaminants, according to the manufacturer's instructions. RNA samples were reverse-transcribed to cDNA using RT^2 first strand kit provided according to the manufacturer's instructions (SA Bioscience, MD). Thermal cycling was performed using iQ5 machine (BioRad, Hercules, CA) and the cycling conditions are as follows: 95 ºC for 10 mins, 40 cycles of denaturation at 95 ºC for 15 s, annealing and

extension at 60 ºC for 1 min, followed by melt curve analysis (95°C, 1 min; 65 °C, 2 min (OPTICS OFF); 65 °C to 95 °C at 2 °C / min (OPTICS ON)). Gene expression was normalized to internal control housekeeping gene (GAPDH) to determine fold changes in gene expression between control (DMSO) and test (treated with analogue) samples. Average ΔCt value for each gene across triplicate arrays for each treatment group was calculated. ΔΔCt for each gene across control and experimental group were determined. Finally the fold difference was computed for each gene from control and other group as 2^ (- ΔΔCt).

4.2.11 Statistical analysis

Statistical significance for treatment groups were analyzed using the two-tailed Student's *t*-test (SPSS, Chicago, IL). The difference between values for each treatment concentration and the respective controls was considered to be statistically significant when $P < 0.05$.

4.3 Results

4.3.1 Purity of curcumin analogues synthesized

The purity of all final compounds were at least ± 0.4 % or 95% AUC based on elemental analysis and HPLC respectively (Appendix 2).

4.3.2 Preliminary evaluation of curcumin analogues on the inhibition of Wnt-3A-induced Wnt activity in HEK293T cells

Preliminary screening of curcumin analogues for potent inhibition of the Wnt/β-catenin signaling pathway was first performed with a cell-based screening system using HEK293T cells. Cells were stimulated with Wnt-3A CM following co-transfection with TOPGlow and CMV-RL renilla control vector for normalization of transfection efficiency. The transfectants were treated with increasing concentrations of curcumin analogues (1-20 µM) for 24 h. HEK293T cells have low β-catenin/TCF transcriptional activity because of low endogenous levels of β-catenin protein [254] and are thus suitable cell model for screening Wnt inhibitory activities [255, 256]. Wnt/β-catenin signaling in HEK293T cells is stimulated by incubation with Wnt-3A CM, which causes the accumulation of and stabilization of unphosphorylated β-catenin [257]. As expected, β-catenin/TCF transcriptional activities were increased approximately 30-fold with Wnt-3A CM treatment in our experiments. Table 4-2 shows the normalized luciferase activity in the presence of curcumin analogues (1-20 µM), expressed as % of DMSO with Wnt-3A activation. Compared with control, Wnt-3A CM-induced β-catenin response transcription (CRT) was inhibited by approximately 18.5 % and 38.2 % with 1 0 µM an d 2 0 µM curcumin treatment respectively (Table 4-2). Given that our lead compound, curcumin (compound **1-1**) was found to have an EC_{50} value of 20.67 ± 0.82 µM, a total of 16 other analogues (Table 4-2, bold and indicated with *) that were capable of suppressing the Wnt-3A-induced CRT by more than 50 % at 20 µM or lower concentrations (i.e. more potent than curcumin) were shortlisted for EC_{50} determinations and subsequent experiments.

Table 4-2. Screening of Series 1-5 for Wnt-3A-induced Wnt inhibitory activity in HEK293T cells.

Compound	Normalized luciferase activity (Firefly/Renilla)[a]			
	Concentration of curcumin analogues			
	1µM	5µM	10µM	20µM
Series 1 Analogues				
1-1 (curcumin)	99.36 ± 3.64	98.20 ± 3.25	82.50 ± 7.86	62.82 ± 12.43
1-2 *	**101.58 ± 3.85**	**69.97 ± 1.73**	**46.51 ± 7.23**	**N.D [b]**
1-3	99.74 ± 3.11	110.28 ± 3.12	104.61 ± 10.28	112.77 ± 1.05
1-4	108.92 ± 4.38	104.09 ± 3.44	107.10 ± 0.78	97.18 ± 7.52
1-5	97.69 ± 0.93	107.44 ± 4.01	107.46 ± 4.23	101.41 ± 6.09
1-6	100.33 ± 8.28	77.73 ± 1.80	72.47 ± 0.56	69.08 ± 1.90
1-7	83.32 ± 9.01	92.19 ± 0.54	89.20 ± 19.22	93.10 ± 20.00
Series 2 Analogues				
2-1	118.41 ± 4.13	110.87 ± 10.53	110.36 ± 23.04	90.35 ± 12.99
2-2	107.13 ± 1.15	107.55 ± 0.12	108.61 ± 0.18	103.39 ± 1.05
2-3 *	**82.49 ± 4.05**	**38.79 ± 4.05**	**34.36 ± 7.72**	**N.D [b]**
2-4	92.95 ± 2.42	82.68 ± 9.03	79.70 ± 14.16	77.94 ± 17.69
2-5	100.43 ± 5.73	113.88 ± 3.38	102.71 ± 2.53	102.89 ± 4.83
2-6 *	**62.29 ± 2.35**	**51.30 ± 6.61**	**51.97 ± 4.99**	**37.82 ± 3.55**
2-7	102.95 ± 12.98	100.02 ± 12.46	110.08 ± 6.17	110.85 ± 9.73
2-8	83.32 ± 4.79	91.17 ± 10.68	70.43 ± 9.61	57.04 ± 5.33
2-9	82.26 ± 1.03	85.89 ± 9.32	69.38 ± 2.90	64.60 ± 3.38
Series 3 Analogues				
3-1 *	**86.13 ± 0.83**	**28.92 ± 5.58**	**21.33 ± 3.76**	**N.D [b]**
3-2 *	**97.67 ± 3.10**	**64.33 ± 7.73**	**62.77 ± 3.54**	**40.82 ± 7.13**
3-3 *	**37.30 ± 1.89**	**27.70 ± 1.52**	**24.73 ± 3.69**	**21.36 ± 1.86**
3-4 *	**85.77 ± 5.65**	**49.57± 6.14**	**40.60 ± 9.16**	**39.01 ± 11.22**
3-5	93.28 ± 11.15	60.65 ± 17.70	72.65 ± 5.78	81.51 ± 21.17
3-6 *	**51.88 ± 5.86**	**26.87 ± 3.49**	**26.33 ± 4.33**	**16.65 ± 2.85**
3-7	94.54 ± 3.15	125.86 ± 14.37	117.90 ± 7.36	113.71 ± 7.28
3-8 *	**52.20 ± 1.78**	**21.86 ± 1.50**	**14.46 ± 0.63**	**20.85 ± 3.64**
3-9	96.07 ± 9.85	119.07 ± 22.15	105.06 ± 22.08	103.61 ± 12.14
3-10	70.25 ± 5.39	65.23 ± 6.27	61.58 ± 8.81	60.18 ± 2.29
Series 4 Analogues				
4-1 *	**91.57 ± 5.80**	**54.09 ± 3.98**	**37.50 ± 2.31**	**13.29 ± 2.71**
4-2 *	**88.86 ± 2.67**	**65.91 ± 6.72**	**55.48 ± 6.18**	**39.14 ± 7.24**
4-3 *	**52.57 ± 6.70**	**45.04 ± 4.96**	**39.48 ± 4.14**	**39.19 ± 4.99**
4-4 *	**82.66 ± 4.01**	**41.48 ± 5.41**	**25.28 ± 6.32**	**18.38 ± 2.08**

4-5	92.30 ± 3.09	72.74 ± 2.69	72.02 ± 5.56	61.33 ± 9.42
4-6 *	**34.34 ± 1.49**	**28.25 ± 3.16**	**19.63 ± 3.31**	**7.99 ± 2.35**
4-7	71.04 ± 7.59	73.11 ± 6.01	60.20 ± 2.41	59.50 ± 6.74
4-8	79.97 ± 12.11	75.70 ± 12.09	85.27 ± 5.60	72.80 ± 4.70
4-9	123.83 ± 16.40	119.20 ± 5.37	109.00 ± 10.25	102.60 ± 7.07
4-10	119.50 ± 10.83	112.53 ± 15.60	105.43 ± 6.10	107.71 ± 5.35
Series 5 Analogues				
5-1	111.96 ± 8.25	115.28 ± 13.91	86.91 ± 9.69	69.64 ± 6.69
5-2	94.95 ± 6.48	86.63 ± 7.68	60.30 ± 4.34	41.58 ± 5.45
5-3 *	**95.72 ± 3.92**	**53.85 ± 6.94**	**41.95 ± 4.71**	**25.72 ± 2.79**
5-4 *	**101.46 ± 5.68**	**90.57 ± 14.07**	**69.03 ± 8.78**	**18.91 ± 5.43**
5-5	106.81 ± 4.31	107.79 ± 6.37	111.19 ± 10.51	72.94 ± 7.04
5-6	92.72 ± 1.70	89.57 ± 8.74	70.85 ± 0.41	68.31 ± 6.96
5-7	117.13 ± 14.80	111.53 ± 13.34	90.21 ± 15.68	59.08 ± 6.77

[a] Results are presented as the mean ± S.E.M of normalized luciferase activity (Firefly/Renilla) from three independent experiments, expressed as % of DMSO under Wnt-3A induced condition. (*) indicates analogues designated as 'actives' and shortlisted for EC_{50} determinations (With an estimated EC_{50} value of less than 20 µM compared to curcumin (EC_{50} 20.67 ± 0.82). [b] Not determined (N.D). Tested at 1, 5 and 10 µM because of toxicity at higher concentrations.

4.3.3 Determination of EC_{50} values for Wnt-3A-induced Wnt inhibitory activity of 'active' curcumin analogues in HEK293T cells

EC_{50} values were used for the qualitative comparison of Wnt inhibitory activity for the 16 selected active curcumin analogues (Table 4-2, bolded and indicated with *) and found to be more potent than curcumin (**1-1**). As shown in Table 4-3, Series 3 and Series 4 analogues were the most promising, with several members such as **3-3**, **3-6**, **3-8**, **4-3** and **4-6** having EC_{50} values in the submicromolar ranges. Specifically, the most potent analogue from these series, **3-3** (EC_{50} 0.35 ± 0.03 µM) and **4-6** (EC_{50} 0.41 ± 0.02 µM) were approximately 60 and 51 times more potent than curcumin (EC_{50} 20.67 ± 0.82 µM) in inhibiting CRT respectively. The other analogues were between 1.2- and 40.4-fold more potent that curcumin. Transcriptional activities of the negative control FOPglow

plasmids were unaffected with treatment of all analogues at the EC_{50} values (Table 4-3), indicating that these analogues specifically inhibited β-catenin/TCF transcription. Except for **1-2**, **3-1**, **3-2**, **4-1**, and **4-2**, all the other analogues have limited cytotoxicity at their EC_{50} for inhibition of TOPGlow β-catenin/TCF transcriptional activity (Table 4-3). Taken together, we have identified several novel curcumin analogues (**3-3**, **3-6**, **3-8**, **4-3** and **4-6)** with novel effects of inhibiting the Wnt/β-catenin pathway, yet with limited cell cytotoxicity at submicromolar concentrations.

Table 4-3. EC_{50} values of selected curcumin analogues in HEK293T cells.

Series	Compound	R_1	R_2	EC_{50} of Wnt inhibition (μM)[a]	Potency (fold)[b]	Cell viability (%)[c]	FOPGlow (%)[c]
Series 1	1-1	OCH_3	OH	20.67 ± 0.82	1.0	42.43 ± 2.34	89.3 ± 3.64
	1-2	OCH_3	OCH_3	8.34 ± 0.19	2.5	41.58 ± 0.09	117.6 ± 17.36
Series 2	2-3	OH	OCH_3	1.84 ± 0.34	11.2	86.57 ± 1.52	105.1 ± 16.0
	2-6	H	OH	3.16 ± 0.24	6.5	99.2 ± 6.90	100.4 ± 11.1
Series 3	3-1	OCH_3	OH	2.63 ± 0.21	7.9	57.64 ± 12.42	87.6 ± 7.09
	3-2	OCH_3	OCH_3	15.86 ± 0.38	1.3	62.13 ± 8.65	103.6 ± 6.40
	3-3	OH	OCH_3	0.34 ± 0.01	59.7	91.64 ± 7.59	93.8 ± 8.27
	3-4	H	H	2.04 ± 0.26	10.1	99.99 ± 11.85	90.7 ± 7.08
	3-6	H	OH	0.80 ± 0.03	25.8	105.85 ± 10.14	85.1 ± 9.24
	3-8 [#]	2'F	H	0.90 ± 0.10	22.8	87.01 ± 1.84	93.0 ± 4.49
Series 4	4-1	OCH_3	OH	5.91 ± 0.46	3.5	38.40 ± 7.81	90.8 ± 4.77
	4-2	OCH_3	OCH_3	17.07 ± 1.80	1.2	40.02 ± 9.45	85.2 ± 5.97
	4-3	OH	OCH_3	0.51 ± 0.04	40.4	86.94 ± 4.52	110.2 ± 12.33
	4-4	H	H	3.08 ± 0.39	6.7	83.53 ± 3.34	82.9 ± 7.15
	4-6	H	OH	0.40 ± 0.01	50.5	81.43 ± 1.77	101.3 ± 11.3
Series 5	5-3	OH	OCH_3	3.89 ± 0.46	5.3	87.15 ± 6.87	130.7 ± 11.7
	5-4	H	H	10.95 ± 0.99	1.9	73.09 ± 12.37	111.9 ± 6.49

[a] The concentration of curcumin analogues that inhibits 50 % of TOPGlow β-catenin/TCF transcriptional activity. EC_{50} values are presented as the mean $\pm$ S.E.M from three independent experiments repeated in triplicate at least.

[b] Potency fold: EC_{50} values of curcumin/ EC_{50} values of other analogues.

[c] Normalized FOPglow transcriptional activities and cell viability of the cells on treatment with analogues at the concentrations of EC_{50}[a].

Ring substitutions at 2' Position.

4.3.4 Inhibition of the intrinsic downstream β-catenin/TCF transcriptional activity by active curcumin analogues in U2OS cells

The effects of several potent and specific curcumin analogues **2-3, 3-3, 4-3, 2-6, 3-6** and **4-6** on the intrinsic downstream β-catenin/TCF transcriptional activity were further evaluated in U2OS osteosarcoma cells. These cells present with activated Wnt/β-catenin signaling which culminates in the abnormal accumulation of β-catenin in the nucleus [73, 74]. These six analogues were selected based on the observations that analogues with 3'-OH-4'OCH$_3$ and 4'OH ring substituent have the most promising Wnt inhibitory effects (Table 4-3). Cells were transiently transfected with either TOPglow or the inactive mutant FOPglow luciferase reporter plasmids, together with the pCMV-RL renilla control vector for normalization of transfection efficiency followed by incubation with increasing concentrations of curcumin analogues for 24 h. We have previously shown that curcumin significantly inhibited β-catenin/TCF transcriptional activity in U2OS cells by approximately 27.1 % and 59.3 % at 10 μM and 20 μM respectively (Figure 4-1). As shown in Figure 4-1, curcumin analogues **2-3, 3-3, 4-3, 2-6, 3-6** and **4-6** were more potent than curcumin in suppressing β-catenin/TCF transcriptional activity in U2OS. Our findings were in parallel to our previous results using HEK293T cells which showed that these analogues were 7- to 60-fold more potent than curcumin (Table 4-3). Specifically, at as low as 0.5 μM, analogue **3-3, 4-3** and **3-6** significantly reduced β-catenin/TCF transcriptional activity in U2OS cells by approximately 27.5 %, 35.1 % and 29.2 % respectively (Figure 4-1). Compared with control, β-catenin/TCF transcriptional activities were reduced by 25.7 % and 37.0 % with analogue **2-6** and **4-6** treatments at 1 μM. The least potent analogue among those tested was also capable of significantly suppressing

49.4 % of β-catenin/TCF transcriptional activity in U2OS cells at 5 μM. Transcriptional activities of the negative control FOPglow plasmids were again unaffected in all instances, indicating that the curcumin analogues specifically inhibited β-catenin/TCF transcription in U2OS osteosarcoma cells. Taken together, our results demonstrated that curcumin analogue **2-3, 3-3, 4-3, 2-6, 3-6** and **4-6** were more potent than curcumin in suppressing β-catenin/TCF transcription in U2OS osteosarcoma cells and are promising candidates for treatment of osteosarcoma.
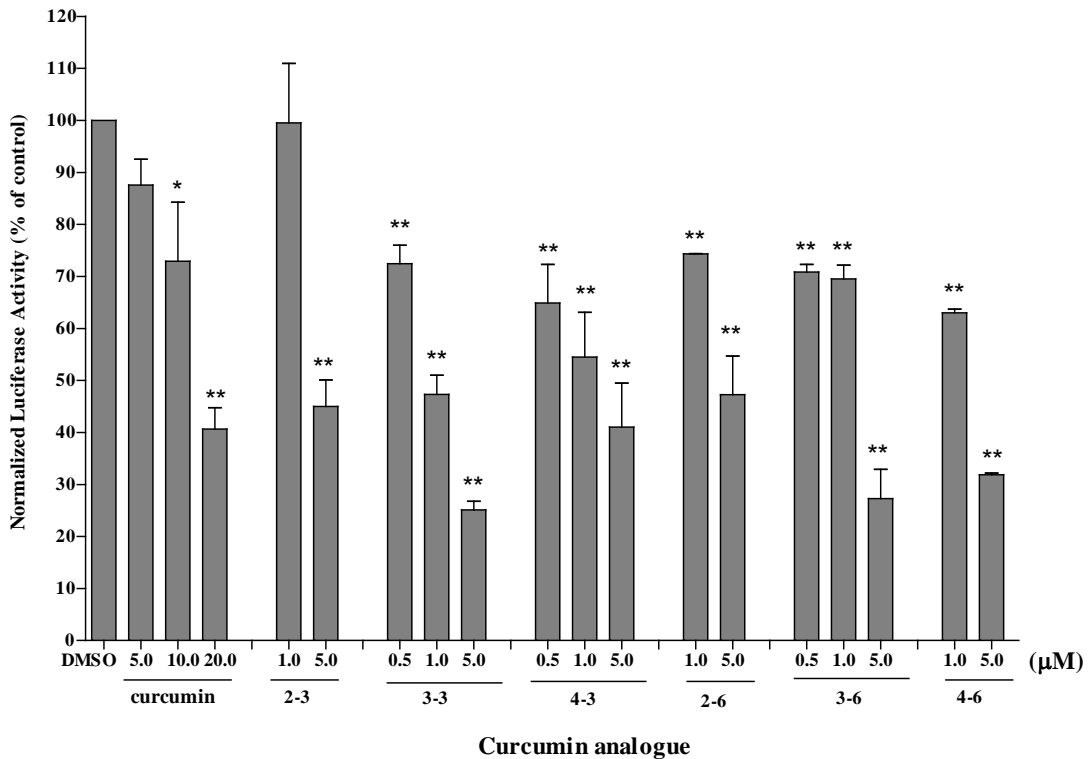
Figure 4-1. Effects of curcumin analogues on the transcriptional activity of β-catenin/TCF in U2OS cell line. U2OS cells were co-transfected with reporter genes harboring Tcf-4 binding sites (TOPglow) or a mutant TCF-4 binding site (FOPglow) and CMV Renilla gene. 20 hours post-transfection, increasing amount of test compounds were added to the cells. Firefly luciferase activity was determined 24h post-treatment, normalized against values for the corresponding Renilla luciferase activity. Results were expressed as the means ± SEM of normalized ratios of firefly luciferase and renilla luciferase measurements of three independent experiments. Reporter activity in compound-treated cells is expressed as the percentage of DMSO-treated samples. * P<0.05, ** P<0.01.

4.3.5 Effects of selected curcumin analogues on the nuclear translocation of β-catenin in U2OS cells

The activation of β-catenin/TCF transcriptional activity results from the accumulation of nuclear β- catenin [77]. As we have previously shown that curcumin was capable of disrupting the translocation of β-catenin into the nucleus without changing the total cellular levels [195], we asked the question if the analogues were also able to effect changes in the cellular contents and localization of β-catenin protein. Both nuclear and cytosolic U2OS cell lysates were collected and used for western blot analysis to determine the amount of β-catenin in each cellular fraction following treatment with 1 μM and 5 μM curcumin analogues for 24 h. As shown in Figure 4-2c, we found that the amount of β-catenin in the cytoplasm was not altered by treatments with **3-3, 2-6** and **4-6**, whereas those in the nuclear fractions were decreased by **3-3, 2-6** and **4-6** at 5 μM, suggesting that these analogues disrupted the translocation of nuclear β-catenin. Specifically, treatment with analogues **3-3, 2-6** and **4-6** resulted in an approximately 41.8 %, 52.9 % and 41.9 % reduction in nuclear β-catenin protein expression respectively (Figure 4-2d). β-catenin protein levels of both the nuclear and cytoplasmic fractions were, however, not altered with treatment of these analogues at 1 μM (Figure 4-2a-b). In contrast to analogues **3-3, 2-6**, **4-6**, and curcumin, treatment with the other analogues (**2-3, 4-3** and **3-6**) had no effects on either the nuclear or cytoplasmic β-catenin protein levels at any of the concentrations tested (Figure 4-2), suggesting that the substitution groups on the benzene rings may affect the components of the Wnt/ß-catenin cascade differentially to effect Wnt inhibition. In addition, we cannot rule out the possibility that other novel

mechanisms may be involved. Further experiments are needed to investigate the specific mechanisms of Wnt inhibition by the curcumin analogues.

(a)

Curcumin analogues (1µM)

| 2-6 | 3-6 | 4-6 | DMSO | 2-3 | 3-3 | 4-3 |

Nuclear β-catenin

Lamin A/C

Cytoplasmic β-catenin

α-Tubulin

(b)

(c)

Curcumin analogue (5 µM)

DMSO	2-3	3-3	4-3

Nuclear β-catenin

Lamin A/C

Cytoplasmic β-catenin

α-Tubulin

Curcumin analogue (5 µM)

DMSO	2-6	3-6	4-6

Nuclear β-catenin

Lamin A/C

Cytoplasmic β-catenin

α-Tubulin
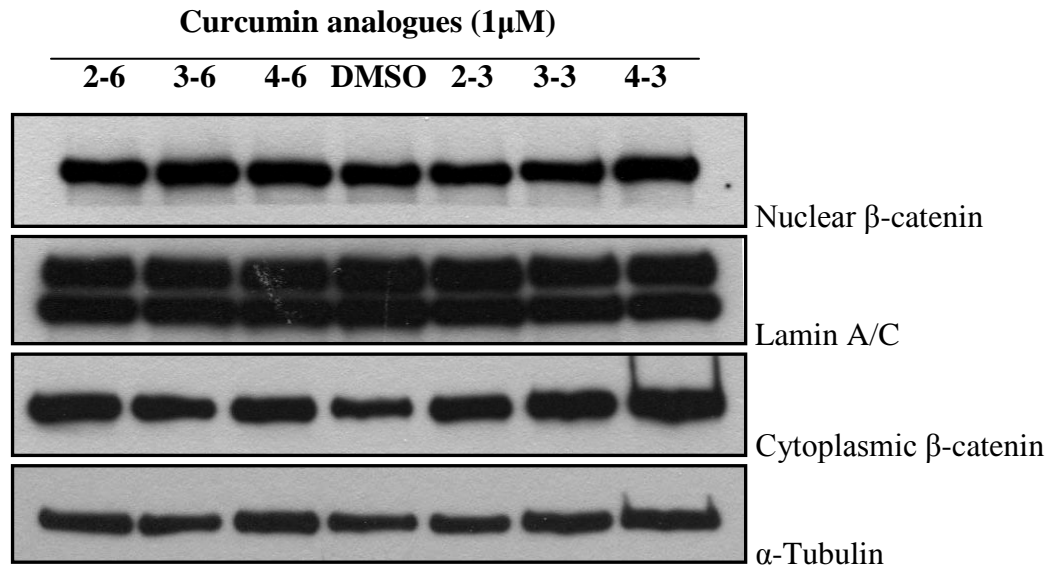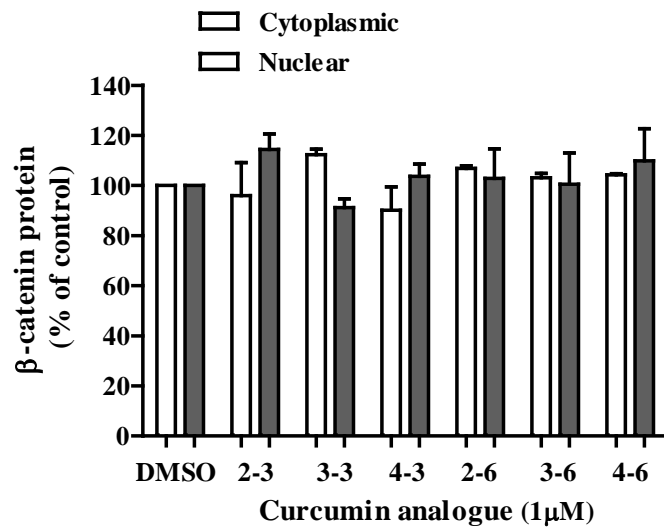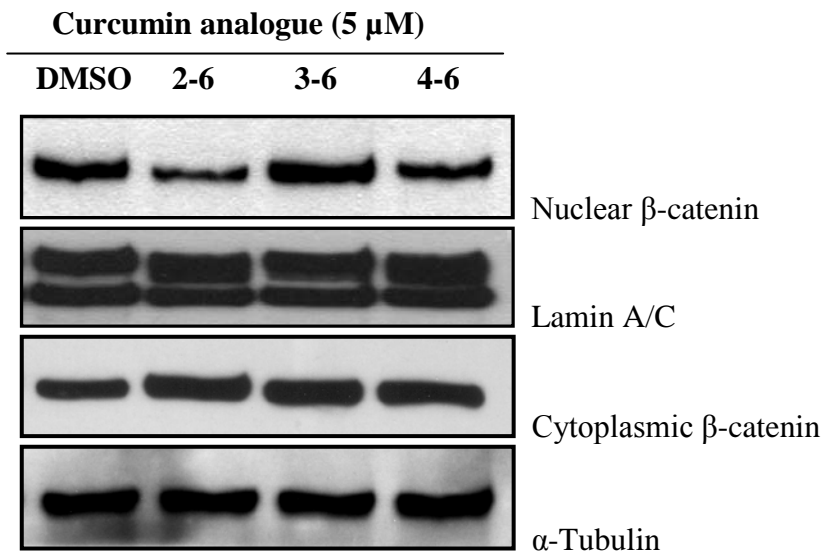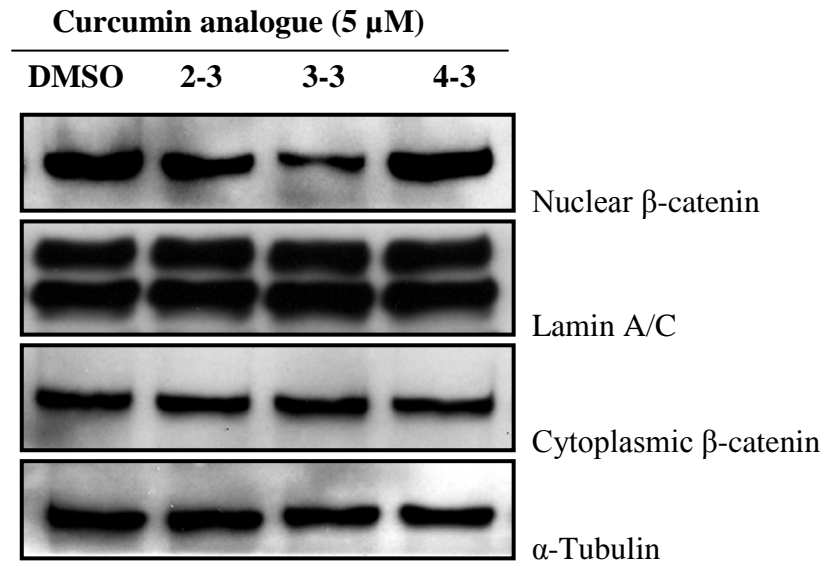
(d)
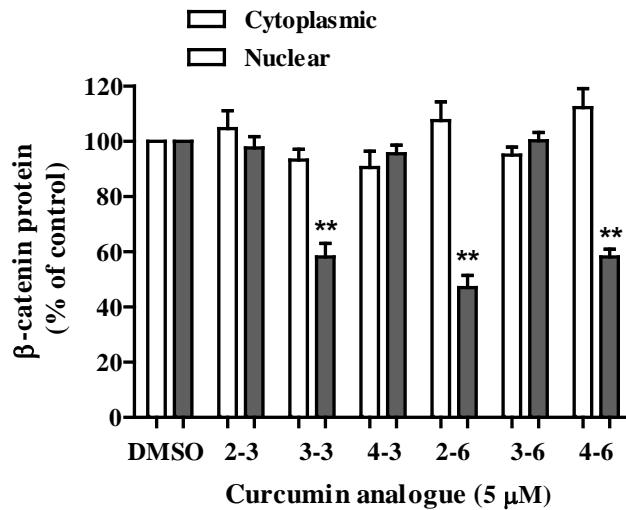
Figure 4-2 Effects of curcumin analogues treatment on the cellular and nuclear accumulation of β-catenin. **(a, c)** U2OS cells were pre-treated with curcumin analogues at the stated concentrations for 24 h, followed by collection of protein from the cytoplasmic and nuclear fraction. α-tubulin and lamin A/C were used for cytoplasmic and nuclear protein loading controls respectively. **(b,d)** β-catenin protein expression in analogue-treated cells were expressed as the percentage of DMSO-treated samples. *$,P<0.05$, ** $P<0.01$.

4.3.6 Effects of selected curcumin analogues in inhibiting U2OS cell invasion

We have recently reported that activation of the Wnt/β-catenin pathway via forced expression of wild-type β-catenin plasmid drastically enhanced the invasive capacity of U2OS cells, but this effect was significantly reversed by curcumin in a dose-dependent manner [195]. To determine if curcumin analogues could exert similar, but more potent anti-invasive effects, we next performed Matrigel invasion assays using U2OS cells. U2OS has been reported to be highly metastatic [213], but as shown in Figure 4-3a the curcumin analogues significantly reduced the ability of U2OS cells to invade through the Matrigel-coated inserts over a period of 48 h dose-dependently. While curcumin treatment significantly reduced the invasive capacity of U2OS cells by 29.0 ± 5.1 % at 5

µM, treatment with analogue **2-3, 3-3, 4-3, 2-6, 3-6** and **4-6** drastically suppressed U2OS cell invasiveness by 63.0 ± 2.4 %, 76.2 ± 1.4 %, 69.3 ± 4.9 %, 81.6 ± 2.6 %, 74.5 ± 5.4 %, 72.8 ± 0.96 % at the same respectively concentration (Figure 4-3b). We found that these analogues were also effective in suppressing U2OS cell invasion by between 34.8 ± 2.2 % to 71.0 ± 5.9 % at a lower treatment concentration of 1 µM. The anti-invasive effects of these analogues were observed at concentration ranges (1-5 µM) that are shown to inhibit downstream β-catenin/TCF transcriptional activities (Figure 4-1) and were not a result of cell toxicity given that U2OS cells did not exhibit significant growth inhibition at these concentrations (Figure 4-3c). Altogether, our results suggest that analogues **2-3, 3-3, 4-3, 2-6, 3-6** and **4-6** were more potent than the parental curcumin in inhibiting U2OS invasiveness.

(a)

Curcumin Analogues (1 µM)

DMSO 2-3 3-3 4-3

2-6 3-6 4-6
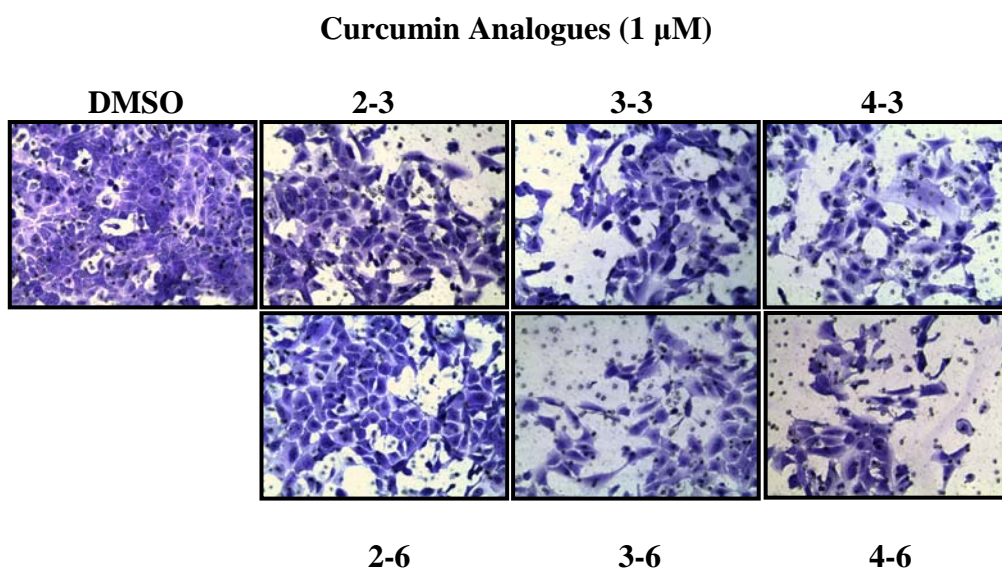
(b)
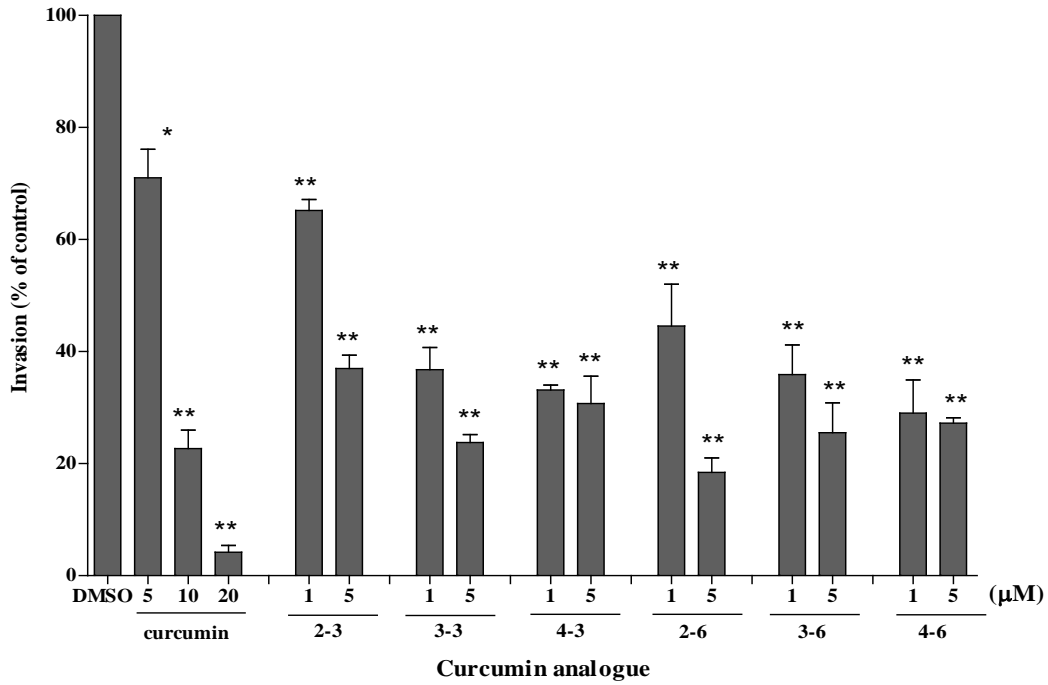
(c)
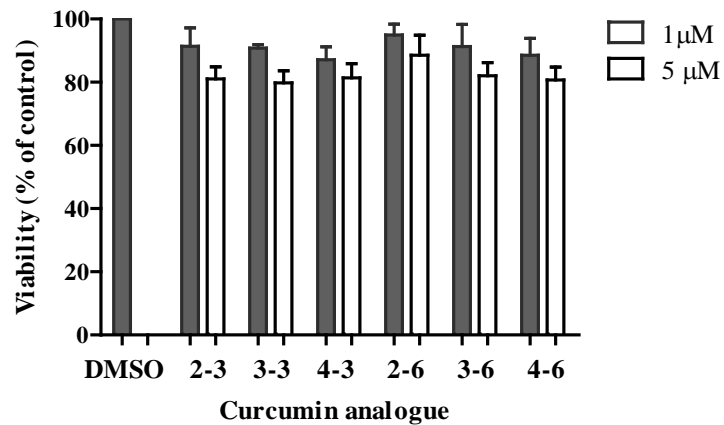
Figure 4-3. Dose-dependent inhibition of U2OS cell invasion by curcumin analogues.
(a) Representative images from three independent experiments showing a dose- and time-dependent inhibition of U2OS migration by curcumin analogues at 1 μM. **(b)** U2OS cells

pre-treated with curcumin analogues or DMSO for 24 h were seeded into Matrigel-coated inserts. Cells that invaded to the lower surface of the insert over a period of 48 h were captured with a light microscope at 200x magnification after staining with crystal violet dye. Ten random fields were counted for the number of invaded U2OS cells. Data were presented as means ± SEM of three independent experiments. Cell invasion in compound-treated cells was expressed as the percentage of DMSO-treated samples, *, $P<0.05$, **, $P<0.01$. (c) Effect of curcumin analogues on osteosarcoma cell proliferation. MTS cell cytotoxicity assay was used to evaluate the cytotoxic profile of the curcumin analogues. U2OS cells were treated with curcumin analogues for 24 h at the concentrations indicated. The results shown were means ± SEM from three independent experiments repeated in triplicate. Cell viability in compound-treated cells was expressed as the percentage of DMSO-treated samples.

4.3.7   Effects of selected curcumin analogues on protein expression of Wnt responsive genes (MMP-9 and cyclin D1) in U2OS cells.

MMPs play important roles in the degradation of extracellular matrix to facilitate osteosarcoma cancer cell invasion and metastasis [216]. In particular, MMP-9 is a well known Wnt target gene that is associated with enhanced osteosarcoma tumor invasion and metastasis [217-219]. Indeed, in our earlier study, we showed that curcumin elicited a reduction in the secretion of MMP-9 under conditions of either endogenous and/or exogenous Wnt/β-catenin activation, possibly giving rise to reduced invasiveness of U2OS cells (Figure 3-9). Thus using Western blotting, we further examined whether reduced invasion with curcumin analogues treatment correlated with MMP-9 protein levels in U2OS cells. As shown in Figure 4-4, we observed reductions in MMP-9 protein expression with analogue treatments at 1 μM and 5 μM. These effects correlated to the reduced anti-invasive effects of these analogues at similar concentrations used in the Matrigel invasion assays (Figure 4-3). Taken together, our findings suggest that curcumin analogues elicited a reduction in the MMP-9 protein expression at more potent

concentrations compared to curcumin, possibly explaining the reduced invasiveness of U2OS cells as seen in Figure 4-3.

Besides MMP-9 levels, we also tested the effects of curcumin analogue treatments on other Wnt downstream markers such as cyclin D1. As shown in Figure 4-4 , we observed a dose-dependent suppression of cyclin D1 with treatment of the analogues.
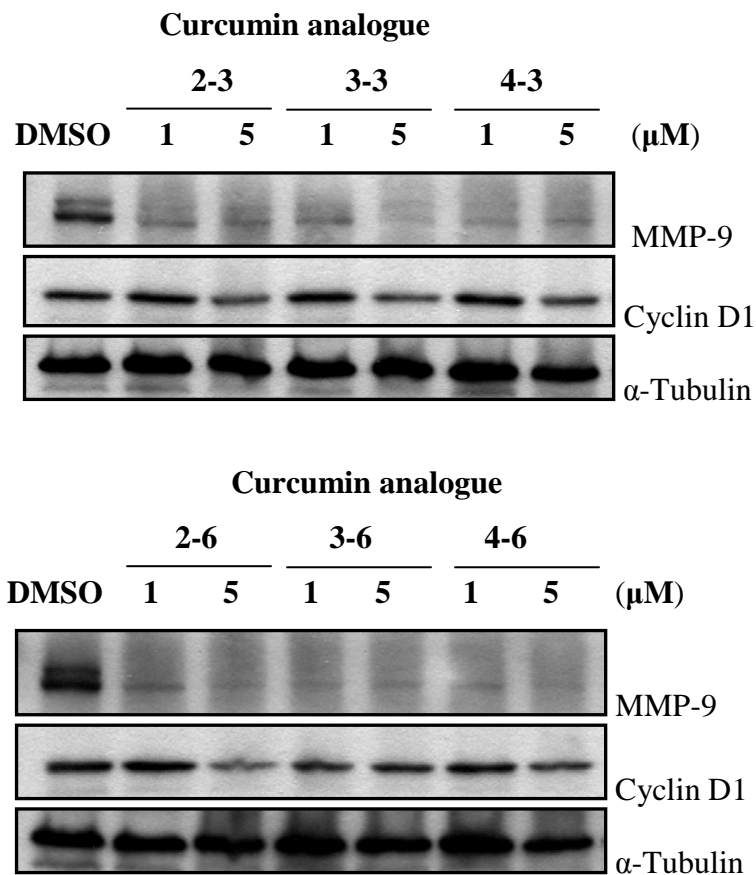
Figure 4-4. Curcumin analogues inhibit MMP-9 and cyclin D1 protein expression in osteosarcoma. U2OS cells were treated with indicated concentrations of curcumin analogues or DMSO for 24 h before proteins were collected for western blot. These blots shown were representative of three independent experiments. α-Tubulin was used as a loading control.

4.3.8 Structure-Activity-Relationship (SAR) Analysis of the Wnt-inhibitory activity of curcumin analogues

To have a better understanding of the structural features important for Wnt inhibitory effects, we examined the SAR among the curcumin analogues. As shown in Tables 4-2 and 4-3, out of 16 compounds identified to be more potent than curcumin (**1-1**, EC_{50} 20.67 ± 0.82 μM), 11 were from Series 3 and 4, in which the terminal phenyl rings were linked by conformationally restricted dibenzylidene-cyclopentanone and dibenzylidene-cyclohexanone ring structures. All non-fluorinated cyclic analogues from both series, except those with 3'-methoxy ring substituent (**3-5** and **4-5**) were found to be more potent than curcumin. These active cyclic analogues significantly reduced luciferase activity in HEK293T cells by approximately 78.1 % to 34.1 % at as low as 5μM. A few others such as **3-3, 3-6, 3-8, 4-3** and **4-6** significantly suppressed Wnt activity at even lower concentrations of 1 μM. Interestingly, compound **3-8**, which was mono-fluorinated at the 2' position, was found to be active, with luciferase activity reduced to only approximately 45.7 % and 15.0 % at 5 μM and 10 μM concentrations respectively. This trend was however not seen for compound 4-8 in Series 4. Nor was it observed among other fluorinated analogs (4'-F or 3', 4'-diF) represented across the different series. We also observed that analogues that were substituted with a methoxy group at the 3' position showed consistently poor activity in all series. On the other hand, the inclusion of another methoxy group to give 3'4'-dimethoxy improved activity in Series 1, 3 and 4. Next, comparison of the EC_{50} values among analogues from Series 2-5 with various aromatic ring substitutions showed that Wnt inhibitory effects were influenced by the nature of the ring substituent which may be broadly ranked in the sequence: 3'-OH-4'-OCH3 ≈ 4'-

OH (most active) >> 3'-H-4'-H > 3'-OCH3 4'-OH > 3'-OCH$_3$ -4'-OCH$_3$ >> 3'-OCH$_3$ ≈ 4'-F ≈ 3' -4'-F (least active). For Series 1 analogues, the only compound that exhibited significantly greater Wnt activity than curcumin was compound **1-2**, which has a 3'-4'-di-methoxyl substituent. A couple of chalcones, which lacks structural symmetry is capable of suppressing Wnt activity with an EC$_{50}$ values that were at least 2-fold higher than curcumin.

4.3.9 Real time PCR array analysis of related Wnt components and target genes with curcumin analogue 3-3 treatment in U2OS cells

The global changes in gene expression of related Wnt components with analogue **3-3** treatment (most potent) was tested using the Human Signaling Pathway RT^2 Profiler^{TM} PCR array. As mentioned in Section 4.2.10 (Material and Methods), these 84 genes comprises representative upstream and downstream components of the canonical Wnt/β-catenin pathway. Expressions of selected genes that were significantly up- or down-regulated (p-value < 0.05) were presented in Table 4-4 while the others were reported in Appendix 3. As shown in Table 4-4, the expressions of β-TrCP and Transducin-like Enhancer of Split 2 (TLE2) were significantly up-regulated 1.54- and 2.40-fold following analogue **3-3** treatment at 1 µM for 24 h respectively. On the other hand, the gene expressions of Wnt ligands including WNT 5a, 5b, 6, 7a, 7b, 8a, 10a and 11 were significantly suppressed, while all 16 Wnt ligands tested, except WNT 2b, were down-regulated with curcumin analogue **3-3** treatment (Appendix 3). Similarly, the gene expression of all FZD (FZD1-8) were decreased following 1 µM curcumin analogue **3-3** treatment, but statistical significance was observed only for FZD2, FZD3 and FZD4, with

3.77-, 1.34- and 2.60-fold reduction respectively. Furthermore, expressions of several Wnt target genes that are critical for cancer tumorigenesis and metastasis such as FOS-like antigen 1 (FOSL1), PITX2, WISP1 and cyclin D1 were markedly suppressed in U2OS cells after treatment with curcumin analogue **3-3**. T-cell specific transcription factor 7-like 1 (TCF7L1), a member of TCF/LEF transcription factors that function as a mediator of the Wnt/β-catenin transcription, was also inhibited. Much to our surprise, we found a reduction in the gene expressions of two negative regulators of the Wnt/β-beta-catenin/TCF signaling pathway. These two genes were SFRP1 belonging to a family of five glycoprotein (SFRP1-5) that competes with FZD for binding of Wnt ligands and Naked Cuticle Homolog 1 (NKD1), a dishevelled-binding protein (Table 4-4). Taken together, this global analysis has provided some preliminary observations that may explain the mechanism of Wnt inhibition by curcumin analogue **3-3** in U2OS cells. Our results suggest that down-regulation of target oncogenes critical for cancer tumorigenesis and metastatic transformation including FOSL1, PITX2, WISP1 and cyclin D1, may possibly contribute synergistically to the reduction of invasiveness of U2OS cells observed in the preceding invasion assay (Figure 4-3).

Table 4-4. Effects of curcumin analogue 3-3 on related Wnt components and target genes in U2OS cells using Human Wnt signaling real time PCR array analysis.

Gene	Gene symbol	Function	Fold change	p-value	Up (↑) / down (↓) Regulation
Beta-transducin repeat containing	β-TrCP	A component of an E3 ubiquitin ligase complex, which functions in phosphorylation-dependent ubiquitination of cytoplasmic β-catenin, thus destabilizes it.	1.54	0.047	↑
Transducin-like enhancer of split 2	TLE2	Mammalian homologue of the Drosophila groucho which serves as a nuclear transcriptional co-repressor by interacting with TCF family of proteins to block TCF/β-catenin transcription and thus repress Wnt target oncogenes	2.41	0.00052	↑
Cyclin D1	CCND1	Wnt target oncogene that stimulates tumor cell proliferation and cell cycle progression in the G1/S phase.	1.46	0.042	↓
FOS-like antigen 1	FOSL1	Member of FOS protein family that is implicated as regulator of tumor cell proliferation, invasion, motility, differentiation and transformation.	4.57	0.044	↓
Frizzled receptor 2	FZD2	Member of the 'frizzled' gene family encode 7-transmembrane domain proteins receptors that interacts with Wnt signaling proteins to initiate Wnt signaling.	3.77	0.030	↓
Frizzled receptor 3	FZD3		1.34	0.015	↓
Frizzled receptor 4	FZD4		2.60	0.029	↓
naked cuticle	NKD1	A Dishevelled-binding protein that functions as a negative	2.29	0.017	↓

homolog 1		regulator of the Wnt/β-beta-catenin/TCF signaling pathway			
paired-like homeodomain 2	PITX2	A transcriptional factor of the Wnt/β-catenin signaling that promotes tumorigenesis by directly activating cyclin D1, cyclin D2 and c-Myc expressions.	3.85	0.030	↓
secreted frizzled-related protein 1	SFRP1	Belongs to a family of five glycoprotein (SFRP1-5) that competes with Frizzled receptors for bind Wnt ligands, but has been shown to be capable of increasing Wnt signaling rather than antagonizing it in some conditions	1.56	0.00062	↓
T-cell specific transcription factor 7-like 1	TCF7L1	Member of TCF/LEF transcription factors that function as mediator of the Wnt/β-catenin transcription	2.92	0.031	↓
WNT1 inducible signaling pathway protein 1	WISP1	A member of the connective tissue growth factor that is frequently over-expressed in various tumors, and is involve in the regulation of various processes leading to tumorigenesis and malignant transformation including cell proliferation, migration, adhesion, angiogenesis and extracellular matrix formation.	2.82	0.027	↓
Wingless-type MMTV integration site family, member 5a	WNT 5a	Secreted signaling protein that are implicated in oncogenesis and in several developmental processes	2.55	0.019	↓
Wingless-type MMTV integration site family, member 5b	WNT 5b		2.36	0.012	↓

Wingless-type MMTV integration site family, member 6	WNT 6	4.37	0.029	↓
Wingless-type MMTV integration site family, member 7a	WNT 7a	2.47	0.039	↓
Wingless-type MMTV integration site family, member 7b	WNT 7b	4.21	0.011	↓
Wingless-type MMTV integration site family, member 8a	WNT 8a	1.35	0.0055	↓
Wingless-type MMTV integration site family, member 10a	WNT 10a	3.40	0.015	↓
Wingless-type MMTV integration site family, member 11	WNT 11	9.89	0.000005	↓

Selected genes that are involved in the Wnt/β-catenin signaling in U2OS cells treated with curcumin analogue **3-3** were listed. The gene symbol, gene function, fold-change, p-value, status of transcription has been described for each gene. The fold-changes in gene expression and p-values of the full list of the 84 genes were reported in Appendix 3.

4.4 Discussion

We have established in Chapter 3 that Wnt inhibition mediated by curcumin could result in reduced osteosarcoma proliferation and invasion. However, the clinical application of curcumin as a Wnt inhibitor is likely to be curtailed given its poor bioavailability due to poor absorption and rapid metabolism, and high concentrations needed for effective Wnt inhibition for good *in vivo* pharmacological bioavailability [243, 244, 246]. We thus aimed in this chapter to identify more potent curcumin analogues, elucidate important chemical features for improved Wnt inhibitory potency and provide preliminary observations on their mechanism of action.

Based on the rationale of drug design as described in (Sections 4.2.2 and 4.2.3), we have synthesized and evaluated five series of curcumin analogues for improved potency as Wnt inhibitors in osteosarcoma. Our preliminary screening yielded 16 compounds that were 1.2- to 40.4-fold more potent than curcumin in suppressing CRT (Table 4-3). A study of SAR revealed that Series 3 (dibenzylidene-cyclohexanones) and Series 4 (dibenzylidene-cyclopentanones) analogues, both with conformationally restricted and bulkier tethers between the terminal phenyl rings, exhibited much higher Wnt inhibitory potency than the other analogues in which the terminal rings were linked by longer and more flexible carbon spacers such as the diarylheptanoids (Series 1), diarylpentanoids, (Series 2) and chalcones (Series 5). Specifically, 11 of the 16 analogues that were identified to be more potent than our lead compound (curcumin, **1-1**) in suppressing the Wnt-3A-mediated transcriptional activity were from Series 3 and 4. In addition, all analogues from Series 3 and 4, except compounds **3-5** and **4-5** were capable of inhibiting

activated Wnt activity in HEK293T cells. Besides having the largest number of potent analogues, cyclic analogues (Series 3 and 4) also gave rise to the most potent analogues such as compound **3-3** (EC_{50} 0.34 ± 0.01 μM) and **4-6** (EC_{50} 0.40 ± 0.01 μM) which were 51- to 60-fold more potent than curcumin (**1-1**, EC_{50} 20.67 ± 0.82 μM), strongly suggesting the importance of restricting the flexibility of the central linker for Wnt inhibitory potency. In fact, in terms of number of rotatable bonds, the Series 3 and 4 compounds (two rotatable bonds) have the most restricted carbon tethers. This is followed by the chalcones (three rotatable bonds), series 2 (four rotatable bonds) and series 1 (five rotatable bonds). There is also a change in lipophilicity across the five series. Based on analogs with unsubstituted phenyl rings (**1-4,2-4, 3-4, 4-4, 5-4**), lipophilicities estimated by ClogP decreased in the order **3-4** (ClogP 5.33) > **4-4** (ClogP 4.77) > **1-4** (ClogP 4.57) > **2-4** (ClogP 4.20) > **5-4** (ClogP 3.62). It is notable that besides restricting flexibility, embedded ring structures within the linker as in Series 3 and 4, led to increases in lipophilicity. However, no significant correlation could be established between EC_{50} for Wnt inhibition and ClogP values.

In curcumin, the terminal phenyl rings were substituted with 3'-OCH_3-4'-OH substituent. A recent study by Ryu et al. showed that natural derivatives of curcumin, such as demethoxycurcumin and bisdemethoxycurcumin, which lack one or more methoxy groups on both rings, suppressed the transcriptional co-activator, CBP/p300, but had no effects on the protein expression of both cytoplasmic and nuclear ß-catenin and nuclear TCF-4 whereas removal of the double bond in tetrahudrocurcumin abolished Wnt inhibitory activity entirely [96]. In our study, the importance of maintaining these

substituents at the terminal rings of Series 1-5 compounds was investigated by various permutations centered on the OH/OCH$_3$ groups. Thus, the positions of these groups were reversed (3'-OH-4'-OCH$_3$) or replaced with 3'4'-di-OCH$_3$ or one group was omitted or both were removed to give the unsubstituted ring. One or more fluorine atoms were also introduced to the rings to test the bioisosteric relationship of F and H. Compounds in Series 1 bear the same scaffold as curcumin. It is seen that the Wnt inhibitory activity of this Series was significantly affected by the type of substituent on the terminal phenyl rings. Except for the dimethoxy analog **1-2** which was more potent than curcumin, the other analogs in this Series fared poorly in terms of Wnt inhibitory activity. Thus, it would seem that there is limited tolerance for the type of groups that can be introduced into phenyl rings of the Series 1 template. A similar trend was observed in Series 2 and 5 where no more than 2 different substitution patterns were permissible. As mentioned earlier, the central linker in these Series are of intermediate flexibility. It is observed that for both Series 2 and 5, the preferred substituent were 3'-OH-4'-OCH$_3$ and not dimethoxy as noted for Series 1. It is evident that optimal ring substitution pattern is influenced in part by the type of linker present and would be expected to vary from one series to another.

In contrast to the earlier series, Series 3 and 4 have restricted and lipophilic linkers and interestingly, their Wnt inhibitory activities were less influenced by the type of substituent on the terminal phenyl rings. Thus, the shortlisted compounds in Series 3 represent six out of the 10 different substitution patterns investigated, while in Series 4, they represent five out of the 10 different substitution patterns. Notwithstanding the

greater tolerance for different substituent on the phenyl rings, there were some groups that fared better than others, notably the 3'OH-4'OCH$_3$ identified for Series 2 and 5, as well as 4-OH emerged as top contenders. The good activity associated with the 4'-OH group (**3-6, 4-6**) is notable as 4'-OH groups are also present on the phenyl rings of curcumin. On the other hand, a 3'-OCH$_3$ group is also present in curcumin but no analog with 3'-OCH$_3$ (Series 1-5) was shortlisted for EC$_{50}$ determination.

The poor activity of the 3'OCH$_3$ analogs may suggest the need to restrain the steric dimensions of groups at this position. It may also reflect a preference for groups that are not electron withdrawing at this position. It is notable that 3'OCH$_3$ is electron withdrawing unlike 4'OCH$_3$ which is electron donating, as seen from their Hammett sigma values (σp OCH$_3$ -0.27 ; σm OCH$_3$ = 0.12). Inhibitory activity may be determined by an interplay of the size and electrostatic nature of groups at this position. Thus, the poor activity of 3'F analogs would suggest that the strong electron withdrawing effect of F has more than offset its small steric dimensions while the moderate activities of analogs with unsubstituted phenyl rings (**3-4, 4-4**) may be attributed to their limited size requirements. Taken together, it is tempting to suggest that Wnt inhibitory activity is favored by the absence of electron withdrawing groups on the terminal phenyl rings of Series 3 and 4. Support for this view is seen from the exceptionally good activities of the 4'OH analogs (**3-6, 4-6**) and the 3'OH-4'OCH$_3$ analogs (**3-3, 4-3**). As to why switching 3'OH-4'OCH$_3$ to 3'OCH$_3$-4'OH resulted in analogs (**3-1, 4-1**) with a modest decline in activity, this may be attributed to the location of the bulkier OCH$_3$ at the 3' position. A

larger lost in inhibitory activity was observed when both 3' and 4' positions were occupied by OCH_3 groups.

Taken together, some general structure activity trends may be deduced from the present results (Figure 4-5). First, reducing the flexibility of the intermediate linker joining the terminal phenyl rings improved inhibitory activity. Notably, incorporating the linker as part of a ring structure like those represented in Series 3 and 4 resulted in several compounds with outstanding activities. Second, the flexibility of the intermediate side chain influenced the substitution on the terminal phenyl rings that were required for good activity. In those compound series (Series 1, 2, 5) that had more flexible linkers, only limited substitution patterns were tolerated at the phenyl rings. In contrast, a wider range of substitution patterns were permitted in compound series that had less flexible linkers (Series 3, 4). In Series 3 and 4, the preferred substituent were deduced to be electron donating and/or of limited size requirements if sited at the 3' position. These requirements may reflect the involvement of these groups in key interactions with target proteins and would require further confirmation with additional analogs. These SAR trends observed would be highly valuable and may served as leads for future rational drug design for even more potent Wnt antagonists.
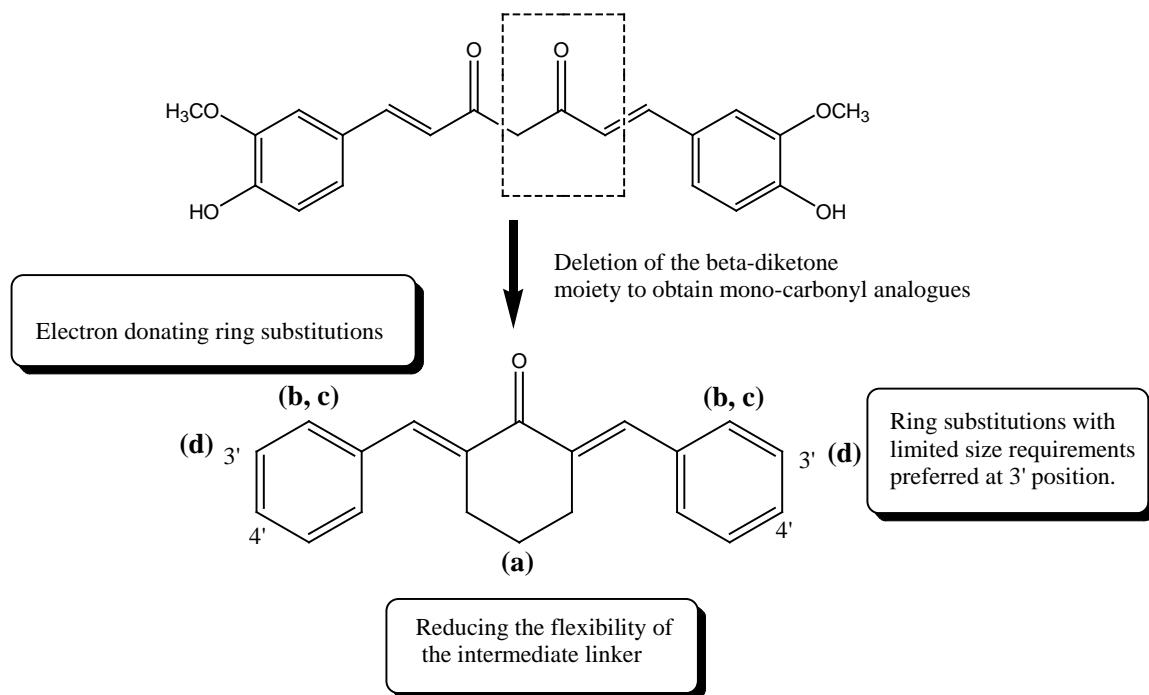
Figure 4-5. Structural features of curcumin analogues important for enhanced Wnt inhibitory activity. (a) Reducing the flexibility of the intermediate linker joining the terminal phenyl rings improved Wnt inhibitory activity. Incorporating the linker as part of a ring structure such as dibenzylidene-cyclohexanone (Series 3) and dibenzylidene-cyclopentanone (Series 4) spacers are favored. **(b)** Flexibility of the intermediate side chain influenced the substitution on the terminal phenyl rings. Only limited ring substitution patterns were tolerated in analogues with flexible linkers (Series 1, 2, 5), but a wider range of substitution patterns were permitted in analogues that had less flexible linkers (Series 3, 4). **(c)** Electron donating ring substitutions are more favorable. **(d)** Ring substitutions with limited size requirements are preferred at the 3' position.

To provide preliminary understanding of the interactions of curcumin analogues with various critical Wnt players, perturbations in gene levels of 84 Wnt signaling components and target genes by curcumin analogue **3-3** (the most potent analogue) were evaluated using the Human Wnt Signaling Pathway RT^2 Profiler^{TM} PCR Array. Our preliminary findings support a model in which analogue **3-3** is likely to attenuate the Wnt/β-catenin signaling pathway at various points of the pathway including interruption of receptor-ligand interactions at the cell surface, enhancement of proteasomal degradation of

cytoplasmic β-catenin, disruption of β-catenin/TCF complexation and transcription and inactivation of Wnt target oncogenes within the nucleus. This is supported by these observations: Firstly, suppression of mRNA expressions of several frizzled receptors (FZD2, FZD 3, FZD4) and Wnt ligands (WNT 10a, 11, 5a, 5b, 6, 7a, 7b, 8a) suggest that analogue **3-3** may attenuate receptor-ligand interactions and thus block signal initiation at the membranous level. However, it is practically challenging to determine precise binding affinities and specificities of the native WNT-FZD complexes due to the lack of purified Wnt ligands and the sheer number of members identified to date [37, 38]. Secondly, the significant up-regulation of β-TrCP protein, a component of an E3 ubiquitin ligase complex, indicated that analogue **3-3** could have increased the phosphorylation-dependent ubiquitination of β-catenin, thus destabilizing β-catenin in the cytoplasm and consequently reducing its nuclear translocation. A similar mechanism of Wnt inhibition was previously observed with curcumin, which was reported to induce G2/M phase arrest and apoptosis of HCT116 colon cells through caspase-mediated degradation of cytoplasmic β-catenin [193, 207]. Thirdly, analogue **3-3** may be capable of disrupting β-catenin/TCF complexation and transcription through attenuating the nuclear translocation of β-catenin protein (Figure 4-2) and regulating the expression of several transcriptional factors such as TLE2, TCF7L1 and PITX2: TLE2 gene is a mammalian homologue of the Drosophila transcriptional repressor groucho which serves as a nuclear transcriptional co-repressor by interacting with TCF family of proteins to block TCF/β-catenin transcription and thus repress Wnt target oncogenes [129, 258, 259] while PITX2, a bicoid-related homeodomain factor [260], has been shown as a downstream gene target and a transcriptional factor of the Wnt/β-catenin signaling

pathway by interacting with LEF-1 and β-catenin to activate Wnt target genes [141, 261, 262]. Collectively, analogue **3-3** may possibly disrupt β-catenin/TCF transcriptional activity and complexation through up-regulating transcriptional repressor, groucho, inhibiting TCF7L1 and/or suppressing level of PITX2 transcription factor. In particular, PITX2 is required for the temporally ordered and growth factor-dependent recruitment of a series of specific co-activator complexes that prove necessary for cyclin D1, cyclin D2 and c-Myc gene induction [261, 263]. Furthermore, silencing of PITX2 gene by hypermethylation has been closely associated with prognosis, metastasis-free survival and reduced risk of developing disease recurrence in breast cancer patients [264]. Most recently, Huang et al demonstrated that knockdown of PITX2 gene expression in human thyroid cancer cells and mouse in *in vivo* models significantly suppressed cell proliferation and soft-agar colony formation by down-regulating cyclin D1 and cyclin D2 [265]. Parallel to results from our western blot analysis (Figure 4-4), we found a suppression of cyclin D1 mRNA level with analogue **3-3** treatment. Given that both PITX2 mRNA levels, as well as cyclin D1 protein and mRNA expressions, were suppressed in U2OS cells by analogue **3-3** treatment, it is tempting to speculate that attenuation of PITX2/Wnt/β-catenin pathway may have resulted in the down-regulation of cyclin D1 in U2OS cells, although further studies using chromatin immunoprecipitaion and/or reporter assays would be necessary to confirm this.

Our curcumin analogues were also found to be effective in reducing osteosarcoma cell invasiveness by between 34.8 - 71.0 % and 63.0 - 81.6 % at 1 µM and 5 µM respectively (Figure 4-3). The observed anti-invasive effects correlated with the down-regulation of

MMP-9 protein expressions with curcumin analogue treatment (Figure 4-4). In addition, through our global analysis, we found that the most potent compound (**3-3**) could effectively suppress the mRNA expressions of several other oncogenes including WISP1 and FOSL1 that play critical roles in promoting tumorigenesis and metastatic transformation in various tumor models. WISP-1, a member of the connective tissue growth factor that belongs to the Cry61, CTGF and Noc (CCN) super family, is involved in the regulation of various processes leading to tumorigenesis and malignant transformation including cell proliferation, migration, adhesion, angiogenesis and extracellular matrix formation [266]. Several lines of evidence support a role for WISP-1 in tumorigenesis, although none has been reported with osteosarcoma. WISP-1 is over-expressed in many tumors types, including breast, colon, cholangiocarcinoma and plexiform neurofibromas [267-270]. Moreover, forced expression of WISP-1 in normal kidney fibroblasts was sufficient to induce morphological transformation, accelerate cell growth and induce tumor formation in nude mice [146]. Elevated levels of WISP-1 in both primary breast and rectal cancers correlated with more advanced features such as late-stage disease, lymph node involvements and larger tumor size [269, 271]. Similarly, FOSL1, shown to be over-expressed in numerous cancers, promotes invasion, metastasis and angiogenesis [272]. For instance, Debinski at el. demonstrated that gliomas over-express FOSL1, which is capable of modulating malignant properties in these cancer cells including morphology changes, anchorage-dependent growth and tumorigenic potential [273]. On the other hand, down-regulation of FOSL1 was reported to suppress breast cancer cell motility and proliferation through inhibition of tumor progression-association proteins including MMP-9, VEGF, MMP-1 and cyclin D1 [274]. Given their

oncogenic properties, the potential implications of regulating WISP-1 and FOSL1 expressions in osteosarcoma pathogenesis is highly relevant. Further studies are however needed to fully understand the contributory roles of these oncogenes in regulating osteosarcoma metastasis and tumorigenesis.

Anomalous observation was made with regards to two genes, namely SFRP1 and NKD1. The down-regulation of mRNA SFRP1 level following treatment with analogue **3-3** is not unexpected since SFRP1 has been shown to be capable of increasing Wnt signaling in some conditions [54, 275], although it belongs to a family of five gylcoproteins (SFRP1-5) that disrupts the pathway at the cell surface by competing with Frizzled receptors for Wnt ligands [55]. NKD1, a protein that binds to PDZ domain of DVL, is known for its function as a negative regulator of the Wnt-beta-catenin-TCF signaling pathway [106, 276]. Our observation that NKD1 was down-regulated in U2OS cells following treatment with analogue **3-3** suggested that NKD1 or/and DVL-NKD1 complex could have mediated other unknown Wnt-independent signal transduction. We also cannot rule out the possibility of compensatory response or biphasic effects of NKD1 on Wnt signaling.

CHAPTER 5.   Role of SFRPs as tumor suppressors in human osteosarcoma

5.1 Introduction

SFRPs, a family of five glycoproteins (SFRP1-5) are the largest family of endogenous Wnt inhibitors. Structurally, SFRPs contain an N-terminal cysteine–rich domain (CRD) which share 30-50 % sequence similarity with those of the ligand binding domain of the FZD and a netrin (NTR) domain. The NTR domains of SFRP1, SFRP2 and SFRP5 share a similar pattern of cysteine spacing that is related to that of netrin 1, whereas those of SFRP3 and SFRP4 display a different cysteine-spacing pattern and thus a distinct pattern of disulphide bonds [54]. Crystallographic resolution studies revealed a number of different mechanisms by which SFRPs can modulate Wnt signaling: (1) sequestering WNT ligands through both the CRD and NTR domains; (2) functioning as a dominant-negative form by formation of inactive complexes with FZD; (3) titrating out one another's activity to favor Wnt signaling; (4) favoring Wnt-FZD interaction by binding to both molecules simultaneously and (5) binding of CRD to FZD [277].

Epigenetic silencing due to hypermethylation of the promoter regions of SFRP1, 2, 4 and 5 has been found in different human cancers, suggesting tumor suppressor function of these SFRPs [61, 62, 278]. On the other hand, restoration of sFRP functions in these tumor types has been shown to effectively attenuate Wnt signaling even in the presence of downstream mutation [61]. Unlike the other SFRPs, SFRP3 does not have the CpG-islands in its promoter region. Instead, chromosomal deletion and loss of heterozygosity of the SFRP3 gene may account for its down-regulation in human malignancies, given

that the SFRP3 gene is located at 2q where frequent deletion and loss of heterozygosity are observed.

Differences in the biological effects of the various SFRPs have previously been reported in various malignancies. This is not surprising given that SFRPs do not bind to Wnt ligands in an equivalent manner, neither in terms of specificity and number of binding sites nor in terms of interaction domain. Furthermore, post-translation modifications may very likely confer additional differences that might further diversify the functions of different SFRP family members.

Recently, the loss of SFRP3 expression was reported in osteogenic sarcoma biopsy specimens and several osteosarcoma cells lines [56]. Despite strong evidence of their status as tumor suppressors, the functional significance of other family members including SFRP1, 2, 4 and 5 in the pathogenesis of osteosarcoma has yet been reported. Therefore, we hypothesized that these genes function as tumor suppressors and restoration of these may inhibit osteosarcoma tumorigenesis and metastasis. The objective of this chapter is thus to examine functional roles and mechanisms of SFRPs as tumor suppressors in regulating osteosarcoma cell proliferation, motility and invasion. Understanding this may be useful in the development of SFRPs as a therapeutic strategy in osteosarcoma.

We first examined the transcriptional expressions of SFRP genes and showed that these Wnt antagonists were down-regulated in several metastatic osteosarcoma cells lines,

compared to human fetal osteoblasts. Using SFRPs-stably transfected U2OS cell lines, we further demonstrated that forced expressions of these genes effectively suppressed β-catenin/TCF transcriptional activities and β-catenin protein levels, as well as resulted in redistribution of β-catenin protein from the nucleus to the membrane of U2OS cells. We found that ectopic expressions of SFRPs are capable of disrupting the cascade of events that leads to osteosarcoma tumorigenesis and/or metastasis including inhibition of anchorage-dependent growth rates, colony formation efficiencies, cell invasion, migration, as well as induction of G0/G1 cell cycle arrest and apoptosis. These tumor suppressing effects may be mediated though down-regulation of protein expressions of several Wnt responsive oncogenes such as MMP-2, cyclin D1, c-Myc and survivin. Furthermore, using the Human Wnt Signaling Pathway RT^2 $Profiler^{TM}$ PCR Array analysis, we identified additional Wnt target genes including WISP1, Brachyury, SLC9A3R1 and JUN that may account for the tumor-suppressing effects of SFRP2 and SFRP5 in U2OS cells. Lastly, we observed dysregulation of several Wnt signaling proteins when SFRP2 or SFRP5 expressions were restored in U2OS cells, suggesting that the molecular mechanisms of SFRP2 and SFRP5 functions may involve disruption of the Wnt signaling via interrupting WNT-FZD interactions, enhancing proteasomal degradation of cytoplasmic β-catenin, disrupting of β-catenin/TCF complexation and transcription, inactivating Wnt target oncogenes as well as up-regulating tumor suppressors genes. Taken together, our findings strongly suggest that SFRPs function as tumor suppressors in osteosarcoma, and that restoration of these genes in SFRPs-deficient osteosarcoma may be exploited as a new therapeutic approach for the treatment and prevention of osteosarcoma disease progression.

5.2 Experimental Methods

5.2.1 Cell culture, plasmids and stable transfection

The human osteosarcoma cell lines CRL11226, CRL1423, OS1, OS2 and OS3 were kindly provided by Dr Saminathan S. Nathan (Department of Orthopaedic Surgery, Yong Loo Lin School of Medicine, NUS) and have been described previously [194]. CRL11226, CRL1423, OS1-3 cells were cultured in RPMI, McCoy's 5A and RPMI: DMEM 9:1 media respectively. Human fetal osteoblasts (hFOB1.19) are a gift from Dr Tong Cao (Department of Dentistry, NUS) and were maintained in DMEM/F-12 medium. U2OS cells stably transfected with SFRPs were cultured in McCoy's 5A medium supplemented with 400 µg/ml of G418. All media were supplemented with 10-15 % FBS (Invitrogen, Carlsbad, CA), 10U/ml penicillin G and 100µg/ml streptomycin. The cells were cultured in a humidified atmosphere at 37 ºC containing 5% CO_2. TOPglow and FOPglow reporters used in the luciferase reporter gene assays were purchased from Upstate Biotechnology (Lake Placid, NY) while the pSV-β-galactosidase control vector was from Invitrogen (Carlsbad, CA). pcDNA3.1-HIS-SFRPs plasmids and pcDNA3.1-HIS empty vector controls were generous gift from Dr. Hiromu Suzuki (Sapporo Medical University, Sapporo, Japan) [61]. For stable transfection, U2OS cells were transfected with one of the pcDNA3.1-HIS-SFRP vectors or pcDNA3.1-HIS empty vector, using Lipofectamin 2000 (Invitrogen, Carlsbad, CA), according to the manufacturer's protocol. Transfected cells were selected with G418 (400 µg/ml) for 14 days, starting 48 h after transfection.

5.2.2 Western blot analysis

Western blot analyses used to examine the protein expression levels of β-catenin, active-β-catenin, SFRP1, SFRP2, SFRP4, SFRP5, MMP-2, MMP-9, cyclin D1, c-Myc and survivin in U2OS transfectants, were carried out as previously described (section 3.2.5). Anti-active-β-catenin antibody (clone 8E7), which is specific for β-catenin dephosphorylated on Ser31 and Thr41, was purchased from Upstate (Lake Placid, NY, USA). Antibodies for SFRP1, SFRP2 and SFRP4 were from Santa Cruz Biotechnology, Inc. (Santa Cruz, CA) while that of SFRP5 was purchased from ThermoFisher Scientific, (Waltham, MA).

5.2.3 Polymerase Chain Reaction (PCR)

Total RNA from the osteosarcoma cell lines was extracted using Qiagen's RNeasy mini kit (Qiagen, Valencia, CA), according to the manufacturer's instructions. Samples were treated with DNase (Ambion DNA-free kit, Applied Biosystems, Austin, TX) to remove genomic contaminants. RNA samples were reverse-transcribed to cDNA using iSCRIPT cDNA synthesis kit (BioRad, Hercules, CA), after which cDNA was amplified by PCR with primers specific for SFRP1, SFRP2, SFRP4, SFRP5 and GAPDH, using iTaq DNA polymerase kit (BioRad, Hercules, CA) and dNTP Mix (BioRad, Hercules, CA). The cycling conditions were as follows: 95 ºC for 3 mins, 30-35 cycles of denaturation at 95 ºC for 30s, annealing at 55 ºC for 30s and extension at 72 ºC for 45s, followed by a 10 mins final extension at 72 ºC. The PCR products were analyzed by electrophoresis on 3 % agarose gels. The specific primers listed in Appendix 4 were kindly provided by Dr. Hiromu Suzuki (Sapporo Medical University, Sapporo, Japan).

5.2.4 Luciferase reporter gene assay

Luciferase reporter gene assays using the U2OS transfectants were performed with Luciferase assay systems kit (Promega, Madison, WI) according to the manufacturer's instructions, as detailed previously (section 3.2.3). Results were expressed as mean ± SEM of normalized ratios of luciferase and β-galactosidase activities for each triplicate sets. Reporter activities in U2OS/SFRPs transfectants were expressed as the percentage of that in U2OS/pcDNA3.1-HIS control cells.

5.2.5 Immunofluorescence microscopy analysis

U2OS stable transfectants were seeded and cultured in tissue culture-treated Lab-Tek™ Chambered Coverglass (Bio Laboratories, Singapore). On the following day, the cells were washed with PBS, fixed with 4 % formaldehyde, permeabilized with 0.5 % Triton X-100 and blocked in 1% Bovine Serum Albumin. The cells were then incubated with anti-β-catenin antibody (Santa Cruz, CA), followed by FITC-conjugated secondary antibody (Invitrogen, Carlsbad, CA). The cell nuclei were also counterstained with DAPI (Invitrogen, Carlsbad, CA). Images were acquired on an LSM 5 DUO inverted confocal microscope (Carl Zesis Inc, Germany).

5.2.6 Anchorage-dependent MTT cell proliferation assay

The effects of SFRPs on the proliferation of U2OS cells were assessed using MTT assays. U2OS transfectants were seeded into 96-well plates at a density of 10×10^3 cells/well and cultured over a period of 3, 5 and 7 days before cell growth was analyzed by adding 100 µl of 1mg/ml MTT (Sigma Chemical Co., St Louis, MO). Following an incubation period of 4 h, DMSO was added to lyse the cells and dissolve the purple formazan crystals. The

absorbance of the formazan product was determined at λ_{max} of 595 nm using a Tecan Spectra Fluor spectrophotometer (MTX Lab Systems Inc., Vienna, VA). Cell growth over the periods of 3, 5 and 7 days was expressed relative to that on Day 1 (set as 1.0).

5.2.7   Colony formation assay

U2OS cells were transfected with each of the pcDNA3.1-HIS-SFRP vectors or pcDNA3.1-HIS empty vector, using Lipofectamine 2000 (Invitrogen, Carlsbad, CA), according to the manufacturer's protocol. Transfected cells were then reseeded in 100-mm culture dishes at a density of 1:20 and selected with G418 (400 µg/ml) for 14 days. Colonies were then fixed with 70% ethanol and stained with 0.2% w/v crystal violet before they were enumerated.

5.2.8   Cell migration and invasion assay

U2OS cell migration and invasion were determined using the wound healing and Matrigel invasion assays as previously described (section 3.2.4).

5.2.9   Cell cycle analysis

The effect of SFRPs over-expression on the cell cycle distribution was accessed by flow cytometry after staining the cells with PI as described earlier (section 3.2.8).

5.2.10 Gene expression profiling using real-time PCR array

The Human Wnt Signaling Pathway RT^2 Profiller^{TM} PCR Array (SA Bioscience, MD) was used to identify changes in expression of 84 key genes related to Wnt-mediated

signaling transduction with forced expressions of either SFRP2 or SFRP5 in U2OS cells as described earlier in section 4.2.10.

5.2.11 Statistical analysis

Statistical significance for treatment groups were analyzed using the two-tailed Student's t-test (SPSS, Chicago, IL). The difference between values for each treatment concentration and the respective controls was considered to be statistically significant when $P < 0.05$.

5.3 Results

5.3.1 Analysis of Wnt antagonist genes, SFRP1, 2, 4 and 5 in osteosarcoma cell lines

Down-regulation of SFRP genes through epigenetic silencing was commonly found in various malignancies [58, 61, 62, 278, 279]. While the loss of SFRP3 expression has previously been observed in osteogenic sarcoma biopsy specimens and several osteosarcoma cells lines [56], the functional roles of SFRP1, 2, 4 and 5 as potential tumor suppressors in osteosarcoma have yet been explored. We therefore hypothesized that a loss of SFRP1, 2, 4 or 5 may contribute to the activation of Wnt signaling and, thus be implicated in the pathogenesis of osteosarcoma. To this end, we first compared the expression status of these Wnt genes in a panel of eight osteosarcoma cell lines against hFOB using PCR. As osteosarcoma is a mesenchymal neoplasm that can result from morphologically abnormal osteoblastic cells producing defective immature bone (osteoid), hFOB have been commonly used in previous studies as normal control of gene profile

against osteosarcoma cell lines and tissue samples [19, 26, 56, 65]. As shown in Figure 5-1, SFRP1, 2 and 5, but not SFRP4 mRNA were expressed in hFOB cells. Compared to hFOB cells, the expression of SFRP1 was down-regulated in U2OS, HOS, CRL1423 and OS2 cell lines and completely absent in SaOS-2 cells. We found that SFRP2 mRNA expression was completely absent in four of the eight osteosarcoma cell lines tested (U2OS, CRL11226, CRL1423 and OS3) and was down-regulated in HOS, compared to hFOB. While SFRP4 expression was absent in HOS and CRL11226 cell lines, the other cell lines showed varied expressions of SFRP4 gene: strong expression in OS1 and weak but detectable expressions in U2OS, SaOS-2, CRL1423, OS2 and OS3 cell lines. On the other hand, SFRP5 expression was markedly suppressed in all eight osteosarcoma cell lines tested compared to hFOB cells, and completely absent in U2OS and CRL1423 cells. To investigate the anti-tumor effects of SFRPs in osteosarcoma, U2OS cells were used for the restoration of SFRPs in subsequent studies, given that they consistently showed low expressions of SFRP1, 2 and 5 compared to hFOB.
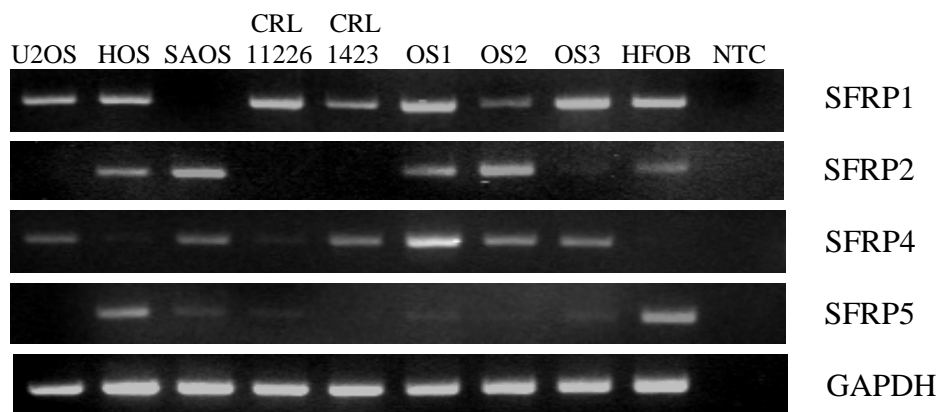
Figure 5-1. Frequent inactivation of Wnt antagonist genes, SFRP1, 2, 4 and 5 in osteosarcoma cell lines. RT-PCR analysis of SFRP1, 2, 4 and 5 in hFOB, together with eight osteosarcoma cell lines. GAPDH was used as a loading control. NTC, no template control was included as a negative control.

5.3.2 Establishment of stable transfectants of SFRP1, 2, 4 and 5 in U2OS cells

To elucidate the role of SFRP1, 2, 4 and 5 in osteosarcoma disease progression, we stably transfected U2OS cells with each of the SFRPs under study and pcDNA3.1-HIS control vectors. The reexpressions of the SFRPs genes in stable clones were confirmed by western blotting and RT-PCR (Figure 5-2). U2OS/SFRP1 clone #2, U2OS/SFRP2 clone #7, U2OS/SFRP4 clone #1 and U2OS/SFRP5 clone #3 were selected and used for subsequent experiments as the mRNA and protein expressions of SFRPs in these clones were highly up-regulated in U2OS/SFRP cells compared with the U2OS/pcDNA3.1-HIS cells. Other clones were not selected as the SFRPs expressions in these clones were either low or totally absent.

(a)
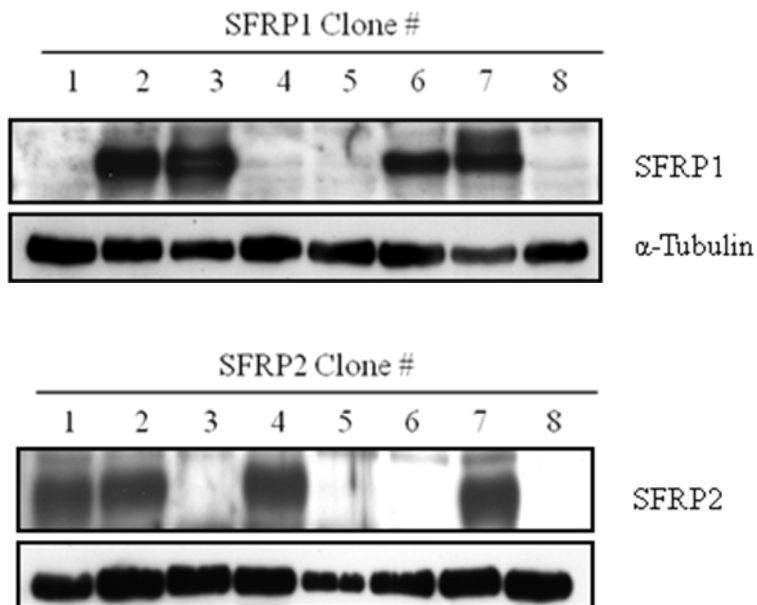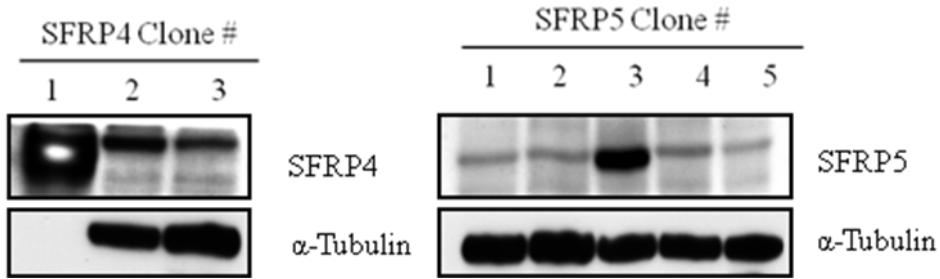
(b)
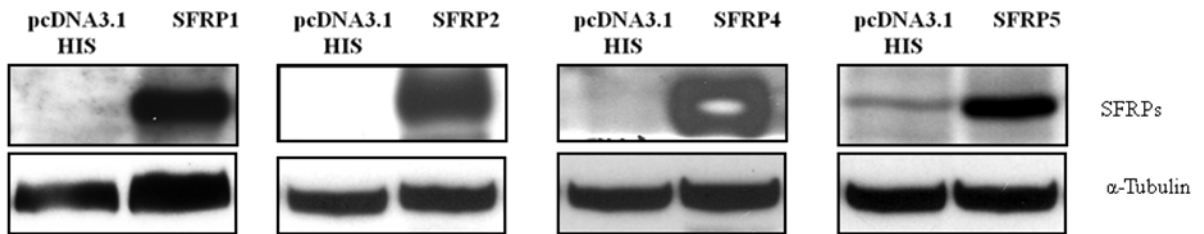
(c)
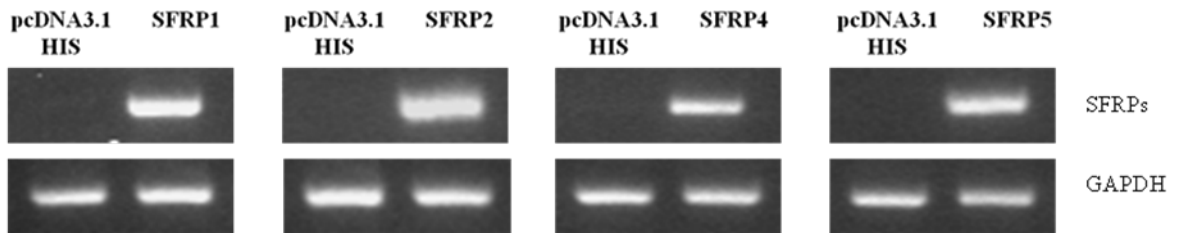
Figure 5-2. Successful establishment of stable transfectants of SFRP1, 2, 4 and 5 in U2OS cell. (a) Successful selection of several stable clones, verified by western blots using antibodies against the respective SFRPs. α-Tubulin was used as a loading control. **(b-c)** Selected stable clones to be used for subsequent experiments, with SFRPs protein and mRNA expressions verified using **(b)** western blot analysis and **(c)** RT-PCR analysis respectively. GAPDH was used as a loading control in RT-PCR.

5.3.3 Restoration of SFRPs expression decreased β-catenin production and inhibited TCF-dependent transcriptional activity

Activation of the Wnt/β-catenin signaling pathway results in phosphorylation of GSK-3β and stabilization of cytosolic β-catenin leading to activation of TCF-mediated transcriptional activity [35]. To evaluate the effects of SFRP1, 2, 4 and 5 on the downstream β-catenin/TCF transcriptional activity in osteosarcoma cells, U2OS/SFRP1, U2OS/SFRP2, U2OS/SFRP4 and U2OS/SFRP5 stable transfectants were transiently co-transfected with reporter plasmids containing either wild-type (TOPGlow) or mutant (FOPGlow) consensus TCF/LEF binding elements and pSV-β-galatosidase control vector for normalization of transfection efficiency. As shown in Figure 5-3a, β-catenin/TCF transcriptional activities were significantly suppressed in all the stable transfectants. Compared to the U2OS/pcDNA3.1-HIS control cells, TCF-mediated transcription were inhibited by approximately 88 %, 57 %, 49 % and 62 % in the U2OS/SFRP1, U2OS/SFRP2, U2OS/SFRP4 and U2OS/SFRP5 cells respectively. Transcriptional activity for FOPGlow remained low at all instances. Consistently, the suppression of β-catenin/TCF transcriptional activities in the U2OS/SFRPs transfectants were accompanied by marked decrease in total β-catenin protein expressions (Figure 5-3b).

(a)
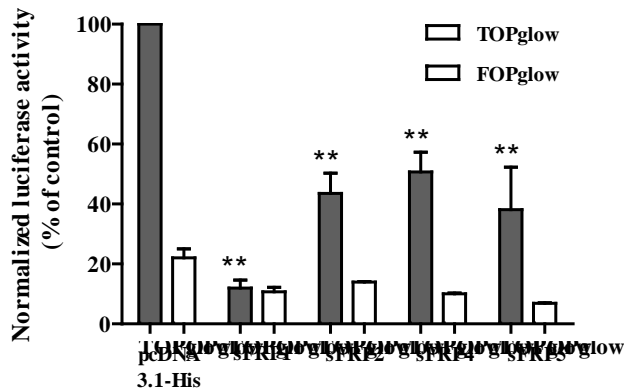
(b)
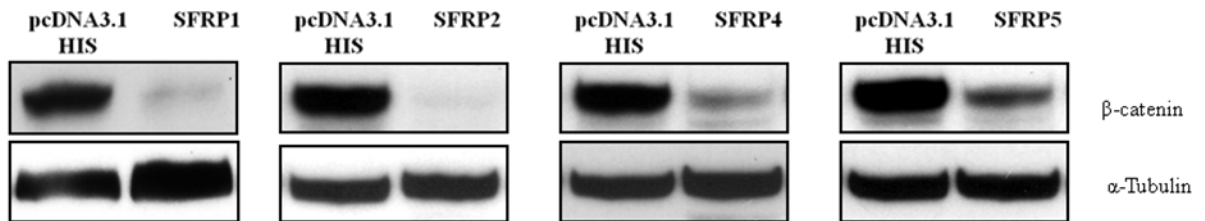
Figure 5-3. SFRPs over-expression inhibited TCF-dependent transcriptional activity and decrease β-catenin protein. **(a)** Luciferase reporter gene assays by using either reporter gene TOPGlow or a negative control with mutant TCF-4 binding sites (FOPGlow) was used to analyze TCF-dependent transcriptional activity. Results were expressed as mean ± SEM of normalized ratios of luciferase and β-galactosidase activities for each triplicate sets. Reporter activities in U2OS/SFRPs transfectants were expressed as the percentage of that in U2OS/pcDNA3.1-HIS control cells. ** $P > 0.01$, compared with U2OS/pcDNA3.1-HIS control group. (b) Western blot analysis of total β-catenin protein expression in U2OS/SFRPs stable transfectants. α-Tubulin was used as a loading control.

5.3.4 Ectopic expressions of SFRP1, 2, 4 and 5 decreased nuclear β-catenin and facilitated the translocation of β-catenin protein to the cell membrane

Using immunofluorescence microscopy analysis, we next examined whether over-expression of SFRPs were associated with changes in the localization of β-catenin protein. As shown in Figure 5-4, over-expression of SFRP1, 2, 4 or 5 is associated with a

reduction in nuclear β-catenin immunofluorescence signal and a corresponding increase in membranous β-catenin localization compared to the control vector pcDNA3.1 U2OS cells, suggesting that restoration of SFRPs resulted in β-catenin translocating from the nucleus to adherent junctions of the cell membrane in U2OS cells.

DAPI	β-catenin	Merged
U2OS/pcDNA3.1-HIS	U2OS/pcDNA3.1-HIS	U2OS/pcDNA3.1-HIS
U2OS/SFRP1	U2OS/SFRP1	U2OS/SFRP1
U2OS/SFRP2	U2OS/SFRP2	U2OS/SFRP2

| DAPI | β-catenin | Merged |
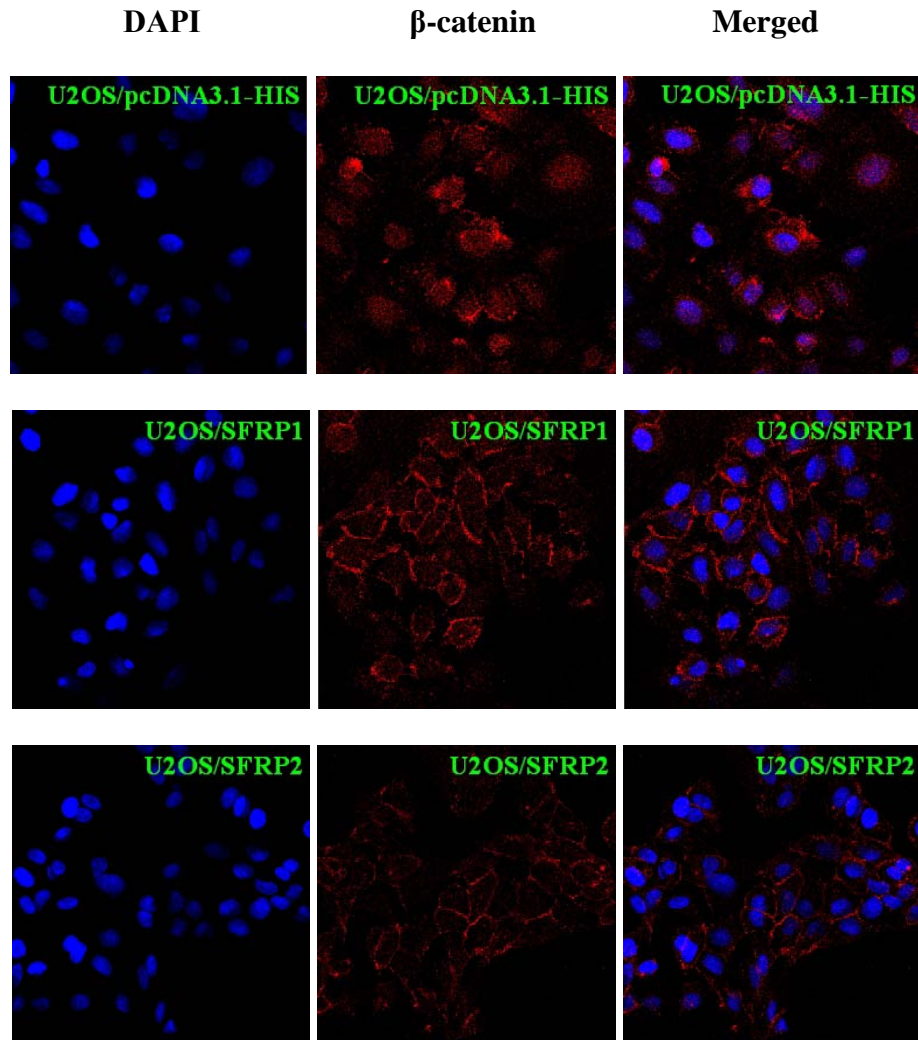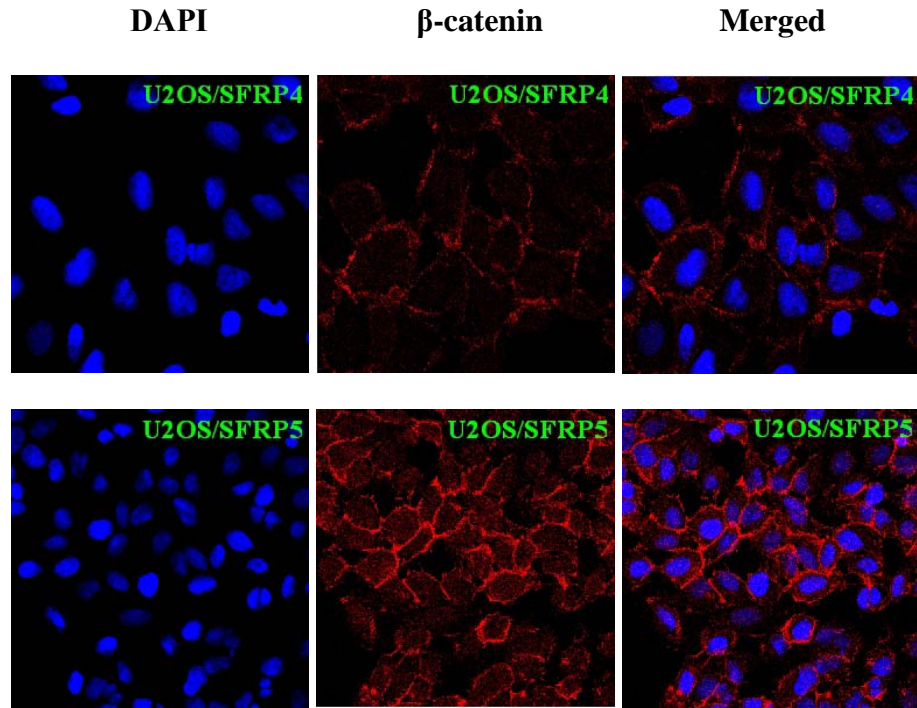
Figure 5-4. Immunofluorescence microscopy analysis of β-catenin protein localization in U2OS cells over-expressing SFRPs. The cells were incubated with anti-β-catenin antibody and the nuclei were also counter stained with DAPI. Representative images from three independent experiments shown were acquired on an LSM 5 DUO inverted confocal microscope.

5.3.5   Over-expression of SFRPs suppressed both anchorage-dependent cell growth, colony formation and disrupted cell cycle progression through affecting proliferation-associated Wnt-responsive genes expressions in U2OS cells

Previous studies have reported that disruption of Wnt/β-catenin signaling using DN-LRP5 inhibited both *in vitro* and *in vivo* osteosarcoma growth [52]. We have also recently demonstrated that PKF118-310, a specific Wnt/β-catenin antagonist, induced apoptosis and G2/M phase cell cycle arrest but suppressed osteosarcoma cell proliferation [195]. Given that β-catenin/TCF signaling and its gene products such as cyclin D1, c-Myc and survivin are known to collectively regulate cell proliferation, cell cycle

distribution and apoptosis, we next investigated the effects of SFRP1, 2, 4 and 5 on the expressions of these Wnt responsive oncogenes such as cyclin D1, c-Myc and survivin [97, 98].

As shown in Figure 5-5a, we observed a significant decrease in cyclin D1 protein expression in all the SFRPs transfectants. Survivin protein expression was also down-regulated with over-expression of SFRP2, 4 and 5 while the protein expression for c-Myc was markedly suppressed by the restoration of SFRP2, but up-regulated by ectopic expressions of SFRP4 and SFRP5. Given the observations, we further asked if the perturbation of cyclin D1, c-Myc and survivin protein expressions correlated with anti-proliferation and pro-apoptotic effects with over-expression of SFRPs antagonist in U2OS cells.

Anchorage-dependent growth of each transfectant was determined using the MTT cell proliferation assay, Figure 5-5b showed correspondingly lower rate of growth over a period of 7 days in SFRPs transfected U2OS cells compared to that of U2OS/pcDNA3.1-HIS control cells. Specifically, transfection with SFRP1, 2, 4 and 5 exhibited approximately 1.5-, 2.0-, 2.7- and 1.6-fold lower rate of anchorage-dependent growth than the U2OS/pcDNA3.1-HIS control cells after 7 days of cell seeding respectively.

Consistent with both the suppression of proliferation-associated Wnt responsive targets and the inhibition of anchorage-dependent growth, results from the colony formation assay demonstrated that restoration of SFRP1, 2, 4 and 5 attenuated anchorage-independent growths of osteosarcoma cells (Figure 5-5c). Compared with the

147

U2OS/pcDNA3.1-HIS control cells, transfection of SFRP-1, 2, 4 and 5 resulted in 88.7 %, 83.2 %, 65.6 % and 72.9 % reduction in the number of colonies formed respectively.

To examine if SFRPs could exert their anti-proliferative effects through disruption of cell cycle progression and/or apoptosis, we performed flow cytometry analysis. Our results revealed that over-expression of SFRP4 and SFRP5 significantly induced the rate of apoptosis (Sub-G1 phase) by 229.3 % and 249.2 % respectively, compared to the U2OS/pcDNA3.1-HIS control cells (Figure 5-5d). We also found that restoration of SFRP1, 2 and 5 resulted in an increase in the number of cells in the G0/G1 phase (66.3 % in control vs. 72.8 %, 74.8 % and 68.5 % respectively), with a corresponding decrease in the number of cells in the G2/M phase (17.2 % in control vs. 10.7 %, 12.6 % and 10.6 % respectively), suggesting an induction of G0/G1 phase arrest. On the other hand, a G2/M phase arrest was observed for over-expression of SFRP4, as indicated by the accumulation of cells in the G2/M phase (51.06 %), but a reduction in the number of cells in the G0/G1 phase (6.6 %). Taken together, our studies showed that restoration of SFRPs in U2OS cells resulted in the suppression of both anchorage-dependent (Figure 5-5b) and -independent growth (Figure 5-5c), possibly through disruptions of the cell cycle progression (Figure 5-5d) and alterations of proliferation-associated Wnt target oncogenes (Figure 5-5a).

(a)

				Cyclin D1
				Survivin
				c-Myc
				α -Tubulin

(b)

SFRP1

SFRP2

SFRP4

SFRP5

149
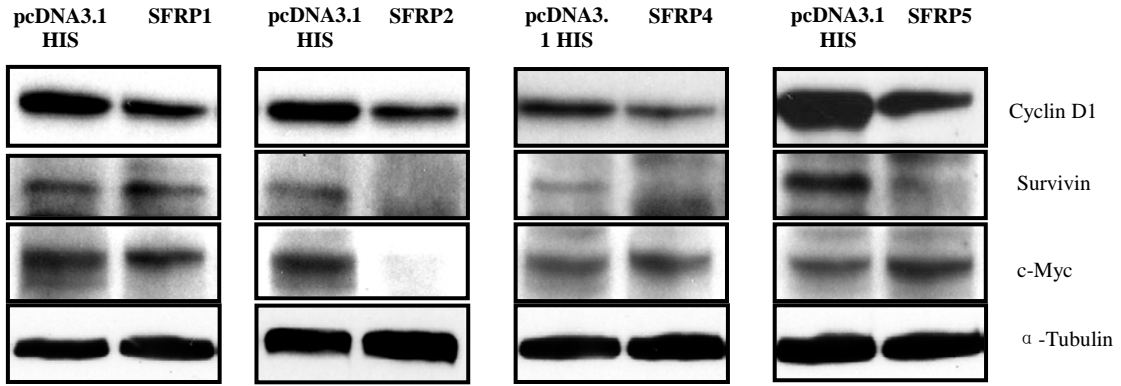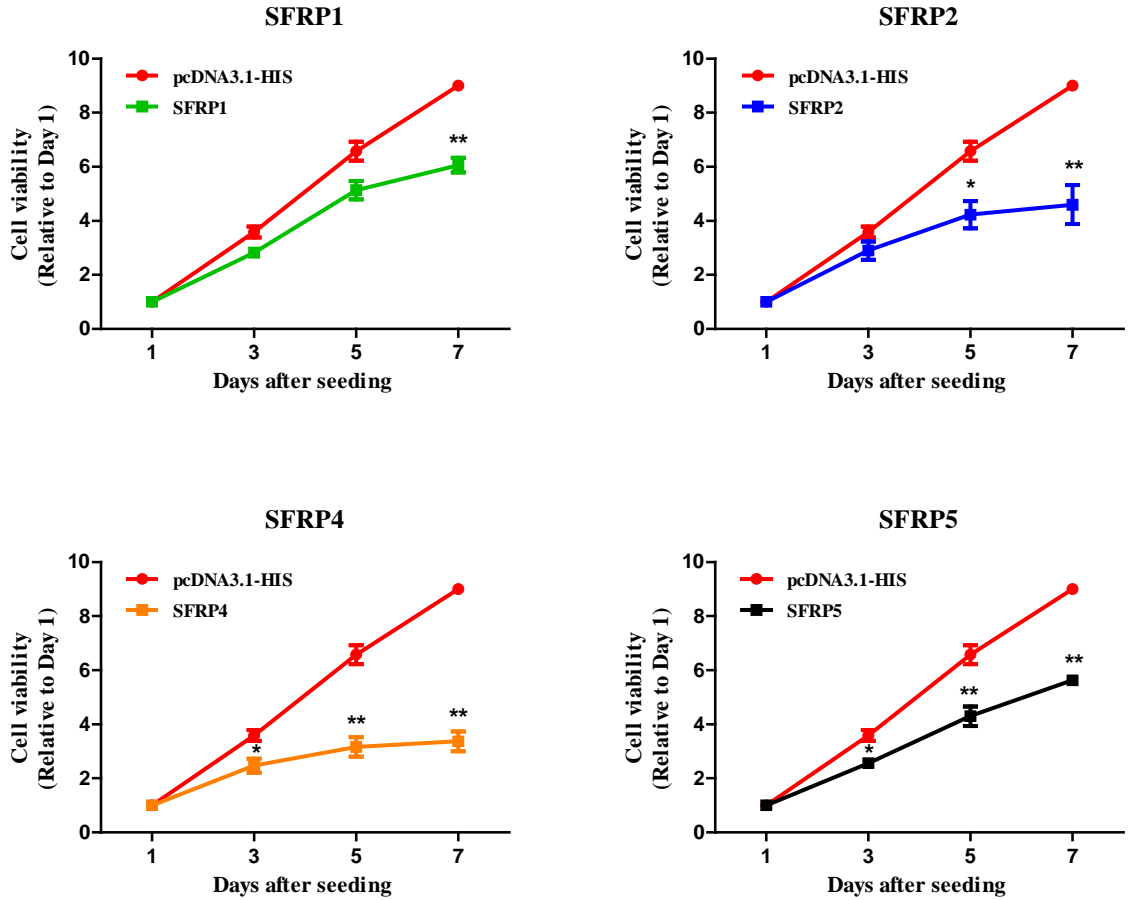
(c)
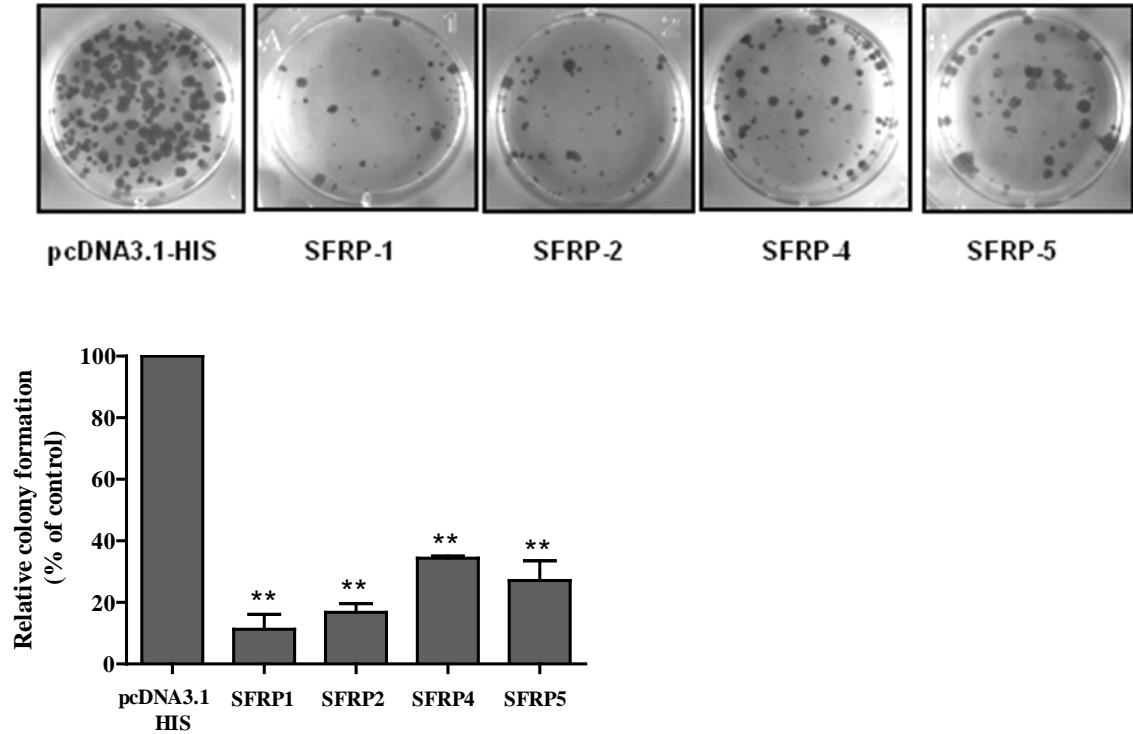
(d)
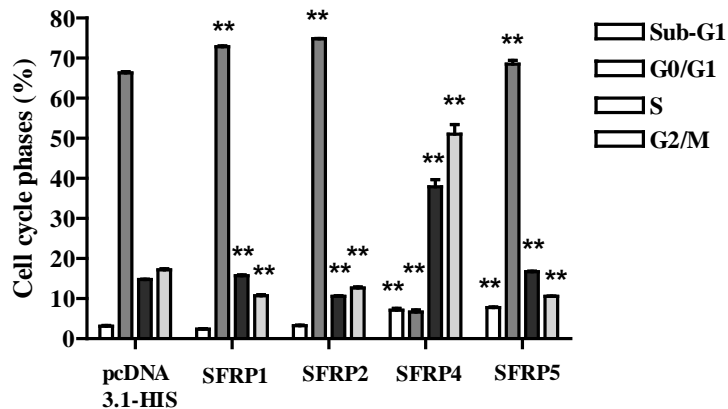
Figure 5-5. Over-expression of SFRP1, 2, 4 and 5 suppressed anchorage-dependent cell growth and colony formation, disrupted cell cycle progressions through down-regulating proliferation-associated Wnt-responsive genes in U2OS cells. (a) Western blot analysis of proliferation-associated Wnt target oncogenes such as cyclin D1, c-Myc and survivin in U2OS/SFRPs stable transfectants. α-Tubulin was used as a loading control. **(b)** Anchorage-dependent growth over periods of 3, 5 and 7 days were evaluated by MTT proliferation assay and expressed as mean ± SEM relative to that on Day 1 (set

150

as 1.0). **(c)** Representative images from three independent experiments showing a decrease in the number of colonies formed with U2OS cells stably transfected with SFRP, compared to pcDNA3.1-HIS control vector, after selection with G418 (400μg/ml) for 14 days. Relative colony formation was expressed as the percentage of colonies formed with U2OS transfected with empty vector, pcDNA3.1-HIS. ** *P<0.01*, compared with the pcDNA3.1-HIS control vector group. **(d)** Cell cycle distribution of the U2OS transfectants was measured by flow cytomerty analysis and the results were plotted as the percentage of cell in each cell cycle phase. Data were presented as mean ± S.E.M from three independent experiments. ** *P<0.01*, indicated the difference in the various cell cycle phases with SFRP over-expression, compared with the pcDNA3.1-HIS control vector group.

5.3.6 Restoration of SFRPs expression inhibited U2OS cell invasion and migration through regulating MMP-2 and MMP-9 proteins

Our group and several others have recently shown that inhibition of Wnt/β-catenin signaling using either PKF118-310, a specific antagonist of the pathway or endogenous inhibitors such as DN-LRP5 and DKK-3 could result in the suppression of cell invasiveness and motility of osteosarcoma cells [52, 63, 195]. Given these observations, we also examined the *in vitro* invasiveness and motility of U2OS cells expressing SFRP1, SFRP2, SFRP4, SFRP5 or pcDNA3.1-HIS vector control in Matrigel invasion and wound healing assays. As shown in Figure 5-6a, the capacity of SFRP1, SFRP2, SFRP4 and SFRP5-transfected U2OS cells to invade through the Matrigel-coated inserts over a period of 24 h were significantly decreased (80.3 %, 53.4 %, 73.9 % and 83.0 % respectively) compared with control cells (100 %). Except for SFRP4, over-expressions of SFRP1, 2 and 5 resulted in a parallel reduction in cell motility in U2OS cells using the wound healing assay (Figure 5-6b).

MMPs play important roles in the degradation of extracellular matrix to facilitate cancer cell metastasis [216]. Given that MMP-2 and MMP-9 are the two major extracellular

matrix degradation enzymes associated with enhanced osteosarcoma tumor invasion and metastasis [217-219], we examined whether reduced invasion with ectopic expression of SFRP1, 2, 4 and 5 correlated with MMP-2 and MMP-9 protein expressions in U2OS cells. Western blot analysis showed that restoration of SFRP1 and SFRP4 resulted in a decrease in both MMP-2 and MMP-9 protein expressions (Figure 5-6c). On the other hand, with over-expression of SFRP2, we observed a reduction in MMP-9 expression but an unexpected increase in MMP-2 protein expression. SFRP5 did not have any effects on both the MMP-2 and MMP-9 protein expressions, although the invasive capacity and motility of U2OS cells were markedly reduced with ectopic expression of this Wnt antagonist gene. Altogether, our results suggest that restoration of SFRPs in U2OS cells significantly inhibited U2OS cell invasiveness (Figure 5-6a) and/or motility (Figure 5-6b), and that other metastasis-associated genes, besides MMP-2 or MMP-9, may be involved in regulating U2OS metastasis.

(a)

U2OS/pcDNA3.1-HIS   U2OS/SFRP1   U2OS/SFRP2

U2OS/SFRP4   U2OS/SFRP5
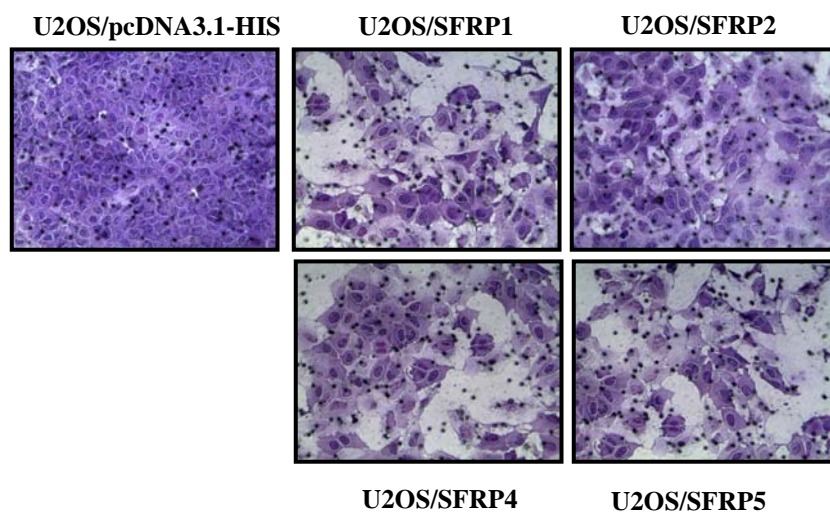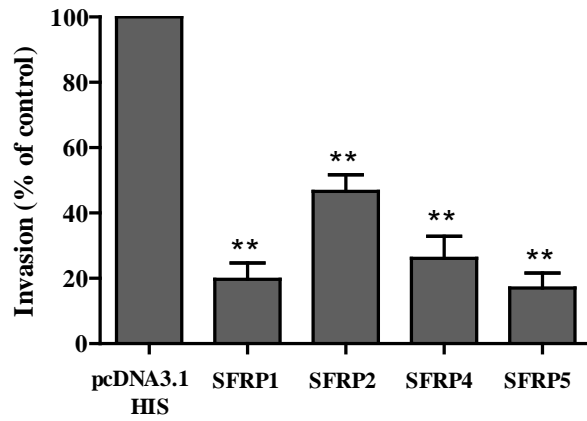
(b)
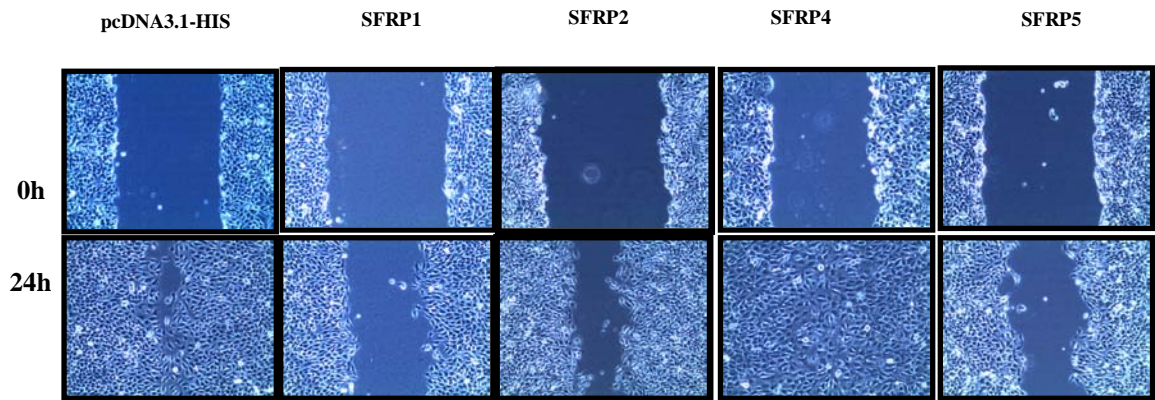
(c)

Figure 5-6. SFRPs over-expression inhibited OS cell metastasis through suppressing MMP-2 and MMP-9 protein. (a) Inhibition of U2OS cell invasion by SFRPs over-expression. Cells invaded through to the lower surface of the Matrigel-coated inserts over a period of 24 h were captured on a light microscope at 200 x magnification after staining

with crystal violet. Ten random fields were enumerated and data were presented as means ± SEM of three independent experiments. Cell invasion in U2OS/SFRP transfectants were expressed as the percentage of invasion in U2OS/pcDNA3.1-HIS. ** *P>0.01*, compared to the U2OS/pcDNA3.1-HIS group. **(b)** Representative images from three independent experiments showing differential wound closure rates of U2OS cells stably transfected with SFRPs or empty vector, pcDNA3.1-HIS, captured using microscope at 10 x objective. **(c)** Western blot analysis of MMP-2 and MMP-9 protein expressions in U2OS/SFRPs stable transfectants. α-Tubulin was used as a loading control.

5.3.7 Changes in gene expression profile induced by over-expression of SFRP2 or SFRP5 in U2OS cells

To identify critical targets of Wnt inhibition, we next examined the global changes in gene expression of 84 genes related to Wnt-mediated signal transduction in U2OS cells over-expressed with either SFRP2 or SFRP5 using the Human Signaling Pathway RT^2 Profiler^{TM} PCR arrays. Expressions of selected genes that were significantly up- or down-regulated (p-value < 0.05) were presented in (Table 5-1) while the others were reported in Appendix 5 and 6. As shown in Table 5-1, over-expression of SFRP2 resulted in the significant up-regulation of several endogenous Wnt antagonists such as DKK1, WIF-1 and SFRP1 while the transcription levels of DKK1 and FRZB were elevated with restoration of SFRP5. With ectopic expression of SFRP2, the levels of several Wnt ligands and receptors including WNT 5a, WNT 5b, WNT 11, FZD2, FZD4, FZD6 and FZD7 were significantly suppressed. In contrast, those of WNT 1, WNT 2, WNT 2b, WNT 3, WNT 7a, WNT 8a, WNT 9a, WNT 16, FZD3, FZD5 and FZD8 were up-regulated. The expressions of a different set of Wnt ligands and receptors were perturbated with over-expression of SFR5: Compared with pcDNA3.1 HIS control U2OS cells, mRNA levels of WNT 5a, WNT 11, FZD4 and FZD7 were significantly suppressed,

while those of WNT 10a, WNT 16, WNT 2b and FZD3 were up-regulated in U2OS cells over-expressing SFRP5.

Furthermore, the transcriptional expressions of several Wnt signaling components that play important roles in facilitating the phosphorylation-dependent ubiquitination of cytoplasmic β-catenin including APC, β-TrCP, CSNK1G1, FBXW2 and FBXW11 and were significantly up-regulated in both SFRP2 and SFRP5 over-expressed U2OS cells (Table 5-1). Forced expression of SFRP5 also resulted in a significant up-regulation of SENP2 mRNA levels. The expressions of other Wnt signaling components necessary for ubiquitination of cytoplasmic β-catenin such as CSNK1D, GSK-3β and FBXW4 were enhanced with restoration of SFRP2, but remained unchanged in U2OS cell over-expressing SFRP5.

We also found perturbations in several genes that play critical roles in TCF/β-catenin transcription when SFRPs are over-expressed in U2OS cells. Our gene array analysis showed a 2.2-fold increased in AES gene which encodes groucho, a nuclear transcriptional co-repressor that blocks TCF/β-catenin transcription with ectopic expression of SFRP5 in U2OS cells (Table 5-1). The expressions of transcriptional co-repressor proteins such as CTBP2 and TLE1 were up-regulated 2.03- and 2.00-fold respectively, while levels of LEF transcriptional factor was significantly suppressed with restoration of SFRP2.

In addition, forced expressions of both SFRP2 and SFRP5 resulted in the suppression of oncogene WISP1 but induced levels of T tumor suppressor gene. The expressions of other Wnt target oncogenes such as JUN and c-Myc were also significantly down-regulated in U2OS cells stably transfected with SFRP2 and SFRP5 respectively. Consistent with results from the western blot analysis Figure 5-5a, we further observed that the cyclin D1 transcriptional levels were suppressed by approximately 2-fold in SFRP2 stable transfectants, but an increased in cyclin D2 mRNA was also observed.

Much to our surprise, we found up-regulations in the gene expressions of several activators of the Wnt/β-catenin/TCF signaling pathway such as DVL1 and DVL2 while NKD1, a dishevelled-binding protein was significantly suppressed with restoration of either SFRP2 or SFRP5. Unexpectedly, TCFL1 expression was found to be up-regulated in U2OS cells over-expressing SFRP5.

Taken together, we identified several novel Wnt signaling components and target genes that may possibly explain the mechanism of Wnt inhibition and tumor suppressive effects of SFRP2 and SFRP5 in U2OS cells observed in the preceding anti-cancer functional assays.

Table 5-1. Wnt signaling components and target genes that significantly dysregulated with over-expression of SFRP2 or SFRP5 in U2OS cells.

Gene (Gene Symbol)	Function	SFRP2 over-expression			SFRP5 over-expression		
		Fold change	p-value	Up (↑) / down (↓) Regulation	Fold change	p-value	Up (↑) / down (↓) Regulation
Amino-terminal enhancer of split (AES)	Mammalian homologue of the Drosophila groucho which serves as a nuclear transcriptional co-repressor by interacting with TCF family of proteins to block TCF/β-catenin transcription and thus repress Wnt target oncogenes	-	-	-	2.16	0.041	↑
Adenomatosis polyposis coli (APC)	Tumor suppressor gene which facilitates the degradation of β-catenin by binding it and recruiting it to the APC-Axin-GSK-3β β-catenin destructive complex as well as by exporting nuclear β-catenin	2.16	0.0019	↑	1.79	0.038	↑
Beta-transducin repeat containing (β-TrCP)	A component of an E3 ubiquitin ligase complex, which functions in phosphorylation-dependent ubiquitination of cytoplasmic β-catenin, thus destabilizes it.	1.23	0.011	↑	1.79	0.040	↑
Cyclin D1	Wnt target oncogene that stimulates tumor cell proliferation and cell cycle	1.97	0.00030	↓	-	-	-

(CCND1)	progression in the G1/S phase.						
Cyclin D2 (CCND2)	Wnt target oncogene that stimulates tumor cell proliferation and cell cycle progression in the G1/S phase, compensatory increase in cyclin D2 was observed with cyclin D2 knockdown	2.63	0.000076	↑	-	-	-
Casein kinase 1, delta (CSNK1D)	Facilitate phosphorylation and destabilization of cytoplasmic β-catenin	1.96	0.0010	↑	-	-	-
Casein kinase 1, gamma 1 (CSNK1G1)		3.47	0.00026	↑	2.05	0.00046	↑
C-terminal binding protein 2 (CTBP2)	A transcriptional co-repressor that function as a scaffold protein to recruit chromatin-modifying enzymes to TCF/LEF family of DNA-binding transcriptional factors, thus facilitating the transcriptional repression activity of TCF/LEF, as well as antagonizing the activity of p300 co-activator complex	2.03	0.00054	↑	-	-	-
Dickkopf 1 (DKK1)	Endogenous Wnt antagonist that attenuates Wnt signaling by binding to LRP and Kremen receptors, and sterically hindering Wnt interaction with LRPs	3.32	0.000005	↑	1.178	0.037	↑
Dishevelled	A critical cytoplasmic transducer regulator	1.38	0.0075	↑	1.447	0.019	↑

homolog 1 (DVL1)	that functions to release β-catenin from ubiquitin-dependent degradation						
Dishevelled homolog 2 (DVL2)		2.24	0.0011	↑	1.395	0.046	↑
F-box and WD repeat domain containing 2 (FBXW2)	A member of the F-box protein family that constitutes one of the four subunits of ubiquitin protein ligase complex called SCFs (SKP1-cullin-F-box), which function in phosphorylation-dependent ubiquitination.	3.78	0.0010	↑	2.76	0.019	↑
F-box and WD repeat domain containing 4 (FBXW4)		1.66	0.0061	↑	-	-	-
F-box and WD repeat domain containing 11 (FBXW11)		1.49	0.0030	↑	1.44	0.0066	↑
Frizzled receptor 2 (FZD2)	Member of the 'frizzled' gene family encode 7-transmembrane domain proteins receptors that interacts with Wnt signaling proteins to initiate Wnt signaling.	1.87	0.0052	↓	-	-	-
Frizzled receptor 3 (FZD3)		1.81	0.00075	↑	1.811	0.045	↑

		2.70	0.0037	↓	2.55	0.016	↓
Frizzled receptor 4 (FZD4)		2.70	0.0037	↓	2.55	0.016	↓
Frizzled receptor 5 (FZD5)		2.63	0.00032	↑	-	-	-
Frizzled receptor 6 (FZD6)		5.02	0.000032	↓	-	-	-
Frizzled receptor 7 (FZD7)		3.72	0.00062	↓	1.34	0.052	↓
Frizzled receptor 8 (FZD8)		1.62	0.0013	↑	-	-	-
Glycogen synthase kinase 3β (GSK3β)	A component of Axin-GSK-3β β-catenin destructive complex which function in phosphorylation-dependent ubiquitination of cytoplasmic β-catenin, thus destabilize it.	1.48	0.0016	↑	-	-	-
Jun oncogene (JUN)	A Wnt target oncogene that is over-expressed in osteosarcoma, and its suppression inhibited growth and metastasis of osteosarcoma in an orthotopic spontaneously metastasizing neoplasia model	1.72	0.00039	↓	-	-	-
Lyphoid enhancing factor 1	Member of TCF/LEF transcription factors that function as mediator of the Wnt/β-catenin transcription, also a Wnt target	1.43	0.053	↓	-	-	-

Gene	Description						
(LEF1)	gene						
V-myc myelocytomatosis viral oncogene homolog (MYC)	A multifunctional, nuclear phosphoprotein that is frequently over-expressed in various malignancies, and plays a role in cell cycle progression, apoptosis and cellular transformation, as well as functions as a transcription factor that regulates transcription of specific target genes.	-	-	-	2.81	0.047	↑
Naked cuticle homolog 1 (NKD1)	A Dishevelled-binding protein that functions as a negative regulator of the Wnt/β-beta-catenin/TCF signaling pathway	1.63	0.0048	↓	1.61	0.016	↓
Frizzled-related protein 1 (SFRP1)	Belongs to a family of five glycoprotein (SFRP1-5) that competes with Frizzled receptors for bind Wnt ligands and silencing of this tumor suppressor gene is implicated in several malignancies	1.49	0.0026	↑	-	-	-
Frizzled-related protein 3 (FRZB)		-	-	-	2.445	0.010	↑
SUMO1/sentrin/SMT3 specific peptidase 2 (SENP2)	Axin-binding protein that promotes β-catenin ubiquitination and degradation	-	-	-	1.66	0.052	↑
Solute carrier family 9 (sodium/	β-catenin-associating protein that potentiates β-catenin/TCF-dependent	1.15	0.011	↓	-	-	-

Gene	Description						
hydrogen exchanger), member 3 regulator 1 (SLC9A3R1)	transcription, and function as a tumor suppressor to regulate anti-cancer activities						
T, brachyury homolog (T)	Epigenetic silencing of this tumor suppressor is implicated in non-small-cell lung cancer	1.62	0.0048	↑	1.44	0.027	↑
T-cell specific transcription factor 7-like 1 (TCF7L1)	Member of TCF/LEF transcription factors that function as mediator of the Wnt/β-catenin transcription	-	-	-	1.36	0.0073	↑
Transducin-like enhancer of split 1 (TLE1)	Mammalian homologue of the Drosophila groucho which serves as a nuclear transcriptional co-repressor by interacting with TCF family of proteins to block TCF/β-catenin transcription and thus repress Wnt target oncogenes	1.97	0.00030	↑	-	-	-
WNT inhibitor factor 1 (WIF1)	A Wnt antagonist that is frequently silenced in many tumors including osteosarcoma, and restoration of this tumor suppressor gene suppressed cell proliferation, invasiveness and in vivo lung metastasis in many cancers	3.32	0.000005	↑	-	-	-

WNT1 inducible signaling pathway protein 1 (WISP1)	A member of the connective tissue growth factor that is frequently over-expressed in various tumors, and is involve in the regulation of various processes leading to tumorigenesis and malignant transformation including cell proliferation, migration, adhesion, angiogenesis and extracellular matrix formation.	7.67	0.00025	↓	2.85	0.0021	↓
Wingless-type MMTV integration site family, member 1 (WNT1)	Secreted signaling protein that are implicated in oncogenesis and in several developmental processes	3.32	0.000005	↑	-	-	-
Wingless-type MMTV integration site family, member 2 (WNT2)		3.21	0.00005	↑	-	-	-
Wingless-type MMTV integration site family, member 2B (WNT2B)		1.16	0.0047	↑	1.37	0.011	↑
Wingless-type MMTV integration site family,		1.41	0.0036	↑	-	-	-

member 3 (WNT3)						
Wingless-type MMTV integration site family, member 5A (WNT5A)	1.85	0.0022	↓	1.47	0.022	↓
Wingless-type MMTV integration site family, member 5B (WNT5B)	1.52	0.0054	↓	-	-	-
Wingless-type MMTV integration site family, member 7A (WNT7A)	3.38	0.0053	↑	-	-	-
Wingless-type MMTV integration site family, member 8A (WNT8A)	1.92	0.00061	↑	-	-	-
Wingless-type MMTV integration site family, member 9A	2.15	0.0034	↑			

(WNT9A)						
Wingless-type MMTV integration site family, member 10A (WNT10A)	-	-	-	1.66	0.0015	↑
Wingless-type MMTV integration site family, member 11 (WNT11)	11.21	0.00025	↓	5.57	0.00044	↓
Wingless-type MMTV integration site family, member 16 (WNT16)	3.32	0.000005	↑	1.57	0.041	↑

Selected genes that are involved in the Wnt/β-catenin signaling with forced expression of SFRP2 in U2OS cells were listed. The gene symbol, gene function, fold-change, p-value, status of transcription has been described for each gene. The fold-changes in gene expression and p-values of the full list of the 84 genes were reported in Appendix 5.

5.4 Discussion

The Wnt/β-catenin pathway was first linked to cancer formation when it was found to be chronically activated in spontaneous forms of colon cancer. Approximately 90 % of colon cancers showed aberrant Wnt signaling, usually as a result of mutation in APC (80 %) [79-81], and less frequently due to mutations in β-catenin [76, 77] or Axin [85, 86]. On the other hand, mutations in APC and β-catenin are rare in osteosarcoma, despite accumulation of β-catenin protein [73, 74]. Instead, epigenetic silencing of genes encoding upstream components seemed to be the preferred route to chronic Wnt signaling dysfunction in osteosarcoma. Attention has therefore been focused on the contributory role of Wnt upstream components in osteosarcoma pathogenesis.

Indeed, over-expressions of numerous upstream membrane-bound Wnt components including Wnt ligands (Wnt 1, 4, 5a, 7, 10b, 11) [47, 48], Frizzled receptors (FZD1-10) [47] and LRP5 co-receptor [47, 51, 52] have been implicated in osteosarcoma tumorigenesis and metastasis. Epigenetic silencing of genes encoding endogenous Wnt pathway cell surface inhibitors such as DKK3 [63] and WIF-1 [65, 149] were observed to promote osteosarcoma disease progression. Furthermore, it has been previously reported that SFRP3 transcription was severely suppressed in osteogenic sarcoma biopsy specimens and several osteosarcoma cells lines [56], while the forced expression of SFRP3 inhibited *in vivo* tumor growth and lung metastasis [232]. However, the molecular functions of other members of the SFRPs family in the pathogenesis of osteosarcoma have not been reported, despite strong evidence of their status as tumor suppressors.

166

Therefore, we hypothesized that SFRP1, 2, 4 or 5 function as tumor suppressor genes and restoration of these may inhibit osteosarcoma tumorigenesis and metastasis.

To test our hypothesis, we first established the constitutive levels of SFRPs in osteosarcoma cells by PCR. In general, SFRPs expressions in osteosarcoma cells are down-regulated compared hFOB cell lines (Figure 5-1). However, we did not detect mRNA expression of SFRP4 in hFOB cells. In agreement with our observations, several studies have previously reported undetectable mRNA levels of one or more SFRPs levels in normal human tissues or cell lines such as normal breast, lung and mesothelioma [58, 280]. Despite lacking abundant expression in hFOB, SFRP4 may nevertheless bear crucial tumor-suppressive functions that only become effective under certain tumorigenic circumstances. This speculation is supported by a study which found that low levels of SFRP5 was readily inducible by activating Wnt signaling through forced expression of Wnt-1 or treatment with LiCl [281]. Effective inhibitions of the Wnt/β-catenin pathway by restoration of SFRPs in U2OS cells were subsequently shown by marked suppression of both β-catenin/TCF transcriptional activities (Figure 5-3a) and total β-catenin protein levels (Figure 5-3b), as well as re-distribution of β-catenin protein from the nucleus to the cell membrane (Figure 5-4) using luciferase reporter assays, western blotting and immunofluorescence confocal microscopy analyses respectively.

Upon restoration of the SFRPs, anchorage-dependent (Figure 5-5b) and –independent (Figure 5-5c) growths of osteosarcoma cells were found to be negatively regulated. Analysis of cell cycle progression by flow cytometry further revealed that ectopic

expressions of SFRP1, 2 and 5 resulted in G0/G1 mitosis exit abnormity while a G2/M phase delay was observed with over-expression of SFRP4 in U2OS cells, accounting for the anti-proliferation effects of SFRPs in U2OS (Figure 5-5d). High apoptotic rate in SFRP4 and SFRP5 over-expressing cells might contribute additionally to cell proliferation suppression in U2OS cells (Figure 5-5d). Our western blot results demonstrated that perturbations of protein expressions of several Wnt target proliferation-associated oncogenes including cyclin D1, c-Myc and survivin [234-241], correlated with anti-proliferation and pro-apoptotic effects with over-expression of SFRPs antagonist in U2OS cells.

Interestingly, we observed an up-regulation of c-Myc protein expression in U2OS over-expressing SFRP4 or SFRP5. Consistent with these results, c-Myc mRNA level was also significantly induced 2.8-fold in U2OS cell over-expressing SFRP5 (Table 5-1). c-Myc is known to play multiple roles in cell cycle progression, apoptosis and cellular transformation, and is regulated in a multi-factorial and tissue specific manner [98]. Our observation that restoration of SFRP4 and SFRP5 up-regulated c-Myc protein expression, but induced anti-proliferative and pro-apoptotic effects in U2OS cell, is thus not unexpected. A similar phenomenon was reported previously by Thompson et al. who found that both a decrease and increase of c-Myc led to apoptosis [282]. In another study, a decreased expression of c-Myc was found in human colorectal adenocarcinoma cells over-expressing β-catenin [283]. Furthermore, c-Myc may be positively or negatively regulated based on combinatorial interactions involving E2F transcriptional factors and other classes of transcriptional activators and repressors [284].

Besides their anti-proliferative effects, SFRPs may function as anti-invasive agents in osteosarcoma by inhibiting U2OS cell invasion and motility. As shown in Figure 5-6, we found that ectopic expressions of SFRP1, 2 and 5 decreased the invasiveness and motility of U2OS. On the other hand, restoration of SFRP4 inhibited U2OS cell invasion but had no effect on U2OS cell migration, suggesting that SFRP4 has less effects on motility in U2OS cells than the other members of the SFRPs family of Wnt antagonists. Reduction in MMP-2 and MMP-9 protein was observed only in SFRP1 and SFRP4 transfectants, suggesting that other invasion-associated genes may be involved in regulating osteosarcoma cell invasion and migration. In agreement with our observations, Zhao et al also found no significant correlation between SFRP5 expression and MMP-2 or MMP-9 expressions in gastric cancer cells, however, both MMP-7 and MT1-MMP mRNA expressions correlated inversely with SFRP5 expressions in these cell lines [285]. Further experiments are necessary to investigate the roles of other members of the MMP family, such as MMP-1 [286], MMP-3 [287] MMP-7 [288] , MMP-13 [289], MMP-26 [101], MT1-MMP [290], MT3-MMP [231], that may be affected through direct or indirect Wnt activation.

As a means to elucidate novel targets that can mediate the anti-tumor effects of SFRPs restoration, we examined changes in the global expressions of 84 Wnt signaling components and target genes expression profile induced by SFRP2 and SFRP5 over-expressions in U2OS stable transfectants using the Human Wnt Signaling Pathway RT^2 Profiler^{TM} PCR Array. SFRP2 and SFRP5 were chosen for Wnt array analysis over SFRP1 or SFRP4 for the following reasons: (1) SFRP2 and SFRP5 are less well known

members of the SFRPs family; (2) Both SFRP2 and SFRP5 are markedly down-regulated in U2OS cells and in many other osteosarcoma cell lines while the suppression of the other SFRPs was less obvious (Figure 5-1) and (3) To test our hypothesis that Novel Wnt target genes, besides MMPs (Figure 5-6), may play a more significant role in regulating the anti-metastatic effects of SFRP2 or SFRP5.

Firstly, based on the RT-PCR array data, we observed suppressions of mRNA expressions of specific frizzled receptors (SFRP2: FZD2, FZD 4, FZD6, FZD7; SFRP5: FZD4, FZD7) and Wnt ligands (SFRP2: WNT 5a, WNT 5b, WNT 11; SFRP5: WNT 5a, WNT 11), suggesting that restoration of SFRP2 or SFRP5 may disrupt specific WNT-FZD interactions and thus block signal initiation at the membranous level. Up-regulation of expressions of other endogenous antagonists such as DKK-1, SFRP1, SFRP3 and/or WIF-1 by SFRP5 and SFRP2 over-expression respectively may additionally prevent or reduce Wnt signaling by binding competitively to the LRP5 and/or FZD receptors. Notably, these Wnt antagonists function as tumor suppressor genes and were previously reported to inhibit both *in vitro* and *in vivo* cell proliferation, invasion, migration, angiogenesis as well as induce apoptosis in several malignancies such as osteosarcoma [56, 65, 149], prostate [232], liver multiple myeloma [279, 291], breast [62] and kidney [292]. Given that epigenetic silencing of SFRP3 and WIF-1 have been implicated in the pathogenesis of osteosarcoma [56, 65] and that restoration of WIF-1 and DKK3 have been shown to inhibit *in vivo* lung metastasis and invasiveness of osteosarcoma cells respectively [63], our findings suggest that SFRP2 or SFRP5 may offer a clinically relevant role in activating the tumor suppressive functions of DKK-1, SFRP1, SFRP3 and

WIF-1 in osteosarcoma to achieve effective therapy. However, further studies are needed to examine the specific effects for the disruption of the native WNT-FZD complexes by SFRP2 and SFRP5.

Secondly, it is tempting to speculate that over-expressions of SFRP2 or SFRP5 could have attenuated Wnt signaling in U2OS cells through enhancing the phosphorylation-dependent ubiquitination and destabilization of cytoplasmic β-catenin, given that restorations of SFRP2 and SFRP5 both resulted in a collective up-regulations of signaling components that are responsible for these processes such as APC, CSNK1G1, CSNK1D, GSK3β, β-TrCP, FBXW2, FBXW4, FBXW11 and SENP2. As shown in Table 5-1, over-expression of SFRP2 or SFRP5 increased the mRNA expression of APC, a tumor suppressor which plays critical roles in facilitating the degradation of β-catenin by binding and recruiting it to the APC-Axin-GSK-3β β-catenin destructive complex as well as by exporting nuclear β-catenin [109, 131, 293]. Furthermore, as proposed by Ha et al. who found that the subsequent phosphorylation of APC by CSNK slowed the release of β-catenin from the destructive complex [294], the up-regulation of CSNK observed with ectopic expressions of SFRP2 and SFRP5 may possibly further enhance ubiquitination of β-catenin in U2OS cells. Phosphorylated β-catenin is then recognized by and associates with specific member of the SCF (SKP1-cullin-F-box) family of the E3 ubiquitin ligase complex, the Beta-transducin repeat containing and F-box proteins before it gets degraded by the proteosome [295].

Thirdly, SFRP2 may be capable of disrupting β-catenin/TCF complexation and transcription through attenuating the nuclear translocation of β-catenin protein by redistribution to the cell membrane (Figure 5-4) and regulating the expression of several transcriptional factors such as TLE1, LEF1, and CTBP2. TLE1 gene is a mammalian homologue of the Drosophila transcriptional repressor groucho which serves as a nuclear transcriptional co-repressor by interacting with TCF/LEF family of proteins to block TCF/β-catenin transcription and thus repress Wnt target oncogenes [129, 258, 259]. As a co-repressor, CTBP2 primarily functions as a scaffold protein to recruit chromatin-modifying enzymes, including HDACS, histone methyltranferases and polycomb group proteins, to TCF/LEF family of DNA-binding transcriptional factors, thus facilitating the transcriptional repression activity of TCF/LEF [296, 297] and antagonizing the activity of p300 co-activator complex [298]. Notably, mutations which affect the CTBP2 interaction with TCF/LEF have been reported to contribute to carcinogenesis [93, 299]. Given that LEF1, a DNA binding transcriptional factor, has been shown to be a bona fide target gene [300, 301], down-regulation of LEF may possibly reduce the magnitude of Wnt activation since a smaller amount of LEF protein would be available for complex formation with β-catenin. Taken together, SFRP2 may possibly disrupt β-catenin/TCF transcriptional activity and complexation through up-regulating transcriptional repressors such as groucho and CTBP2, while suppressing the level of LEF1 transcription factor. On the other hand, SFRP5 may be capable of disrupting β-catenin/TCF transcription by up-regulating expressions of AES gene which encodes groucho, a nuclear transcriptional co-repressor.

Lastly, ectopic expression of both SFRP2 and SFRP5 were found to effectively suppress the mRNA expressions of oncogene WISP1 but induced expression of tumor suppressor T gene, Brachyury. Both WISP1 and Brachyury genes play critical roles in regulating tumorigenesis and metastatic transformation in various tumor models. Indeed, several lines of evidence support a role for WISP-1 in tumorigenesis: WISP-1, a member of the connective tissue growth factor that belongs to the Cry61, CTGF and Noc (CCN) super family, has been shown to promote cell proliferation, migration, adhesion, angiogenesis and extracellular matrix formation [266, 302]. WISP-1 is over-expressed in many tumors types, including breast, colon, cholangiocarcinoma and plexiform neurofibromas [267-270] and its over-expression correlated with more advanced features such as late-stage disease, lymph node involvements and larger tumor size in both primary breast and rectal cancers [269, 271]. In *in-vivo* mouse models, forced expression of WISP-1 in normal kidney fibroblasts were found to induce morphological transformation, accelerate cell growth and induced tumor formation [146]. On the other hand, Brachyury was recently identified as a tumor suppressor gene in non-small-cell lung cancer [303] whereas other members of the T-box family genes that share T box motif with Brachyury such as TBX2 and TBX3, are known to be transcriptional repressors that inhibit cell proliferation and oncogenic transformation [304]. Since our earlier results from the western blot analysis showed that protein expressions of MMP-2 and MMP-9 remained unaltered and did not correspond to the reduction in invasive capacity of SFRP5 over-expressing U2OS cells, it is tempting to speculate that other metastasis-associated Wnt target genes including WISP1 and Brachyury might play a significant contributory role in regulating osteosarcoma metastasis and disease progression and additional experiments using

siRNA or forced expressions of these genes would be necessary to fully elucidate their effects in regulating osteosarcoma cell invasion by SFRP5.

Furthermore, we observed suppressions of several other Wnt target oncogenes such as SLC9A3R1, JUN and cyclin D1 with forced expression of SFRP2. Parallel to results from the western blot analysis (Figure 5-5a), we found a reduction of cyclin D1 mRNA level in U2OS cell over-expressing SFRP5. On the other hand, we observed an up-regulation of cyclin D2 in these cells. Such compensated effects of cyclin D2 with the knockdown of cyclin D1 was previously observed in mantle lymphoma cells as well as in an *in vivo* mouse model, but more studies are required to explain these observed phenomenon. SLC9A3R1, a β-catenin-associating protein that potentiates β-catenin/TCF-dependent transcription [305] was found to be up-regulated in breast cancer [306], schwannoma [307] and hepatocellular carcinomas [305] compared to their non-tumor counterparts. Elevated level of SLC9A3R1 is closely associated with the invasive behavior of malignant glioma cells *in vivo* and *in vitro*, and when silenced, tumor cells exhibited reduced migratory activity, leading to an increased susceptibility to chemotherapy [308]. Furthermore, SLC9A3R1 has been reported to regulate formation of invadopodia-cell structures that mediate tumor cell migration and invasion [309]. Another Wnt target gene, JUN has been found to be over-expressed in many cancers including osteosarcoma [310-312]. Indeed, JUN plays a critical role in the tumorigenesis and metastasis of osteosarcoma as reported recently by Dass et al. who demonstrated that knockdown of JUN using a c-jun DNAzyme, encapsulated within a novel cationic multi-lamellar vesicle liposome inhibited the growth and metastasis of osteosarcoma in an

orthotopic spontaneously metastasizing model of the disease [313]. Consistent with our results, JUN was suppressed in breast cancer cells that ectopically expressed SFRP2 [314]. While the suppression of WISP1, Brachyury, SLC9A3R1 and JUN in U2OS cells over-expressing SFRP2 correlated with inhibition of U2OS cell proliferation, invasion and migration, further studies are needed to fully understand the contributory roles of these oncogenes in regulating osteosarcoma metastasis and tumorigenesis. Nevertheless, the potential implications of regulating WISP-1 and Brachyury expressions by either over-expression of SFRP2 or SFRP5 in osteosarcoma pathogenesis are highly relevant and deserve in-depth investigation, given their oncogenic properties.

Much to our surprise, we observed significant up-regulations in the gene expressions of several activators of the Wnt/β-catenin/TCF signaling pathway such as DVL 1 and 2, as well as TCFL1 while suppression of NKD1, a dishevelled-binding protein with forced expressions of either SFRP2 or SFRP5. The expressions of several Wnt ligands and receptors were also induced with restoration of either SFRP2 or SFRP5 in U2OS cells. A possible explanation to the discordant results is that external stimuli such as the forced expression of SFRP2 or SFRP5 may have induced a protective auto-regulatory positive feedback mechanism to enhanced Wnt signaling in U2OS cells. Other reasons to these aberrant effects may include the presence of unclassified biphasic functions of these signaling components in Wnt signaling and their multiple roles in regulating other cross talk signaling pathways.

Taken together, we identified several novel Wnt signaling components and target genes that possibly explain the mechanism of Wnt inhibition and tumor suppressive effects of SFRP2 or SFRP5 in U2OS cells. Further studies are however needed to gain a comprehensive understanding of the underlying mechanism of Wnt inhibition by these secreted proteins in U2OS cells. Nevertheless, our findings supplemented the limited existing knowledge in understanding the interactions of SFRPs with the various molecular Wnt targets, which are essential for designing more effective SFRPs-based therapeutics for the treatment of osteosarcoma.

At present, we cannot rule out the fact that tumor-suppressive functions of SFRPs may be mediated through both Wnt/β-catenin-dependent and -independent signaling. In fact, restoration of SFRP4 expression in both β-catenin-dependent and β-catenin-deficient cell mesothelioma cell lines have been shown to promote apoptosis, suppress cancer cell growth and down-regulate Wnt signaling [315]. Another study showed that ectopic expression of SFRP1 reduced cell proliferation even though β-catenin/TCF is not activated in prostate cancer cells [316]. Recently, Shih et al. also found that β-catenin-deficient SK-Hep1 hepatoma cell treated with SFRP1 shRNA showed enhanced cell growth, implicating involvement of Wnt-independent signaling [317]. Furthermore, analysis of global expression reveled that over-expression of SFRP2 repressed numerous genes that are implicated in Wnt/β-catenin-dependent signaling. More experiments involving the knockdown of the individual SFRPs in β-catenin-deficient osteosarcoma cell lines such as CRL1423 would be needed to clarify the contributory role of Wnt/β-

catenin-independent signaling by SFRPs in regulating tumor-suppressive effects in osteosarcoma.

CHAPTER 6.   Conclusions and Perspective

The overall aim of this thesis is to develop novel Wnt-targeted therapeutics for the treatment of osteosarcoma. We tested the hypothesis of disrupting the Wnt/β-catenin signaling pathway as an effective therapeutic strategy in preventing osteosarcoma progression. The hypothesis was investigated using a two-pronged approach: The first approach builds on novel identification of small molecule compounds derived from natural sources as potent inhibitors of the Wnt pathway. Using curcumin as a lead compound, a series of 43 functionalized curcumin analogues were chemically synthesized to determine if structural modification would result in more potent Wnt antagonists. This part of the study also aimed at identifying critical structural motifs for Wnt inhibitory activity and understanding the underlying mechanism of Wnt inhibition of the most potent curcumin analogue. The second approach focuses on understanding the functional roles and mechanisms of SFRPs as tumor suppressors in regulating osteosarcoma cell proliferation, motility and invasion.

In aim (1), several natural occurring small molecule compounds such as curcumin and PKF118-310 were successfully identified as effective Wnt antagonists in osteosarcoma (Chapter 3). We showed that curcumin significantly inhibited Wnt/β-catenin signaling and reverses Wnt/β-catenin-induced cell invasiveness and MMP-9 expression in U2OS cells. Furthermore, PKF118-310 inhibited osteosarcoma cell invasion, migration and proliferation, as well as induced apoptosis and G2/M phase cell cycle arrest, through down-regulating Wnt target genes including MMP-9, cyclin D1, c-Myc and survivin.

In aim (2), functionlization of curcumin was found to be an attractive approach of enhancing the potency of Wnt inhibitory activity (Chapter 4). Modification of the curcumin structure was made to the central linker between the terminal phenyl rings and various permutations centered on the OH/OCH_3 groups as ring substitutions. Despite these simple structural modifications, we identified six analogues (**2-3, 3-3, 4-3, 2-6, 3-6, 4-6**) that were more potent than parental curcumin in suppressing β-catenin/TCF transcriptional activities and inhibition of U2OS cell invasiveness. These analogues were approximately 6.5- to 60-fold more potent than parental curcumin. SAR analysis of the whole panel of 43 curcumin analogues provided four important observations relating to the Wnt inhibitory activity (Figure 4-5): Firstly, reducing the flexibility of the intermediate linker joining the terminal phenyl rings improved inhibitory activity. Incorporating the linker as part of a ring structure like those represented in Series 3 (dibenzylidene-cyclohexanone) and Series 4 (dibenzylidene-cyclopentanone) resulted in several compounds with outstanding activities. Secondly, the flexibility of the intermediate side chain influenced the substitution on the terminal phenyl rings that were required for good activity. Thirdly, specifically for Series 3 and 4 analogues, the preferred substituents were deduced to be electron donating. Lastly, ring substitutions with limited size requirements are favored if sited at the 3' position.

In aim (3), we investigated the functional role of SFRP1, 2, 4 and 5 and found that these secreted Wnt antagonists differentially suppressed anchorage-dependent growth, colony formation efficiency, invasion and migration in U2OS cells (Chapter 5). These anti-tumor

activities were mediated through down-regulations of Wnt responsive oncogenes including matrix metalloproteinases-2, cyclin D1, c-Myc and survivin. Lastly, using the Human Wnt Signaling Pathway RT^2 Profiler^{TM} PCR Array, we identified additional Wnt target genes such as WISP1, Brachyury, SLC9A3R1 and JUN that might play significant contributory role in regulating osteosarcoma tumorigenesis and metastasis. By analyzing significant perturbations of Wnt signaling components mRNA levels, we also identified potential critical targets for Wnt inhibition by the restoration of SFRP2 or SFRP5 or treatment of analogue **3-3** in U2OS cells.

The present work has raised several issues to be pursued in future investigations. In Chapter 4, we evaluated a set of curcumin analogues with improved potency and high selectivity as Wnt/β-catenin antagonists. An important outcome of this study is the recognition of the curcumin backbone as a potential lead for compounds with potent Wnt inhibitory activity. Additional analogues with the symmetrical terminal phenyl rings substituted with electron-donating groups such as $N(OCH_3)_2$ (σp $N(OCH_3)_2$, -0.63 ; σm $N(OCH_3)_2$, -0.10) and NH_2 (σp NH_2, -0.57 ; σm NH_2, -0.09) would be required to confirm our findings that Wnt inhibitory activity is favored by the absence of electron-withdrawing groups at these phenyl rings. In addition, the structural modifications described here have been fairly limited and there is ample scope for further exploration with more structurally diverse curcumin analogues. These proposed modifications are summarized in Figure 6-1. For example, would tri- or multiple-substitutions of the phenyl rings with electron-donating groups further improve Wnt inhibitory activity? How would Wnt inhibitory activity be affected by replacing both the terminal phenyl rings with other

aromatic rings such as furan, thiophene, pyrrole or naphthalene? Would incorporation of other aromatic rings as part of the linker and varying the substitutions on these rings lead to enhanced Wnt inhibition?
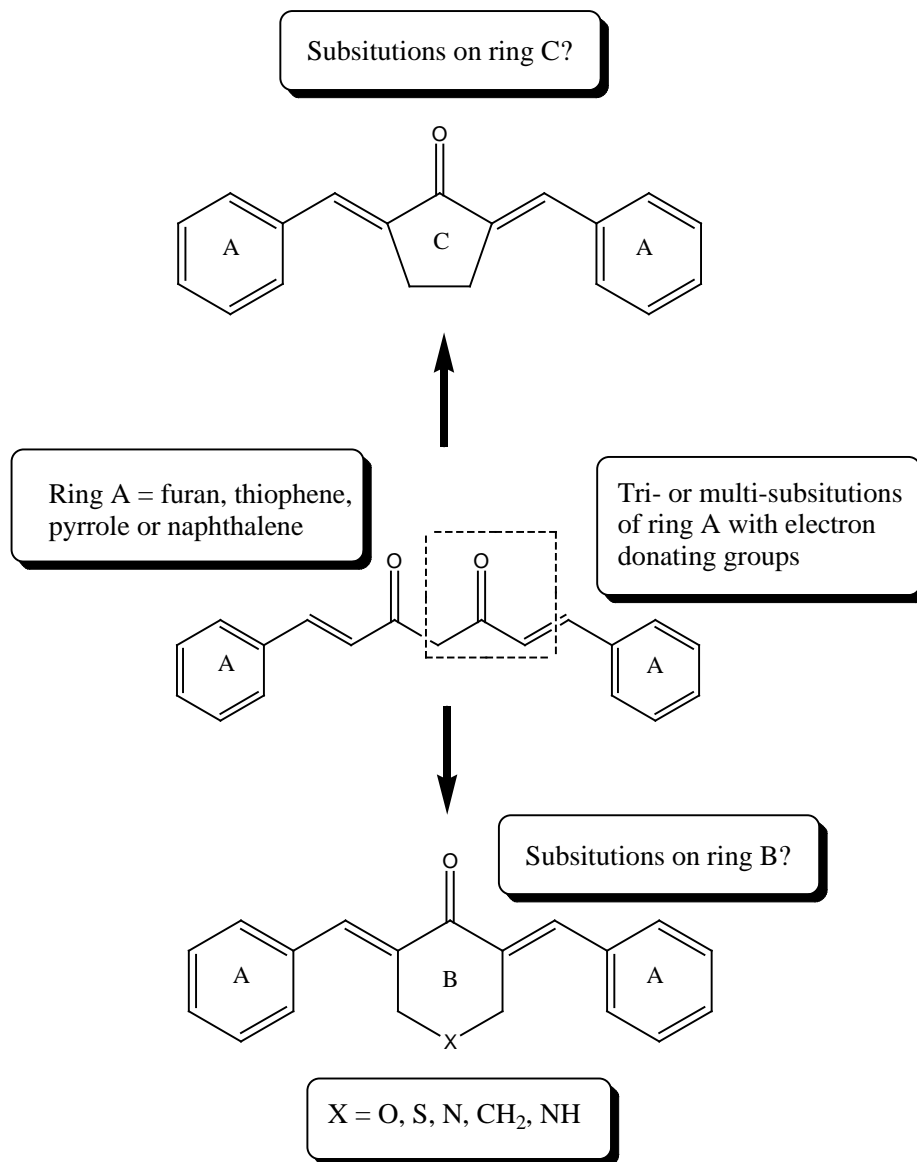
Figure 6-1. Proposed modifications of curcumin template for improved Wnt inhibitory activity.

Another objective of this thesis is to examine the underlying mechanism of Wnt inhibition of curcumin analogues (Chapter 4) and SFRPs (Chapter 5). Perturbations in

mRNA levels of several Wnt targeted genes following treatment with either the most potent analogue (**3-3**) or U2OS cells over-expressing SFRP2 or 5 collectively suggest that **3-3** and forced expressions of SFRP2 or 5 attenuated the Wnt/β-catenin signaling pathway at various critical nodal points of the pathway. However, further experiments are needed to verify and confirm our results: (1) Perturbations were observed on the mRNA levels, thus these findings needs to be validated at the protein levels using immunohistochemistry or western blotting; (2) Anti-sense and siRNA strategies against tumor-suppressor genes including Brachyury and WIF1 that are up-regulated with our treatments would be essential to verify their contributory roles in regulating osteosarcoma growth and metastasis; (3) On the other hand, additional experiments using forced expressions of other oncogenes including WISP1, FOSL1, JUN and cyclinD2 that are down-regulated are necessary to further elucidate their effects in inhibiting various anti-tumor activities in osteosarcoma; (4) Further immunoprecipitation assays needs to be performed to investigate protein interactions of the various components of the APC-Axin-GSK-3β-β-catenin complex to fully elucidate its role in enhancing phosphorylation-dependent ubiquitination of β-catenin following treatment with analogue **3-3** and restoration of SFRP2 or 5 respectively; (5) Lastly, it would be interesting to examine the specificities for disruption of the native WNT-FZD complexes interacts by over-expression of SFRP2 or 5 using appropriate binding assays and X-ray crystallography.

Our results suggest that manipulating this pathway through new small molecule compounds or recombinant/therapeutic molecules is of great promise for osteosarcoma therapy. Nevertheless, the application of Wnt therapeutics may be relevant in only a

subset of osteosarcoma tumors since only a few osteosarcoma cell lines were studied. Future studies with a wider range of osteosarcoma cell lines, primary tumors and patient tissue samples are required to confirm and supplement our findings and to better clarify the implication of canonical Wnt signaling pathway in osteosarcoma tumorigenesis and metastasis. Furthermore, our *in vitro* results may be encouraging but the true therapeutic potential of the Wnt/β-catenin inhibitors will only become evident when their *in vivo* efficacies as anti-tumor agents are rigorously tested in nude mice tumor models.

Other challenges remain to be overcome before Wnt therapeutics becomes a reality for osteosarcoma treatment. Given that the Wnt/β-catenin signaling pathway is also involved in normal developmental processes such as the regulation of tissue regeneration and stem cell renewal in the bone marrow and gut, persistent inhibition of this signaling pathway may result in potential fatal side effects including anemia, immunosuppression and gastrointestinal damages. The challenge of this study will therefore be to ensure both therapeutic strategies of using small molecule antagonists and SFRPs secreted inhibitors result in sufficient selectivity to avoid these detrimental side effects resulting from inappropriate disruption of Wnt signaling in normal tissues. Finally, Wnt/β-catenin signaling pathway does not occur in isolation from other signaling pathways, and there is considerable evidence suggesting that other cross-talk pathways can cooperate in unexpected ways in the pathogenesis of osteosarcoma. The mechanism by which this combinatorial signaling occurs and whether it is functionally significant in osteosarcoma are largely unknown. As such, the potential benefit of combining the use of inhibitors of

different pathways with Wnt therapeutics for osteosarcoma treatment needs further attention.

Most recently, Cai et al. reported that canonical Wnt/β-catenin signaling appear to be inactive in osteosarcoma and concluded that silencing of Wnt signaling may contribute to osteosarcoma tumorigenesis [318]. They found that β-catenin expression was localized to the cytoplasm and cell membrane, rather than the nucleus. They also demonstrated that a GSK3β inhibitor, GIN, inhibited osteosarcoma cell growth and stimulated markers of osteoblast differentiation. In contrast to their findings, we found the majority of the β-catenin protein localized in the nucleus of U2OS cells (Figure 5-4). The effects of GIN on osteosarcoma should be verified using a specific Wnt antagonist, especially since GSK3β kinase plays multiple roles in cellular processes, aside from those linked to β-catenin. In addition, there are no examples of signaling pathways that have been identified where gain-in-function clearly results in tumor suppression in one tumor type, but stimulate tumor formation in others. Therefore, the findings from this isolated report need further confirmation.

In this thesis, we have proven the hypothesis that osteosarcoma tumorigenesis and metastasis may be delayed by small molecule Wnt inhibitors or restoration of endogenous antagonist SFRPs. The contributory role of aberrant canonical Wnt/β-catenin signaling in osteosarcoma disease progression has been demonstrated by enhanced U2OS cell invasion with forced expression of β-catenin (Figure 3-10b). In Chapter 3, we further provided important *in-vitro* proof-of-concept for the potential use of small molecule

Wnt/β-catenin inhibitors to delay osteosarcoma progression and metastasis (Aim 1). In Chapter 4, we evaluated and identified curcumin analogues with enhanced Wnt inhibitory potency and reported critical structural motifs for Wnt inhibitory activity using structure-activity–relationship analysis (Aim 2). Lastly, we demonstrated the role of SFRPs as tumor suppressors in delaying osteosarcoma disease progression (Chapter 5, Aim 3). All in all, our findings strongly supported the prevailing view that activated Wnt/β-catenin signaling is critical in the pathogenesis of osteosarcoma and that Wnt targeted therapeutics hold great promises for the treatment of osteosarcoma.

BIBLIOGRAPHY

1.   Arndt, C.A. and W.M. Crist, *Common musculoskeletal tumors of childhood and adolescence.* N Engl J Med, 1999. **341**(5): p. 342-52.
2.   Kansara, M. and D.M. Thomas, *Molecular pathogenesis of osteosarcoma.* DNA Cell Biol, 2007. **26**(1): p. 1-18.
3.   Link, M.P., et al., *The effect of adjuvant chemotherapy on relapse-free survival in patients with osteosarcoma of the extremity.* N Engl J Med, 1986. **314**(25): p. 1600-6.
4.   Bielack, S.S., B. Kempf-Bielack, and K. Winkler, *Osteosarcoma: relationship of response to preoperative chemotherapy and type of surgery to local recurrence.* J Clin Oncol, 1996. **14**(2): p. 683-4.
5.   Bielack, S.S., et al., *Prognostic factors in high-grade osteosarcoma of the extremities or trunk: an analysis of 1,702 patients treated on neoadjuvant cooperative osteosarcoma study group protocols.* J Clin Oncol, 2002. **20**(3): p. 776-90.
6.   Ozger, H., et al., *[Survival analysis and the effects of prognostic factors in patients treated for osteosarcoma].* Acta Orthop Traumatol Turc, 2007. **41**(3): p. 211-9.
7.   Ferrari, S., et al., *Postrelapse survival in osteosarcoma of the extremities: prognostic factors for long-term survival.* J Clin Oncol, 2003. **21**(4): p. 710-5.
8.   Kempf-Bielack, B., et al., *Osteosarcoma relapse after combined modality therapy: an analysis of unselected patients in the Cooperative Osteosarcoma Study Group (COSS).* J Clin Oncol, 2005. **23**(3): p. 559-68.
9.   Petrilli, A.S., et al., *Results of the Brazilian Osteosarcoma Treatment Group Studies III and IV: prognostic factors and impact on survival.* J Clin Oncol, 2006. **24**(7): p. 1161-8.
10.   Lee, E.J., et al., *Cyclooxygenase-2 promotes cell proliferation, migration and invasion in U2OS human osteosarcoma cells.* Exp Mol Med, 2007. **39**(4): p. 469-76.
11.   Naruse, T., et al., *Meloxicam inhibits osteosarcoma growth, invasiveness and metastasis by COX-2-dependent and independent routes.* Carcinogenesis, 2006. **27**(3): p. 584-92.
12.   Harimaya, K., et al., *Antioxidants inhibit TNFalpha-induced motility and invasion of human osteosarcoma cells: possible involvement of NFkappaB activation.* Clin Exp Metastasis, 2000. **18**(2): p. 121-9.
13.   Felx, M., et al., *Endothelin-1 (ET-1) promotes MMP-2 and MMP-9 induction involving the transcription factor NF-kappaB in human osteosarcoma.* Clin Sci (Lond), 2006. **110**(6): p. 645-54.
14.   Abdeen, A., et al., *Correlation between clinical outcome and growth factor pathway expression in osteogenic sarcoma.* Cancer, 2009. **115**(22): p. 5243-50.
15.   Do, S.I., et al., *Expression of insulin-like growth factor-II mRNA binding protein 3 (IMP3) in osteosarcoma.* Oncol Res, 2008. **17**(6): p. 269-72.

16. Do, S.I., et al., *The expression of epidermal growth factor receptor and its downstream signaling molecules in osteosarcoma.* Int J Oncol, 2009. **34**(3): p. 797-803.

17. Ryu, K., et al., *Activation of signal transducer and activator of transcription 3 (Stat3) pathway in osteosarcoma cells and overexpression of phosphorylated-Stat3 correlates with poor prognosis.* J Orthop Res, 2010. **28**(7): p. 971-8.

18. Chen, C.L., et al., *Signal transducer and activator of transcription 3 is involved in cell growth and survival of human rhabdomyosarcoma and osteosarcoma cells.* BMC Cancer, 2007. **7**: p. 111.

19. Li, G.D., et al., *[Gene profiling of MAPK pathway in human osteosarcoma].* Zhonghua Zhong Liu Za Zhi, 2009. **31**(5): p. 340-5.

20. Gazitt, Y., et al., *Targeted therapy of human osteosarcoma with 17AAG or rapamycin: characterization of induced apoptosis and inhibition of mTOR and Akt/MAPK/Wnt pathways.* Int J Oncol, 2009. **34**(2): p. 551-61.

21. Morioka, K., et al., *Orphan receptor tyrosine kinase ROR2 as a potential therapeutic target for osteosarcoma.* Cancer Sci, 2009. **100**(7): p. 1227-33.

22. Enomoto, M., et al., *Autonomous regulation of osteosarcoma cell invasiveness by Wnt5a/Ror2 signaling.* Oncogene, 2009. **28**(36): p. 3197-208.

23. Yang, C., et al., *The kinase Mirk is a potential therapeutic target in osteosarcoma.* Carcinogenesis, 2010. **31**(4): p. 552-8.

24. Hayden, J.B. and B.H. Hoang, *Osteosarcoma: basic science and clinical implications.* Orthop Clin North Am, 2006. **37**(1): p. 1-7.

25. Wolf, M., et al., *Novel findings in gene expression detected in human osteosarcoma by cDNA microarray.* Cancer Genet Cytogenet, 2000. **123**(2): p. 128-32.

26. Fuchs, B., et al., *Identification of twenty-two candidate markers for human osteogenic sarcoma.* Gene, 2001. **278**(1-2): p. 245-52.

27. Khanna, C., et al., *Metastasis-associated differences in gene expression in a murine model of osteosarcoma.* Cancer Res, 2001. **61**(9): p. 3750-9.

28. Nakano, T., et al., *Biological properties and gene expression associated with metastatic potential of human osteosarcoma.* Clin Exp Metastasis, 2003. **20**(7): p. 665-74.

29. Sharma, R.P. and V.L. Chopra, *Effect of the Wingless (wg1) mutation on wing and haltere development in Drosophila melanogaster.* Dev Biol, 1976. **48**(2): p. 461-5.

30. Nusse, R. and H.E. Varmus, *Many tumors induced by the mouse mammary tumor virus contain a provirus integrated in the same region of the host genome.* Cell, 1982. **31**(1): p. 99-109.

31. Rijsewijk, F., et al., *The Drosophila homolog of the mouse mammary oncogene int-1 is identical to the segment polarity gene wingless.* Cell, 1987. **50**(4): p. 649-57.

32. Wodarz, A. and R. Nusse, *Mechanisms of Wnt signaling in development.* Annu Rev Cell Dev Biol, 1998. **14**: p. 59-88.

33. Willert, K. and R. Nusse, *Beta-catenin: a key mediator of Wnt signaling.* Curr Opin Genet Dev, 1998. **8**(1): p. 95-102.

34. Clevers, H., *Wnt/beta-catenin signaling in development and disease.* Cell, 2006. **127**(3): p. 469-80.

35. Moon, R.T., et al., *WNT and beta-catenin signalling: diseases and therapies.* Nat Rev Genet, 2004. **5**(9): p. 691-701.

36. Johnson, M.L. and N. Rajamannan, *Diseases of Wnt signaling.* Rev Endocr Metab Disord, 2006. **7**(1-2): p. 41-9.

37. Bhanot, P., et al., *A new member of the frizzled family from Drosophila functions as a Wingless receptor.* Nature, 1996. **382**(6588): p. 225-30.

38. Tamai, K., et al., *LDL-receptor-related proteins in Wnt signal transduction.* Nature, 2000. **407**(6803): p. 530-5.

39. Kuhl, M., et al., *The Wnt/Ca2+ pathway: a new vertebrate Wnt signaling pathway takes shape.* Trends Genet, 2000. **16**(7): p. 279-83.

40. Chen, A.E., D.D. Ginty, and C.M. Fan, *Protein kinase A signalling via CREB controls myogenesis induced by Wnt proteins.* Nature, 2005. **433**(7023): p. 317-22.

41. Katoh, M., et al., *WNT2B2 mRNA, up-regulated in primary gastric cancer, is a positive regulator of the WNT- beta-catenin-TCF signaling pathway.* Biochem Biophys Res Commun, 2001. **289**(5): p. 1093-8.

42. Mazieres, J., et al., *Wnt2 as a new therapeutic target in malignant pleural mesothelioma.* Int J Cancer, 2005. **117**(2): p. 326-32.

43. Milovanovic, T., et al., *Expression of Wnt genes and frizzled 1 and 2 receptors in normal breast epithelium and infiltrating breast carcinoma.* Int J Oncol, 2004. **25**(5): p. 1337-42.

44. Rhee, C.S., et al., *Wnt and frizzled receptors as potential targets for immunotherapy in head and neck squamous cell carcinomas.* Oncogene, 2002. **21**(43): p. 6598-605.

45. You, L., et al., *Inhibition of Wnt-2-mediated signaling induces programmed cell death in non-small-cell lung cancer cells.* Oncogene, 2004. **23**(36): p. 6170-4.

46. You, L., et al., *Wnt-1 signal as a potential cancer therapeutic target.* Drug News Perspect, 2006. **19**(1): p. 27-31.

47. Hoang, B.H., et al., *Expression of LDL receptor-related protein 5 (LRP5) as a novel marker for disease progression in high-grade osteosarcoma.* Int J Cancer, 2004. **109**(1): p. 106-11.

48. Chen, K., et al., *Wnt10b induces chemotaxis of osteosarcoma and correlates with reduced survival.* Pediatr Blood Cancer, 2008. **51**(3): p. 349-55.

49. To, K.F., et al., *Alterations of frizzled (FzE3) and secreted frizzled related protein (hsFRP) expression in gastric cancer.* Life Sci, 2001. **70**(4): p. 483-9.

50. Kirikoshi, H., H. Sekihara, and M. Katoh, *Up-regulation of Frizzled-7 (FZD7) in human gastric cancer.* Int J Oncol, 2001. **19**(1): p. 111-5.

51. Guo, Y., et al., *Blocking Wnt/LRP5 signaling by a soluble receptor modulates the epithelial to mesenchymal transition and suppresses met and metalloproteinases in osteosarcoma Saos-2 cells.* J Orthop Res, 2007. **25**(7): p. 964-71.

52. Guo, Y., et al., *Dominant negative LRP5 decreases tumorigenicity and metastasis of osteosarcoma in an animal model.* Clin Orthop Relat Res, 2008. **466**(9): p. 2039-45.

53. Bjorklund, P., G. Akerstrom, and G. Westin, *An LRP5 receptor with internal deletion in hyperparathyroid tumors with implications for deregulated WNT/beta-catenin signaling.* PLoS Med, 2007. **4**(11): p. e328.

54. Kawano, Y. and R. Kypta, *Secreted antagonists of the Wnt signalling pathway.* J Cell Sci, 2003. **116**(Pt 13): p. 2627-34.

55. Shi, Y., et al., *Roles of secreted frizzled-related proteins in cancer.* Acta Pharmacol Sin, 2007. **28**(9): p. 1499-504.

56. Mandal, D., et al., *Severe suppression of Frzb/sFRP3 transcription in osteogenic sarcoma.* Gene, 2007. **386**(1-2): p. 131-8.

57. Fukui, T., et al., *Transcriptional silencing of secreted frizzled related protein 1 (SFRP 1) by promoter hypermethylation in non-small-cell lung cancer.* Oncogene, 2005. **24**(41): p. 6323-7.

58. Lee, A.Y., et al., *Expression of the secreted frizzled-related protein gene family is downregulated in human mesothelioma.* Oncogene, 2004. **23**(39): p. 6672-6.

59. Liu, T.H., et al., *CpG island methylation and expression of the secreted frizzled-related protein gene family in chronic lymphocytic leukemia.* Cancer Res, 2006. **66**(2): p. 653-8.

60. Wong, S.C., et al., *Expression of frizzled-related protein and Wnt-signalling molecules in invasive human breast tumours.* J Pathol, 2002. **196**(2): p. 145-53.

61. Suzuki, H., et al., *Epigenetic inactivation of SFRP genes allows constitutive WNT signaling in colorectal cancer.* Nat Genet, 2004. **36**(4): p. 417-22.

62. Suzuki, H., et al., *Frequent epigenetic inactivation of Wnt antagonist genes in breast cancer.* Br J Cancer, 2008. **98**(6): p. 1147-56.

63. Hoang, B.H., et al., *Dickkopf 3 inhibits invasion and motility of Saos-2 osteosarcoma cells by modulating the Wnt-beta-catenin pathway.* Cancer Res, 2004. **64**(8): p. 2734-9.

64. Urakami, S., et al., *Epigenetic inactivation of Wnt inhibitory factor-1 plays an important role in bladder cancer through aberrant canonical Wnt/beta-catenin signaling pathway.* Clin Cancer Res, 2006. **12**(2): p. 383-91.

65. Kansara, M., et al., *Wnt inhibitory factor 1 is epigenetically silenced in human osteosarcoma, and targeted disruption accelerates osteosarcomagenesis in mice.* J Clin Invest, 2009. **119**(4): p. 837-51.

66. Ai, L., et al., *Inactivation of Wnt inhibitory factor-1 (WIF1) expression by epigenetic silencing is a common event in breast cancer.* Carcinogenesis, 2006. **27**(7): p. 1341-8.

67. Batra, S., et al., *Wnt inhibitory factor-1, a Wnt antagonist, is silenced by promoter hypermethylation in malignant pleural mesothelioma.* Biochem Biophys Res Commun, 2006. **342**(4): p. 1228-32.

68. Mazieres, J., et al., *Wnt inhibitory factor-1 is silenced by promoter hypermethylation in human lung cancer.* Cancer Res, 2004. **64**(14): p. 4717-20.

69. Wissmann, C., et al., *WIF1, a component of the Wnt pathway, is down-regulated in prostate, breast, lung, and bladder cancer.* J Pathol, 2003. **201**(2): p. 204-12.

70. Okino, K., et al., *Up-regulation and overproduction of DVL-1, the human counterpart of the Drosophila dishevelled gene, in cervical squamous cell carcinoma.* Oncol Rep, 2003. **10**(5): p. 1219-23.

71. Uematsu, K., et al., *Activation of the Wnt pathway in non small cell lung cancer: evidence of dishevelled overexpression.* Oncogene, 2003. **22**(46): p. 7218-21.
72. Uematsu, K., et al., *Wnt pathway activation in mesothelioma: evidence of Dishevelled overexpression and transcriptional activity of beta-catenin.* Cancer Res, 2003. **63**(15): p. 4547-51.
73. Haydon, R.C., et al., *Cytoplasmic and/or nuclear accumulation of the beta-catenin protein is a frequent event in human osteosarcoma.* Int J Cancer, 2002. **102**(4): p. 338-42.
74. Iwao, K., et al., *Frequent beta-catenin abnormalities in bone and soft-tissue tumors.* Jpn J Cancer Res, 1999. **90**(2): p. 205-9.
75. Sunaga, N., et al., *Constitutive activation of the Wnt signaling pathway by CTNNB1 (beta-catenin) mutations in a subset of human lung adenocarcinoma.* Genes Chromosomes Cancer, 2001. **30**(3): p. 316-21.
76. Morin, P.J., et al., *Activation of beta-catenin-Tcf signaling in colon cancer by mutations in beta-catenin or APC.* Science, 1997. **275**(5307): p. 1787-90.
77. Polakis, P., *Wnt signaling and cancer.* Genes Dev, 2000. **14**(15): p. 1837-51.
78. Rubinfeld, B., et al., *Stabilization of beta-catenin by genetic defects in melanoma cell lines.* Science, 1997. **275**(5307): p. 1790-2.
79. Korinek, V., et al., *Constitutive transcriptional activation by a beta-catenin-Tcf complex in APC-/- colon carcinoma.* Science, 1997. **275**(5307): p. 1784-7.
80. Miyoshi, Y., et al., *Somatic mutations of the APC gene in colorectal tumors: mutation cluster region in the APC gene.* Hum Mol Genet, 1992. **1**(4): p. 229-33.
81. Powell, S.M., et al., *APC mutations occur early during colorectal tumorigenesis.* Nature, 1992. **359**(6392): p. 235-7.
82. Dahmen, R.P., et al., *Deletions of AXIN1, a component of the WNT/wingless pathway, in sporadic medulloblastomas.* Cancer Res, 2001. **61**(19): p. 7039-43.
83. Satoh, S., et al., *AXIN1 mutations in hepatocellular carcinomas, and growth suppression in cancer cells by virus-mediated transfer of AXIN1.* Nat Genet, 2000. **24**(3): p. 245-50.
84. Nakajima, M., et al., *Reduced expression of Axin correlates with tumour progression of oesophageal squamous cell carcinoma.* Br J Cancer, 2003. **88**(11): p. 1734-9.
85. Lammi, L., et al., *Mutations in AXIN2 cause familial tooth agenesis and predispose to colorectal cancer.* Am J Hum Genet, 2004. **74**(5): p. 1043-50.
86. Liu, W., et al., *Mutations in AXIN2 cause colorectal cancer with defective mismatch repair by activating beta-catenin/TCF signalling.* Nat Genet, 2000. **26**(2): p. 146-7.
87. Ishizaki, Y., et al., *Immunohistochemical analysis and mutational analyses of beta-catenin, Axin family and APC genes in hepatocellular carcinomas.* Int J Oncol, 2004. **24**(5): p. 1077-83.
88. Graveel, C., et al., *Activating Met mutations produce unique tumor profiles in mice with selective duplication of the mutant allele.* Proc Natl Acad Sci U S A, 2004. **101**(49): p. 17198-203.
89. Wang, Z., et al., *Mutational analysis of the tyrosine phosphatome in colorectal cancers.* Science, 2004. **304**(5674): p. 1164-6.

90. Rowley, J.D., *Rearrangements involving chromosome band 11Q23 in acute leukaemia.* Semin Cancer Biol, 1993. **4**(6): p. 377-85.

91. Guo, C., et al., *Allelic deletion at 11q23 is common in MYCN single copy neuroblastomas.* Oncogene, 1999. **18**(35): p. 4948-57.

92. Knosel, T., et al., *Incidence of chromosomal imbalances in advanced colorectal carcinomas and their metastases.* Virchows Arch, 2002. **440**(2): p. 187-94.

93. Duval, A., et al., *Frequent frameshift mutations of the TCF-4 gene in colorectal cancers with microsatellite instability.* Cancer Res, 1999. **59**(17): p. 4213-5.

94. Kim, J., et al., *Suppression of Wnt signaling by the green tea compound (-)-epigallocatechin 3-gallate (EGCG) in invasive breast cancer cells. Requirement of the transcriptional repressor HBP1.* J Biol Chem, 2006. **281**(16): p. 10865-75.

95. Sampson, E.M., et al., *Negative regulation of the Wnt-beta-catenin pathway by the transcriptional repressor HBP1.* EMBO J, 2001. **20**(16): p. 4500-11.

96. Ryu, M.J., et al., *Natural derivatives of curcumin attenuate the Wnt/beta-catenin pathway through down-regulation of the transcriptional coactivator p300.* Biochem Biophys Res Commun, 2008. **377**(4): p. 1304-8.

97. Tetsu, O. and F. McCormick, *Beta-catenin regulates expression of cyclin D1 in colon carcinoma cells.* Nature, 1999. **398**(6726): p. 422-6.

98. He, T.C., et al., *Identification of c-MYC as a target of the APC pathway.* Science, 1998. **281**(5382): p. 1509-12.

99. Brabletz, T., et al., *beta-catenin regulates the expression of the matrix metalloproteinase-7 in human colorectal cancer.* Am J Pathol, 1999. **155**(4): p. 1033-8.

100. Crawford, H.C., et al., *The metalloproteinase matrilysin is a target of beta-catenin transactivation in intestinal tumors.* Oncogene, 1999. **18**(18): p. 2883-91.

101. Marchenko, N.D., et al., *Beta-catenin regulates the gene of MMP-26, a novel metalloproteinase expressed both in carcinomas and normal epithelial cells.* Int J Biochem Cell Biol, 2004. **36**(5): p. 942-56.

102. Levy, L., et al., *Transcriptional activation of interleukin-8 by beta-catenin-Tcf4.* J Biol Chem, 2002. **277**(44): p. 42386-93.

103. Hiendlmeyer, E., et al., *Beta-catenin up-regulates the expression of the urokinase plasminogen activator in human colorectal tumors.* Cancer Res, 2004. **64**(4): p. 1209-14.

104. Mao, B., et al., *Kremen proteins are Dickkopf receptors that regulate Wnt/beta-catenin signalling.* Nature, 2002. **417**(6889): p. 664-7.

105. Bafico, A., et al., *Novel mechanism of Wnt signalling inhibition mediated by Dickkopf-1 interaction with LRP6/Arrow.* Nat Cell Biol, 2001. **3**(7): p. 683-6.

106. Zeng, W., et al., *naked cuticle encodes an inducible antagonist of Wnt signalling.* Nature, 2000. **403**(6771): p. 789-95.

107. Sun, T.Q., et al., *PAR-1 is a Dishevelled-associated kinase and a positive regulator of Wnt signalling.* Nat Cell Biol, 2001. **3**(7): p. 628-36.

108. Hino, S., et al., *Inhibition of the Wnt signaling pathway by Idax, a novel Dvl-binding protein.* Mol Cell Biol, 2001. **21**(1): p. 330-42.

109. Liu, C., et al., *Control of beta-catenin phosphorylation/degradation by a dual-kinase mechanism.* Cell, 2002. **108**(6): p. 837-47.

191

110. Behrens, J., et al., *Functional interaction of an axin homolog, conductin, with beta-catenin, APC, and GSK3beta.* Science, 1998. **280**(5363): p. 596-9.

111. Spiegelman, V.S., et al., *Wnt/beta-catenin signaling induces the expression and activity of betaTrCP ubiquitin ligase receptor.* Mol Cell, 2000. **5**(5): p. 877-82.

112. Liu, C., et al., *beta-Trcp couples beta-catenin phosphorylation-degradation and regulates Xenopus axis formation.* Proc Natl Acad Sci U S A, 1999. **96**(11): p. 6273-8.

113. Drees, F., et al., *Alpha-catenin is a molecular switch that binds E-cadherin-beta-catenin and regulates actin-filament assembly.* Cell, 2005. **123**(5): p. 903-15.

114. Kemler, R., *From cadherins to catenins: cytoplasmic protein interactions and regulation of cell adhesion.* Trends Genet, 1993. **9**(9): p. 317-21.

115. Yamada, S., et al., *Deconstructing the cadherin-catenin-actin complex.* Cell, 2005. **123**(5): p. 889-901.

116. Behrens, J., et al., *Functional interaction of beta-catenin with the transcription factor LEF-1.* Nature, 1996. **382**(6592): p. 638-42.

117. Huber, O., et al., *Nuclear localization of beta-catenin by interaction with transcription factor LEF-1.* Mech Dev, 1996. **59**(1): p. 3-10.

118. Roura, S., et al., *Regulation of E-cadherin/Catenin association by tyrosine phosphorylation.* J Biol Chem, 1999. **274**(51): p. 36734-40.

119. Piedra, J., et al., *p120 Catenin-associated Fer and Fyn tyrosine kinases regulate beta-catenin Tyr-142 phosphorylation and beta-catenin-alpha-catenin Interaction.* Mol Cell Biol, 2003. **23**(7): p. 2287-97.

120. Brembeck, F.H., et al., *Essential role of BCL9-2 in the switch between beta-catenin's adhesive and transcriptional functions.* Genes Dev, 2004. **18**(18): p. 2225-30.

121. Xu, G., et al., *Continuous association of cadherin with beta-catenin requires the non-receptor tyrosine-kinase Fer.* J Cell Sci, 2004. **117**(Pt 15): p. 3207-19.

122. Piedra, J., et al., *Regulation of beta-catenin structure and activity by tyrosine phosphorylation.* J Biol Chem, 2001. **276**(23): p. 20436-43.

123. Castano, J., et al., *Beta-catenin N- and C-terminal tails modulate the coordinated binding of adherens junction proteins to beta-catenin.* J Biol Chem, 2002. **277**(35): p. 31541-50.

124. Adachi, S., et al., *Role of a BCL9-related beta-catenin-binding protein, B9L, in tumorigenesis induced by aberrant activation of Wnt signaling.* Cancer Res, 2004. **64**(23): p. 8496-501.

125. Huber, A.H. and W.I. Weis, *The structure of the beta-catenin/E-cadherin complex and the molecular basis of diverse ligand recognition by beta-catenin.* Cell, 2001. **105**(3): p. 391-402.

126. Hulsken, J., W. Birchmeier, and J. Behrens, *E-cadherin and APC compete for the interaction with beta-catenin and the cytoskeleton.* J Cell Biol, 1994. **127**(6 Pt 2): p. 2061-9.

127. Gottardi, C.J. and B.M. Gumbiner, *Distinct molecular forms of beta-catenin are targeted to adhesive or transcriptional complexes.* J Cell Biol, 2004. **167**(2): p. 339-49.

128. Roose, J. and H. Clevers, *TCF transcription factors: molecular switches in carcinogenesis.* Biochim Biophys Acta, 1999. **1424**(2-3): p. M23-37.

129. Cavallo, R.A., et al., *Drosophila Tcf and Groucho interact to repress Wingless signalling activity.* Nature, 1998. **395**(6702): p. 604-8.

130. Chen, G., et al., *A functional interaction between the histone deacetylase Rpd3 and the corepressor groucho in Drosophila development.* Genes Dev, 1999. **13**(17): p. 2218-30.

131. Henderson, B.R., *Nuclear-cytoplasmic shuttling of APC regulates beta-catenin subcellular localization and turnover.* Nat Cell Biol, 2000. **2**(9): p. 653-60.

132. Neufeld, K.L., et al., *APC-mediated downregulation of beta-catenin activity involves nuclear sequestration and nuclear export.* EMBO Rep, 2000. **1**(6): p. 519-23.

133. Hecht, A., et al., *The p300/CBP acetyltransferases function as transcriptional coactivators of beta-catenin in vertebrates.* EMBO J, 2000. **19**(8): p. 1839-50.

134. Takemaru, K.I. and R.T. Moon, *The transcriptional coactivator CBP interacts with beta-catenin to activate gene expression.* J Cell Biol, 2000. **149**(2): p. 249-54.

135. Kramps, T., et al., *Wnt/wingless signaling requires BCL9/legless-mediated recruitment of pygopus to the nuclear beta-catenin-TCF complex.* Cell, 2002. **109**(1): p. 47-60.

136. Parker, D.S., J. Jemison, and K.M. Cadigan, *Pygopus, a nuclear PHD-finger protein required for Wingless signaling in Drosophila.* Development, 2002. **129**(11): p. 2565-76.

137. Mosimann, C., G. Hausmann, and K. Basler, *Parafibromin/Hyrax activates Wnt/Wg target gene transcription by direct association with beta-catenin/Armadillo.* Cell, 2006. **125**(2): p. 327-41.

138. Daniels, D.L. and W.I. Weis, *Beta-catenin directly displaces Groucho/TLE repressors from Tcf/Lef in Wnt-mediated transcription activation.* Nat Struct Mol Biol, 2005. **12**(4): p. 364-71.

139. Barker, N., et al., *The chromatin remodelling factor Brg-1 interacts with beta-catenin to promote target gene activation.* EMBO J, 2001. **20**(17): p. 4935-43.

140. Kim, S., et al., *Mediator is a transducer of Wnt/beta-catenin signaling.* J Biol Chem, 2006. **281**(20): p. 14066-75.

141. Amen, M., et al., *PITX2 and beta-catenin interactions regulate Lef-1 isoform expression.* Mol Cell Biol, 2007. **27**(21): p. 7560-73.

142. Zhang, T., et al., *Evidence that APC regulates survivin expression: a possible mechanism contributing to the stem cell origin of colon cancer.* Cancer Res, 2001. **61**(24): p. 8664-7.

143. Jamora, C., et al., *Links between signal transduction, transcription and adhesion in epithelial bud development.* Nature, 2003. **422**(6929): p. 317-22.

144. Wong, N.A. and M. Pignatelli, *Beta-catenin--a linchpin in colorectal carcinogenesis?* Am J Pathol, 2002. **160**(2): p. 389-401.

145. Zhang, X., J.P. Gaspard, and D.C. Chung, *Regulation of vascular endothelial growth factor by the Wnt and K-ras pathways in colonic neoplasia.* Cancer Res, 2001. **61**(16): p. 6050-4.

146. Xu, L., et al., *WISP-1 is a Wnt-1- and beta-catenin-responsive oncogene.* Genes Dev, 2000. **14**(5): p. 585-95.

147. Yamaguchi, T.P., et al., *T (Brachyury) is a direct target of Wnt3a during paraxial mesoderm specification.* Genes Dev, 1999. **13**(24): p. 3185-90.

148. Brannon, M., et al., *A beta-catenin/XTcf-3 complex binds to the siamois promoter to regulate dorsal axis specification in Xenopus.* Genes Dev, 1997. **11**(18): p. 2359-70.

149. Rubin, E.M., et al., *Wnt inhibitory factor 1 decreases tumorigenesis and metastasis in osteosarcoma.* Mol Cancer Ther, 2010. **9**(3): p. 731-41.

150. Boon, E.M., et al., *Sulindac targets nuclear beta-catenin accumulation and Wnt signalling in adenomas of patients with familial adenomatous polyposis and in human colorectal cancer cell lines.* Br J Cancer, 2004. **90**(1): p. 224-9.

151. Shao, J., et al., *Prostaglandin E2 Stimulates the beta-catenin/T cell factor-dependent transcription in colon cancer.* J Biol Chem, 2005. **280**(28): p. 26565-72.

152. Castellone, M.D., et al., *Prostaglandin E2 promotes colon cancer cell growth through a Gs-axin-beta-catenin signaling axis.* Science, 2005. **310**(5753): p. 1504-10.

153. Xia, J.J., et al., *Celecoxib inhibits beta-catenin-dependent survival of the human osteosarcoma MG-63 cell line.* J Int Med Res, 2010. **38**(4): p. 1294-304.

154. Hoosein, N.M., et al., *Comparison of the antiproliferative effects of transforming growth factor-beta, N,N-dimethylformamide and retinoic acid on a human colon carcinoma cell line.* Cancer Lett, 1988. **40**(2): p. 219-32.

155. O'Dwyer, P.J., et al., *Effect of 13-cis-retinoic acid on tumor prevention, tumor growth, and metastasis in experimental colon cancer.* J Surg Res, 1987. **43**(6): p. 550-7.

156. Mollersen, L., et al., *Dietary retinoic acid supplementation stimulates intestinal tumour formation and growth in multiple intestinal neoplasia (Min)/+ mice.* Carcinogenesis, 2004. **25**(1): p. 149-53.

157. He, B., et al., *A monoclonal antibody against Wnt-1 induces apoptosis in human cancer cells.* Neoplasia, 2004. **6**(1): p. 7-14.

158. You, L., et al., *An anti-Wnt-2 monoclonal antibody induces apoptosis in malignant melanoma cells and inhibits tumor growth.* Cancer Res, 2004. **64**(15): p. 5385-9.

159. Holcombe, R.F., et al., *Expression of Wnt ligands and Frizzled receptors in colonic mucosa and in colon carcinoma.* Mol Pathol, 2002. **55**(4): p. 220-6.

160. He, B., et al., *Blockade of Wnt-1 signaling induces apoptosis in human colorectal cancer cells containing downstream mutations.* Oncogene, 2005. **24**(18): p. 3054-8.

161. Kaplan, J.M., *Adenovirus-based cancer gene therapy.* Curr Gene Ther, 2005. **5**(6): p. 595-605.

162. Chen, R.H. and F. McCormick, *Selective targeting to the hyperactive beta-catenin/T-cell factor pathway in colon cancer cells.* Cancer Res, 2001. **61**(11): p. 4445-9.

163. Lipinski, K.S., et al., *Optimization of a synthetic beta-catenin-dependent promoter for tumor-specific cancer gene therapy.* Mol Ther, 2004. **10**(1): p. 150-61.

164. Brunori, M., et al., *Replicating adenoviruses that target tumors with constitutive activation of the wnt signaling pathway.* J Virol, 2001. **75**(6): p. 2857-65.

165.	Fuerer, C. and R. Iggo, *Adenoviruses with Tcf binding sites in multiple early promoters show enhanced selectivity for tumour cells with constitutive activation of the wnt signalling pathway.* Gene Ther, 2002. **9**(4): p. 270-81.

166.	Kwong, K.Y., et al., *The suppression of colon cancer cell growth in nude mice by targeting beta-catenin/TCF pathway.* Oncogene, 2002. **21**(54): p. 8340-6.

167.	DeAlmeida, V.I., et al., *The soluble wnt receptor Frizzled8CRD-hFc inhibits the growth of teratocarcinomas in vivo.* Cancer Res, 2007. **67**(11): p. 5371-9.

168.	Tsuji, T., et al., *A REIC gene shows down-regulation in human immortalized cells and human tumor-derived cell lines.* Biochem Biophys Res Commun, 2000. **268**(1): p. 20-4.

169.	Tsuji, T., et al., *Antiproliferative activity of REIC/Dkk-3 and its significant down-regulation in non-small-cell lung carcinomas.* Biochem Biophys Res Commun, 2001. **289**(1): p. 257-63.

170.	Shih, I.M., et al., *The beta-catenin binding domain of adenomatous polyposis coli is sufficient for tumor suppression.* Cancer Res, 2000. **60**(6): p. 1671-6.

171.	Green, D.W., et al., *Beta-catenin antisense treatment decreases beta-catenin expression and tumor growth rate in colon carcinoma xenografts.* J Surg Res, 2001. **101**(1): p. 16-20.

172.	Veeramachaneni, N.K., et al., *Down-regulation of beta catenin inhibits the growth of esophageal carcinoma cells.* J Thorac Cardiovasc Surg, 2004. **127**(1): p. 92-8.

173.	Chung, E.J., et al., *Regulation of leukemic cell adhesion, proliferation, and survival by beta-catenin.* Blood, 2002. **100**(3): p. 982-90.

174.	van de Wetering, M., et al., *Specific inhibition of gene expression using a stably integrated, inducible small-interfering-RNA vector.* EMBO Rep, 2003. **4**(6): p. 609-15.

175.	Verma, U.N., et al., *Small interfering RNAs directed against beta-catenin inhibit the in vitro and in vivo growth of colon cancer cells.* Clin Cancer Res, 2003. **9**(4): p. 1291-300.

176.	Arun, B. and P. Goss, *The role of COX-2 inhibition in breast cancer treatment and prevention.* Semin Oncol, 2004. **31**(2 Suppl 7): p. 22-9.

177.	Natale, R.B., *Irinotecan, cisplatin/carboplatin, and COX-2 inhibition in small-cell lung cancer.* Oncology (Williston Park), 2003. **17**(7 Suppl 7): p. 22-6.

178.	Lepourcelet, M., et al., *Small-molecule antagonists of the oncogenic Tcf/beta-catenin protein complex.* Cancer Cell, 2004. **5**(1): p. 91-102.

179.	Emami, K.H., et al., *A small molecule inhibitor of beta-catenin/CREB-binding protein transcription [corrected].* Proc Natl Acad Sci U S A, 2004. **101**(34): p. 12682-7.

180.	Fuerer, C. and R. Iggo, *5-Fluorocytosine increases the toxicity of Wnt-targeting replicating adenoviruses that express cytosine deaminase as a late gene.* Gene Ther, 2004. **11**(2): p. 142-51.

181.	Lukashev, A.N., et al., *Late expression of nitroreductase in an oncolytic adenovirus sensitizes colon cancer cells to the prodrug CB1954.* Hum Gene Ther, 2005. **16**(12): p. 1473-83.

182.	Iversen, P.L., et al., *Efficacy of antisense morpholino oligomer targeted to c-myc in prostate cancer xenograft murine model and a Phase I safety study in humans.* Clin Cancer Res, 2003. **9**(7): p. 2510-9.

183.   Chen, J.P., et al., *Antisense c-myc fragments induce normal differentiation cycles in HL-60 cells.* Eur J Clin Invest, 2006. **36**(1): p. 49-57.

184.   Whittaker, S.R., et al., *The Cyclin-dependent kinase inhibitor CYC202 (R-roscovitine) inhibits retinoblastoma protein phosphorylation, causes loss of Cyclin D1, and activates the mitogen-activated protein kinase pathway.* Cancer Res, 2004. **64**(1): p. 262-72.

185.   Hidalgo, M. and E.K. Rowinsky, *The rapamycin-sensitive signal transduction pathway as a target for cancer therapy.* Oncogene, 2000. **19**(56): p. 6680-6.

186.   van de Wetering, M., et al., *The beta-catenin/TCF-4 complex imposes a crypt progenitor phenotype on colorectal cancer cells.* Cell, 2002. **111**(2): p. 241-50.

187.   Stadeli, R. and K. Basler, *Dissecting nuclear Wingless signalling: recruitment of the transcriptional co-activator Pygopus by a chain of adaptor proteins.* Mech Dev, 2005. **122**(11): p. 1171-82.

188.   Xing, Y., et al., *Crystal structure of a beta-catenin/APC complex reveals a critical role for APC phosphorylation in APC function.* Mol Cell, 2004. **15**(4): p. 523-33.

189.   Xing, Y., et al., *Crystal structure of a full-length beta-catenin.* Structure, 2008. **16**(3): p. 478-87.

190.   Sampietro, J., et al., *Crystal structure of a beta-catenin/BCL9/Tcf4 complex.* Mol Cell, 2006. **24**(2): p. 293-300.

191.   Graham, T.A., et al., *Crystal structure of a beta-catenin/Tcf complex.* Cell, 2000. **103**(6): p. 885-96.

192.   Shan, J., et al., *Identification of a specific inhibitor of the dishevelled PDZ domain.* Biochemistry, 2005. **44**(47): p. 15495-503.

193.   Jaiswal, A.S., et al., *Beta-catenin-mediated transactivation and cell-cell adhesion pathways are important in curcumin (diferuylmethane)-induced growth arrest and apoptosis in colon cancer cells.* Oncogene, 2002. **21**(55): p. 8414-27.

194.   Pereira, B.P., et al., *Runx2, p53, and pRB status as diagnostic parameters for deregulation of osteoblast growth and differentiation in a new pre-chemotherapeutic osteosarcoma cell line (OS1).* J Cell Physiol, 2009. **221**(3): p. 778-88.

195.   Leow, P.C., et al., *Antitumor activity of natural compounds, curcumin and PKF118-310, as Wnt/beta-catenin antagonists against human osteosarcoma cells.* Invest New Drugs, 2009.

196.   Cho, H.J., et al., *Disulfiram suppresses invasive ability of osteosarcoma cells via the inhibition of MMP-2 and MMP-9 expression.* J Biochem Mol Biol, 2007. **40**(6): p. 1069-76.

197.   Barker, N. and H. Clevers, *Mining the Wnt pathway for cancer therapeutics.* Nat Rev Drug Discov, 2006. **5**(12): p. 997-1014.

198.   Coghlan, M.P., et al., *Selective small molecule inhibitors of glycogen synthase kinase-3 modulate glycogen metabolism and gene transcription.* Chem Biol, 2000. **7**(10): p. 793-803.

199.   Meijer, L., et al., *GSK-3-selective inhibitors derived from Tyrian purple indirubins.* Chem Biol, 2003. **10**(12): p. 1255-66.

200. Park, C.H., et al., *Quercetin, a potent inhibitor against beta-catenin/Tcf signaling in SW480 colon cancer cells.* Biochem Biophys Res Commun, 2005. **328**(1): p. 227-34.

201. Park, C.H., et al., *The inhibitory mechanism of curcumin and its derivative against beta-catenin/Tcf signaling.* FEBS Lett, 2005. **579**(13): p. 2965-71.

202. Goel, A., A.B. Kunnumakkara, and B.B. Aggarwal, *Curcumin as "Curecumin": from kitchen to clinic.* Biochem Pharmacol, 2008. **75**(4): p. 787-809.

203. Singh, S. and A. Khar, *Biological effects of curcumin and its role in cancer chemoprevention and therapy.* Anticancer Agents Med Chem, 2006. **6**(3): p. 259-70.

204. Agullo, G., et al., *Comparative effects of flavonoids on the growth, viability and metabolism of a colonic adenocarcinoma cell line (HT29 cells).* Cancer Lett, 1996. **105**(1): p. 61-70.

205. Hosokawa, N., et al., *Inhibitory effect of quercetin on the synthesis of a possibly cell-cycle-related 17-kDa protein, in human colon cancer cells.* Int J Cancer, 1990. **45**(6): p. 1119-24.

206. Kuo, S.M., *Antiproliferative potency of structurally distinct dietary flavonoids on human colon cancer cells.* Cancer Lett, 1996. **110**(1-2): p. 41-8.

207. Narayan, S., *Curcumin, a multi-functional chemopreventive agent, blocks growth of colon cancer cells by targeting beta-catenin-mediated transactivation and cell-cell adhesion pathways.* J Mol Histol, 2004. **35**(3): p. 301-7.

208. Tomita, M., et al., *Curcumin targets Akt cell survival signaling pathway in HTLV-I-infected T-cell lines.* Cancer Sci, 2006. **97**(4): p. 322-7.

209. Efferth, T., *Willmar Schwabe Award 2006: antiplasmodial and antitumor activity of artemisinin--from bench to bedside.* Planta Med, 2007. **73**(4): p. 299-309.

210. Nakase, I., et al., *Anticancer properties of artemisinin derivatives and their targeted delivery by transferrin conjugation.* Int J Pharm, 2008. **354**(1-2): p. 28-33.

211. Li, L.N., et al., *Artesunate attenuates the growth of human colorectal carcinoma and inhibits hyperactive Wnt/beta-catenin pathway.* Int J Cancer, 2007. **121**(6): p. 1360-5.

212. Gregory, C.A., et al., *The Wnt signaling inhibitor dickkopf-1 is required for reentry into the cell cycle of human adult stem cells from bone marrow.* J Biol Chem, 2003. **278**(30): p. 28067-78.

213. Dass, C.R., et al., *A novel orthotopic murine model provides insights into cellular and molecular characteristics contributing to human osteosarcoma.* Clin Exp Metastasis, 2006. **23**(7-8): p. 367-80.

214. Caca, K., et al., *Beta- and gamma-catenin mutations, but not E-cadherin inactivation, underlie T-cell factor/lymphoid enhancer factor transcriptional deregulation in gastric and pancreatic cancer.* Cell Growth Differ, 1999. **10**(6): p. 369-76.

215. Lu, W., et al., *Suppression of Wnt/beta-catenin signaling inhibits prostate cancer cell proliferation.* Eur J Pharmacol, 2009. **602**(1): p. 8-14.

216. Nelson, A.R., et al., *Matrix metalloproteinases: biologic activity and clinical implications.* J Clin Oncol, 2000. **18**(5): p. 1135-49.

217. Bjornland, K., et al., *Matrix metalloproteinases participate in osteosarcoma invasion.* J Surg Res, 2005. **127**(2): p. 151-6.

218. Uchibori, M., et al., *Increased expression of membrane-type matrix metalloproteinase-1 is correlated with poor prognosis in patients with osteosarcoma.* Int J Oncol, 2006. **28**(1): p. 33-42.

219. Foukas, A.F., et al., *Stage-IIB osteosarcomas around the knee. A study of MMP-9 in surviving tumour cells.* J Bone Joint Surg Br, 2002. **84**(5): p. 706-11.

220. Guo, Y., et al., *Frzb, a secreted Wnt antagonist, decreases growth and invasiveness of fibrosarcoma cells associated with inhibition of Met signaling.* Cancer Res, 2008. **68**(9): p. 3350-60.

221. Johnstone, R.W., A.A. Ruefli, and S.W. Lowe, *Apoptosis: a link between cancer genetics and chemotherapy.* Cell, 2002. **108**(2): p. 153-64.

222. Giodini, A., et al., *Regulation of microtubule stability and mitotic progression by survivin.* Cancer Res, 2002. **62**(9): p. 2462-7.

223. Kim, P.J., et al., *Survivin and molecular pathogenesis of colorectal cancer.* Lancet, 2003. **362**(9379): p. 205-9.

224. Beardmore, V.A., et al., *Survivin dynamics increases at centromeres during G2/M phase transition and is regulated by microtubule-attachment and Aurora B kinase activity.* J Cell Sci, 2004. **117**(Pt 18): p. 4033-42.

225. Li, F., et al., *Control of apoptosis and mitotic spindle checkpoint by survivin.* Nature, 1998. **396**(6711): p. 580-4.

226. Pahlke, G., et al., *Impact of quercetin and EGCG on key elements of the Wnt pathway in human colon carcinoma cells.* J Agric Food Chem, 2006. **54**(19): p. 7075-82.

227. Gardner, S.H., G. Hawcroft, and M.A. Hull, *Effect of nonsteroidal anti-inflammatory drugs on beta-catenin protein levels and catenin-related transcription in human colorectal cancer cells.* Br J Cancer, 2004. **91**(1): p. 153-63.

228. Ryu, M.J., et al., *Natural derivatives of curcumin attenuate the Wnt/beta-catenin pathway through down-regulation of the transcriptional coactivator p300.* Biochem Biophys Res Commun, 2008.

229. Takahashi, M., et al., *Identification of membrane-type matrix metalloproteinase-1 as a target of the beta-catenin/Tcf4 complex in human colorectal cancers.* Oncogene, 2002. **21**(38): p. 5861-7.

230. Marchenko, G.N., et al., *Promoter characterization of the novel human matrix metalloproteinase-26 gene: regulation by the T-cell factor-4 implies specific expression of the gene in cancer cells of epithelial origin.* Biochem J, 2002. **363**(Pt 2): p. 253-62.

231. Lowy, A.M., et al., *beta-Catenin/Wnt signaling regulates expression of the membrane type 3 matrix metalloproteinase in gastric cancer.* Cancer Res, 2006. **66**(9): p. 4734-41.

232. Zi, X., et al., *Expression of Frzb/secreted Frizzled-related protein 3, a secreted Wnt antagonist, in human androgen-independent prostate cancer PC-3 cells suppresses tumor growth and cellular invasiveness.* Cancer Res, 2005. **65**(21): p. 9762-70.

233. Chen, H.W., et al., *Curcumin inhibits lung cancer cell invasion and metastasis through the tumor suppressor HLJ1.* Cancer Res, 2008. **68**(18): p. 7428-38.

234. Osaka, E., et al., *Survivin as a prognostic factor for osteosarcoma patients.* Acta Histochem Cytochem, 2006. **39**(3): p. 95-100.

235. Osaka, E., et al., *Survivin expression levels as independent predictors of survival for osteosarcoma patients.* J Orthop Res, 2007. **25**(1): p. 116-21.

236. Trieb, K., et al., *Survivin expression in human osteosarcoma is a marker for survival.* Eur J Surg Oncol, 2003. **29**(4): p. 379-82.

237. Wang, W., H. Luo, and A. Wang, *Expression of survivin and correlation with PCNA in osteosarcoma.* J Surg Oncol, 2006. **93**(7): p. 578-84.

238. Chiou, S.K., M.K. Jones, and A.S. Tarnawski, *Survivin - an anti-apoptosis protein: its biological roles and implications for cancer and beyond.* Med Sci Monit, 2003. **9**(4): p. PI25-9.

239. Pompetti, F., et al., *Oncogene alterations in primary, recurrent, and metastatic human bone tumors.* J Cell Biochem, 1996. **63**(1): p. 37-50.

240. Gamberi, G., et al., *C-myc and c-fos in human osteosarcoma: prognostic value of mRNA and protein expression.* Oncology, 1998. **55**(6): p. 556-63.

241. Wu, X., Z.R. Chen, and G.J. Zhang, *[Apoptosis-related gene expression and its clinical significance of human osteosarcoma.].* Zhonghua Zhong Liu Za Zhi, 2004. **26**(11): p. 678-81.

242. Zucchini, C., et al., *Apoptotic genes as potential markers of metastatic phenotype in human osteosarcoma cell lines.* Int J Oncol, 2008. **32**(1): p. 17-31.

243. Anand, P., et al., *Bioavailability of curcumin: problems and promises.* Mol Pharm, 2007. **4**(6): p. 807-18.

244. Liang, G., et al., *Exploration and synthesis of curcumin analogues with improved structural stability both in vitro and in vivo as cytotoxic agents.* Bioorg Med Chem, 2009. **17**(6): p. 2623-31.

245. Perkins, S., et al., *Chemopreventive efficacy and pharmacokinetics of curcumin in the min/+ mouse, a model of familial adenomatous polyposis.* Cancer Epidemiol Biomarkers Prev, 2002. **11**(6): p. 535-40.

246. Liang, G., et al., *Synthesis and anti-bacterial properties of mono-carbonyl analogues of curcumin.* Chem Pharm Bull (Tokyo), 2008. **56**(2): p. 162-7.

247. Hagmann, W.K., *The many roles for fluorine in medicinal chemistry.* J Med Chem, 2008. **51**(15): p. 4359-69.

248. Kirk, K.L., *Selective fluorination in drug design and development: an overview of biochemical rationales.* Curr Top Med Chem, 2006. **6**(14): p. 1447-56.

249. Muller, K., C. Faeh, and F. Diederich, *Fluorine in pharmaceuticals: looking beyond intuition.* Science, 2007. **317**(5846): p. 1881-6.

250. Oprea, T.I. and J. Gottfries, *Toward minimalistic modeling of oral drug absorption.* J Mol Graph Model, 1999. **17**(5-6): p. 261-74, 329.

251. Qiu, X., et al., *Synthesis and evaluation of curcumin analogues as potential thioredoxin reductase inhibitors.* Bioorg Med Chem, 2008. **16**(17): p. 8035-41.

252. Handler, N., et al., *Synthesis of novel curcumin analogues and their evaluation as selective cyclooxygenase-1 (COX-1) inhibitors.* Chem Pharm Bull (Tokyo), 2007. **55**(1): p. 64-71.

253. Mazumder, A., et al., *Curcumin analogs with altered potencies against HIV-1 integrase as probes for biochemical mechanisms of drug action.* J Med Chem, 1997. **40**(19): p. 3057-63.

254. Shibamoto, S., et al., *Cytoskeletal reorganization by soluble Wnt-3a protein signalling.* Genes Cells, 1998. **3**(10): p. 659-70.

255. Li, X., et al., *New Wnt/beta-catenin signaling inhibitors isolated from Eleutherine palmifolia.* Chem Asian J, 2009. **4**(4): p. 540-7.

256. Song, G.Y., et al., *Decursin suppresses human androgen-independent PC3 prostate cancer cell proliferation by promoting the degradation of beta-catenin.* Mol Pharmacol, 2007. **72**(6): p. 1599-606.

257. Willert, K., et al., *Wnt proteins are lipid-modified and can act as stem cell growth factors.* Nature, 2003. **423**(6938): p. 448-52.

258. Levanon, D., et al., *Transcriptional repression by AML1 and LEF-1 is mediated by the TLE/Groucho corepressors.* Proc Natl Acad Sci U S A, 1998. **95**(20): p. 11590-5.

259. Roose, J., et al., *The Xenopus Wnt effector XTcf-3 interacts with Groucho-related transcriptional repressors.* Nature, 1998. **395**(6702): p. 608-12.

260. Lin, C.R., et al., *Pitx2 regulates lung asymmetry, cardiac positioning and pituitary and tooth morphogenesis.* Nature, 1999. **401**(6750): p. 279-82.

261. Kioussi, C., et al., *Identification of a Wnt/Dvl/beta-Catenin --> Pitx2 pathway mediating cell-type-specific proliferation during development.* Cell, 2002. **111**(5): p. 673-85.

262. Vadlamudi, U., et al., *PITX2, beta-catenin and LEF-1 interact to synergistically regulate the LEF-1 promoter.* J Cell Sci, 2005. **118**(Pt 6): p. 1129-37.

263. Baek, S.H., et al., *Regulated subset of G1 growth-control genes in response to derepression by the Wnt pathway.* Proc Natl Acad Sci U S A, 2003. **100**(6): p. 3245-50.

264. Duffy, M.J., et al., *Methylated genes as new cancer biomarkers.* Eur J Cancer, 2009. **45**(3): p. 335-46.

265. Huang, Y., et al., *Pituitary homeobox 2 (PITX2) promotes thyroid carcinogenesis by activation of cyclin D2.* Cell Cycle, 2010. **9**(7).

266. Lau, L.F. and S.C. Lam, *The CCN family of angiogenic regulators: the integrin connection.* Exp Cell Res, 1999. **248**(1): p. 44-57.

267. Pasmant, E., et al., *Differential expression of CCN1/CYR61, CCN3/NOV, CCN4/WISP1, and CCN5/WISP2 in neurofibromatosis type 1 tumorigenesis.* J Neuropathol Exp Neurol, 2010. **69**(1): p. 60-9.

268. Pennica, D., et al., *WISP genes are members of the connective tissue growth factor family that are up-regulated in wnt-1-transformed cells and aberrantly expressed in human colon tumors.* Proc Natl Acad Sci U S A, 1998. **95**(25): p. 14717-22.

269. Xie, D., et al., *Elevated levels of connective tissue growth factor, WISP-1, and CYR61 in primary breast cancers associated with more advanced features.* Cancer Res, 2001. **61**(24): p. 8917-23.

270. Tanaka, S., et al., *Human WISP1v, a member of the CCN family, is associated with invasive cholangiocarcinoma.* Hepatology, 2003. **37**(5): p. 1122-9.

271.	Tian, C., et al., *Overexpression of connective tissue growth factor WISP-1 in Chinese primary rectal cancer patients.* World J Gastroenterol, 2007. **13**(28): p. 3878-82.

272.	Young, M.R. and N.H. Colburn, *Fra-1 a target for cancer prevention or intervention.* Gene, 2006. **379**: p. 1-11.

273.	Debinski, W. and D.M. Gibo, *Fos-related antigen 1 modulates malignant features of glioma cells.* Mol Cancer Res, 2005. **3**(4): p. 237-49.

274.	Belguise, K., et al., *FRA-1 expression level regulates proliferation and invasiveness of breast cancer cells.* Oncogene, 2005. **24**(8): p. 1434-44.

275.	Uren, A., et al., *Secreted frizzled-related protein-1 binds directly to Wingless and is a biphasic modulator of Wnt signaling.* J Biol Chem, 2000. **275**(6): p. 4374-82.

276.	Rousset, R., et al., *Naked cuticle targets dishevelled to antagonize Wnt signal transduction.* Genes Dev, 2001. **15**(6): p. 658-71.

277.	Bovolenta, P., et al., *Beyond Wnt inhibition: new functions of secreted Frizzled-related proteins in development and disease.* J Cell Sci, 2008. **121**(Pt 6): p. 737-46.

278.	Nojima, M., et al., *Frequent epigenetic inactivation of SFRP genes and constitutive activation of Wnt signaling in gastric cancer.* Oncogene, 2007. **26**(32): p. 4699-713.

279.	Jost, E., et al., *Epigenetic dysregulation of secreted Frizzled-related proteins in multiple myeloma.* Cancer Lett, 2009. **281**(1): p. 24-31.

280.	Veeck, J., et al., *Epigenetic inactivation of the secreted frizzled-related protein-5 (SFRP5) gene in human breast cancer is associated with unfavorable prognosis.* Carcinogenesis, 2008. **29**(5): p. 991-8.

281.	Stambolic, V., L. Ruel, and J.R. Woodgett, *Lithium inhibits glycogen synthase kinase-3 activity and mimics wingless signalling in intact cells.* Curr Biol, 1996. **6**(12): p. 1664-8.

282.	Thompson, E.B., *The many roles of c-Myc in apoptosis.* Annu Rev Physiol, 1998. **60**: p. 575-600.

283.	Wang, H.L., et al., *Elevated protein expression of cyclin D1 and Fra-1 but decreased expression of c-Myc in human colorectal adenocarcinomas overexpressing beta-catenin.* Int J Cancer, 2002. **101**(4): p. 301-10.

284.	Takahashi, Y., J.B. Rayman, and B.D. Dynlacht, *Analysis of promoter binding by the E2F and pRB families in vivo: distinct E2F proteins mediate activation and repression.* Genes Dev, 2000. **14**(7): p. 804-16.

285.	Zhao, C., et al., *Downregulation of SFRP5 expression and its inverse correlation with those of MMP-7 and MT1-MMP in gastric cancer.* BMC Cancer, 2009. **9**: p. 224.

286.	Masckauchan, T.N., et al., *Wnt5a signaling induces proliferation and survival of endothelial cells in vitro and expression of MMP-1 and Tie-2.* Mol Biol Cell, 2006. **17**(12): p. 5163-72.

287.	Prieve, M.G. and R.T. Moon, *Stromelysin-1 and mesothelin are differentially regulated by Wnt-5a and Wnt-1 in C57mg mouse mammary epithelial cells.* BMC Dev Biol, 2003. **3**: p. 2.

288.	Zhai, Y., et al., *Role of beta-catenin/T-cell factor-regulated genes in ovarian endometrioid adenocarcinomas.* Am J Pathol, 2002. **160**(4): p. 1229-38.

289. Blavier, L., et al., *Matrix metalloproteinases play an active role in Wnt1-induced mammary tumorigenesis.* Cancer Res, 2006. **66**(5): p. 2691-9.

290. Neth, P., et al., *Wnt signaling regulates the invasion capacity of human mesenchymal stem cells.* Stem Cells, 2006. **24**(8): p. 1892-903.

291. Hu, J., et al., *Blockade of Wnt signaling inhibits angiogenesis and tumor growth in hepatocellular carcinoma.* Cancer Res, 2009. **69**(17): p. 6951-9.

292. Kawakami, K., et al., *Functional significance of Wnt inhibitory factor-1 gene in kidney cancer.* Cancer Res, 2009. **69**(22): p. 8603-10.

293. Yanagawa, S., et al., *Casein kinase I phosphorylates the Armadillo protein and induces its degradation in Drosophila.* EMBO J, 2002. **21**(7): p. 1733-42.

294. Ha, N.C., et al., *Mechanism of phosphorylation-dependent binding of APC to beta-catenin and its role in beta-catenin degradation.* Mol Cell, 2004. **15**(4): p. 511-21.

295. Kikuchi, A., S. Kishida, and H. Yamamoto, *Regulation of Wnt signaling by protein-protein interaction and post-translational modifications.* Exp Mol Med, 2006. **38**(1): p. 1-10.

296. Kuppuswamy, M., et al., *Role of the PLDLS-binding cleft region of CtBP1 in recruitment of core and auxiliary components of the corepressor complex.* Mol Cell Biol, 2008. **28**(1): p. 269-81.

297. Shi, Y., et al., *Coordinated histone modifications mediated by a CtBP co-repressor complex.* Nature, 2003. **422**(6933): p. 735-8.

298. Chinnadurai, G., *CtBP, an unconventional transcriptional corepressor in development and oncogenesis.* Mol Cell, 2002. **9**(2): p. 213-24.

299. Saeki, H., et al., *Genetic alterations in the human Tcf-4 gene in Japanese patients with sporadic gastrointestinal cancers with microsatellite instability.* Oncology, 2001. **61**(2): p. 156-61.

300. Atcha, F.A., et al., *A new beta-catenin-dependent activation domain in T cell factor.* J Biol Chem, 2003. **278**(18): p. 16169-75.

301. Hovanes, K., et al., *Beta-catenin-sensitive isoforms of lymphoid enhancer factor-1 are selectively expressed in colon cancer.* Nat Genet, 2001. **28**(1): p. 53-7.

302. Brigstock, D.R., *The connective tissue growth factor/cysteine-rich 61/nephroblastoma overexpressed (CCN) family.* Endocr Rev, 1999. **20**(2): p. 189-206.

303. Park, J.C., et al., *Epigenetic silencing of human T (brachyury homologue) gene in non-small-cell lung cancer.* Biochem Biophys Res Commun, 2008. **365**(2): p. 221-6.

304. Lingbeek, M.E., J.J. Jacobs, and M. van Lohuizen, *The T-box repressors TBX2 and TBX3 specifically regulate the tumor suppressor gene p14ARF via a variant T-site in the initiator.* J Biol Chem, 2002. **277**(29): p. 26120-7.

305. Shibata, T., et al., *EBP50, a beta-catenin-associating protein, enhances Wnt signaling and is over-expressed in hepatocellular carcinoma.* Hepatology, 2003. **38**(1): p. 178-86.

306. Stemmer-Rachamimov, A.O., et al., *NHE-RF, a merlin-interacting protein, is primarily expressed in luminal epithelia, proliferative endometrium, and estrogen receptor-positive breast carcinomas.* Am J Pathol, 2001. **158**(1): p. 57-62.
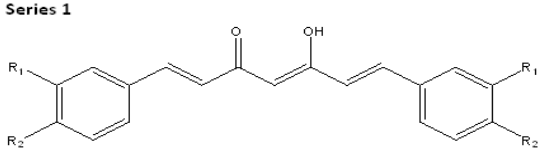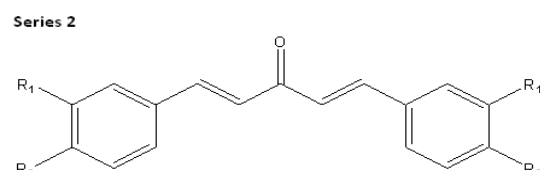
307. Fraenzer, J.T., et al., *Overexpression of the NF2 gene inhibits schwannoma cell proliferation through promoting PDGFR degradation.* Int J Oncol, 2003. **23**(6): p. 1493-500.

308. Kislin, K.L., et al., *NHERF-1: modulator of glioblastoma cell migration and invasion.* Neoplasia, 2009. **11**(4): p. 377-87.

309. Cardone, R.A., V. Casavola, and S.J. Reshkin, *The role of disturbed pH dynamics and the Na+/H+ exchanger in metastasis.* Nat Rev Cancer, 2005. **5**(10): p. 786-95.

310. Salisbury, T.B., et al., *GnRH-regulated expression of Jun and JUN target genes in gonadotropes requires a functional interaction between TCF/LEF family members and beta-catenin.* Mol Endocrinol, 2009. **23**(3): p. 402-11.

311. Franchi, A., A. Calzolari, and G. Zampi, *Immunohistochemical detection of c-fos and c-jun expression in osseous and cartilaginous tumours of the skeleton.* Virchows Arch, 1998. **432**(6): p. 515-9.

312. Papachristou, D.J., et al., *Activation of the JNK-AP-1 signal transduction pathway is associated with pathogenesis and progression of human osteosarcomas.* Bone, 2003. **32**(4): p. 364-71.

313. Dass, C.R., et al., *Downregulation of c-jun results in apoptosis-mediated anti-osteosarcoma activity in an orthotopic model.* Cancer Biol Ther, 2008. **7**(7): p. 1033-6.

314. Lee, J.L., et al., *Secreted frizzled related protein 2 (sFRP2) decreases susceptibility to UV-induced apoptosis in primary culture of canine mammary gland tumors by NF-kappaB activation or JNK suppression.* Breast Cancer Res Treat, 2006. **100**(1): p. 49-58.

315. He, B., et al., *Secreted frizzled-related protein 4 is silenced by hypermethylation and induces apoptosis in beta-catenin-deficient human mesothelioma cells.* Cancer Res, 2005. **65**(3): p. 743-8.

316. Lodygin, D., et al., *Functional epigenomics identifies genes frequently silenced in prostate cancer.* Cancer Res, 2005. **65**(10): p. 4218-27.

317. Shih, Y.L., et al., *SFRP1 suppressed hepatoma cells growth through Wnt canonical signaling pathway.* Int J Cancer, 2007. **121**(5): p. 1028-35.

318. Cai, Y., et al., *Inactive Wnt/beta-catenin pathway in conventional high-grade osteosarcoma.* J Pathol, 2010. **220**(1): p. 24-33.

APPENDICES

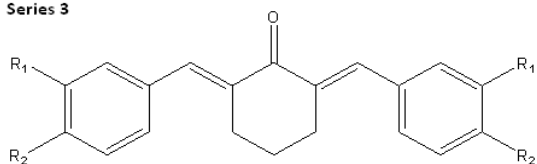**Appendix 1: Table of structures of synthesized compounds and their physiochemical properties**

a C log P/molecular weight values were determined on ChemDraw Ultra 10.0, CambridgeSoft, Cambridge, MA.

b No. of rotatable bonds/No. of hydrogen bond donors and acceptors values were determined on MOE, 2009. 10 Chemical Computing Group

Compound No.	R_1(3')	R_2(4')	Molecular[a] weight	No. of rotatable bonds [b]	No. of hydrogen bond donors [b]	No. of hydrogen bond acceptors[b]	C logP[a]
Series 1 Analogues							
1-1 (curcumin)	OCH_3	OH	368.38	7	2	4	2.94
1-2	OCH_3	OCH_3	396.43	9	0	4	3.89
1-3	OH	OCH_3	368.38	7	2	4	2.94
1-4	H	H	276.33	5	0	0	4.58
1-5	OCH_3	H	336.38	7	0	2	4.41
1-6	H	OH	308.33	5	2	2	3.24
1-7	F	F	348.29	5	0	0	5.01
Series 2 Analogues							
2-1	OCH_3	OH	326.34	6	2	5	2.64
2-2	OCH_3	OCH_3	354.40	8	0	5	3.59
2-3	OH	OCH_3	326.34	6	2	5	2.64
2-4	H	H	234.39	4	0	1	4.28
2-5	OCH_3	H	294.34	6	0	3	4.11
2-6	H	OH	266.29	4	2	3	2.94
2-7	F	F	306.25	4	0	1	4.71

Series 3 Analogues

Series 3

3-1	OCH$_3$	OH	366.41	4	2	5	3.70
3-2	OCH$_3$	OCH$_3$	394.46	6	0	5	4.65
3-3	OH	OCH$_3$	366.41	4	2	5	3.70
3-4	H	H	274.36	2	0	1	5.33
3-5	OCH$_3$	H	334.41	4	0	3	5.17
3-6	H	OH	306.36	2	2	3	4.00
3-7	F	F	346.32	2	0	1	5.76
3-8	2'F		310.34	2	0	1	5.62
3-9	F	H	310.34	2	0	1	5.62
3-10	H	F	310.34	2	0	1	5.62

Series 4 Analogues

Series 4
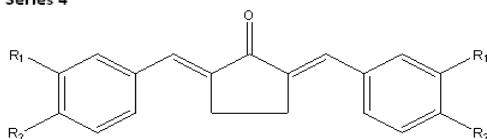
4-1	OCH$_3$	OH	352.38	4	2	5	3.14
4-2	OCH$_3$	OCH$_3$	380.43	6	0	5	4.09
4-3	OH	OCH$_3$	352.38	4	2	5	3.14
4-4	H	H	260.33	2	0	1	4.77
4-5	OCH$_3$	H	320.38	4	0	3	4.61
4-6	H	OH	292.33	2	2	3	3.44
4-7	F	F	332.29	2	0	1	5.20
4-8	2'F		296.31	2	0	1	5.06
4-9	F	H	296.31	2	0	1	5.06
4-10	H	F	296.31	2	0	1	5.06

Series 5 Analogues

Series 5
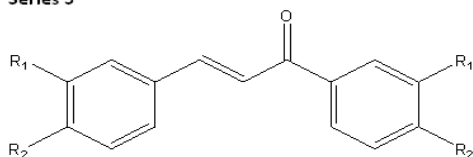
5-1	OCH$_3$	OH	300.31	5	2	5	2.50

5-2	OCH$_3$	OCH$_3$	328.36	7	0	5	3.18
5-3	OH	OCH$_3$	300.31	5	2	5	2.50
5-4	H	H	208.26	3	0	1	3.62
5-5	OCH$_3$	H	268.31	5	0	3	3.77
5-6	H	OH	240.25	3	2	3	2.83
5-7	F	F	280.22	3	0	1	4.16

Appendix 2: Characterization of compounds in Series 1-5

Compound 1-1(Curcumin): $C_{21}H_{20}O_6$. Yellow-orange crystals. Melting point: 183°C. ^{1}H-NMR (300 MHz, CDCl$_3$) δ: 3.95 (6H, s, OCH$_3$ × 2), 5.80 (1H, s, COCH=C), 6.48 (2H, d, J=16Hz, CHCO ×2), 6.93 (2H, d, J=8Hz, Ar-H), 7.05 (2H, s, Ar-H), 7.12(2H, d, J= 8Hz, Ar-H), 7.59 (2H, d, J = 16Hz, Ar-CH=C ×2). ^{13}C-NMR (75 MHz, CDCl$_3$) δ: 55.928, 101.089, 109.626, 114.800, 121.769, 122.828, 127.677, 140.491, 140.491,146.755, 147.823, 151.915, 183.229. MS (APCI) m/z: 369.0 (M+1)[+]. Anal calcd for $C_{17}H_{14}O_5$: C, 68.45; H, 4.73; Found: C, 68.03; H, 4.78.

Compound 1-2: Orange powder. $C_{23}H_{24}O_6$. Melting point: 130-131°C. ^{1}H-NMR (300 MHz, CDCl$_3$) δ: 3.92 (6H, s, OCH$_3$ ×2), 3.93 (6H, s, OCH$_3$ ×2), 5.82(1H, s, COCH=C), 6.50 (2H, d, J=16Hz, CHCO ×2), 6.88 (2H, d, J=8 Hz, Ar-H), 7.10 (4H, m, Ar-H), 7.61(2H, d, J=16 Hz, Ar-CH=C ×2). ^{13}C-NMR (75 MHz, CDCl$_3$) δ: 55.843, 55.912, 76.642, 77.066, 77.490, 101.274, 109.754, 111.096, 121.967, 122.578, 128.002, 140.334, 149.173, 150.992, 183.204. MS (APCI) m/z: 396.9 (M+1)[+]. HPLC (MeOH: H2O=80:20) t_R (min): 9.394. P_{HPLC}/ %: 97.50. HPLC (ACN: H2O=80:20) t_R (min): 2.931. P_{HPLC}/ %: 100.00.

Compound 1-3: Orange powder. $C_{21}H_{20}O_6$. Melting point: 192°C. ^{1}H-NMR (300 MHz, CDCl$_3$) δ: 3.92(6H, s, OCH$_3$ ×2), 5.82 (1H, s, COCH=C), 6.48 (2H, d, J=16 Hz, CHCO ×2), 6.87 (2H, d, J= 8Hz, Ar-H), 7.04 (2H, d, J=8Hz, Ar-H),7.15 (2H, s, Ar-H), 7.53 (2H, d, J=16 Hz, Ar-CH=C ×2). ^{13}C-NMR (75 MHz, CDCl$_3$) δ: MS (APCI) m/z: 369.0 (M+1)[+]. HPLC (MeOH: H2O=80:20) t_R (min): 2.450. P_{HPLC}/ %: 95.97. HPLC (ACN: H2O=80:20) t_R (min): 1.849. P_{HPLC}/ %: 95.48

Compound 1-4: Yellow powder. $C_{19}H_{16}O_2$. Melting point: 138-140°C. ^{1}H-NMR (300 MHz, DMSO-d$_6$) δ: 6.209 (1H, s, COCH=C), 6.953 (2H, d, J=16 Hz, CHCO ×2), 7.442 (6H, s, Ar-H), 7.688 (2H, s, Ar-H),7.719 (2H, m, Ar-H). ^{13}C-NMR (75 MHz, DMSO-d$_6$) δ: 101.752, 124.194, 128.237, 128.878, 13.200, 134.551, 140.264, 183.092 . MS (APCI) m/z: 277.0 (M+1)[+]. HPLC (MeOH: H2O=80:20) t_R (min): 9.281. P_{HPLC}/ %: 99.86. HPLC (ACN: H2O=70:30) t_R (min): 12.003. P_{HPLC}/ %: 98.50

Compound 1-5: Brownish-orange powder. $C_{23}H_{24}O_4$. Melting point: 59-60°C. ^{1}H-NMR (300 MHz, CDCl$_3$) δ: 3.85 (6H, s, OCH$_3$ ×2), 5.86 (1H, s, COCH=C), 6.62 (2H, d, J=16Hz, -CHCO-×2), 6.88 (2H, d, J=2Hz, Ar-H), 6.95 (2H, d, J=10 Hz, Ar-H), 7.08 (2H, s, Ar-H),7.30 (2H, s, Ar-H), 7.633 (2H, d, J= 16 Hz, Ar-CH=C ×2). ^{13}C-NMR (75 MHz, CDCl$_3$) δ: 55.289, 101.794, 113.037, 115.908, 120.794, 124.328, 129.882, 136.329, 140.543, 159.889, 183.230 . MS (APCI) m/z: 337.0 (M+1)[+]. HPLC (MeOH: H2O=80:20) t_R (min): 1.784. P_{HPLC}/ %: 95.81. HPLC (ACN: H2O=80:20) t_R (min): 1.608. P_{HPLC}/ %: 97.30

Compound 1-6: Orange-red crystals. $C_{19}H_{16}O_6$. Melting point: 229-230°C. ^{1}H-NMR (300 MHz, DMSO-d$_6$) δ: 6.03 (1H, s, COCH=C), 6.65 (2H, J = 16 Hz, -CHCO-×2), 6.83 (4H, d, J = 8.4 Hz, Ar-H), 7.53-7.57 (m, 6H, Ar-H + Ar-CH=C ×2), 10.2 (2H, s, OH). ^{13}C-NMR (75 MHz, DMSO-d$_6$) δ: 110.180, 116.095, 120.891, 125.979, 130.464, 140.522,

159.893, 183.325 MS (APCI) m/z: 369.0 (M+1)$^+$. HPLC (MeOH: H2O=80:20) t_R (min): 5.055. P_{HPLC}/ %: 96.85. HPLC (ACN: H2O=80:20) t_R (min): 1.670. P_{HPLC}/ %: 99.14

Compound 1-7: Yellow powder. $C_{19}H_{12}F_4O$. Melting point: 229-230°C. ^{1}H-NMR (300 MHz, DMSO-d$_6$) δ: 5.82 (1H, s, COCH=C), 6.53 (2H, J = 16 Hz, -CHCO-×2), 7.14-7.41 (m, 7H, Ar-H + Ar-CH=C ×2), 7.57 (2H, d, 8Hz, Ar-H). ^{13}C-NMR (75 MHz, DMSO-d$_6$) δ: 76.5764, 77.0000, 77.2022, 77.4236, 78.3575, 102.1870, 116.0418, 117.7460, 117.9771, 124.8419, 132.1689, 138.4753, 182.7933. MS (APCI) m/z: 309.2 (M+1)$^+$. HPLC (MeOH: H2O=80:20) t_R (min): 14.846. P_{HPLC}/ %: 99.85. HPLC (ACN: H2O=70:30) t_R (min): 2.198. P_{HPLC}/ %: 98.68

Compound 2-1: Greenish-yellow powder. $C_{19}H_{18}O_5$. Melting point: 106°C. ^{1}H-NMR (300 MHz, CDCl$_3$) δ: 3.96 (6H, s, OCH$_3$ ×2), 6.90-6.95 (4H, m, Ar-H + COCH= ×2), 7.09-7.17 (m, 4H, Ar-H), 7.68 (2H, d, J=16 Hz, Ar-CH= ×2). ^{13}C-NMR (75 MHz, DMSO-d$_6$) δ: 55.689, 111.350, 115.632, 122.965, 123.334, 126.306, 142.754, 149.942, 188.015 MS (APCI) m/z: 326.9 (M+1)$^+$. HPLC (MeOH: H2O=80:20) t_R (min): 1.794. P_{HPLC}/ %: 95.81. HPLC (ACN: H2O=70:30) t_R (min): 1.608. P_{HPLC}/ %: 97.40

Compound 2-2: Orange-yellow solid. $C_{21}H_{22}O_5$. Yield: 52.0%. Melting point: 93-95°C. ^{1}H-NMR (300 MHz, CDCl$_3$) δ: 3.93(6H, s, OCH$_3$ ×2), 3.95(6H, s, OCH$_3$ ×2), 6.89 (2H, d, J =8.1 Hz, Ar-H), 6.96 (d, J = 16 Hz, COCH= ×2), 7.14-7.21 (m, 4H, Ar-H), 7.69 (d, J = 16 Hz, Ar-CH= ×2). ^{13}C-NMR (75 MHz, CDCl$_3$) δ: 55.845, 55.892, 109.840, 111.035, 123.033, 123.530, 127.763, 142.984, 149.156, 151.252, 188.629 MS (APCI) m/z: 355.0 (M+1)$^+$. HPLC (MeOH: H2O=80:20) t_R (min): 3.129. P_{HPLC}/ %: 95.49. HPLC (ACN: H2O=70:30) t_R (min): 2.762. P_{HPLC}/ %: 94.59

Compound 2-3: Yellow powder. $C_{19}H_{18}O_5$. Yield: 33.27%. Melting point: 189-190°C. ^{1}H-NMR (300 MHz, DMSO-d$_6$) δ: 3.77 (s, 6H, OCH$_3$ ×2), 6.93 (d, 2H, J = 8 Hz, Ar-H), 7.03 (d, 2H, J = 16 Hz, COCH= ×2), 7.14-7.17 (m, 4H, Ar-H), 7.57 (d, J = 16 Hz, 2H, Ar-CH= ×2). ^{13}C-NMR (75 MHz, DMSO-d$_6$) δ: 56.0, 112.592, 114.706, 122.818, 123.919, 128.057, 143.757, 147.087, 150.906, 189.454 MS (APCI) m/z: 327.0 (M+1)$^+$. HPLC (MeOH: H2O=80:20) t_R (min): 3.129. P_{HPLC}/ %: 95.49. HPLC (ACN: H2O=70:30) t_R (min): 2.762. P_{HPLC}/ %: 94.59

Compound 2-4: Yellow crystals. $C_{17}H_{14}O$. Yield: 28.3%. Melting point: 113°C. ^{1}H-NMR (300 MHz, CDCl$_3$) δ: 7.09 (d, J= 16 Hz, 2H, COCH= ×2), 7.26-7.42 (m, 6H, Ar-H), 7.60-7.63 (m, 4H, Ar-H), 7.75 (d, J = 16 Hz, 2H, Ar-CH= ×2). ^{13}C-NMR (75 MHz, CDCl$_3$) δ: 125.327, 128.310, 128.872, 130.411, 134.964, 143.206, 188.805 MS (APCI) m/z: 235.3 (M+1)$^+$.P_{HPLC}/ %: 95.37. HPLC (ACN: H2O=80:20) t_R (min): 3.075. P_{HPLC}/ %: 99.72

Compound 2-5: Yellow solid. $C_{19}H_{18}O_3$. Yield: 45.7%. Melting point: 50-51°C. ^{1}H-NMR (300 MHz, CDCl$_3$) δ: 3.847 (6H, s, CH$_3$-O x2), 6.959(2H, d, J=3.15Hz, Ar-H), 7.056(4H, m, Ar-H), 7.208 (2H, d, J=16Hz, -COCH= x2), 7.326(2H, t, J=8Hz, Ar-H), 7.699(2H, d, J=16Hz, Ar–CH=Cx2). ^{13}C-NMR (75 MHz, CDCl$_3$) δ: 55.100, 113.127, 116.158, 120.915, 113.127, 116.158, 120.915, 125.451, 129.759, 135.958, 143.043,

159.751, 188.641 MS (APCI) m/z: 295.0 $(M+1)^+$. HPLC (MeOH: H2O=80:20) t_R (min): 6.637. P_{HPLC}/ %: 96.48. HPLC (ACN: H2O=80:20) t_R (min): 3.040. P_{HPLC}/ %: 96.71

Compound 2-6: Dark yellow powder. $C_{17}H_{14}O_3$. Yield: 24.26%. Melting point: 236-239°C. ^{1}H-NMR (300 MHz, DMSO-d$_6$) δ: 6.837 (4H, m, Ar-H x4), 7.099(2H, d, J=16Hz, -COCH= x2), 7.644 (6H, m, Ar-H=x4 + Ar–CH=Cx2), 10.062(2H, s, OH). ^{13}C-NMR (75 MHz, DMSO-d$_6$) δ: 115.836, 122.656, 125.821, 130.443, 142.400, 159.821, 188.047. MS (APCI) m/z: 267.2 $(M+1)^+$. HPLC (MeOH: H2O=80:20) t_R (min): 2.738. P_{HPLC}/ %: 99.42. HPLC (ACN: H2O=70:30) t_R (min): 1.793. P_{HPLC}/ %: 99.67

Compound 2-7: Yellow crystals. $C_{17}H_{10}F_4O$. Melting point: 132-133°C. ^{1}H-NMR (300 MHz, DMSO-d$_6$) δ: 6.955(2H, d, J=7.95, Ar-H), 7.199(2H, t, J=8.9Hz, Ar-H), 7.332(2H, d, J= 16Hz, -COCH= x2), 7.443(2H, m, Ar-H), 7.637 (2H, d, J=16Hz, Ar–CH=Cx2). MS (APCI) m/z: 306.9 $(M+1)^+$. HPLC (MeOH: H2O=80:20) t_R (min): 2.728. P_{HPLC}/ %: 99.28. HPLC (ACN: H2O=70:30) t_R (min): 1.793. P_{HPLC}/ %: 99.67

Compound 2-9: $C_{17}H_{12}F_2O$ Melting point: 147-149°C. ^{1}H-NMR (300 MHz, DMSO-d$_6$) δ: 6.981(4H, m, Ar-H), 7.248 (6H, m, Ar-H, -COCH= x2), 7.564 (2H, d, J=16Hz, Ar–CH=Cx2). ^{13}C-NMR (75 MHz, CDCl$_3$) δ: 114.261, 114.550, 117.515, 130.417, 130.523, 136.829, 136.935, 139.640, 142.124, 161.342, 164.616, 188.252 MS (APCI) m/z: 271.0 $(M+1)^+$. HPLC (MeOH: H2O=80:20) t_R (min): 5.418. P_{HPLC}/ %: 99.08. HPLC (ACN: H2O=80:20) t_R (min): 3.195. P_{HPLC}/ %: 97.59

Compound 2-10: $C_{17}H_{12}F_2O$. Melting point: 149-150°C ^{1}H-NMR (300 MHz, DMSO-d$_6$) δ: 7.231(6H, m, Ar-H), 7.781 (6H, m, Ar-H, -COCH= x2, Ar–CH=Cx2) ^{13}C-NMR (75 MHz, CDCl$_3$) δ: 114.936, 115.225, 124.006, 124.034, 129.166, 129.282, 129.908, 141.018, 161.324, 164.655, 187.397 MS (APCI) m/z: 271.2 $(M+1)^+$. HPLC (MeOH: H2O=80:20) t_R (min): 3.373 . P_{HPLC}/ %: 99.16. HPLC (ACN: H2O=80:20) t_R (min): 3.228. P_{HPLC}/ %: 95.74

Compound 3-1: Yellow solid. $C_{22}H_{22}O_5$. Melting point: 177-178°C. ^{1}H-NMR (300 MHz, DMSO-d$_6$) δ: 1.72 (s, 2H, -CH$_2$-), 2.88 (s, 4H, =C-CH$_2$- × 2), 3.81 (s, 6H, OCH$_3$ × 2), 6.85 (d, J = 8.1 Hz, 2H, Ar-H), 7.03 (d, J = 8.4 Hz, 2H, Ar-H), 7.11 (s, Ar-H), 7.57 (s, 2H, CH=C × 2), 9.52 (br s, 2H, OH). ^{13}C-NMR (75 MHz, CDCl$_3$) δ: 55.289, 76.574, 76.994, 77.421, 101.794, 113.037, 115.908, 120.794, 124.328, 129.882, 136.329, 140.543, 159.889, 183.230. MS (APCI) m/z: 367.0 $(M+1)^+$. HPLC (MeOH: H2O=80:20) t_R (min): 3.351. P_{HPLC}/ %: 97.88. HPLC (ACN: H2O=80:20) t_R (min): 3.209. P_{HPLC}/ %: 99.31.

Compound 3-2: Yellow crystals. $C_{24}H_{26}O_5$. Melting point: 149-151°C. ^{1}H-NMR (300 MHz, CDCl$_3$) δ: 1.830(2H, m, J=6Hz ,-CH$_2$-), 2.95(4H, t, J=5Hz =C-CH$_2$- x2), 3.914(6H, s, CH$_3$-O x2), 3.924 (6H, s, CH$_3$-O x2), 6.911(2H, d, J=8.4Hz, Ar-H), 7.023(2H, s, Ar-H), 7.114(2H, d, J=4.2Hz, Ar-H),7.753(2H, s,-CH=C- x2). ^{13}C-NMR (75 MHz, CDCl$_3$) δ: 23.022, 28.503, 55.909, 76.725, 77.150, 77.754, 110.897, 113.714, 123.936, 128.961, 134.490, 136.774, 148.640, 149.603, 189.929 MS (APCI) m/z: 395.1

(M+1)$^{+}$. HPLC (MeOH: H2O=80:20) t_R (min): 5.691. P_{HPLC}/ %: 100.00. HPLC (ACN: H2O=80:20) t_R (min): 2.750. P_{HPLC}/ %: 97.80.

Compound 3-3: Brownish-yellow powder. C$_{22}$H$_{22}$O$_5$. Yield: 31.09%. Melting point: 189°C. ^{1}H-NMR (300 MHz, DMSO-d$_6$) δ: 1.72 (t, J =5Hz, 2H), 2.86 (s, 4H), 3.81 (s, OCH$_3$ × 2), 6.99-7.01(m, 6H, Ar-H + CH=C × 2), 7.48 (s, 2H, Ar-H), 9.18 (br s, 2H, OH). ^{13}C-NMR (75 MHz, DMSO-d$_6$) δ: 22.237, 27.847, 55.504, 111.911, 117.060, 122.884, 129.172, 133.957, 135.691, 146.173, 148.483, 188.514 S MS (APCI) m/z: 367.3 (M+1)$^{+}$. HPLC (MeOH: H2O=80:20) t_R (min): 4.810. P_{HPLC}/ %: 100.00. HPLC (ACN: H2O=80:20) t_R (min): 1.747. P_{HPLC}/ %: 99.83.

Compound 3-4: Yellow crystals. C$_{20}$H$_{18}$O Melting point: 116-120°C. ^{1}H-NMR (300 MHz, CDCl$_3$) δ: δ: 1.79 (t, J=6 Hz , 2H -CH$_2$-), 2.93 (4H, t, J=5 Hz, -CH$_2$- ×2), 7.25-7.48 (10H, m, Ar–H), 7.80 (2H, s,-CH=C- ×2). ^{13}C-NMR (75 MHz, DMSO-d$_6$) δ: 22.994, 28.429, 76.579, 77.002, 100.686, 128.356, 128.556, 130.340, 135.963, 136.175, 136.916, 190.373 . MS (APCI) m/z: 275.1 (M+1)$^{+}$. HPLC (MeOH: H2O=80:20) t_R (min): 12.149. P_{HPLC}/ %: 98.71. HPLC (ACN: H2O=80:20) t_R (min): 5.549. P_{HPLC}/ %: 98.60.

Compound 3-5: Yellow crystals. C$_{22}$H$_{22}$O$_3$. Yield: 41.1%. Melting point: 59-60°C. ^{1}H-NMR (300 MHz, CDCl$_3$) δ: 1.68 (2H, t, J=5Hz, -CH$_2$-), 2.86(4H, s, =C-CH$_2$-x2), 3.835(6H, s, CH$_3$-O), 6.96 (d, J=8 Hz, 2H, ArH), 7.05-7.10 (m, 4H, ArH), 7.32-7.38 (m, 2H, ArH), 7.60 (s, 2H, CH=C- ×2). ^{13}C-NMR (75 MHz, DMSO-d$_6$) δ: 22.287, 27.780, 55.023, 114.502, 115.474, 122.449, 129.459, 135.636, 136.404, 159.109, 188.80 MS (APCI) m/z: 335.0 (M+1)$^{+}$. HPLC (MeOH: H2O=80:20) t_R (min): 5.049. P_{HPLC}/ %: 95.43. HPLC (ACN: H2O=80:20) t_R (min): 4.033. P_{HPLC}/ %: 96.79.

Compound 3-6: Brownish-yellow powder. C$_{20}$H$_{18}$O$_3$. Yield: 25.44%. Melting point: 270-271°C. ^{1}H-NMR (300 MHz, DMSO-d$_6$) δ: 1.71(2H, t, J=6 Hz, -CH$_2$-), 2.85(4H, t, J=5.4Hz, -CH$_2$- ×2), 6.84 (4H, d, J=4Hz, ArH), 7.40(4H, d, J=4 Hz, ArH),7.53 (2H, s, Ar–CH=C ×2), 9.96 (2H, br s, OH ×2). ^{13}C-NMR (75 MHz, DMSO-d$_6$) δ: 22.476, 27.912, 115.464, 126.393, 132.390, 133.242, 135.731, 158.250, 188.443 MS (APCI) m/z: 307.0 (M+1)$^{+}$. HPLC (MeOH: H2O=80:20) t_R (min): 7.542. P_{HPLC}/ %: 98.28. HPLC (ACN: H2O=80:20) t_R (min): 3.075. P_{HPLC}/ %: 97.68.

Compound 3-7: Yellow crystals. C$_{20}$H$_{14}$F$_4$O Yield: 12.5%. Melting point: 105-106°C. ^{1}H-NMR (300 MHz, CDCl$_3$) δ: 1.79-1.87 (m, 2H, -C-CH$_2$-), 2.89 (4H, t, J=5.7Hz, -C-CH$_2$- ×2), 7.18-7.31 (m, 6H, ArH), 7.67 (2H, s, Ar–CH=C ×2). ^{13}C-NMR (75 MHz, DMSO-d$_6$). MS (APCI) m/z: 347.0 (M+1)$^{+}$. HPLC (MeOH: H2O=80:20) t_R (min): 6.923. P_{HPLC}/ %: 92.43. HPLC (ACN: H2O=80:20) t_R (min): 5.013. P_{HPLC}/ %: 96.79.

Compounds 3-8: Yellow powder. C$_{20}$H$_{16}$F$_2$O. Melting point: 95-96°C. ^{1}H-NMR (300 MHz, CHCl$_3$) δ: 1.7821(2H, m,-CH$_2$-), 2.8086(4H, t, J=5.67Hz =C-CH$_2$- x2), 7.1324(4H, m, Ar-H), 7.3441(4H, m, Ar-H), 7.8224(2H, s,-CH=C- x2). ^{13}C-NMR (75 MHz, DMSO-d$_6$) δ: 22.9383, 28.5130, 76.5764, 77.0000, 77.4236, 115.5604, 115.8589, 123.6673, 123.7154, 123.7636, 123.9455, 129.7041, 129.7522, 130.2722, 130.3781, 130.6669, 130.7054, 138.1961, 159.1660, 162.4877, 189.5330. MS (APCI) m/z: 311.0(M+1) $^{+}$.

HPLC (MeOH: H2O=80:20) t_R (min): 5.535. P_{HPLC}/ %: 97.00. HPLC (ACN: H2O=80:20) t_R (min): 4.435. P_{HPLC}/ %: 95.99.

Compound 3-9: Yellow powder. $C_{20}H_{16}F_2O$. Melting point: 84°C. ^{1}H-NMR (300 MHz, CHCl$_3$) δ: 1.8000 (2H, m,-CH$_2$-), 2.9128(4H, t, J=5.28Hz =C-CH$_2$- x2), 7.2148(8H, m, Ar-Hx2), 7.7270(2H, s,-CH=C- x2). ^{13}C-NMR (75 MHz, DMSO-d$_6$) δ: 22.6206, 28.2241, 76.5764, 77.0000, 77.4236, 115.2909, 115.5701, 116.4452, 116.7351, 126.1321, 126.1706, 129.7619, 129.8678, 135.6254, 135.6542, 135.8577, 137.8206, 137.9265, 160.8509, 164.1148, 189.6774. MS (APCI) m/z: 311.0 (M+1) $^+$. HPLC (MeOH: H2O=80:20) t_R (min): 6.683. P_{HPLC}/ %: 99.41. HPLC (ACN: H2O=80:20) t_R (min): 5.609. P_{HPLC}/ %: 97.23

Compound 3-10: Yellow powder. $C_{20}H_{16}F_2O$. Melting point: 151°C. ^{1}H-NMR (300 MHz, CHCl$_3$) δ: 1.8055 (2H, m,-CH$_2$-), 2.8952(4H, t, J=5.28Hz =C-CH$_2$- x2), 7.0943(4H, m, Ar-H), 7.4458(4H, m, Ar-H), 7.7458(2H, s,-CH=C- x2). ^{13}C-NMR (75 MHz, DMSO-d$_6$) δ: 22.8709, 28.3108, 115.3583, 115.6375, 132.1689, 132.2844, 135.6928, 135.8468, 160.9857, 164.2978, 190.0048. MS (APCI) m/z: 310.9 (M+1) $^+$. HPLC (MeOH: H2O=80:20) t_R (min): 5.699. P_{HPLC}/ %: 96.45. HPLC (ACN: H2O=80:20) t_R (min): 5.316. P_{HPLC}/ %: 95.44

Compound 4-1: Dark yellow powder. $C_{21}H_{20}O_5$. Melting point: 198-202 °C. ^{1}H-NMR (300 MHz, DMSO-d$_6$) δ : 3.06 (4H, s, -CH$_2$-CH$_2$), 3.84 (6H, s, OCH$_3$ ×2), 6.89 (2H, d, J=8 Hz, Ar-H), 7.16 (2H, d, J=8 Hz, Ar-H), 7.24(2H, s, Ar-H), 7.35 (2H, s, CH=C×2), 9.69(2H, br s, OH ×2). ^{13}C-NMR (75 MHz, DMSO-d$_6$) δ: 26.914, 56.605, 115.545, 116.922, 125.793, 128.179, 133.841, 135.768, 148.727, 149.537, 195.480. MS (APCI) m/z: 353.0 (M+1)$^+$. HPLC (MeOH: H2O=80:20) t_R (min): 2.464. P_{HPLC}/ %: 98.66. HPLC (ACN: H2O=70:30) t_R (min): 1.953. P_{HPLC}/ %: 100.00.

Compound 4-2: Yellow powder. $C_{23}H_{24}O_5$. Yield: 44.0%. Melting point: 196-199°C. ^{1}H-NMR (300 MHz, CDCl$_3$) δ : 3.10 (4H, s, CH$_2$-CH$_2$), 3.93 (12H, s, OCH$_3$ ×4), 6.93 (2H, d, J= 8 Hz, Ar-H), 7.12-7.27 (m, 4H, Ar-H), 7.53 (2H, s, CH=C×2).^{13}C-NMR (75 MHz, DMSO-d$_6$) δ: 26.387, 55.822, 55.899, 111.112, 113.409, 124.534, 128.946, 133.622, 135.319, 148.856, 150.223, 195.946. MS (APCI) m/z: 381.0 (M+1)$^+$. HPLC (MeOH: H2O=80:20) t_R (min): 7.734. P_{HPLC}/ %: 96.91. HPLC (ACN: H2O=80:20) t_R (min): 2.377. P_{HPLC}/ %: 96.60.

Compound 4-3: Dark yellow powder. $C_{21}H_{20}O_5$. Yield: 27.19%. Melting point: 224-225°C. ^{1}H-NMR (300 MHz, DMSO-d$_6$) δ : 3.02 (4H, s, CH$_2$-CH$_2$), 3.82 (6H, s, OCH$_3$ ×2), 7.02 (2H, d, J= 8 Hz, Ar-H), 7.12-7.14 (m, 4H, Ar-H), 7.28 (2H, s, CH=C × 2), 9.28 (2H, s, OH ×2). ^{13}C-NMR (75 MHz, DMSO-d$_6$) δ: 25.846, 55.534, 112.095, 116.836, 123.566, 128.334, 132.410, 135.260, 146.481, 149.148, 194.795 MS(APCI) m/z: 353.0 (M+1)$^+$.HPLC (MeOH: H2O=80:20) t_R (min): 6.566. P_{HPLC}/ %: 99.28. HPLC (ACN: H2O=80:20) t_R (min): 3.083. P_{HPLC}/ %: 99.79.

Compound 4-4: Yellow powder. $C_{19}H_{16}O$. Yield: 63.9%. Melting point: 194-195°C. ^{1}H-NMR (300 MHz, CDCl$_3$) δ: 3.07 (4H, s, CH$_2$-CH$_2$), 7.35-7.44 (m, 6H, Ar-H), 7.56-7.58 (m, 6H, Ar-H + CH=C ×2). ^{13}C-NMR (75 MHz, CDCl$_3$) δ: 26.434, 128.675, 129.286,

130.652, 133.722, 135.717, 137.212, 196.220 MS (APCI) m/z: 381.0 (M+1)$^+$. HPLC (MeOH: H2O=80:20) t_R (min): 22.011. P_{HPLC}/ %: 97.12. HPLC (ACN: H2O=80:20) t_R (min): 4.199. P_{HPLC}/ %: 99.28

Compound 4-5: Yellow crystals. $C_{21}H_{20}O_3$ Yield: 56.8%. Melting point: 144-147°C. ^{1}H-NMR (300 MHz, CDCl$_3$) δ : 3.05 (4H, s, CH$_2$-CH$_2$), 3.82 (6H, s, MeO ×2), 6.91 (dd, J= 2 Hz, J = 10 Hz, 2H, ArH), 7.08 (s, 2H, ArH), 7.16 (d, J= 8 Hz, 2H, ArH), 7.30-7.35 (m, 2H, Ar-H), 7.52 (s, 2H, CH=C ×2). ^{13}C-NMR (75 MHz, DMSO-d$_6$) δ : 26.387, 55.154, 114.968, 115.888, 123.179, 129.592, 133.647, 136.978, 137.405, 159.579, 196.103. MS (APCI) m/z: 321.0 (M+1)$^+$. HPLC (MeOH: H2O=80:20) t_R (min): 13.048. P_{HPLC}/ %: 98.85. HPLC (ACN: H2O=80:20) t_R (min): 4.022. P_{HPLC}/ %: 99.09

Compound 4-6: Greenish-yellow powder. $C_{19}H_{16}O_3$ Yield: 31.60%. Melting point: 314°C. ^{1}H-NMR (300 MHz, DMSO-d$_6$) δ : 3.02 (4H, s, CH$_2$–CH$_2$), 6.87 (4H, d, J= 8Hz, Ar–H^{3,5} ×2), 7.33 (s, 2H, CH=C ×2), 7.54 (4H, d, J= 8Hz, Ar–H^{2,6}x2), 10.1 (br s, 2H, OH×2). ^{13}C-NMR (75 MHz, DMSO-d$_6$) δ: 26.063, 116.110, 126.800, 132.912, 134.787, 159.078, 195.280MS 795 MS (APCI) m/z: 293.0 (M+1)$^+$. HPLC (MeOH: H2O=80:20) t_R (min): 3.854. P_{HPLC}/ %: 98.60. HPLC (ACN: H2O=70:30) t_R (min): 1.784. P_{HPLC}/ %: 99.66

Compound 4-7: Yellow crystals. $C_{19}H_{12}F_4O$.Yield: 38.5%. Melting point: 239-240°C. ^{1}H-NMR (300 MHz, CDCl$_3$) δ : 3.10(4H, s, CH$_2$–CH$_2$), 7.19-7.45 (m, 6H, Ar-H), 7.50 (s, 2H, CH=C ×2). MS (APCI) m/z: 332.9 (M+1)$^+$. HPLC (MeOH: H2O=80:20) t_R (min): 20.240. P_{HPLC}/ %: 96.92. HPLC (ACN: H2O=70:30) t_R (min): 13.712. P_{HPLC}/ %: 98.41

Compound 4-8: Yellow powder. $C_{19}H_{14}F_2O$. Melting point: 210°C. ^{1}H-NMR (300 MHz, CHCl$_3$) δ: 3.0484(4H, s, CH$_2$–CH$_2$), 7.7.167(4H, m, Ar-H), 7.3667(2H, m, Ar-H),7.5776 (2H, m, Ar-H),7.8111(2H, s, Ar-CH=Cx2) **.**^{13}C-NMR (75 MHz, DMSO-d$_6$) δ: 26.0771, 76.1527, 76.5764, 77.0000, 115.3775, 115.6664, 123.3496, 123.5132, 123.6095, 123.6577, 125.2655, 125.3329, 129.7041, 130.5802, 130.6958, 138.5041, 159.6281, 195.1076. MS (APCI) m/z: 297.0 (M+1) $^+$.HPLC (MeOH: H2O=80:20) t_R (min): 6.816. P_{HPLC}/ %: 99.89. HPLC (ACN: H2O:80=20) t_R (min): 4.057. P_{HPLC}/ %: 94.18

Compound 4-9: Yellow powder. $C_{19}H_{14}F_2O$. Melting point: 191-192°C. ^{1}H-NMR (300 MHz, CHCl$_3$) δ: 2.9969 (4H, s, CH$_2$–CH$_2$), 7.0071(2H, m, Ar-H), 7.2633 (6H, m, Ar-H), 7.4257(2H, s, Ar-CH=Cx2). ^{13}C-NMR (75 MHz, DMSO-d$_6$) δ: 26.3370, 76.5764, 77.0000, 77.4236, 100.6658, 116.1863, 116.4751, 116.5907, 116.8795, 126.7001, 126.7386, 130.1662, 130.2818, 132.7273, 132.7658, 137.6954, 137.8109, 138.0420, 139.6595, 161.1494, 164.4229, 195.9068. MS (APCI) m/z: 297.0 (M+1) $^+$. HPLC (MeOH: H2O=80:20) t_R (min): 5.848. P_{HPLC}/ %: 97.32. HPLC (ACN: H2O=80:20) t_R (min): 4.303. P_{HPLC}/ %: 93.77

Compound 4-10: Yellow powder. $C_{19}H_{14}F_2O$. Melting point: 239-240°C. ^{1}H-NMR (300 MHz, CHCl$_3$) δ: 2.7885(4H, s, CH$_2$–CH$_2$), 6.8292(8H, m, Ar-H), 7.3077 (2H, s, Ar-CH=Cx2). ^{13}C-NMR (75 MHz, DMSO-d$_6$) δ: 26.3274, 76.5764, 77.0000, 77.4236, 115.8108, 116.0996, 131.9956, 132.0437, 132.5444, 132.6599, 132.7177, 136.6556, 161.4864, 164.8177, 196.0416. MS (APCI) m/z: 297.0 (M+1) $^+$. HPLC (MeOH:

H2O=80:20) t_R (min): 7.108. P_{HPLC}/ %: 99.57. HPLC (ACN: H2O=80:20) t_R (min): 4.387. P_{HPLC}/ %: 95.02

Compound 5-1: Yellow powder .$C_{17}H_{16}O_5$. Yield: 34.07%. Melting point: 108-110°C. ^{1}H-NMR (300 MHz, DMSO-d$_6$) δ: 3.87 (6H, s, MeO ×2), 6.82 (1H, d, J= 8 Hz, ArH), 6.91(1H, d, J=8Hz, ArH), 7.27 (1H, d, J= 8 Hz, ArH), 7.48-7.80 (m, 5H, Ar-H + CH=CH), 9.62 (s, 1H, OH), 9.99 (s, 1H, OH). ^{13}C-NMR (75 MHz, DMSO-d$_6$) δ: 55.637, 55.776, 111.519, 111.722, 114.848, 115.540, 118.643, 123.480, 126.445, 129.786, 143.527, 147.711, 149.334, 151.593, 186.957 MS (APCI) m/z: 301.0 (M+1)$^+$. HPLC (MeOH: H2O=80:20) t_R (min): 4.252. P_{HPLC}/ %: 97.30. HPLC (ACN: H2O=80:20) t_R (min): 3.234. P_{HPLC}/ %: 95.495.624

Compound 5-2: Light yellow solid. $C_{19}H_{20}O_5$. Yield: 69.0%. Melting point: 110°C. ^{1}H-NMR (300 MHz, CDCl$_3$) δ: 6.85 (t, 2H, J = 7.8 Hz, Ar-H), 7.12 (m, 1H, Ar-H), 7.18 (d, J = 8.1 Hz, 1H, Ar-H), 7.38 (d, J = 15 Hz, 1H, COCH=), 7.57-7.65 (m, 2H, Ar-H), 7.71 (d, J = 15 Hz, 1H, Ar-CH=). ^{13}C-NMR (75 MHz, CDCl$_3$) δ: 55.788, 55.854, 109.768, 110.044, 110.616, 110.954, 119.404, 122.732, 127.858, 131.334, 143.937, 149.026, 151.084, 152.935, 188.401 MS (APCI) m/z: 329.0 (M+1)$^+$. HPLC (MeOH: H2O=80:20) t_R (min): 7.043. P_{HPLC}/ %: 99.34. HPLC (ACN: H2O=80:20) t_R (min): 3.742. P_{HPLC}/ %: 99.12

Compound 5-3: Yellow powder. $C_{17}H_{16}O_5$. Melting point: 144-147°C. ^{1}H-NMR (300 MHz, CDCl$_3$) δ: 3.94 (s, 3H, OCH$_3$), 3.98 (s, 3H, OCH$_3$), 6.86 (d, J= 8 Hz, 1H, ArH), 6.93 (d, J= 8 Hz, 1H, ArH), 7.13 (dd, J = 1.8 Hz, J = 10 Hz, 1H, ArH), 7.27-7.28 (m, 1H, ArH), 7.39 (d, J = 16 Hz, 1H, COCH=), 7.61-7.63 (m, 2H, ArH), 7.72 (d, J = 16 Hz, 1H, ArCH=). ^{13}C-NMR (75 MHz, DMSO-d$_6$) δ: 56.197, 56.288, 111.821, 112.542, 114.804, 115.151, 119.781, 122.406, 122.779, 128.088, 131.317, 144.265, 146.882, 147.027, 150.793, 152.766, 188.593 MS (APCI) m/z: 301.0 (M+1)$^+$. HPLC (MeOH: H2O=80:20) t_R (min): 3.366. P_{HPLC}/ %: 99.40. HPLC (ACN: H2O=80:20) t_R (min): 2.934. P_{HPLC}/ %: 99.91

Compound 5-4: Light yellow crystals. $C_{15}H_{12}O$. Yield: 66.1%. Melting point: 53-55°C. ^{1}H-NMR (300 MHz, CDCl$_3$) δ: 7.41-7.79 (m, 10H, Ar-H + -CH=CH-), 8.03 (d, J = 7.5 Hz, 2H, Ar-H). ^{13}C-NMR (75 MHz, CDCl$_3$) δ: 121.980, 128.358, 128.407, 128.530, 128.862, 130.450, 132.689, 134.781, 138.104, 144.714, 190.393 MS (APCI) m/z: 209.0 (M+1)$^+$. HPLC (MeOH: H2O=80:20) t_R (min): 8.273. P_{HPLC}/ %: 100.00. HPLC (ACN: H2O=70:30) t_R (min): 4.465. P_{HPLC}/ %: 99.27

Compound 5-5: Yellow liquid. $C_{17}H_{16}O_3$. Yield: 15.8%. Liquid state. ^{1}H-NMR (300 MHz, CDCl$_3$) δ: 3.85 (s, 3H, OMe), 3.88 (s, 3H, OMe), 6.97 (d, J = 8 Hz, 1H, ArH), 7.12-7.61 (m, 8H, Ar-H + COCH=), 7.77 (d, J=16 Hz, 1H, Ar-CH=). ^{13}C-NMR (75 MHz, CDCl$_3$) δ: 121.980, 128.358,55.038, 55.156, 112.704, 113.263, 116.053, 118.978, 120.818, 120.857, 122.060, 129.343, 129.696, 135.993, 144.437, 159.650, 159.700, 189.781 MS (APCI) m/z: 241.2 (M+1)$^+$. HPLC (MeOH: H2O=80:20) t_R (min): 6.073. P_{HPLC}/ %: 98.13. HPLC (ACN: H2O=70:30) t_R (min): 2.867. P_{HPLC}/ %: 97.85

Compound 5-6: Pale yellow powder. $C_{15}H_{12}O_3$. Yield: 12.05%. Melting point: 190-195°C. ^{1}H-NMR (300 MHz, DMSO-d$_6$) δ: 6.80-6.88 (m, 4H, ArH), 7.56-7.62 (m, 4H, ArH + -CH=CH-), 7.94 (d, J = 8 Hz, 2H, Ar-H). MS (APCI) m/z: 241.2 (M+1)$^+$. HPLC (MeOH: H2O=80:20) t_R (min): 3.326. P_{HPLC}/ %: 99.69. HPLC (ACN: H2O=70:30) t_R (min): 2.941. P_{HPLC}/ %: 99.69

Compound 5-7: White crystals. $C_{15}H_8F_4O$. Yield: 14.3%. Melting point: 132-134°C. ^{1}H-NMR (300 MHz, CDCl$_3$) δ: 7.18-7.39 (m, 4H, Ar-H + COCH=), 7.45-7.51 (m, 1H, Ar-H), 7.73 (d, J = 16 Hz, 1H, Ar-CH=), 7.79-7.90 (m, 2H, Ar-H). ^{13}C-NMR (75 MHz, CDCl$_3$) δ: 55100.711, 116.482, 116.715, 117.508, 117.742, 117.894, 117.978, 118.127, 121.670, 121.694, 125.335, 125.403, 131.783, 131.841, 134.884, 143.229, 148.946, 152.249, 187.095 MS (APCI) m/z: 280.9 (M+1)$^+$. HPLC (MeOH: H2O=80:20) t_R (min): 4.523. P_{HPLC}/ %: 95.64. HPLC (ACN: H2O=80:20) t_R (min): 3.812. P_{HPLC}/ %: 96.05

Appendix 3: Effects of curcumin analogue 3-3 on 84 related Wnt components and target genes in U2OS cells using Human Wnt signaling real time PCR array analysis. The gene symbol, gene description, fold-change and p-value were reported for each gene. Genes that are significantly dysregulated (p-value < 0.05) are bold and indicated with *.

Gene symbol	Gene Description	Fold Regulation	p-value
Genes that are up-regulated with cucrumin analogue 3-3 treatment			
BTRC *	**Beta-transducin repeat containing**	**1.540**	**0.0475**
CCND2	Cyclin D2	1.099	0.7502
CTBP2	C-terminal binding protein 2	1.012	0.9960
DKK1	Dickkopf homolog 1 (Xenopus laevis)	1.602	0.0663
FGF4	Fibroblast growth factor 4 (heparin secretory transforming protein, Kaposi sarcoma oncogene)	1.000	0.9596
FRZB	Frizzled-related protein	1.307	0.3766
KREMEN1	Kringle containing transmembrane protein 1	1.031	0.8588
MYC	V-myc myelocytomatosis viral oncogene homolog (avian)	1.606	0.0821
TLE2 *	**Tranducin-like enhancer of split 2 (E(sp1) homolog, Drosophila)**	**2.406**	**0.000526**
WNT2B	Wingless-type MMTV integration site family, member 2B	1.206	0.3665
Genes that are down-regulated with curcumin analogue 3-3 treatment			
AES	Amino-terminal enhancer of split	1.932	0.1798
APC	Adenomatosis polyposis coli	1.663	0.0798
AXIN1	Axin 1	1.050	0.8786
BCL9	B-cell CLL/lymphoma 9	1.498	0.2007
FZD5	Frizzled homolog 5(Drosophila)	1.047	0.8533
CCND1 *	**Cyclin D1**	**1.461**	**0.0421**
CCND3	Cyclin D3	1.146	0.6529
CSNK1A1	Casein kinase 1, alpha 1	1.901	0.1223
CSNK1D	Casein kinase 1, delta 1	1.385	0.4049
CSNK1G1	Casein kinase 1, gamma 1	1.195	0.5570
CSNK2A1	Casein kinase 1, alpha 1 polypeptide	1.211	0.1538
CTBP1	C-terminal binding protein 1	1.832	0.2304
CTNNB1	Catenin(cadherin-associated protein), beta 1, 88kDa	1.461	0.0884
CTNNBIP1	Catenin, beta interacting protein 1	2.009	0.0682
CXXC4	CXXC finger 4	2.651	0.0697
DAAM1	Dishevelled associated activator of	1.035	0.5478

	morphogenesis 1		
DIXDC1	DIX domain containing 1	1.516	0.0675
DVL1	Dishevelled, dsh homolog 1 (Drosophila)	1.110	0.4598
DVL2	Dishevelled, dsh homolog 2 (Drosophila)	1.823	0.3636
EP300	E1A binding protein p300	1.254	0.4232
FBXW11	F-box and WD repeat domain containing 11	1.159	0.5991
FBXW2	F-box and WD repeat domain containing 2	1.047	0.5459
FOSL1 *	**FORolike antigen 1**	**4.574**	**0.0448**
FOXN1	Forkhead box N1	1.451	0.2374
FRAT1	Frequently rearranged in advanced T-cell lymphomas	1.495	0.313
FSHB	Follicle stimulating hormone, beta polypeptide	1.234	0.4260
FZD1	Frizzled homolog 1 (Drosophila)	1.569	0.1054
FZD2 *	**Frizzled homolog 2 (Drosophila)**	**3.776**	**0.0304**
FZD3 *	**Frizzled homolog 3 (Drosophila)**	**1.341**	**0.0153**
FZD4 *	**Frizzled homolog 4 (Drosophila)**	**2.597**	**0.0297**
FZD6	Frizzled homolog 6 (Drosophila)	1.357	0.5118
FZD7	Frizzled homolog 7 (Drosophila)	1.509	0.2087
FZD8	Frizzled homolog 8 (Drosophila)	1.097	0.7414
GSK3A	Glycogen synthase kinase 3 alpha	1.379	0.2654
GSK3B	Glycogen synthase kinase 3 beta	1.226	0.3865
JUN	Jun oncogene	1.686	0.1092
LEF1	Lymphoid enhancer-binding factor 1	1.251	0.1993
LRP5	Low density lipoprotein receptor-related protein 5	1.198	0.6691
LRP6	Low density lipoprotein receptor-related protein 6	1.335	0.1809
NKD1 *	**Naked cuticle homolog 1 (Drosophila)**	**2.292**	**0.0173**
NLK	Nemo-like kinase	1.097	0.7933
PITX2 *	**Paired-like homedomain transcription factor 2**	**3.855**	**0.0306**
PORCN	Porcupine homolog (Drosophila)	1.026	0.8923
PPP2CA	Protein phosphatase 2(formerly 2A), catalytic subunit, alpha isoform	1.341	0.0535
PPP2R1A	Protein phosphatase 2(formerly 2A), regulatory subunit A, alpha isoform	1.678	0.2019
PYGO1	Pygopus homolog (Drosophila)	1.184	0.2637
RHOU	Ras homolog gene family, member U	1.973	0.0833
SENP2	SUMO1/sentrin/SMT3 specific peptidase 2	1.509	0.1791
SFRP1 *	**Secreted frizzled-related protein 1**	**1.562**	**0.000628**
SFRP4	Secreted frizzled-related protein 4	1.606	0.1438
FBXW4	F-box and WD repeat domain containing 4	1.231	0.4354
SLC9A3R1	Solute carrier family 9 (sodium/hydrogen exchanger), member 3 regulator 1	1.447	0.3604

Gene	Description	Value	p-value
SOX17	SRY (sex determining region Y)-box 17	1.162	0.5814
T	T, brachyury homolog (mouse)	1.289	0.2734
TCF7	Transcription factor 7 (T-cell specific, HMG-box)	1.234	0.4260
TCF7L1 *	**Transcription factor 7-like 1 (T-cell specific, HMG-box)**	**2.921**	**0.0307**
TLE1	Tranducin-like enhancer of split 1 (E(sp1) homolog, Drosophila)	1.655	0.0699
WIF1	WNT inhibitory factor 1	1.234	0.4260
WISP1 *	**WNT inducible signaling pathway protein 1**	**2.815**	**0.0276**
WNT1	Wingless-type MMTV integration site family, member 1	1.234	0.4260
WNT10A *	**Wingless-type MMTV integration site family, member 10A**	**3.403**	**0.0151**
WNT11 *	**Wingless-type MMTV integration site family, member 11**	**9.895**	**0.000005**
WNT16	Wingless-type MMTV integration site family, member 16	1.228	0.4311
WNT2	Wingless-type MMTV integration site family, member 2	1.234	0.4260
WNT3	Wingless-type MMTV integration site family, member 3	1.437	0.2642
WNT3A	Wingless-type MMTV integration site family, member 3A	1.323	0.2490
WNT4	Wingless-type MMTV integration site family, member 4	2.292	0.1375
WNT5A *	**Wingless-type MMTV integration site family, member 5A**	**2.549**	**0.0195**
WNT5B *	**Wingless-type MMTV integration site family, member 5B**	**2.357**	**0.0125**
WNT6 *	**Wingless-type MMTV integration site family, member 6**	**4.367**	**0.0295**
WNT7A *	**Wingless-type MMTV integration site family, member 7A**	**2.474**	**0.0397**
WNT7B *	**Wingless-type MMTV integration site family, member 7B**	**4.218**	**0.0115**
WNT8A *	**Wingless-type MMTV integration site family, member 8A**	**1.354**	**0.0055**
WNT9A	Wingless-type MMTV integration site family, member 9A	1.228	0.4040

Appendix 4: Primer sequence for RT-PCR

Gene		Sequence	Product size (bp)
SFRP1	Sense	5'-CCAGC GAGTA CGACT ACGTG AGCTT-3'	497
	Anti-sense	5'-CTCAGATTTCAACTCGTTGTCACAGG-3'	
SFRP2	Sense	5'-ATGAT GATGA CAACG ACATA ATG-3'	322
	Anti-sense	5'-ATGCG CTTGA ACTCT CTCTG C-3'	
SFRP4	Sense	5'-CCAGA CATGA TGGTA CAGGA AAG-3'	380
	Anti-sense	5'-CTTTTACTAAGCTGATCTCTCCAT-3'	
SFRP5	Sense	5'-CAGAT GTGCT CCAGT GACTT TG-3'	346
	Anti-sense	5'-AGAAG AAAGG GTAGT AGAGG GAG-3'	
GAPDH	Sense	5'-CGGAG TCAAC GGATT TGGTC GTAT-3'	307
	Anti-sense	5'-AGCCT TCTCC ATGGT GGTGA AGAC-3'	

Appendix 5: Effects of SFRP2 on 84 related Wnt components and target genes in U2OS cells using Human Wnt signaling real time PCR array analysis. The gene symbol, gene description, fold-change and p-value were reported for each gene. Genes that are significantly dysregulated (p-value < 0.05) are bold and indicated with *.

Gene symbol	Gene Description	Fold Regulation	p-value
Genes that are up-regulated with SFRP2 over-expression			
AES	Amino-terminal enhancer of split	1.774	0.0829
APC *	**Adenomatosis polyposis coli**	**2.163**	**0.0019**
AXIN1	Axin 1	1.102	0.2615
BCL9	B-cell CLL/lymphoma 9	1.050	0.4808
BTRC *	**Beta-transducin repeat containing**	**1.226**	**0.0106**
CCND2 *	**Cyclin D2**	**2.627**	**0.000076**
CCND3	Cyclin D3	1.060	0.6606
CSNK1D *	**Casein kinase 1, delta 1**	**1.959**	**0.0010**
CSNK1G1*	**Casein kinase 1, gamma 1**	**3.466**	**0.00026**
CSNK2A1	Casein kinase 1, alpha 1 polypeptide	1.231	0.3178
CTBP1	C-terminal binding protein 1	1.057	0.2074
CTBP2 *	**C-terminal binding protein 2**	**2.028**	**0.00054**
CTNNBIP1	Catenin, beta interacting protein 1	1.283	0.4021
CXXC4	CXXC finger 4	1.074	0.0945
DIXDC1	DIX domain containing 1	1.230	0.3597
DKK1 *	**Dickkopf homolog 1 (Xenopus laevis)**	**3.317**	**0.000005**
DVL1 *	**Dishevelled, dsh homolog 1 (Drosophila)**	**1.376**	**0.0074**
DVL2 *	**Dishevelled, dsh homolog 2 (Drosophila)**	**2.245**	**0.0011**
EP300	E1A binding protein p300	1.209	0.0957
FBXW2 *	**F-box and WD repeat domain containing 2**	**3.776**	**0.0010**
FBXW4 *	**F-box and WD repeat domain containing 4**	**1.655**	**0.0061**
FBXW11 *	**F-box and WD repeat domain containing 11**	**1.488**	**0.0030**
FGF4	Fibroblast growth factor 4 (heparin secretory transforming protein, Kaposi sarcoma oncogene)	1.335	0.6212
FOXN1	Forkhead box N1	1.251	0.2438
FRZB	Frizzled-related protein	1.495	0.1817
FSHB	Follicle stimulating hormone, beta polypeptide	2.378	0.061762
FZD3 *	**Frizzled homolog 3 (Drosophila)**	**1.811**	**0.00075**
FZD5 *	**Frizzled homolog 5(Drosophila)**	**2.627**	**0.0003**
FZD8 *	**Frizzled homolog 8 (Drosophila)**	**1.617**	**0.00134**
GSK3B *	**Glycogen synthase kinase 3 beta**	**1.480**	**0.00167**
KREMEN1	Kringle containing transmembrane protein 1	1.014	0.7771

LRP5	Low density lipoprotein receptor-related protein 5	1.128	0.2017
LRP6	Low density lipoprotein receptor-related protein 6	1.128	0.0796
NLK	Nemo-like kinase	2.751	0.2345
PITX2	Paired-like homedomain transcription factor 2	1.079	0.6196
PPP2R1A	Protein phosphatase 2(formerly 2A), regulatory subunit A, alpha isoform	1.286	0.4072
RHOU	Ras homolog gene family, member U	1.220	0.1463
SENP2	SUMO1/sentrin/SMT3 specific peptidase 2	1.526	0.2469
SFRP1 *	**Secreted frizzled-related protein 1**	**1.491**	**0.0026**
SFRP4	Secreted frizzled-related protein 4	1.149	0.4850
SOX17	SRY (sex determining region Y)-box 17	1.338	0.3052
T *	**T, brachyury homolog**	**1.625**	**0.0048**
TCF7	Transcription factor 7 (T-cell specific, HMG-box)	1.231	0.5227
TLE1 *	**Tranducin-like enhancer of split 1 (E(sp1) homolog, Drosophila)**	**1.968**	**0.0003**
TLE2	Tranducin-like enhancer of split 2 (E(sp1) homolog, Drosophila)	1.733	0.2065
WIF1 *	**WNT inhibitory factor 1**	**3.317**	**0.000005**
WNT1 *	**Wingless-type MMTV integration site family, member 1**	**3.317**	**0.000005**
WNT10A	Wingless-type MMTV integration site family, member 10A	1.021	0.8557
WNT16 *	**Wingless-type MMTV integration site family, member 16**	**3.317**	**0.000005**
WNT2 *	**Wingless-type MMTV integration site family, member 2**	**3.317**	**0.000005**
WNT2B *	**Wingless-type MMTV integration site family, member 2B**	**1.159**	**0.0047**
WNT3 *	**Wingless-type MMTV integration site family, member 3**	**1.408**	**0.0369**
WNT3A	Wingless-type MMTV integration site family, member 3A	1.526	0.0967
WNT4	Wingless-type MMTV integration site family, member 4	1.021	0.8764
WNT6	Wingless-type MMTV integration site family, member 6	1.289	0.2158
WNT7A*	**Wingless-type MMTV integration site family, member 7B**	**3.379**	**0.0053**
WNT8A *	**Wingless-type MMTV integration site family, member 8A**	**1.919**	**0.0006**

WNT9A *	Wingless-type MMTV integration site family, member 9A	2.154	0.0034
Genes that are down-regulated with SFRP2 over-expression			
CCND1 *	Cyclin D1	1.973	0.00029
CSNK1A1	Casein kinase 1, alpha 1	1.424	0.1171
CTNNB1	Catenin(cadherin-associated protein), beta 1, 88kDa	1.099	0.1991
DAAM1	Dishevelled associated activator of morphogenesis 1	1.110	0.3138
FOSL1	FORolike antigen 1	1.190	0.6883
FRAT1	Frequently rearranged in advanced T-cell lymphomas	1.151	0.4000
FZD1	Frizzled homolog 1 (Drosophila)	1.260	0.0893
FZD2 *	Frizzled homolog 2 (Drosophila)	1.875	0.0052
FZD4 *	Frizzled homolog 4 (Drosophila)	2.701	0.0037
FZD6 *	Frizzled homolog 6 (Drosophila)	5.016	0.000032
FZD7 *	Frizzled homolog 7 (Drosophila)	3.724	0.00062
GSK3α	Glycogen synthase kinase 3α	1.020	0.8131
JUN *	Jun oncogene	1.721	0.00039
LEF1 *	Lymphoid enhancer-binding factor 1	1.434	0.0533
MYC	V-myc myelocytomatosis viral oncogene homolog (avian)	1.077	0.5938
NKD1 *	Naked cuticle homolog 1 (Drosophila)	1.628	0.0048
PORCN	Porcupine homolog (Drosophila)	1.257	0.3911
PPP2CA	Protein phosphatase 2(formerly 2A), catalytic subunit, alpha isoform	1.140	0.2990
PYGO1	Pygopus homolog (Drosophila)	2.357	0.0806
SLC9A3R1 *	Solute carrier family 9 (sodium/hydrogen exchanger), member 3 regulator 1	1.146	0.0118
TCF7L1	Transcription factor 7-like 1 (T-cell specific, HMG-box)	1.162	0.1494
WISP1 *	WNT inducible signaling pathway protein 1	7.569	0.00025
WNT11 *	Wingless-type MMTV integration site family, member 11	11.210	0.00025
WNT5A *	Wingless-type MMTV integration site family, member 5A	1.853	0.0022
WNT5B *	Wingless-type MMTV integration site family, member 5B	1.519	0.0054
WNT7B	Wingless-type MMTV integration site family, member 7B	1.064	0.6405

Appendix 6: Effects of SFRP5 on 84 related Wnt components and target genes in U2OS cells using Human Wnt signaling real time PCR array analysis. The gene symbol, gene description, fold-change and p-value were reported for each gene. Genes that are significantly dysregulated (p-value < 0.05) are bold and indicated with *.

Gene symbol	Gene Description	Fold Regulation	p-value
Genes that are up-regulated with SFRP5 over-expression			
AES *	**Amino-terminal enhancer of split**	**2.163**	**0.0410**
APC *	**Adenomatosis polyposis coli**	**1.794**	**0.0380**
AXIN1	Axin 1	1.141	0.4515
BTRC *	**Beta-transducin repeat containing**	**1.798**	**0.0404**
FZD5	Frizzled homolog 5(Drosophila)	1.289	0.2411
CCND3	Cyclin D3	1.060	0.6979
CSNK1D	Casein kinase 1, delta 1	1.045	0.5434
CSNK1G1*	**Casein kinase 1, gamma 1**	**2.052**	**0.00046**
CTBP1	C-terminal binding protein 1	1.060	0.6914
CTBP2	C-terminal binding protein 2	1.089	0.5701
CTNNB1	Catenin(cadherin-associated protein), beta 1, 88kDa	1.372	0.1697
CTNNBIP1	Catenin, beta interacting protein 1	1.023	0.8274
CXXC4	CXXC finger 4	1.055	0.5615
DAAM1	Dishevelled associated activator of morphogenesis 1	1.043	0.7656
DIXDC1	DIX domain containing 1	1.220	0.2515
DKK1 *	**Dickkopf homolog 1 (Xenopus laevis)**	**1.178**	**0.0373**
DVL1 *	**Dishevelled, dsh homolog 1 (Drosophila)**	**1.447**	**0.0193**
DVL2 *	**Dishevelled, dsh homolog 2 (Drosophila)**	**1.395**	**0.0458**
EP300	E1A binding protein p300	1.401	0.2063
FBXW2 *	**F-box and WD repeat domain containing 2**	**2.757**	**0.0186**
FBXW11 *	**F-box and WD repeat domain containing 11**	**1.437**	**0.0066**
FGF4	Fibroblast growth factor 4 (heparin secretory transforming protein, Kaposi sarcoma oncogene)	1.181	0.5367
FOSL1	FORolike antigen 1	1.461	0.1373
FOXN1	Forkhead box N1	1.502	0.1666
FRZB *	**Frizzled-related protein**	**2.445**	**0.00968**
FZD1	Frizzled homolog 1 (Drosophila)	1.263	0.2806
FZD3 *	**Frizzled homolog 3 (Drosophila)**	**1.811**	**0.0445**
FZD8	Frizzled homolog 8 (Drosophila)	1.226	0.1030
GSK3B	Glycogen synthase kinase 3 beta	1.120	0.4285
LEF1	Lymphoid enhancer-binding factor 1	1.043	0.8003
LRP6	Low density lipoprotein receptor-related	1.102	0.5302

	protein 6		
MYC *	**V-myc myelocytomatosis viral oncogene homolog (avian)**	**2.809**	**0.0473**
NLK	Nemo-like kinase	1.115	0.5519
PPP2CA	Protein phosphatase 2(formerly 2A), catalytic subunit, alpha isoform	1.464	0.1466
PPP2R1A	Protein phosphatase 2(formerly 2A), regulatory subunit A, alpha isoform	1.069	0.6371
SENP2 *	**SUMO1/sentrin/SMT3 specific peptidase 2**	**1.659**	**0.0524**
SFRP4	Secreted frizzled-related protein 4	1.505	0.0686
FBXW4	F-box and WD repeat domain containing 4	1.272	0.1951
SLC9A3R1	Solute carrier family 9 (sodium/hydrogen exchanger), member 3 regulator 1	1.040	0.6586
SOX17	SRY (sex determining region Y)-box 17	1.526	0.2289
T *	**T, brachyury homolog (mouse)**	**1.441**	**0.0265**
TCF7 *	**Transcription factor 7 (T-cell specific, HMG-box)**	**1.357**	**0.00737**
TLE2	Tranducin-like enhancer of split 2 (E(sp1) homolog, Drosophila)	1.209	0.1542
WNT10A *	**Wingless-type MMTV integration site family, member 10A**	**1.659**	**0.00149**
WNT16 *	**Wingless-type MMTV integration site family, member 16**	**1.566**	**0.0407**
WNT2B *	**Wingless-type MMTV integration site family, member 2B**	**1.366**	**0.0107**
WNT3	Wingless-type MMTV integration site family, member 3	1.283	0.3457
WNT3A	Wingless-type MMTV integration site family, member 3A	1.128	0.6488
WNT4	Wingless-type MMTV integration site family, member 4	1.072	0.6682
WNT5B	Wingless-type MMTV integration site family, member 5B	1.117	0.1867
WNT6	Wingless-type MMTV integration site family, member 6	1.198	0.4048
WNT7B	Wingless-type MMTV integration site family, member 7B	1.107	0.7392
WNT8A	Wingless-type MMTV integration site family, member 8A	1.385	0.0757
WNT9A	Wingless-type MMTV integration site family, member 9A	1.278	0.2706
Genes that are down-regulated with SFRP5 over-expression			
BCL9	B-cell CLL/lymphoma 9	1.045	0.8588

CCND1	Cyclin D1	1.278	0.2336
CCND2	Cyclin D2	1.128	0.4163
CSNK1A1	Casein kinase 1, alpha 1	1.002	0.8883
CSNK2A1	Casein kinase 1, alpha 1 polypeptide	1.107	0.4711
FRAT1	Frequently rearranged in advanced T-cell lymphomas	1.326	0.3332
FSHB	Follicle stimulating hormone, beta polypeptide	1.016	0.9750
FZD2	Frizzled homolog 2 (Drosophila)	1.094	0.8241
FZD4 *	**Frizzled homolog 4 (Drosophila)**	**2.549**	**0.0156**
FZD6	Frizzled homolog 6 (Drosophila)	1.354	0.1132
FZD7 *	**Frizzled homolog 7 (Drosophila)**	**1.341**	**0.0517**
GSK3A	Glycogen synthase kinase 3 alpha	1.141	0.4442
JUN	Jun oncogene	1.170	0.6445
KREMEN1	Kringle containing transmembrane protein 1	1.115	0.1604
LRP5	Low density lipoprotein receptor-related protein 5	1.149	0.7137
NKD1 *	**Naked cuticle homolog 1 (Drosophila)**	**1.613**	**0.0158**
PITX2	Paired-like homedomain trnascription factor 2	1.079	0.5783
PORCN	Porcupine homolog (Drosophila)	1.089	0.3624
PYGO1	Pygopus homolog (Drosophila)	1.014	0.8092
RHOU	Ras homolog gene family, member U	1.434	0.0734
SFRP1	Secreted frizzled-related protein 1	1.587	0.1410
TCF7L1	Transcription factor 7-like 1 (T-cell specific, HMG-box)	1.016	0.9750
TLE1	Tranducin-like enhancer of split 1 (E(sp1) homolog, Drosophila)	1.263	0.0800
WIF1	WNT inhibitory factor 1	1.016	0.9750
WISP1 *	**WNT inducible signaling pathway protein 1**	**2.848**	**0.00205**
WNT1	Wingless-type MMTV integration site family, member 1	1.016	0.9750
WNT11 *	**Wingless-type MMTV integration site family, member 11**	**5.566**	**0.00044**
WNT2	Wingless-type MMTV integration site family, member 2	1.016	0.9750
WNT5A *	**Wingless-type MMTV integration site family, member 5A**	**1.471**	**0.0218**
WNT7A	Wingless-type MMTV integration site family, member 7A	1.411	0.1683